

Gene Mapping of Morphological Traits in Chickens

Jingyi Li

Dissertation submitted to the faculty of the Virginia Polytechnic Institute and State

University in partial fulfillment of the requirements for the degree of

Doctor of Philosophy

In

Animal and Poultry Sciences

Paul B. Siegel, Chair

Leif Andersson

Elizabeth Ruth Gilbert

D. Phillip Sponenberg

March 23, 2017

Blacksburg, Virginia

Keywords: Linkage mapping, feather patterns, feathered legs, polydactyly, chickens

Copyright 2017, Jingyi Li

Gene Mapping of Morphological Traits in Chickens

Jingyi Li

Abstract (Public)

Chickens, one of the major protein sources in diets for humans, have a long cultural, sport and religious history since their initial domestication during the neolithic period. Darwin wrote of the importance of variation, which today we see for example in size of body, length of shank, number of toes, distribution of feathers, comb types, and plumage color patterns resulting in a plethora of breeds of chickens that differ in appearance. Some of these traits are “simply” inherited, which in the molecular era facilitates the study of relationships between DNA sequences and phenotypes. This dissertation focuses on identification of differences in DNA sequences among chickens responsible for these “simply” inherited phenotypes. The 12 phenotypes that were studied included 6 plumage color patterns (Pattern, Columbian, Melanotic, mottling, Blue, and chocolate), 2 forms of feathered-legs, polydactyly, dark brown eggshell color, vulture hock, and creeper. Designed were ten 3-generation populations to produce 1,880 chickens. An additional 339 DNA samples from other populations were included. Of the 12 phenotypes, 8 involved genotyping of pooled DNA samples, a cost-effective initial screen to target DNA sequences. This was followed by genotyping individual samples in 5 of the more promising studies. Candidate genes identified as associated with these 5 phenotypes underwent further studies which identified differences in DNA sequences associated with 4 of them (mottling, feathered-leg, Blue, and chocolate). These findings provide insights of how DNA sequences contribute to the phenotypic appearance of animals.

Gene Mapping of Morphological Traits in Chickens

Jingyi Li

Abstract (Academic)

Chickens exhibit considerable variation in morphological traits, with some populations having undergone intensive selection for uniqueness and uniformity. These populations are a source of experimental material to study the genetics of morphological traits. An important first step in such studies is to map the genes and the causal mutations that influence these traits. This research focused on gene mapping of 12 morphological traits including 4 intra-feather color patterns (Pattern, Columbian, Melanotic, and mottling), 2 inter-feather color patterns (Blue and chocolate), 2 forms of feathered-legs, polydactyly, dark brown eggshell color, vulture hock, and creeper. Ten backcross and/or F₂ populations were designed to produce 1,880 individuals. An additional 339 DNA samples from other populations were included. The procedures for gene mapping were: 1. Pooling of DNA samples of backcross or F₂ individuals based on their shared phenotypes, followed by microarray assays for genotyping, a cost-effective initial screen for the candidate genomic regions, 2. Linkage mapping to narrow the range of candidate genes, 3. Sequencing to identify the candidate mutations, 4. Diagnostic tests to confirm the association between the candidate mutation and the phenotype. Of the 12 traits studied, 3 (mottling, Blue, and chocolate) made progress into step 4. Complexities due to genomic context, modifiers, and environmental factors precluded step 4 for the first form of the feathered-leg gene, step 3 for the mapping of Melanotic, and earlier stages for the mapping of Pattern, Columbian, dark brown egg, vulture hock, and the second form of feathered-leg. These findings provide insights of the complexity of how background

genome can influence the phenotypic expression of single genes (gene \times genetic background interactions) and an understanding of cellular and molecular mechanisms involved in morphogenesis.

Acknowledgements

Dr. Paul Siegel

In my hardest time during the past 4 years, you have rescued me in many ways. By accepting me as your graduate student and treating me with respect and kindness like that of your own son, I have become a better person and scientist. My vision was broadened by your many life experiences, and by default, you have encouraged me to explore other topics outside of my field of study.

Dr. Leif Andersson

I appreciate all the assistance you have provided, including advising and partial funding for my projects. Most of our communication has been through email, which in my view should have been inefficient, but to my surprise, it was very beneficial to me. I came to realize that you trusted me enough not to micro-manage me, which coincidentally helped me to build my confidence in research. Therefore, I decided to have an academic career for the rest of life.

Dr. Elizabeth Gilbert

I remember the day we met for my interview in Beijing more than 4 years ago. I appreciate your kindness, and without your help, I may not have been accepted by Virginia Tech. Moreover, I am grateful for your suggestions regarding my research.

Dr. Phillip Sponenberg

Your inputs in my research projects were insightful. Your broad knowledge of chickens and other species developed my thought process and will benefit my current and future academic careers.

Dr. Ben Dorshorst

I am grateful for the opportunity that you afforded me. I have gained hands on experience in the poultry genetics laboratory and in establishing mapping populations for my research. Thank you for accepting me as your first graduate student and also for all your input in our lab and my research.

Members of my research group

Thanks to Dez-Ann Sutherland, Michelle Jambui, Christa Honaker, and undergraduate students in our lab. Thanks to John Thomas. You directly contributed to my projects, such as DNA isolation, pooling of DNA samples, and husbandry of chickens. I also want to thank you for establishing long lasting friendships, making the past 4 years such a wonderful time.

Researchers and breeders who provided the samples

Chickens, blood samples, and DNA samples involved in this dissertation were provided by multiple researchers and chicken breeders. Without your help, these projects would not be possible.

My family, Mei Liu, Jie Li, and Sijia Xie

Thanks to my parents and girlfriend who supported me. Special thanks to my mother who spent almost an entire year in Blacksburg, which alleviated my homesickness.

Table of contents

Abstract (Public).....	ii
Abstract (Academic).....	iii
Acknowledgements.....	v
List of tables.....	xii
List of figures.....	xiv
Chapter 1. Introduction and literature review.....	1
Introduction.....	1
Literature review of plumage color patterns.....	1
Tables and figures.....	10
References.....	11
Chapter 2. General materials and methods.....	13
Animals.....	13
Genotyping of DNA pools.....	13
Linkage mapping and diagnostic test	14
Individual genotyping using 600K SNP array.....	15
PCR and sequencing.....	16
Bioinformatics analysis.....	18
Tables and figures.....	19
References.....	26
Chapter 3. Pattern (<i>Pg</i>) gene mapping.....	28
Abstract.....	28
Introduction.....	28

Materials and methods.....	29
Results and discussion.....	30
Tables and figures.....	32
References.....	35
Chapter 4. Columbian (<i>Co</i>) gene mapping.....	36
Abstract.....	36
Introduction.....	36
Materials and methods.....	37
Results and discussion.....	38
Tables and figures.....	41
References.....	42
Chapter 5. Melanotic (<i>MI</i>) gene mapping.....	43
Abstract.....	43
Introduction.....	43
Materials and methods.....	44
Results and discussion.....	45
Tables and figures.....	48
References.....	50
Chapter 6. Mottling (<i>mo</i>) gene mapping.....	51
Abstract.....	51
Introduction.....	51
Materials and methods.....	54
Results.....	55

Discussion.....	58
Tables and figures.....	62
References.....	66
Chapter 7. Feathered-leg in chickens is associated with a SNP on chromosome 15 and a region on chromosome 12.....	68
Authors.....	68
Affiliations.....	68
Summary.....	68
Introduction.....	69
Materials and methods.....	71
Results.....	73
Discussion.....	75
Acknowledgements.....	78
References.....	78
Figures.....	80
Supporting information.....	81
Chapter 8. Polydactyly 2 (<i>Po-2</i>) gene mapping	82
Abstract.....	82
Introduction.....	82
Materials and methods.....	85
Results and discussion.....	85
Tables and figures.....	89
References.....	91

Chapter 9. Bl (<i>Bl</i>) gene mapping	92
Abstract.....	92
Introduction.....	92
Materials and methods.....	94
Results and discussion.....	97
Tables and figures.....	102
References.....	107
Chapter 10. A missense mutation in <i>TYRPI</i> causes the chocolate plumage color in chicken and alters melanosome structure.....	108
Authors.....	108
Affiliations.....	108
Abstract	109
Significance.....	109
Key-words.....	110
Introduction.....	110
Methods.....	111
Results.....	118
Discussion.....	121
Conclusion.....	123
Acknowledgements.....	124
References.....	124
Tables and figures.....	127
Supporting information.....	132

Chapter 11. Peripheral Experiments.....	138
Abstract.....	138
Literature review.....	138
Materials and methods.....	145
Results and discussion.....	148
Tables and figures.....	161
References.....	176
Chapter 12. Summary.....	178
Abbreviations.....	180

List of tables

Table 2.1. Details of 6 mapping populations.....	19
Table 2.2. Eighty-five breeds or lines used in the diagnostic tests.....	20
Table 2.3. Fifty-six chicken samples for individual genotyping via 600K SNP chips.....	22
Table 2.4. Groups in back cross and F ₂	23
Table 2.5. SNPs used in linkage mapping of individual analysis.....	24
Table 2.6. PCR primers for Sanger sequencing.....	25
Table 3. Genes within the genomic regions that contain SNPs with absRAFdif greater than 0.5 when comparing stippling and partridge groups.....	32
Table 6.1. Polymorphisms identified in the chicken <i>EDNRB2</i> gene.....	62
Table S1 ¹ . Linkage mapping of feathered-leg using individual SNP analysis.....	81
Table 9.1. PCR primers and probes used for analyzing the causal mutation of the Blue gene.....	102
Table 1 ² . Fifteen haplotypes identified among 78 individuals.....	127
Table S1 ² . List of non-chocolate breeds or lines used to provide control samples for the <i>TYRPI</i> His214Asn genotyping.....	132
Table S2 ² . List of the 9 SNPs used in linkage mapping for <i>choc</i> mutation.....	135
Table S3 ² . PCR primers and conditions for <i>TYRPI</i> sequencing.....	135
Table S4 ² . Design of the pyrosequencing test for the <i>choc</i> mutation.....	136
Table 11.1. Details of 4 chicken populations discussed in Chapter 11.....	161
Table 11.2. Phenotypes recorded in the Cross_9 F ₂ population.....	162

¹ Table title followed the paper “Feathered-leg in chickens is associated with a SNP on chromosome 15 and a region on chromosome 12” which is submitted to Animal Genetics.

² Table title followed the paper “A missense mutation in TYRP1 causes the Chocolate plumage color in chicken and alters melanosome structure” which is submitted to Pigment Cell & Melanoma Research.

Table 11.3. Correlations (<i>r</i>) between different locations on the eggshell for color measurements.....	163
Table 11.4. Correlations (<i>r</i>) between different color measurements at 3 locations on the eggshell.....	163
Table 11.5. Means, their standard errors, and estimated repeatability of Cross_8 F ₁ eggshell color for different locations of egg and color measurements.....	164
Table 11.6. Means, their standard errors, and estimated Cross_8 F ₁ individual effects on F ₁ eggshell color using the average color measurements of each egg.....	165
Table 11.7. Means, their standard errors, and homogeneity test of variances of LT7, 1D7, and 4D7 between the Cross_9 F ₂ and the red jungle fowl.....	166
Table 11.8. Means, their standard errors, and estimated <i>Po</i> genotypic effect on ED, 1D, 4D, HE, and LT in Cross_9 F ₂	167
Table 11.9. Means, their standard errors, and estimated feathered-leg and vulture hock effects on the total length of the 4th digit (4D) in Cross_9 F ₂	168
Table 11.10. Means, their standard errors, and estimated hookless and its genotypic effects on the total length of the tarsometatarsus in Cross_9 F ₂	169
Table 11.11. Means, their standard errors, and estimated sex and vulture hock effect on percentage relative asymmetry (RA) in Cross_9 F ₂ at week 7.....	170
Table 11.12. Candidate genes of <i>Cp</i>	171

List of figures

Figure 1.1. Examples of intra-feather patterns.....	10
Figure 3. Genome-wide absRAFDif values, for <i>Pg</i> mapping.....	34
Figure 4. Genome-wide absRAFDif values, for <i>Co</i> mapping.....	41
Figure 5.1. Genome-wide absRAFDif values, for <i>Ml</i> mapping.....	48
Figure 5.2. The absRAFDif values of SNPs on chromosome 1, for <i>Ml</i> mapping.....	49
Figure 6.1. Genome-wide absRAFDif values, for <i>mo</i> mapping.....	64
Figure 6.2. The absRAFDif values of SNPs on chromosome 4, for <i>mo</i> mapping.....	65
Figure 1 ¹ . Linkage mapping of feathered-leg using backcross individuals.....	80
Figure 2 ¹ . Genomic regions associated with intermediate feathered-leg.....	81
Figure 8.1. Genome-wide absRAFDif values for <i>Po-1</i> mapping.....	89
Figure 8.2. The absRAFDif values of SNPs on chromosome 2, for <i>Po-1</i> mapping.....	90
Figure 9.1. Genome-wide absRAFDif values, for <i>Bl</i> mapping.....	104
Figure 9.2. The absRAFDif values of SNPs on chromosome 1, for <i>Bl</i> mapping.....	105
Figure 9.3. The organization of the <i>bl^d/bl^d</i> and <i>bl^d/bl⁺</i> , and the relative positions of the amplicons involved in the CNV analysis.....	106
Figure 1 ² . Linkage mapping of the <i>chocolate</i> mutation using F ₂ females.....	128
Figure 2 ² . Position of the SNP identified in the gene capture experiment according to the structure of the <i>TYRP1</i> gene.....	129

¹ Figure title followed the paper “Feathered-leg in chickens is associated with a SNP on chromosome 15 and a region on chromosome 12” which is submitted to Animal Genetics.

² Figure title followed the paper “A missense mutation in TYRP1 causes the Chocolate plumage color in chicken and alters melanosome structure” which is submitted to Pigment Cell & Melanoma Research.

Figure 3 ¹ . Scheme of the <i>TYRP1</i> gene summarizing the various polymorphisms associated with coat color or feather color variation in domestic animals.....	130
Figure 4 ¹ . Electron microscope pictures of melanosomes from feather follicles.....	131
Figure S1 ¹ . The network of TYRP1 haplotypes extracted from the gene capture experiment.....	140
Figure 11.1. Genome-wide ABSdif_H values for <i>Cp</i> mapping.....	172
Figure 11.2. The ABSdif_H values of SNPs on chromosome 7 for <i>Cp</i> mapping.....	173
Figure 11.3. Genome-wide -log _p values calculated by dominant model in PLINK, for <i>Cp</i> mapping.....	174
Figure 11.4. The -log _p values calculated by dominant model in PLINK of SNPs on chromosome 7, for <i>Cp</i> mapping.....	175

¹ Figure title followed the paper “A missense mutation in TYRP1 causes the Chocolate plumage color in chicken and alters melanosome structure” which is submitted to Pigment Cell & Melanoma Research.

Chapter 1

Introduction and literature review

Introduction

Morphogenesis, defined as structural changes observed during embryogenesis (Bard, 1990), involves the responsible cellular and molecular mechanisms (Yu et al., 2002). Mapping of genes and the causal mutations that influence morphological traits are important first steps in understanding these mechanisms. They, in turn, can trigger the discovery of principles in morphology and thus have broad applications. Via phenotypic selection, favorable genes that contribute to the fine details of the different morphological traits are assumed to be fixed in backyard poultry flocks which exhibit a large variety of inter-feather patterns, intra-feather patterns, and other morphological traits. Populations of chickens varying in plumage patterns were established to provide a range of experimental material for study. My dissertation focuses on mapping of 12 genes or loci associated with morphological traits in chickens. They include genes or loci for 6 plumage color patterns, 2 feathered-legs genes, 1 each for polydactyly, dark brown egg, vulture hock, and creeper. Plumage color patterns are reviewed in this chapter; other traits are reviewed in Chapters 7, 8, and 11.

Literature review of plumage color patterns

Plumage color patterns are examples of morphological diversity (Prum and Williamson, 2002). While chickens only deposit melanin (eumelanin and pheomelanin) into feathers (Smyth, 1990), other avian species also deposit carotene into feathers

(Delhey et al., 2010). Thus, the mechanisms of feather color pattern formation are less complex in chickens than they are in some other avian species.

Inter-feather patterns

Inter-feather or primary feather patterns are color patterns that involve all feather tracts of the chicken. The color patterns include mapped genes such as extended black (*E*), dominant white (*I*), recessive white (*c*), and silver (*S*). The causal mutations of these 4 genes primarily influence melanin production within the melanosomes (Kerje et al., 2003, 2004; Chang et al., 2006; Gunnarsson et al., 2007). Melanosomes are lysosome-related organelles in melanocytes in which melanin pigments are synthesized and stored (Loubéry et al., 2012). There are 2 major steps in the development of melanosomes. First, from undifferentiated vesicles an immature and unpigmented premelanosome is formed (stage I), followed by elongation and formation of internal fibrils (stage II). Then, there is the maturation of premelanosomes through synthesis of melanin with deposition on the internal fibrils (stage III), which become heavily pigmented melanocytes (stage IV) (Chi et al., 2006). Mature melanosomes containing melanin are transported through the microtubule network to the periphery of the cell where they are transferred to keratinocytes (Delevoe et al., 2011).

Baxter et al. (2009) has reviewed several genes. They include Microphthalmia-Associated Transcription Factor (MITF), Paired Box Gene 3 (PAX3), and the SRY-box containing gene 10 (SOX10), which are 3 transcription factors with central roles in the main pathways and mechanisms involved in melanocyte development. MITF has been termed the “melanocyte master regulator” and is required for melanocyte differentiation and survival because it activates transcription of most of the melanogenic proteins. PAX3

is responsible for the early development of myoblasts and maintaining melanocyte stem cells as well as serving as an upstream activator of MITF. SOX10 regulates specification of melanocytes. It strongly activates MITF, acts synergistically with PAX3, and also regulates expression of other melanogenic proteins.

Among those melanogenic proteins, we have a relatively better understanding of the roles of melanocortin 1 receptor (MC1R), premelanosome protein (PMEL), tyrosinase (TYR), tyrosinase-related-protein 1 (TYRP1), TYRP2 (also known as dopachrome tautomerase, DCT), and solute carrier family 45, member 2, protein (SLC45A2). MC1R, a transmembrane receptor expressed on the membrane of melanocytes, is equivalent to the extended black (E) locus controlling plumage color in chickens (Kerje et al., 2003). Alleles of the E locus (E , E^R , e^{Wh} , e^+ , e^b , e^s , e^{bc} and e^y) can influence variation in inter- and intra-feather patterns. Although the *MC1R* gene is relatively short and has only one exon, there are abundant polymorphisms. Because none of those mutations has complete association with the E locus (Kerje et al., 2003; Guo et al., 2010; Dávila et al., 2014), each mutation on the *MC1R* gene may affect pigmentation dependent on other mutations, or on the genetic background specific to the breed of chicken. The binding of α -melanocyte stimulating hormone (α -MSH) to MC1R results in an induction of TYR and increased eumelanin synthesis (Kerje et al., 2003), while the binding of Agouti signaling protein (ASIP) to MC1R stimulates pheomelanin synthesis and inhibits eumelanin synthesis as well as melanocyte differentiation (Oribe et al., 2012). Lin et al. (2013) studied the formation of 3 other intra-feather patterns, namely arrays of offset dots, spangling, and single lacing. They observed undifferentiated melanocytes present in unpigmented regions. The modulator, which is responsible for the undifferentiation, might

be secreted from adjacent mesenchyme. They suggested ASIP as one such modulator, so that MC1R may be involved in formation of those intra-feather patterns.

A type I integral membrane protein, PMEL (also known as PMEL17), facilitates a crucial role in the premelanosomes for the normal development of eumelanosomes by restructuring stage I melanosomes into elongated and fibrillar structured stage II melanosomes (Kerje et al., 2004). In this way, eumelanosomes are elliptical and highly structured, thus allowing melanin to be deposited in an orderly fashion. Without the activity of PMEL, eumelanosomes are poorer in internal vesicles than pheomelanosomes, which is opposite from the normal situation (Lamoreux et al., 1995). This alternation of eumelanosome structure, however, has only a subtle effect on visible pigmentation (Hellström et al., 2011). In contrast, insertions or deletions of several amino acids in the PMEL transmembrane region are associated with dominant white, dun, and smoky color variants in chickens (Kerje et al., 2004).

TYR is a membrane protein integrated on the stage I premelanosomes (Chang et al., 2006). Highly activated TYR will recruit TYRP1 and TYRP2 to form the TYRP complex, which is necessary for eumelanogenesis. The initial step in melanogenesis is to transform tyrosine to dopaquinone via TYR. Dopaquinone can be transferred into pheomelanins after several chemical reactions. It also can become eumelanin: either when dopachrome is converted into 5, 6-dihydroxyindole (DHI) then complex quinone through the TYRP1 enzyme or when converted into DHI-2-carboxylic acid (DHICA) by TYRP2 and forms a complex quinone which is catalyzed by TYRP1. The complex quinone is then polymerized into eumelanin (Hearing, 2011). Neither TYRP1 nor TYRP2 are expressed in cells producing pheomelanin and the TYRP complex is not formed on

pheomelanosomes (Lamoreux et al., 1995). Although TYR has a key role in both eumelanogenesis and pheomelanogenesis, reduced tyrosinase activity affects pheomelanogenesis more than eumelanogenesis (Lamoreux et al., 2001). Mutations on the *TYR* gene have strong negative effects on pigmentation in chickens, i.e. albino (Tobita-Teramoto et al., 2000) and recessive white (Chang et al., 2006).

SLC45A2, previously denoted as membrane-associated transporter protein (MATP), acts as a sodium-proton exchanger located on the membrane of melanosomes, which together with other exchangers regulates pH inside melanosomes (Ito and Wakamatsu, 2011). SLC45A2 may have the same mechanism as sucrose transporters in plants which utilize the proton gradient to transport sucrose into the cytoplasm (Meyer et al., 2011). Active SLC45A2 can increase intramelanosomal pH which is critical for TYR activity and/or TYRP complex formation (Bin et al., 2015). Deletion of one nucleotide (106delT) on the *SLC45A2* gene results in a frameshift and a premature stop codon. This recessive null mutation can be the causal mutation of sex-linked imperfect albinism in chickens (Gunnarsson et al., 2007). Two other non-synonymous mutations (Tyr277Cys and Leu347Met) were also associated with the silver phenotype in chickens (Gunnarsson et al., 2007). This phenotype can be used in sex identification of chicks at hatch because *SLC45A2* is located on the Z chromosome.

Intra-feather patterns

Intra-feather or secondary feather patterns are color patterns that appear on individual feathers (**Figure 1.1**). Only a few of the intra-feather pattern genes (e.g. sex-linked barring and dark brown) have been mapped in chickens. Hypothetically, both of

these causal mutations affect the development and change the cell fate of melanocytes (Hellström et al., 2010; Gunnarsson et al., 2011).

Barring is a pattern that consists of horizontal white and black bars on a single feather vane, and its inheritance can be either autosomal or sex-linked (Hutt, 1949). In sex-linked barring, premature melanocyte cell differentiation in the lower bulge of the growing feather follicle leads to the formation of white bars lacking melanocytes on the feather vane. Then, new melanocytes are recruited from stem cells to produce melanin and form the next black bar. The results of such fluctuating distribution of melanocytes cause the periodically striped pigment distribution on the feather vane, which results in visible horizontal black and white barring (Lin et al., 2013). The progenitor distribution pattern in the lower bulge may be caused by gain-of-function alterations in the cyclin-dependent kinase inhibitor 2A/B (*CDKN2A/B*) tumor suppressor locus, because linkage mapping has shown that *CDKN2A/B* is the sex-linked barring gene (Hellström et al., 2010). Although sex-linked barring is probably the most studied intra-feather pattern in chickens, additional research is necessary to unravel the mechanisms of intra-feather pattern formation. Part of this reasoning is that while a single gene controls sex-linked barring (*B*), expression of most other intra-feather patterns involve multiple genes and can be affected by modifier genes.

Dark brown (*Db*), one of the genes involved in intra-feather pattern traits in chickens, restricts eumelanin distribution and enhances expression of pheomelanin in certain parts of the plumage (Moore et al., 1978). In this way, the dark brown mutation mainly affects inter-feather patterns and it is associated with the *SOX10* gene (Gunnarsson et al., 2011), which should influence the inter-feather patterns reviewed above. However, the *Db*

mutation is also necessary for single lacing and spangling (two intra-feather patterns, that will be reviewed in Chapter 4), together with pattern (*Pg*), columbian (*Co*), and melanotic (*MI*) (Carefoot, 1986, 1992). Information is lacking on how changes in *SOX10* expression influence the distribution of plumage pigments in all feather tracts and also within the vane of a single feather. The identification of genes or loci in charge of *Pg*, *Co*, and *MI* should further our understanding of how they interact during intra-feather pattern formation.

Other pigmentation processes that may relate to both inter- and intra- feather pattern formation include melanocyte migration and transferring of melanosomes from melanocytes into feather keratinocytes. Melanocytes are differentiated from melanoblasts which migrate dorsolaterally from the neural crest to their destination, which in the case of feather pigmentation, are the feather follicles in the dermal tracts (Reedy et al., 1998). Several mechanisms guarantee that melanoblasts migrate dorsolaterally: ephrin and its receptor ephrin receptor B2 (EPHB2); Slit-family proteins (Slits) and its receptor Roundabout1 (Robo1), Robo2; endothelin3 (ET3) and its receptor endothelin receptor B subtype 2 (EDNRB2). The expression of ephrin, Slits, and ET3 in the posterior of somites and in the dorsolateral pathway excludes nonmelanoblast neural crest cells. That these three receptors are expressed only in melanoblasts not only allows melanoblasts to survive in ephrin, Slits, and ET3, but to act as chemoattractants to migrate dorsolaterally (Harris and Erickson, 2007; Harris et al., 2008). Other factors present in the dorsolaterally pathway that restrict the migration of nonmelanoblasts include spondins, chondroitin sulfate proteoglycans, and PNA-binding molecules (Jia et al., 2005). Kinoshita et al. (2014) presented strong evidence that the Arg332His substitution in the

EDNRB2 gene was responsible for mottling (*mo*), an intra-feather pattern seen in some Japanese breeds of chickens. This supports the thesis that the EDNRB2 receptor is not only important for melanoblast migration, but also for melanocyte differentiation and proliferation even within the feather follicle and probably finally contributes to the formation of intra-feather patterns. Other genes involved in melanocyte migration, differentiation, and proliferation, such as *EDNRB2*, may be considered as candidate genes for feather pigment pattern formations.

The distribution of pigments in feathers can also be regulated by (1) ability of melanocyte translocations to locate matured melanosomes peripherally, (2) keratinocyte phagocytic ability to transfer melanosomes from their neighboring melanocytes, and (3) distribution and degradation of the transferred melanosomes by the recipient keratinocyte. The first step is accomplished by melanocyte cytoskeletal elements, microfilaments, and microtubules; and is regulated primarily by α -MSH (Boissy, 2003). A triprotein complex, composed of a member of the RAS oncogene family (Rab27a), melanophilin (MLPH), and myosin VA (MYOVA), is necessary to anchor melanosomes to the actin cytoskeleton and thus facilitates their transport within the melanocyte (Nascimento et al., 2003). Protease-activated receptor-2 (PAR-2) is located on the membrane of keratinocytes and its activation results in increased phagocytic activity of keratinocytes towards melanosomes. Keratinocyte growth factor and its receptor (KGF-KGFR) signaling pathway are well-known factors that regulate keratinocytes' phagocytosis via an actin-dependent mechanism (Cardinali et al., 2008). Inside keratinocytes, the translocation of melanosomes is also mediated by cytoskeletal elements and microtubule-associated motor proteins. During translocation, melanosomes may be degraded by

keratinocytes using hydrolytic enzymes (Boissy, 2003). Any modifications that occur during these processes may alter the distribution of pigments in the feather vane and contribute to intra-feather pattern formations (Prum and Williamson, 2002). For example, in chickens a single nucleotide mutation found in the *MLPH* gene is responsible for a diluted pigmentation phenotype named lavender.

It is evident that there is considerable variation in plumage color patterns in chickens. These morphological differences have fascinated poultry fanciers and breeders for thousands of years. It is only during recent decades that the mechanistic respects could be addressed via molecular methodology. In my dissertation, mapping populations were formed using backcross and F₂ matings in an effort to discover the mechanisms of morphological procedures. The next chapter describes the mating designs that were employed and results are presented in Chapters 3 - 11.

Tables and figures



Figure 1.1. Examples of intra-feather patterns. All feathers are breast feathers from hens.

References

- Bard, J. B. L. 1990. Morphogenesis: the cellular and molecular processes of developmental anatomy. Page 1. Cambridge University Press, Cambridge, United Kingdom.
- Baxter, L. L., S. K. Loftus, W. J. Pavan. 2009. Networks and pathways in pigmentation, health, and disease. Wiley Interdisciplinary Reviews: Systems Biology and Medicine. 1:359-371.
- Bin, B-H., J. Bhin, S. H. Yang, M. Shin, Y-J. Nam, D-H. Choi, D. W. Shin. A-Y. Lee, D. Hwang, E-G. Cho, T. R. Lee. 2015. Membrane-associated transporter protein (MATP) regulates melanosomal PH and influences tyrosinase activity. PLoS One. 10:e0129273.
- Boissy, R. E. 2003. Melanosome transfer to and translocation in the keratinocyte. Experimental Dermatology. 12 Supplement 2:5-12.
- Cardinali, G., G. Bolasco, N. Aspite, G. Lucania, L. V. Lotti, M. R. Torrisi, M. Picardo. 2008. Melanosome transfer promoted by keratinocyte growth factor in light and dark skin-derived keratinocytes. Journal of Investigative Dermatology. 128:558-567.
- Carefoot, W. C. 1986. Laced and double-laced plumage pattern phenotypes of the domestic fowl. British Poultry Science. 27:90-96.
- Carefoot, W. C. 1992. Inheritance of the lace-tailed laced plumage pattern of the sebright bantam. British Poultry Science. 33:297-302.
- Chang, C. M., J. L. Coville, Ge. Coquerelle, D. Gourichon, A. Oulmouden, M. Tixier-Boichard. 2006. Complete association between a retroviral insertion in the tyrosinase gene and the recessive white mutation in chickens. BMC Genomics. Doi: 10.1186/1471-2164-7-19.
- Chi, A., J. C. Valencia, Z. Z. Hu, H. Watabe, H. Yamaguchi, N. J. Mangini, H. Huang, V. A. Canfield, K. C. Cheng, F. Yang, R. Abe, S. Yamagishi, J. Shabanowitz, V. J. Hearing, C. Wu, E. Appella, D. F. Hunt. 2006. Proteomic and bioinformatic characterization of the biogenesis and function of melanosomes. Journal of Proteome Research. 5:3135-3144.
- Dávila, S. G., M. G. Gil, P. Resino-Talaván, J. L. Campo. 2014. Association between polymorphism in the melanocortin 1 receptor gene and E locus plumage color phenotype. Poultry Science. 93:1089-1096.
- Delevoeye, C., F. Giordano, G. van Niel, G. Raposo. 2011. Biogenesis of melanosomes: the chessboard of pigmentation. Medecine Sciences. 27:153-162.
- Delhey, K., C. Burger, W. Fiedler, A. Peters. 2010. Seasonal changes in colour: a comparison of structural, melanin- and carotenoid-based plumage colours. PLoS One. 5:e11582.
- Gou, X. L., X. L. Li, Y. Li, Z. L. Gu, C. S. Zheng, Z. H. Wei, J. S. Wang, R. Y. Zhou, L. H. Li, H. Q. Zheng. 2010. Genetic variation of chicken MC1R gene in different plumage colour populations. British Poultry Science. 51:734-739.
- Gunnarsson, U., A. R. Hellström, M. Tixier-Boichard, F. Minvielle, B. Bed'Hom, S. Ito, P. Jensen, A. Rattink, A. Vereijken, L. Andersson. 2007. Mutations in SLC45A2 cause plumage color variation in chicken and Japanese quail. Genetics. 175:867-877.
- Gunnarsson, U., S. Kerje, B. Bed'hom, A. S. Sahlqvist, O. Ekwall, M. Tixier-Boichard, O. Kämpe, L. Andersson. 2011. The dark brown plumage color in chickens is caused by an 8.3-kb deletion upstream of SOX10. Pigment Cell & Melanoma Research. 24:268-274.
- Harris, M. L., C. A. Erickson. 2007. Lineage specification in neural crest cell pathfinding. Developmental Dynamics. 236:1-19.
- Harris, M. L., R. Hall, C. A. Erickson. 2008. Directing pathfinding along the dorsolateral path - the role of EDNRB2 and EphB2 in overcoming inhibition. Development. 135:4113-4122.
- Hearing, V. J. 2011. Determination of melanin synthetic pathways. Journal of Investigative Dermatology. 131:E8-E11.
- Hellström, A. R., B. Watt, S. S. Fard, D. Tenza, P. Mannström, K. Narfström, B. Ekesten, S. Ito, K. Wakamatsu, J. Larsson, M. Ulfendahl, 2011. Inactivation of Pmel alters melanosome shape but has only a subtle effect on visible pigmentation. PLoS Genetics. 7:e1002285.
- Hellström, A. R., E. Sundström, U. Gunnarsson, B. Bed'Hom, M. Tixier-Boichard, C. F. Honaker, A. S. Sahlqvist, P. Jensen, O. Kämpe, P. B. Siegel, S. Kerje, L. Andersson. 2010. Sex-linked barring in chickens is controlled by the *CDKN2A/B* tumour suppressor locus. Pigment Cell & Melanoma Research. 23:521-530.
- Hutt, F. B. 1949. Genetics of the Fowl. Pages 47, 212 & 216. McCraw-Hill Book Company, New York, United States.

- Ito, S., K. Wakamatsu. 2011. Human hair melanins: what we have learned and have not learned from mouse coat color pigmentation. *Pigment Cell & Melanoma Research*. 24:63-74.
- Jia, L., L. Cheng, J. Raper. 2005. Slit/Robo signaling is necessary to confine early neural crest cells to the ventral migratory pathway in the trunk. *Developmental Biology*. 282:411-421.
- Kerje, S., J. Lind, K. Schütz, P. Jensen, L. Andersson. 2003. Melanocortin 1-receptor (MC1R) mutations are associated with plumage colour in chicken. *Animal Genetics*. 34:241-248.
- Kerje, S., P. Sharma, U. Gunnarsson, H. Kim, S. Bagchi, R. Fredriksson, K. Schütz, P. Jensen, G. V. Heijne, R. Okimoto, L. Andersson. 2004. The Dominant white, Dun and Smoky color variants in chicken are associated with insertion/deletion polymorphisms in the PMEL17 gene. *Genetics*. 168:1507-1518.
- Kinoshita, K., T. Akiyama, M. Mizutani, A. Shinomiya, A. Ishikawa, H. H. Younis, M. Tsudzuki, T. Namikawa, Y. Matsuda. 2014. Endothelin receptor B2 (EDNRB2) is responsible for the tyrosinase-independent recessive white (mo w) and mottled (mo) plumage phenotypes in the chicken. *PLoS One*. 9:e86361.
- Lamoreux, M. L., B. K. Zhou, S. Rosemlat, S. J. Orlov. 1995. The pinkeyed-dilution protein and the eumelanin/pheomelanin switch: in support of a unifying hypothesis. *Pigment Cell Research*. 8:263-270.
- Lamoreux, M. L., K. Wakamatsu, S. Ito. 2001. Interaction of major coat color gene functions in mice as studied by chemical analysis of eumelanin and pheomelanin. *Pigment Cell Research*. 14:23-31.
- Lin, S. J., J. Foley, T. X. Jiang, C. Y. Yeh, P. Wu, A. Foley, C. M. Yen, Y. C. Huang, H. C. Cheng, C. F. Chen, B. Reeder, S. H. Jee, R. B. Widelitz, C. M. Chuong. 2013. Topology of feather melanocyte progenitor niche allows complex pigment patterns to emerge. *Science*. 340:1442-1445.
- Loubéry, S., C. Delevoye, D. Louvard, G. Raposo, E. Coudrier. 2012. Myosin VI regulates actin dynamics and melanosome biogenesis. *Traffic*. 13:665-680.
- Meyer, H., O. Vitavska, H. Wiczorek. 2011. Identification of an animal sucrose transporter. *Journal of Cell Science*. 124:1984-1991.
- Moore, J. W., H. L. Classen, J. R. Smyth. 1978. Further studies on the Db plumage color locus in the Fowl. *Poultry Science*. 57:829-834.
- Nascimento, A. A., J. T. Roland, V. I. Gelfand. 2003. Pigment cells: a model for the study of organelle transport. *Annual Review of Cell and Developmental Biology*. 19:469-491.
- Oribe, E., A. Fukao, C. Yoshihara, M. Mendori, K. G. Rosal, S. Takahashi, S. Takeuchi. 2012. Conserved distal promoter of the agouti signaling protein (ASIP) gene controls sexual dichromatism in chickens. *General and Comparative Endocrinology*. 177:231-237.
- Prum, R. O., S. Williamson. 2002. Reaction-diffusion models of within-feather pigmentation patterning. *Proceedings of the Royal Society of London B: Biological Sciences*. 269:781-792.
- Reedy, M. V., C. D. Faraco, C. A. Erickson. 1998. The delayed entry of thoracic neural crest cells into the dorsolateral path is a consequence of the late emigration of melanogenic neural crest cells from the neural tube. *Developmental Biology*. 200:234-246.
- Smyth, J. R. Jr. 1990. Genetics of plumage, skin and eye pigmentation in chickens. Pages 109-110 in "Poultry Breeding and Genetics". Crawford, R. D. ed. Elsevier, Amsterdam, Netherlands.
- Tobita-Teramoto, T., G. Y. Jang, K. Kino, D. W. Salter, J. Brumbaugh, T. Akiyama, 2000. Autosomal albino chicken mutation (c^a/c^a) deletes hexanucleotide (- Δ GACTGG817) at a copper-binding site of the tyrosinase gene. *Poultry Science*. 79:46-50.
- Yu, M., P. Wu, R. B. Widelitz, C. M. Chuong. 2002. The morphogenesis of feathers. *Nature*. 420:308-312.

Chapter 2

General materials and methods

Animals

Procedures for this study were approved by the Institutional Animal Care and Use Committee at Virginia Tech. Six mapping populations were constructed to map the 8 genes shown in **Table 2.1**. Each mapping population (Cross_1, Cross_2, ... Cross_6) consisted of 2 parental populations (F_0), 1 crossbred population (F_1), 1 back cross and/or 1 F_2 population. In either the back cross or F_2 population for each mapping population, the objective was that phenotypic segregation would allow classification into groups based on their shared phenotypes. In addition, samples of 315 chickens from 85 different breeds and lines (**Table 2.2**) were used to measure associations between candidate mutations and phenotypes. Among them, samples of 57 chickens from 23 different stocks and populations of experimental lines were selected (**Table 2.3**) for individual genotyping using 600K SNP arrays. Blood samples were collected at 4 weeks of age.

Genotyping of DNA pools

After isolation of DNA from blood (following Qiagen, Puregene Tissue Core Kit B, DNA Isolation Protocol for Avian Blood, with minor modifications) for each individual, 23 samples of pooled DNA were constructed (**Table 2.4**). Each individual contributed 250 ng of DNA to a pool sample which was composed of all the DNA samples extracted from individuals within a group. Genotyping of a group was via high-density 600K chicken SNP genotyping array (by Affymetrix, 560,086 SNPs in total, used in Chapters 3, 4, 5, and 10) or high-density 60K SNP Illumina iSelect chicken array (57,636 SNPs in

total, used in Chapters 6, 7, 8, and 9). These arrays had an intensity reading for the 2 alleles (X and Y) at each SNP. The relative allelic frequencies (RAF) at each SNP for each DNA pool were calculated as $X / (X + Y)$, where X and Y represent the intensity signals at the SNP's 2 alleles. An absolute RAF difference (absRAFdif) was calculated for each SNP between the RAFs of 2 DNA pools (Wells et al., 2012) and the absRAFdif values were plotted against the SNP genomic locations (see details in **Table 2.4**).

Linkage mapping and diagnostic test

Estimated allele frequencies from microarrays using pooled samples are arbitrary because of microarray-based and pool-construction errors (Macgregor, 2007). Linkage mapping was therefore necessary to refine the localization of the target gene, especially when the absRAFdif plotting showed significant peak regions which contained multiple candidate genes. Thus, the linkage mappings described in Chapters 5, 6, 7, 8, and 9 involved genotyping each individual in a population via the Kompetitive allele-specific PCR assay (KASP) developed by LGC Genomics (Beverly, MA, USA; www.lgcgenomics.com) (Semagn et al., 2014). From the markers involved in the SNP chips used in this project, SNPs for linkage mapping were chosen from the genomic regions either within or flanking the absRAFdif peak which had relatively high absRAFdif values. Individual genotyping using KASP was also a procedure used to detect SNPs found in the *MC1R* gene for data reported in Chapters 3 and 4. The KASP assays were conducted with a mix of 2.5 μ l of KASP V4.0 2X Mastermix (LGC Genomics, Beverly, MA, US; www.lgcgenomics.com), 1.5 μ l PCR grade water, 1 μ l DNA (50 ng/ μ l), and 0.07 μ l of primers mix (12 μ M each of allele-specific primer,

carrying standard FAM or HEX compatible tails, and 32 μM of allele-flanking primer). Amplifications using 2 protocols were carried out on Bio-Rad C1000 Touch™ Thermal Cycler. The fluorescent signal was detected by a CFX384 Touch™ Real-Time PCR Detection System. PCR amplification protocol 1 (KASP-1) began at 94 °C for 15 min, 10 cycles of 94 °C for 20 s and 61 °C (-0.6 °C/cycle) for 1 min each, followed by 26 cycles of 94 °C for 20 s and 55 °C for 1 min each. KASP-2 began with 94 °C for 15 min, 10 cycles of 94 °C for 20 s and 66 °C (-0.6 °C/cycle) for 1 min each, followed by 26 cycles of 94 °C for 20 s and 57 °C for 1 min each. KASP-3 began with 94 °C for 15 min, 10 cycles of 94 °C for 20 s and 58 °C (-0.6°C/cycle) for 1 min each, followed by 26 cycles of 94 °C for 20 s and 52 °C for 1 min each. All 3 protocols ended with an endpoint fluorescence reading after 37 °C for 1 min. Readings were analyzed by Bio-Rad CFX Manager™ Software. Genotyping results for each sample were validated by at least 2 amplification runs. Details for these KASP assays are presented in **Table 2.5**. Pedigree and genotyping information from the linkage mapping results were input into CRIMAP software for analysis (Green et al., 1990) and genetic distances between each SNP and the target gene were calculated.

The candidate mutations reported in Chapters 6 and 8 were also genotyped via the same KASP assay. The samples were obtained from 310 chickens from 84 stocks and experimental lines.

Individual genotyping using 600K SNP array

Most of the 57 individuals selected for individual genotyping using the 600K SNP array had inferred genotypes of feather pattern, polydactyly, or feathered leg genes based

on their phenotypes and breeds (**Table 2.3**). Each individual sample was genotyped via a high-density 600K chicken SNP genotyping array. Results from each SNP for each individual was either AA, AB, BB (3 genotypes), or No Call. All results were analyzed using PLINK 1.07 software (Purcell et al., 2007; Author: Shaun Purcell; URL: <http://pngu.mgh.harvard.edu/purcell/plink/>). There were 3 criteria for quality control: excluding individuals with a call rate lower than 90% (PLINK commands, similarly hereinafter: --mind 0.1), excluding SNPs with a call rate lower than 90% (--geno 0.1), and excluding SNP with a minimal allele frequency less than 0.05 (--maf 0.05). After quality control, 6 models were used for association analysis: Association (--assoc), Fisher exact (--fisher), Cochran-Armitage Trend (--mode), Dominance (--model --fisher), Genotypic (--model --fisher), and Recessive (--model --fisher). For each model, a p-value was generated for each SNP to indicate the association between this SNP and the inferred genotypes within all involved individuals. All p-values were $-\log$ transformed and plotted against the SNP genomic locations.

PCR and sequencing

Polymerase chain reactions (PCR): 1 Blue and 1 Black Sumatra, 1 Blue and 1 Black Ameraucana, 1 Black Langshan, and 1 splash phenotype chickens were used to sequence *MITF*; 4 Chocolate Wyandottes and 4 Black Langshans were used to sequence *TYRP1*; 4 Mottled Houdans, 2 Mille Fleurs, and 3 Black Langshans were used to sequence *EDNRB2*; 7 B (Wild-type) chickens (See **Table 2.1**), 16 Partridge Plymouth Rocks, 16 Silver Spangled Hamburgs, and 16 Silver Sebrights were used to sequence *MC1R*. According to the *MITF*, *TYRP1*, *EDNRB2*, and *MC1R* DNA sequences of chicken

(GenBank accession numbers NC_006099.3, NC_006127.3, NC_006091.3, and NC_006098.3, respectively), 24 pairs of primers were designed by the Primer3Plus webtool (<http://www.bioinformatics.nl/cgi-bin/primer3plus/primer3plus.cgi>), to amplify and Sanger sequence the exons and UTR regions of chicken *MITF*, *TYRP1*, *EDNRB2*, and *MC1R*. Sequences of the primers are shown in **Table 2.6**. The KAPA2G Robust HotStart PCR system (Kapa Biosystems) was used with 1X KAPA2G GC Buffer, 0.2 mM dNTPs, 0.2 mM of each primer, 0.4 U of KAPA2G Robust HotStart DNA Polymerase, and 50 ng of DNA in a total volume of 10 μ l. A touchdown thermal cycling protocol was used for all the PCR of 95 °C for 5 min, 16 cycles of 95 °C for 30 s, 68 °C (-1.0 °C/cycle) for 30 s, and 72 °C for 30 s (60 s for reactions amplifying products longer than 1 kb) each, followed by 24 cycles of 95 °C for 30 s, 52 °C for 30 s, and 72 °C for 30 s (60 s for reactions amplifying products longer than 1 kb) each. Amplifications were carried out on a Bio-Rad C1000 Touch™ Thermal Cycler. PCR products were assessed by agarose gel electrophoresis.

Sequencing: PCR products were purified before sending to the Biocomplexity Institute at Virginia Tech for Sanger sequencing. Purifications were done with 1X Exonuclease I Buffer, 2 U of Exonuclease, 0.08 U of Alkaline Phosphatase, and 5.82 μ l of PCR product in a total volume of 20 μ l. An ExoSAP treatment program was used for all purifications at 37 °C for 60 min and 85 °C for 15 min. Treatment programs were carried out on Bio-Rad C1000 Touch™ Thermal Cycler. All sequences were visually edited, assembled and aligned with the SeqMan procedure of DNASTAR software (<http://www.dnastar.com>). Whole genome sequencings were conducted at Uppsala

University using individual samples (Chapters 5, 7, 9, and 10), for candidate mutation screening.

Bioinformatics analysis

An online GO (Gene Ontology) search engine (Smedley et al., 2015; www.biomart.org) was used to identify candidate genes which had a molecular function, biological process, or cellular component related to the target genes. The PROSITE webtool (Sigrist et al., 2013; <http://prosite.expasy.org/>) was used to predict the motifs on the TYRP1 protein sequence. The function-changing potential of the candidate mutation on EDNRB2 and TYRP1 was predicted by the PolyPhen webtool (Adzhubei et al., 2010; <http://genetics.bwh.harvard.edu/pph2/>), automatically giving a probability score for the mutation to be either possibly damaging or benign. The EDNRB2 mRNA secondary structure was predicted by the RNAstructure webtool (Mathews et al., 1999; <http://rna.urmc.rochester.edu/RNAstructureWeb/index.html>), giving the schematic secondary structure and the strength of each binding.

Tables and figures

Table 2.1. Details of 6 mapping populations

Population	Target Gene ¹	Number, Breed and Genotype of F ₀ Males	Number, Breed and Genotype of F ₀ Females	Number and Genotype of F ₁ Males	Number and Genotype of F ₁ Females	Number of F ₂ or Back Crosses
Cross_1	<i>Pg</i>	3 B (Wild-type) ² <i>e⁺/e⁺ pg⁺/pg⁺</i>	5 Partridge Plymouth Rock <i>e^b/e^b Pg/Pg</i>	Back cross ³	24 <i>e⁺/e^b Pg/pg⁺</i>	92 ⁴
Cross_2	<i>Co</i>	3 Silver Spangled Hamburg <i>E^R/E^R co⁺/co⁺ Db/Db Ml/Ml Pg/Pg</i>	5 Silver Sebright <i>E^R/E^R Co/Co Db/Db Ml/Ml Pg/Pg</i>	Back cross ³	22 <i>E^R/E^R Co/co⁺ Db/Db Ml/Ml Pg/Pg</i>	178
Cross_3	<i>Ml</i>	2 Partridge Plymouth Rock <i>e^b/e^b ml⁺/ml⁺ Pg/Pg</i>	4 Dark Cornish <i>e^{wh}/e^{wh} ? Ml/Ml Pg/Pg</i>	Back cross ³	17 <i>e^{wh}/e^b ? Ml⁺/ml⁺ Pg/Pg</i>	126 ⁴
Cross_4	<i>mo</i>	3 Mottled Houdan <i>mo/mo pti-1⁺/pti-1⁺ Po-2/Po-2</i>	6 Black Langshan <i>Mo⁺/Mo⁺ Pti-1/Pti-1 po-2⁺/po-2⁺</i>	Back cross ³	25 <i>Mo⁺/mo Pti-1/pti-1⁺</i>	222
	<i>Pti-1</i>			3 <i>Po-2/ po-2⁺</i>	24 <i>Po-2/ po-2⁺</i>	175
Cross_5	<i>Bl</i>	2 Black Langshan <i>bl⁺/bl⁺</i>	4 D (Splash) ² <i>Bl/Bl</i>	4 <i>Bl/bl⁺</i>	16 <i>Bl/bl⁺</i>	205
Cross_6	<i>choc</i>	3 Chocolate Wyandotte <i>choc/choc</i>	5 Black Langshan <i>Choc⁺/W</i>	5 <i>Choc⁺/choc</i>	12 <i>choc/W</i>	140

¹ *Pg*: pattern, *Co*: columbian, *Ml*: melanotic, *mo*: mottling, *Pti-1*: ptilopody-1, *Po-2*: polydactyly-2, *Bl*: blue, *choc*: chocolate

² Not a standard breed, provided by David D. Caveny. Other breeds were purchased from Murray McMurray Hatchery, except Chocolate Wyandotte, which was purchased from Greenfire Farms

³ Back cross to all the F₀ males. In other populations, F₁ were mated *inter se*

⁴ Females only

Table 2.2. Eighty-five breeds or lines used in the diagnostic tests

Breed	Plumage Color	Source	Total
A (B ^{SD}) ¹	Sex-linked Dilution	CO State University	10
A (B ^{SD}) ¹	Sex-linked Dilution	Arizona	10
Ameraucana	Black	APA Show Lucasville, OH	2
Ameraucana	Blue	APA Show Lucasville, OH	2
American Longtail	Wild-type	H & H Longtails	10
Andalusian	Blue	Marshfield, WI	1
Australorp	Black	Marshfield, WI	1
Ayam Cemani	Black	Minnesota	7
B (Wild-type)	Wild-type	CO State University	7
Brahma	Buff	Cape Fear Poultry Assoc.	2
Brahma	Dark	APA Show Lucasville, OH	1
Brahma	Light	NC State University	2
Buttercup	Buttercup	Murray McMurray	9
Buttercup	Buttercup	APA Show Lucasville, OH	10
C (Black)	Black	CO State University	8
Campine	Golden	NC State Fair	2
Chantecler	Partridge	APA Show Lucasville, OH	1
Cochin	Buff	Cape Fear Poultry Assoc.	1
Cochin	Golden Laced	APA Show Lucasville, OH	1
Cochin	Partridge	Murray McMurray	2
Cornish	Dark	Murray McMurray	10
D (Splash)	Splash	CO State University	10
D'Uccle Belgian	Mille Fleur	APA Show Lucasville, OH	2
Dorking	Silver Gray	Murray McMurray	6
Faverolles	Salmon	Murray McMurray	6
Faverolles	White	APA Show Lucasville, OH	2
Frizzle	Red	NC State Fair	1
Frizzle	White	NC State Fair	2
Hamburg	Golden Penciled	Murray McMurray	2
Hamburg	Silver Spangled	Murray McMurray	10
Hamburg	Silver Spangled	Cape Fear Poultry Assoc.	2
Houdan	Mottled	Murray McMurray	10
Houdan	Mottled	APA Show Lucasville, OH	1
Houdan	Mottled	Murray McMurray	6
Langshan	Black	Murray McMurray	2
Langshan	Black	APA Show Lucasville, OH	10
Leghorn	Black tail, Red	APA Show Lucasville, OH	2
Leghorn	Single Comb Dark Brown	NC State University	1
Leghorn	Single Comb Light Brown	NC State University	1
Leghorn	Single Comb Light Brown	APA Show Lucasville, OH	1
Leghorn	White	Virginia Tech	10
Marans	Birchen	Greenfire	3
Marans	Birchen	Virginia Tech	5
Marans	Copper	APA Show Lucasville, OH	2
Marans	Wheaten	APA Show Lucasville, OH	2
Old English	Spangled	APA Show Lucasville, OH	2
Orpington	Black	Marshfield, WI	1
Orpington	Buff	Cape Fear Poultry Assoc.	2
Orpington	Buff	APA Show Lucasville, OH	1
Phoenix	Silver	Marshfield, WI	1
Plymouth Rock	Barred	NC State University	2

Breed	Plumage Color	Source	Total
Plymouth Rock	Barred	Virginia Tech	1
Plymouth Rock	Barred	NC State University	6
Plymouth Rock	Partridge	Murray McMurray	10
Plymouth Rock	Silver Penciled	Murray McMurray	2
Polish	Buff Laced	Cape Fear Poultry Assoc.	2
Polish	White Crested Black	NC State University	1
Polish	White Crested Black	Marshfield, WI	2
Polish	White Crested Black, non-bearded	APA Show Lucasville, OH	1
Polish	White Crested Blue, non-bearded	APA Show Lucasville, OH	1
Polish	White, non-bearded	APA Show Lucasville, OH	1
Rhode Island	Red	Cape Fear Poultry Assoc.	1
Rhode Island	Red	APA Show Lucasville, OH	2
Junglefowl	Red	Richardson line	6
Sebright	Golden	Cape Fear Poultry Assoc.	1
Sebright	Golden	APA Show Lucasville, OH	2
Sebright	Silver	Murray McMurray	10
Sebright	Silver	Cape Fear Poultry Assoc.	2
Silkie	Black	NC State Fair	5
Silkie	White	NC State Fair	3
Silkie	White	NC State University	10
Silkie	White	UW-Madison	3
Spitzhauben	German	NC State University	2
Sultan	White	Cape Fear Poultry Assoc.	2
Sultan	White	NC State University	2
Sumatra	Black	APA Show Lucasville, OH	2
Sumatra	Black	NC State University	10
Sumatra	Blue	APA Show Lucasville, OH	2
Sumatra	Blue	Marshfield, WI	1
Sussex	Speckled	Cape Fear Poultry Assoc.	2
Svarthöna	Black	Uppsala University	4
Wyandotte	Chocolate	Greenfire	5
Wyandotte	Partridge	Murray McMurray	2
Wyandotte	Silver Penciled	Murray McMurray	1
Yokohama	Red Shoulder	APA Show Lucasville, OH	1
		Grand Total	315

¹ B^{SD}: Barred Sex-linked Dilution

Table 2.3. Fifty-six chicken samples for individual genotyping via 600K SNP chips¹

Breed	Variety	Pattern	n	Inferred Genotype ²					
				<i>Pg</i>	<i>Co</i>	<i>Ml</i>	<i>mo</i>	<i>Pti</i>	<i>Po</i>
Campine	Golden	Autosomal Barred	2	<i>Pg</i>	-	<i>ml</i> ⁺	<i>Mo</i> ⁺	<i>pti</i> ⁺	<i>po</i> ⁺
Leghorn	Light Brown	Stippled	1	<i>pg</i> ⁺	<i>co</i> ⁺	<i>ml</i> ⁺	<i>Mo</i> ⁺	<i>pti</i> ⁺	<i>po</i> ⁺
Leghorn	Dark Brown	Stippled	1	<i>pg</i> ⁺	<i>co</i> ⁺	<i>ml</i> ⁺	<i>Mo</i> ⁺	<i>pti</i> ⁺	<i>po</i> ⁺
Sussex	Speckled	Mottled Tri-color	2	<i>pg</i> ⁺ ?	<i>Co</i>	-	<i>mo</i>	<i>pti</i> ⁺	<i>po</i> ⁺
Brahma	Buff	Columbian	2	<i>pg</i> ⁺ ?	<i>Co</i>	-	-	<i>Pti-1</i>	<i>po</i> ⁺
Hamburg	Silver Spangled	Spangled	2	<i>Pg</i>	<i>co</i> ⁺	<i>Ml</i>	<i>Mo</i> ⁺	<i>pti</i> ⁺	<i>po</i> ⁺
Polish	Buff Laced	Single Laced	2	<i>Pg</i>	<i>Co</i>	<i>Ml</i>	<i>Mo</i> ⁺	<i>pti</i> ⁺	<i>po</i> ⁺
Cochin	Buff	No pattern	1	-	-	-	-	<i>Pti-2</i>	<i>po</i> ⁺
Orpington	Buff	No pattern	1	-	-	-	-	<i>pti</i> ⁺	<i>po</i> ⁺
Sebright	Golden	Single Laced	2	<i>Pg</i>	<i>Co</i>	<i>Ml</i>	<i>Mo</i> ⁺	<i>pti</i> ⁺	<i>po</i> ⁺
Sebright	Silver	Single Laced	2	<i>Pg</i>	<i>Co</i>	<i>Ml</i>	<i>Mo</i> ⁺	<i>pti</i> ⁺	<i>po</i> ⁺
Brahma	Light	Columbian	2	<i>pg</i> ⁺ ?	<i>Co</i>	-	-	<i>Pti-1</i>	<i>po</i> ⁺
Hamburg	Golden Penciled	Autosomal Barred	2	<i>Pg</i>	-	<i>ml</i> ⁺	<i>Mo</i> ⁺	<i>pti</i> ⁺	<i>po</i> ⁺
Cochin	Partridge	Concentric Pencilled	2	<i>Pg</i>	<i>co</i> ⁺	<i>ml</i> ⁺	<i>Mo</i> ⁺	<i>Pti-2</i>	<i>po</i> ⁺
Wyandotte	Silver Penciled	Concentric Pencilled	2	<i>Pg</i>	<i>co</i> ⁺	<i>ml</i> ⁺	<i>Mo</i> ⁺	<i>pti</i> ⁺	<i>po</i> ⁺
Plymouth Rock	Silver Penciled	Concentric Pencilled	2	<i>Pg</i>	<i>co</i> ⁺	<i>ml</i> ⁺	<i>Mo</i> ⁺	<i>pti</i> ⁺	<i>po</i> ⁺
Wyandotte	Partridge	Concentric Pencilled	1	<i>Pg</i>	<i>co</i> ⁺	<i>ml</i> ⁺	<i>Mo</i> ⁺	<i>pti</i> ⁺	<i>po</i> ⁺
Faverolles	Salmon	Stippled or Laced	5	-	<i>co</i> ⁺	-	-	<i>Pti-1</i>	<i>Po-2</i>
Dorking	Silver Gray	Stippled	6	<i>pg</i> ⁺	<i>co</i> ⁺	<i>ml</i> ⁺	<i>Mo</i> ⁺	<i>pti</i> ⁺	<i>Po-2</i>
Houdan	Mottled	Mottled	5	<i>pg</i> ⁺ ?	<i>co</i> ⁺	-	<i>mo</i>	<i>pti</i> ⁺	<i>Po-2</i>
Faverolles		Stippled or Laced	4	-	-	-	-	<i>Pti-1</i>	<i>Po-2</i>
Sultan	White	No pattern	6	-	-	-	-	<i>Pti-2</i>	<i>Po-1</i>
Silkie	Black	No pattern	2	-	-	-	-	<i>Pti-2</i>	<i>Po-1</i>
		Grand Total	57						

¹ High-density 600K chicken SNP genotyping array (by Affymetrix, 560,086 SNPs in total)

² *Pg*: pattern, *Co*: columbian, *Ml*: melanotic, *mo*: mottling, *Po-2*: polydactyly-2, *Pti-1*: ptilopody-1; “-”

indicates that the SNP genotyping results of this sample was not used in this data analysis because of an unknown genotype of this target gene

Table 2.4. Groups in back cross and F₂

Population ¹	Group in Back Cross or F ₂	Number	Phenotype	Expecting Genotype ²	DNA Pool	abdRAFdif Result
Cross_1	Group 1_1	27	Pencilling	<i>Pg/pg</i> ⁺	Pool 1_1	Figure 3
	Group 1_2	29	Stippling	<i>pg</i> ⁺ / <i>pg</i> ⁺	Pool 1_2	
	Group 1_3	23	Intermediate	?	Pool 1_3	-
	Group 1_4	13	Non-pattern	?	Pool 1_4	
Cross_2	Group 2_1	77	Lacing	<i>Co/co</i> ⁺	Pool 2_1	Figure 4
	Group 2_2	81	Spangling	<i>co</i> ⁺ / <i>co</i> ⁺	Pool 2_2	
	Group 2_3	20	Intermediate	?	Pool 2_3	-
Cross_3	Group 3_1	43	Double Lacing	<i>MI/ml</i> ⁺	Pool 3_1	Figure 5.1, 5.2
	Group 3_2	60	Pencilling	<i>ml</i> ⁺ / <i>ml</i> ⁺	Pool 3_2	
	Group 3_3	23	Intermediate	?	Pool 3_3	-
Cross_4	Group 4_1	108	Black	<i>MI</i> ⁺ / <i>mo</i>	Pool 4_1	Figure 6.1, 6.2
	Group 4_2	113	Mottling	<i>mo/mo</i>	Pool 4_2	
	Group 4_3	100	Feathered leg	<i>Pti-1/pti-1</i> ⁺	Pool 4_3	Figure 1 ³
	Group 4_4	82	Clean-leg	<i>pti-1</i> ⁺ / <i>pti-1</i> ⁺	Pool 4_4	
	Group 4_5	108	Polydactyly	<i>Po-2/</i>	Pool 4_5	Figure 8.1, 8.2
	Group 4_6	67	4 toes	<i>po-2</i> ⁺ / <i>po-2</i> ⁺	Pool 4_6	
Cross_5	Group 5_1	104	Blue	<i>Bl/bl</i> ⁺	Pool 5_1	-
	Group 5_2	38	Splash	<i>Bl/Bl</i>	Pool 5_2	Figure 9.1, 9.2
	Group 5_3	63	Black	<i>bl</i> ⁺ / <i>bl</i> ⁺	Pool 5_3	
Cross_6	Group 6_1	45	Black Male	<i>Choc</i> ⁺ / <i>choc</i>	Pool 6_1	-
	Group 6_2	29	Chocolate Male	<i>choc/choc</i>	Pool 6_2	
	Group 6_3	32	Black Female	<i>Choc</i> ⁺ / <i>W</i>	Pool 6_3	Figure 1 ⁴
	Group 6_4	34	Chocolate Female	<i>choc/W</i>	Pool 6_4	

¹ Corresponds with **Table 2.1**

² *Pg*: pattern, *Co*: columbian, *MI*: melanotic, *mo*: mottling, *Pti-1*: ptilopody-1, *Po-2*: polydactyly-2, *Bl*: blue, *choc*: chocolate

³ Figure title followed the paper “Feathered-leg in chickens is associated with a SNP on chromosome 15 and a region on chromosome 12” which is submitted to Animal Genetics.

⁴ Figure title followed the paper “A missense mutation in TYRP1 causes the Chocolate plumage color in chicken and alters melanosome structure” which is submitted to Pigment Cell & Melanoma Research.

Table 2.5. SNPs used in linkage mapping of individual analysis

Target Gene ¹	SNP	absRAFdif ²	Chromosome	Position (bp)	KASP Protocol	Genetic Distance from the Target Gene (cM) ³
<i>Ml</i>	rs313722403	0.417	1	86,460,521	KASP-1	15.8
	rs316117302	0.496	1	89,274,893	KASP-1	3.9
	rs314066698	0.489	1	91,633,144	KASP-1	1.9
	rs314825166	0.447	1	93,227,649	KASP-2	2.9
	rs13908401	0.409	1	96,648,937	KASP-1	8.7
	rs317883641	0.367	1	100,530,188	KASP-1	10.7
<i>mo</i>	rs14424110	0.386	4	6,902,583	KASP-3	9.5
	rs314222717	0.382	4	8,362,322	KASP-1	7.6
	rs315977835	0.403	4	9,637,573	KASP-1	4.0
	rs16360752	0.437	4	10,757,507	KASP-1	2.2
	rs313943998	-	4	11,216,160	KASP-2	0.0
	rs317734713	0.369	4	11,654,812	KASP-1	2.7
	rs316670962	0.349	4	12,599,648	KASP-1	8.8
	rs14430948	0.344	4	13,361,011	KASP-1	9.6
rs14433304	0.326	4	15,532,449	KASP-2	13.5	
<i>Pti-1</i>	rs13528978	0.358	15	10784395	KASP-3	7.9
	rs14096198	0.417	15	11721706	KASP-1	1.1
	rs316054667	0.427	15	12316957	KASP-2	0.0
	rs14096597	0.445	15	12515894	KASP-1	0.0
	rs15787779	0.274	15	12695726	KASP-1	0.0
<i>Bl</i>	rs14081238	0.668	1	1453101	KASP-1	4.2
	rs15185947	0.784	1	2889499	KASP-1	2.0
	rs13823450	0.812	1	3538398	KASP-1	0.5
	rs13827504	0.763	1	4171054	KASP-1	0
	rs13827135	0.794	1	4662337	KASP-1	1.0
	rs13621783	0.774	1	5569798	KASP-1	1.5
	rs16756550	0.688	1	6732356	KASP-1	3.0
<i>choc</i>	rs316461371	0.563	Z	24,320,139	KASP-2	10.2
	rs16106682	0.476	Z	28,269,887	KASP-1	1.0
	rs16080645	0.641	Z	30,154,038	KASP-1	0.0
	rs14687394	0.704	Z	30,485,550	KASP-2	0.0
	TYRP1_CANDIDATE	-	Z	30,830,367	KASP-1	0.0
	rs14778077	0.580	Z	31,836,731	KASP-2	5.7
	rs14762884	0.642	Z	32,081,991	KASP-1	5.7
	rs312841286	0.592	Z	33,347,891	KASP-1	7.2
	rs14764310	0.408	Z	35,683,084	KASP-2	15.8
rs14765167	0.261	Z	37,190,373	KASP-2	18.7	
<i>MC1R</i>	rs314881228	-	11	2409000	KASP-1	-
	rs315815196	-	11	2409560	KASP-1	-

¹ *Ml*: melanotic, *mo*: mottling, *Bl*: blue, *choc*: chocolate, *Pti-1*: ptilopody-1

² Corresponding the absRAFdif shown in **Figure 5.2, 6.2, 9.2,** and **Figure 1** in Chapter 7 and 10.

³ Calculated using the CRIMAP software

Table 2.6. PCR primers for Sanger sequencing

Target Element	Primer Name ¹	Primer Sequence (5'-3')	Product Size (bp)
<i>MC1R</i>	MC1R_F1	CTTTGTAGGTGCTGCAGTTGTG	1049
	MC1R_R1	ATCCATCCATCCTCCTGTCTGT	
<i>EDNRB2</i> exon 1	E_E1_F	GATGGCAGCAAGACCCTTTAGT	1321
	E_E1_R	CCTCCAAAATCTCCATCAGACC	
<i>EDNRB2</i> exon 2	E_E2_F	GCAGAAGAGATTGTGTGGGATG	1046
	E_E2_R	ATCATCGGAGTGGGTTCTGTTT	
<i>EDNRB2</i> exon 3	E_E3_F1	AGACTCCCAAACAAGCAGGAAG	1384
	E_E3_R1	ATAGACATTGATGGGCAGAGCA	
	E_E3_F2	AGACCAAGACCCAAGCAAAGA	780
<i>EDNRB2</i> exon 4 & 5	E_E3_R2*	TCTGGATGTGTGTGTGCGTAA	991
	E_E4&5_F*	GCTGCTCTTTGTGGGCTTCT	
<i>EDNRB2</i> exon 6	E_E4&5_R	CCCATTGCTGTGTCTTCC	1107 or 982 ²
	E_E6_F*	GGGAGTGGTGTCTTTGAATGT	
<i>EDNRB2</i> exon 7 & 8	E_E6_R	TCTGCCCTTCTGCTATGTTT	686
	E_E7&8_F	CACGAGAAGAGGGTGTCTTTG	
<i>EDNRB2</i> exon 9	E_E7&8_R*	TACCTGATGCCTGCCTTCC	645
	E_E9_F*	TTCATTTCCAAGCCACACCA	
<i>MITF</i> 5'-UTR	E_E9_R	TTTCTACCCATCTCCTCACC	1548
	M_5' F1	ACTTGAAATTGCTGTGCTGGAA	
	M_5' R	TGCACCCTTCATGTCTTTCCT	
<i>MITF</i> exon 1	M_5' F2†	CCCAGCTCGTACTTTTCCAC	-
	M_E1_F	GTTGATGGCTCTTGAATGTTGC	804
M_E1_R*	TATTTCCCCACATCCCTACTG		
<i>MITF</i> exon 1 (Specific to melanocyte)	M_M1_F	TCAGCACCTTGAAATCCTTCTG	765
	M_M1_R*	ATGTCCCCATTCAATTTTGTG	
<i>MITF</i> exon 2	M_E2_F	GTGTAAACTGGAAAGCCCAAGC	810
	M_E2_R*	TTCCTGTGTGCATCAAGCAAG	
<i>MITF</i> exon 3	M_E3_F*	GGACTGAGACTGTGCCATGAAC	546
	M_E3_R	TCACAGACGGATTAAGCAGTTT	
<i>MITF</i> exon 4	M_E4_F*	GGATAGTGGGATTGGATTTGGA	764
	M_E4_R	AGTTGCAGACAACAGGTTTGGGA	
<i>MITF</i> exon 5	M_E5_F*	TCAAGTGAGCTGTGCTTCCTTT	768
	M_E5_R	AGCCTCACCATGCAGTATTCT	
<i>MITF</i> exon 6 & 7	M_E6&7_F	ACGTAGGGGAAGGTATGTTGGA	1467
	M_E6&7_R	TAATGGAAGTTCTCCCCAAAG	
<i>MITF</i> exon 8	M_E8_F	TTTTGCTGTTGTTGCACAGAGA	805
	M_E8_R*	CTGCTTTGTGGATTAGCTGTGG	
<i>MITF</i> exon 9	M_E9_1_F	TTTTCCAGCTCTTTCAGTGTG	1427
	M_E9_1_R	CAAAAGGAAAACCCAAATCAGC	
	M_E9_2_F	AAACCACTCCGTTCCATTGAGA	797
	M_E9_2_R	CGCCAGTGCTGAAATAAAACAC	
	M_E9_3_F	ATTCTGATTTGCATGGGTTCT	
M_E9_3_R	AGACCCCAAAGCACTACCACAG	1182	
<i>TYRP1</i> 5'-UTR	T_5' F*	ACGTCGGAGTGTTC AATTTCT	916
	T_5' R	TACAAACCTCCAGTCCAGTCT	
<i>TYRP1</i> exon 1	T_E1_F*	TCTGGGAAGTCTTAGATGTCA	746
	T_E1_R	AAATCAACATGCCAACAGACAG	

Target Element	Primer Name ¹	Primer Sequence (5'-3')	Product Size (bp)
<i>TYRP1</i> exon 2	T_E2_F	CATTCAAAGGGCTGAATAAGG	717
	T_E2_R*	TGAAATTGAAGCAAAATTTCAATG	
<i>TYRP1</i> exon 3	T_E3_F*	ACCGCTGTTGTGAGGCTTTT	934
	T_E3_R	CTCCGCTCCTGGAGACATTC	
<i>TYRP1</i> exon 4	T_E4_F*	TGTGCAAAGGACTAGCACACA	909
	T_E4_R	ATCCTTCAGCACATCCAGCA	
<i>TYRP1</i> exon 5	T_E5_F*	AAACGTAACGGCTGGCAAAT	996
	T_E5_R	AGGATGTGCAAGGCAACTGA	
<i>TYRP1</i> exon 6 & 7	T_E6&7_F	GACCTTTGACGCTGTTGCAG	1597
	T_E6&7_R	CCAGCACAAATGGAAGCACAT	

¹ Primers with * are used in PCR only, primer with † are used in sequencing only, all other primers are used for both PCR and sequencing.

² Variation of product size was caused by an indel mutation

References

- Adzhubei, I. A., S. Schmidt, L. Peshkin, V. E. Ramensky, A. Gerasimova, P. Bork, A. S. Kondrashov, S. R. Sunyaev. 2010. A method and server for predicting damaging missense mutations. *Nature Methods*. 7:248-249.
- Green P, K. Falls, S. Crooks. 1990. Documentation for CRIMAP, version 2.4. Washington University School of Medicine, St Louis, MO.
- Macgregor, S. 2007. Most pooling variation in array-based DNA pooling is attributable to array error rather than pool construction error. *European Journal of Human Genetics*. 15:501-504.
- Mathews, D. H., J. Sabina, M. Zuker, D. H. Turner. 1999. A perspective on mammalian upstream open reading frame function. *Journal of Molecular Biology*. 288:911-940.
- Purcell, S., B. Neale, K. Todd-Brown, L. Thomas, M. A. Ferreira, D. Bender, J. Maller, P. Sklar, P. I. De Bakker, M. J. Daly, P. C. Sham. 2007. PLINK: a tool set for whole-genome association and population-based linkage analyses. *The American Journal of Human Genetics*. 81:559-575.
- Semagn K., R. Babu, S. Hearne, M. Olsen. 2014. Single nucleotide polymorphism genotyping using Kompetitive Allele Specific PCR (KASP): overview of the technology and its application in crop improvement. *Molecular Breeding*. 33:1-14.
- Sigrist, C.J., E. De Castro, L. Cerutti, B. A. Cuche, N. Hulo, A. Bridge, L. Bougueleret, I. Xenarios, 2013. New and continuing developments at PROSITE. *Nucleic Acids Research*. D344-7.
- Smedley, D., S. Haider, S. Durinck, L. Pandini, P. Provero, J. Allen, O. Arnaiz, M. H. Awedh, R. Baldock, G. Barbiera, P. Bardou, T. Beck, A. Blake, M. Bonierbale, A. J. Brookes, G. Bucci, I. Buetti, S. Burge, C. Cabau, J. W. Carlson, C. Chelala, C. Chrysostomou, D. Cittaro, O. Collin, R. Cordova, R. J. Cutts, E. Dassi, A. D. Genova, A. Djari, A. Esposito, H. Estrella, E. Eyra, J. Fernandez-Banet, S. Forbes, R. C. Free, T. Fujisawa, E. Gadaleta, J. M. Garcia-Manteiga, D. Goodstein, K. Gray, J. A. Guerra-Assunção, B. Haggarty, D. J. Han, B. W. Han, T. Harris, J. Harshbarger, R. K. Hastings, R. D. Hayes, C. Hoede, S. Hu, Z. L. Hu, L. Hutchins, Z. Kan, H. Kawaji, A. Keliet, A. Kerhornou, S. Kim, R. Kinsella, C. Klopp, L. Kong, D. Lawson, D. Lazarevic, J. H. Lee, T. Letellier, C. Y. Li, P. Lio, C. J. Liu, J. Luo, A. Maass, J. Mariette, T. Maurel, S. Merella, A. M. Mohamed, F. Moreews, I. Nabihoudine, N. Ndegwa, C. Noirrot, C. Perez-Llomas, M. Primig, A. Quattrone, H. Quesneville, D. Rambaldi, J. Reecy, M. Riba, S. Rosanoff, A. A. Saddiq, E. Salas, O. Sallou, R. Shepherd, R. Simon, L. Sperling, W. Spooner, D. M. Staines, D. Steinbach, K. Stone, E. Stupka, J. W. Teague, A. Z. Dayem Ullah, J. Wang, D. Ware, M. Wong-Erasmus, K. Youens-Clark, A. Zadissa, S. J. Zhang, A. Kasprzyk. 2015. The BioMart community portal: an innovative alternative to large, centralized data repositories. *Nucleic Acids Research*. 43:W589-W598.
- Wells, K. L., Y. Hadad, D. Ben-Avraham, J. Hillel, A. Cahaner, D. J. Headon. 2012. Genome-wide SNP scan of pooled DNA reveals nonsense mutation in FGF20 in the scaleless line of featherless chickens. *BMC Genomics*. Doi: 10.1186/1471-2164-13-25.

Chapter 3

Pattern (*Pg*) gene mapping

Abstract

The pattern (*Pg*) gene, located on chromosome 1 in chickens, is involved in the expression of multiple intra-feather patterns. In an attempt to identify the genomic region associated with *Pg*, a mapping population was constructed by crossing Partridge Plymouth Rock females with wild-type plumage color males and backcrossing the F₁ females to the F₀ male. Unfortunately, there was an insufficient number of individuals in the backcross population that expressed clear pencilling or stippling intra-feather patterns necessary for determining the associated genomic region.

Introduction

The pattern (*Pg*) gene (Carefoot, 1985) can interact with other genes or loci that result in different intra-feather patterns including pencilling, autosomal barring (Carefoot, 2002), single lacing (Carefoot, 1987a), double lacing (Smyth, 1990), and spangling (Carefoot, 1992) phenotypes (**Figure 1.1**). Although referred to as autosomal barring (*Ab* or *Bg*) or lacing (*Lg*) by Hutt (1949) and Kimball (1959), they were subsequently shown to be the same as *Pg* (Carefoot, 1986a, 1986b). *Pg* was previously called the penciling gene, because this mutant allele could change stippling (dots of black pigment evenly distributed on the background color, wild type pattern) into pencilling (concentric rings wholly contained within the feather) when in the background of e^b (Carefoot, 1985). The pencilling pattern in Partridge Plymouth Rock chickens results from an interaction between e^b and *Pg* and is expressed only in females (Smyth, 1965).

Linkage relationships between the following genes and loci have been estimated to be *Pg*--10--*Ml*--10--*Db*--28--*P* (*P* for pea comb, numbers are in unit of cM) (Carefoot, 1987b, 1987c, 1990). After the mapping of *Db* (51 Mb in Chromosome 1) (Gunnarsson et al., 2011) and *P* (66 Mb in Chromosome 1) (Wright et al., 2009), the physical positions of *Pg* and *Ml* were estimated as 41.9 Mb and 46.5 Mb in Chromosome 1, respectively. The objective of this experiment was to map *Pg* by segregating stippling and pencilling intra-feather patterns in a backcross population.

Materials and methods

Details of the mating used in this Chapter are shown in **Table 2.1** (Cross_1). Briefly 2 B (Wild-type) males were mated to 5 Partridge Plymouth Rock females to produce 24 F₁ females that when backcrossed to the F₀ males produced 92 female progeny. When 12 weeks of age, the stippling and pencilling patterns of these 92 females were observed and classified by the same individual. In the backcross population, only females were classified and considered in the analysis because intra-feather patterns are not observed in males. Individual DNA samples were isolated from blood, and then pooled into 4 pooled DNA samples (**Table 2.4**). Genotyping of pooled samples was via high-density 600K chicken SNP genotyping arrays. Values of absRAFDif were calculated by comparing each pair of pooled samples. Individual samples were genotyped via the same arrays. The association between each SNP and the inferred genotypes were calculated by PLINK. Genotypes were inferred in 2 ways: 1. “*pg*⁺?” individuals (see **Table 2.3**) were not included in the analysis, which although a more confident way for determining the inferred genotypes reduced sample size; 2. “*pg*⁺?” individuals were considered as “*pg*⁺”

genotypes, which while less confident increased sample size. The *MC1R* gene was sequenced (**Table 2.6**) in the parental lines of the mapping population. See details in Chapter 2.

Results and discussion

SNP mapping

Clear stippling or pencilling phenotypes were observed in 29 and 27 of the 92 backcross females, respectively. The remaining 36 females were assigned to either intermediate (n = 23) or non-pattern (n = 13) groups based on their plumage patterns. No obvious peak region was found when comparing stippling and pencilling groups (**Figure 3**), which was the same as for comparing other groups (e.g. non-pattern and pencilling groups, data not shown). The reasons could be an insufficient number of individuals and/or that the 2 genotypes (Pg/pg^+ and pg^+/pg^+) did not separate clearly into pencilling and stippling groups.

In both ways of analyzing individual genotyping data (more and less confident ways), lacking was a significant genomic region showing an association with the inferred *Pg* genotypes (data not shown). The reasons could be different genetic backgrounds among involved individuals and/or insufficient sample size.

Identification of modifier genes

Modifier genes, other than *Pg*, segregating in the backcross population could influence the phenotypic expression of stippling and pencilling patterns. The most likely modifier gene was the *E* locus (Carefoot, 1986b), because independent of *Pg*, genotypes e^+/e^b and e^+/e^+ should also segregate in the backcross population (see **Table 2.1**). Thus,

the *MC1R* gene (*E* locus, by Kerje et al., 2003) was sequenced (see Chapter 2) and a second possible modifier, *Db*, was genotyped (following the assay described by Gunnarsson et al., 2011) in the founders of the mapping population. That all founders were fixed for the db^+ allele, while B (Wild-type) was fixed for the e^+ allele and Partridge Plymouth Rocks were fixed for the e^b allele (Ling et al., 2003; Kerje et al., 2003; Dávila et al., 2014) consistent with the expectation (Smyth, 1965). Thus, it is necessary to know the presence of e^b in each backcross female to more accurately infer *Pg* genotypes and then to increase the sample sizes of stippling and pencilling pools.

The G274A mutation in *MC1R* (rs314881228, corresponding to the amino acid change Glu92Lys) was chosen for genotyping via KASP (see Chapter 2) to differentiate between e^+ and e^b alleles in the 92 backcross females. Among them, there were 48 with e^+/e^+ and 44 with e^+/e^b which matched the expected 1:1 ($p = 0.68$). The frequencies of e^+/e^b in previous stippling, partridge, intermediate, and non-pattern groups (0.276, 0.667, 0.391, and 0.692, respectively) showed a genotypic effect ($p < 0.01$) of the *E* locus on these feather patterns. Although such frequencies in stippling and partridge groups were different ($p < 0.01$), no peak region was found containing the *MC1R* gene when comparing these 2 groups (**Figure 3**). This suggests that within the 600K SNPs involved in the microarray, lacking is SNP linked with the *MC1R* gene. Thus, the power to detect the genes associated with *Pg* might be decreased with the similar reason. Based on **Figure 3**, genes within the genomic regions that contain SNPs with $absRAF_{dif}$ greater than 0.5 were listed in **Table 3**, which could be the candidate genes. Most of them are expected to be false positively associated because of the sample sizes (29 stippling and 27 pencilling individuals). Meanwhile, at least 2 of them are associated with melanoma

(*PTPRT* and *KIT*, reported by Scott and Wang in 2011 and Yang et al. in 2012, respectively) and thus may be involved in melanogenesis. It was hypothesized that females showing stippling phenotypes with e^+/e^+ genotypes (n = 21) should be homozygous for pg^+ . However, it remains difficult to infer the existence of the *Pg* allele in other individuals (data not shown). One reason for the difficulty of phenotypic classification may be a leaking effect between and *Pg* and pg^+ as well as e^+ and e^b . Little is known about the effect of these two heterozygotes. Until *Pg* genotypes can be inferred more accurately, it is not feasible to map the *Pg* gene.

Tables and figures

Table 3. Genes within the genomic regions that contain SNPs with absRAFdif greater than 0.5 when comparing stippling and partridge groups

Gene	Title	Chromosome	Position (Mb)
<i>EIF2S3L</i>	Putative eukaryotic translation initiation factor 2 subunit 3-like protein	1	118.2
<i>KLHL15</i>	kelch-like family member 15	1	118.2
<i>SATI</i>	spermidine/spermine N1-acetyltransferase 1	1	118.3
<i>ACOT9</i>	acyl-CoA thioesterase 9	1	118.3
<i>MYD88</i>	myeloid differentiation primary response 88	2	4.8
<i>XIRP1</i>	xin actin-binding repeat containing 1	2	5.0
<i>GORASP1</i>	golgi reassembly stacking protein 1, 65kDa	2	5.3
<i>WDR48</i>	WD repeat domain 48	2	5.3
<i>ACVR2B</i>	activin A receptor, type IIB	2	5.8
<i>NUB1</i>	negative regulator of ubiquitin-like proteins 1	2	6.2
<i>PRKAG2</i>	protein kinase, AMP-activated, gamma 2 non-catalytic subunit	2	6.4
<i>INSIG1</i>	insulin induced gene 1	2	7.9
<i>EN2</i>	engrailed homeobox 2	2	7.9
<i>SHH</i>	sonic hedgehog	2	8.1
<i>LMBR1</i>	limb development membrane protein 1	2	8.5
<i>MNX1</i>	motor neuron and pancreas homeobox 1	2	8.6
<i>UBE3C</i>	ubiquitin protein ligase E3C	2	8.6
<i>DNAJB6</i>	DnaJ (Hsp40) homolog, subfamily B, member 6	2	8.7
<i>VIPR2</i>	vasoactive intestinal peptide receptor 2	2	9.7
<i>GTPBP4</i>	GTP binding protein 4	2	10.4
<i>HIBADH</i>	3-hydroxyisobutyrate dehydrogenase	2	32.9
<i>TAX1BP1</i>	Tax1 (human T-cell leukemia virus type 1) binding protein 1	2	33.0
<i>JAZF1</i>	JAZF zinc finger 1	2	33.1
<i>KLHL4</i>	kelch like family member 4	4	8.1

Gene	Title	Chromosome	Position (Mb)
<i>NFKB1</i>	nuclear factor of kappa light polypeptide gene enhancer in B-cells 1	4	61.2
<i>UBE2D3</i>	ubiquitin-conjugating enzyme E2D 3	4	61.3
<i>PDLIM3</i>	PDZ and LIM domain 3	4	61.5
<i>TLR3</i>	toll-like receptor 3	4	61.7
<i>CYP4V2</i>	cytochrome P450, family 4, subfamily V, polypeptide 2	4	61.7
<i>ASAHI</i>	N-acylsphingosine amidohydrolase (acid ceramidase) 1	4	63.2
<i>PCMI</i>	pericentriolar material 1	4	63.2
<i>FGL1</i>	fibrinogen-like 1	4	63.3
<i>SLC7A2</i>	solute carrier family 7 (cationic amino acid transporter, y ⁺ system), member 2	4	63.4
<i>FET1</i>	female expressed transcript 1	4	63.5
<i>CNOT7</i>	CCR4-NOT transcription complex, subunit 7	4	63.6
<i>PAICS</i>	phosphoribosylaminoimidazole carboxylase, phosphoribosylaminoimidazole succinocarboxamide synthetase	4	65.1
<i>PPAT</i>	phosphoribosyl pyrophosphate amidotransferase	4	65.2
<i>NMU</i>	neuromedin U	4	65.5
<i>CLOCK</i>	clock circadian regulator	4	65.5
<i>KDR</i>	kinase insert domain receptor (a type III receptor tyrosine kinase)	4	65.6
<i>KIT</i>	v-kit Hardy-Zuckerman 4 feline sarcoma viral oncogene homolog	4	65.7
<i>PDGFRA</i>	platelet-derived growth factor receptor, alpha polypeptide	4	65.8
<i>SGCB</i>	sarcoglycan, beta (43kDa dystrophin-associated glycoprotein)	4	66.6
<i>TEC</i>	tec protein tyrosine kinase	4	66.9
<i>CNGA1</i>	cyclic nucleotide gated channel alpha 1	4	67.0
<i>YIPF7</i>	Yip1 domain family, member 7	4	68.1
<i>NELFA</i>	negative elongation factor complex member A	4	83.8
<i>PITX1</i>	paired-like homeodomain 1	13	15.7
<i>PCBD2</i>	pterin-4 alpha-carbinolamine dehydratase/dimerization cofactor of hepatocyte nuclear factor 1 alpha (TCF1) 2	13	15.7
<i>CAMLG</i>	calcium modulating ligand	13	15.8
<i>TRPC4AP</i>	transient receptor potential cation channel, subfamily C, member 4 associated protein	20	2.7
<i>PTPRT</i>	protein tyrosine phosphatase, receptor type T	20	3.2
<i>DFFB</i>	DNA fragmentation factor, 40kDa, beta polypeptide (caspase-activated DNase)	21	0.9
<i>HES5</i>	hes family bHLH transcription factor 5	21	1.4
<i>PGD</i>	phosphogluconate dehydrogenase	21	3.7
<i>APITD1</i>	apoptosis-inducing, TAF9-like domain 1	21	3.7
<i>BARX2</i>	BARX homeobox 2	24	1.3
<i>AC005943.2</i>	Cytochrome b-c1 complex subunit 10	28	2.4
<i>MBD3</i>	methyl-CpG binding domain protein 3	28	2.5
<i>ATP8B1</i>	ATPase, class I, type 8B, member 1	Z	0.3
<i>LOX</i>	lysyl oxidase	Z	81.0

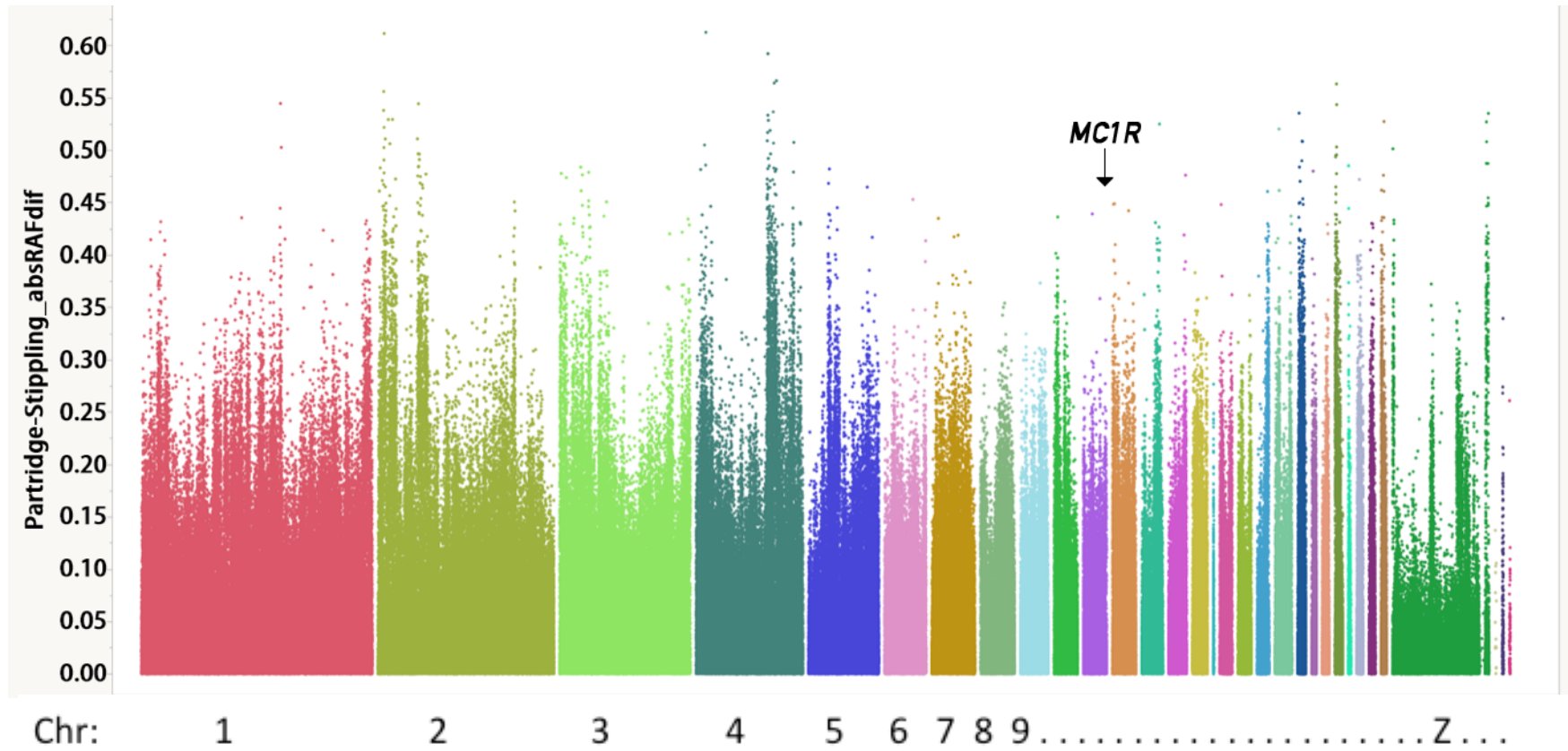


Figure 3. Genome-wide absRAFdif values, for *Pg* mapping. Calculated by contrasting Pools 1_1 and 1_2 of all 600K SNPs, plotted against the genomic location.

The position of the *MC1R* gene is labeled.

References

- Carefoot, W. C. 1985. Effect of the eumelanin restrictor Db on plumage pattern phenotypes of the domestic fowl. *British Poultry Science*. 26:409-412.
- Carefoot, W. C. 1986a. Laced and double-laced plumage pattern phenotypes of the domestic fowl. *British Poultry Science*. 27:90-96.
- Carefoot, W. C. 1986b. Pencilled and double-laced plumage pattern phenotypes in the domestic fowl. *British Poultry Science*. 27:431-433.
- Carefoot, W. C. 1987a. Inheritance of the plumage pattern of the double-laced Barnevelder bantam. *British Poultry Science*. 28:173-175.
- Carefoot, W.C. 1987b. Test for linkage between the eumelanin restrictor (Db) and the eumelanin extension (Ml) genes in the domestic fowl. *British Poultry Science*. 28:69-73.
- Carefoot, W. C. 1987c. Relative positions of the loci of the peacomb (P), eumelanin restrictor (Db), eumelanin extension (Ml) and plumage pattern (Pg) genes of the domestic fowl. *British Poultry Science*. 28:347-350.
- Carefoot, W. C. 1990. Test for linkage between the Eumelanin dilution blue (Bl), the extended black (E) allele at the e - locus and the linked pea comb (p) and eumelanin extension (Ml) genes in the domestic fowl. *British Poultry Science*. 31:465-472.
- Carefoot, W. C. 1992. Inheritance of the lace-tailed laced plumage pattern of the sebright bantam. *British Poultry Science*. 33:297-302.
- Carefoot, W. C. 2002. Hen-feathering mutation HF*H may act as a eumelanising factor and modify the expression of autosomal barring. *British Poultry Science*. 43:391-394.
- Dávila, S. G., M. G. Gil, P. Resino-Talaván, J. L. Campo, 2014. Association between polymorphism in the melanocortin 1 receptor gene and E locus plumage color phenotype. *Poultry Science*. 93:1089-1096.
- Gunnarsson, U., S. Kerje, B. Bed'hom, A. S. Sahlqvist, O. Ekwall, M. Tixier-Boichard, O. Kämpe, L. Andersson. 2011. The dark brown plumage color in chickens is caused by an 8.3-kb deletion upstream of SOX10. *Pigment Cell & Melanoma Research*. 24:268-274.
- Hutt, F. B. 1949. *Genetics of the Fowl*. Pages 47, 212 & 216. McCraw-Hill Book Company, New York, United States.
- Kerje, S., J. Lind, K. Schütz, P. Jensen, L. Andersson. 2003. Melanocortin 1-receptor (MC1R) mutations are associated with plumage colour in chicken. *Animal Genetics*. 34:241-248.
- Kimball, E. 1959. Barred Hamburg plumage pattern. *Poultry Science*. 38:224-225.
- Ling, M. K., M. C. Lagerström, R. Fredriksson, R. Okimoto, N. I. Mundy, S. Takeuchi, H. B. Schiöth. 2003. Association of feather colour with constitutively active melanocortin 1 receptors in chicken. *European Journal of Biochemistry*. 270:1441-1449.
- Scott, A., Z. Wang. 2011. Tumour suppressor function of protein tyrosine phosphatase receptor-T. *Bioscience Reports*. 31:303-307.
- Smyth, J. R. Jr. 1965. Allelic relationship of genes determining extended black, wild type and brown plumage patterns in the fowl. *Poultry Science*. 44:89-98.
- Smyth, J. R. Jr. 1990. Genetics of plumage, skin and eye pigmentation in chickens. Page 127 in "Poultry Breeding and Genetics". Crawford, R. D. ed. Elsevier, Amsterdam, Netherlands.
- Wright, D., H. Boije, J. R. Meadows, B. Bed'hom, D. Gourichon, A. Vieaud, M. Tixier-Boichard, C. J. Rubin, F. Inslund, F. Hallböök, L. Andersson. 2009. Copy number variation in intron 1 of SOX5 causes the Pea-comb phenotype in chickens. *PLoS Genetics*. 5:e1000512.
- Yang, P., Z. Yu, J. A. Gandahi, X. Bian, L. Wu, Y. Liu, L. Zhang, Q. Zhang, Q. Chen. 2012. The identification of c-Kit-positive cells in the intestine of chicken. *Poultry Science*. 91:2264-2269.

Chapter 4

Columbian (*Co*) gene mapping

Abstract

Chickens homozygous for the Columbian gene (*Co*) phenotypically exhibit the columbian distribution of eumelanin with e^+ , e^b or e^{Wh} alleles on the *E* locus. The presence of *Co* is responsible for differences in intra-feather patterns between Silver Sebright and Silver Spangled Hamburg. A mapping population was constructed in an attempt to identify the genomic region associated with *Co* by crossing Silver Spangled Hamburg males to Silver Sebright females and then backcrossing the F_1 to Hamburg males. Unfortunately, such a genomic region was not found. The reason being that the backcross lacked individuals that exhibited either clear single lacing or spangling intra-feather patterns which, in turn, precluded locating the associated genomic region.

Introduction

The columbian plumage pattern in chickens is one in which eumelanin is restricted to the hackle, wing, and tail feathers (American Poultry Association, 1910). This phenotype could be the result of a mutant allele *Co* when in the presence of e^+ , e^b or e^{Wh} (Smyth and Some, 1965). The mutant is an autosomal partial dominant that effectively inhibits eumelanin in males more than females (Some and Smyth, 1965). In addition to its effects on eumelanin, *Co* also changes the color of pheomelanin to an orange-gold or ginger (Campo and Orozco, 1984). The phenotypic expression of *Co* in down is extremely variable and influenced by the presence of other genes, mostly *E* alleles (Smyth, 1990; Campo, 1997).

For intra-feather patterns, *Co* is involved in the formations of single lacing (Carefoot, 1987), speckling (Smyth, 1990), and mille fleur (Somes, 1980). Single lacing consists of an outer ring of eumelanin that conforms to the edge of the feather (Carefoot, 1992) (**Figure 1.1**), while speckling and mille fleur are characterized by a white tip, followed by a V-shaped black band, with the rest of the feather being buff or red-brown (Somes, 1980). Crossbreeding experiments have shown that the single lacing feather pattern of Silver Sebright bantams is a combination of E^R , *Co*, *Db*, *Ml* and *Pg*. The spangling pattern (a V-shaped eumelanin spangle located at the distal end of the feather, see **Figure 1.1**) of Silver Spangled Hamburgs is due to the same combination with co^+ rather than *Co* (Carefoot, 1992). To my knowledge, linkage mapping results on *Co* are lacking. The objective of this experiment was to attempt to map *Co*.

Materials and methods

A mapping population was founded by mating 3 Silver Spangled Hamburg males with 5 Silver Sebright females. The 22 F₁ females were then backcrossed to the F₀ males to produce 178 backcross progeny. See details in **Table 2.1** (Cross_2). Phenotypes of the backcrosses (breast, covert, secondary, saddle feathers, and the general degree of eumelanination) were classified at 12 and 18 weeks by the same individual. Individual DNA samples were isolated from blood, and then pooled into 3 pooled DNA samples (**Table 2.4**). Genotyping of pooled samples was via high-density 600K chicken SNP genotyping arrays. Values for absRAFDif were calculated by comparing each pair of pooled samples. Individual samples (**Table 2.3**) were genotyped via the same arrays. The association between each SNP and the inferred genotypes were calculated by PLINK.

The *MC1R* gene was sequenced in the parental lines of the mapping population (**Table 2.6**). See details in Chapter 2.

Results and discussion

SNP mapping

At 12 and 18 weeks, of the 178 backcross progeny, only 5 and 11 individuals showed clear single lacing or spangling phenotypes, respectively, through their plumage across all feather tracts. These numbers were not sufficient for gene mapping. Thus, individuals with most of their feathers (breast, covert, secondary, and saddle feathers) showing clear phenotypes were also included in DNA pools (Pool 2_1, i.e. the lacing pool, $n = 77$; Pool 2_2, i.e. the spangling pool, $n = 81$. see **Table 2.4**) for SNP mapping. Because the phenotyping was not fully accurate, possibly reducing the power to detect the association, no obvious peak was observed (**Figure 4**).

A significantly associated genomic region was also lacking after the analysis of individual genotypes (data not shown). The reasons could be different genetic backgrounds among involved individuals and/or small sample size.

Identification of modifier genes

That *Co* is a partial dominant may be one of the reasons that lacing phenotypes were not obvious in the *Co/co*⁺ backcross individuals. Other than *Co*, modifier genes including *E*^R, *Db*, *Ml* and *Pg* are required for standard single lacing and spangling patterns (Carefoot, 1992). Thus, the questionable phenotypes observed in the backcross population may be due to the absence of those alleles. Among them, the DNA sequences responsible for *E* locus and *Db* were reported (Kerje et al., 2003; Gunnarsson et al., 2011).

Therefore, the *MC1R* gene (*E* locus, by Kerje et al., 2003) was sequenced (see Chapter 2) and the *Db* gene was genotyped (following the assay described by Gunnarsson et al., 2011) in the founders of this mapping population.

All founders were fixed for the *Db* allele, a result consistent with the expectation. Thus, the backcross population should have been fixed for *Db* which should not have a negative effect on the expression of either clear single lacing or spangling patterns. However, one synonymous mutation C843T (rs315815196) in *MC1R* was different in Silver Spangled Hamburgs and Silver Sebrights. The Hamburgs were fixed for C alleles whereas 2 of the founder Sebrights were heterozygotes and the other 3 were T allele homozygotes. That this mutation was not fixed in Sebrights, is synonymous and found in both *E* and *e^{bc}* alleles (Dávila et al., 2014), should not influence the function of MC1R. However, this mutation was the only polymorphism observed in the known modifier genes in the founders. As expected, only 2 genotypes of this mutation were detected in the backcross population via a KASP assay (see Chapter 2), which were homozygotes of the C allele and heterozygotes. The percentages of homozygous C in lacing feathers were higher than other patterns in 2 types of wing feathers, i.e. covert feathers (71.2% in lacing group, 53.9% in spangling group, and 31.5% in intermediate group, $p < 0.01$) and secondary feathers (100.0% in lacing group, 79.0% in double lacing group, 54.8% in barring group, and 25.0% in spangling group, $p < 0.01$). This effect may be caused by a regulatory change in *MC1R* or in a closely linked gene.

Sequences of the *MC1R* gene showed that Hamburg and Sebright breeds shared 3 non-synonymous mutations (G274A, G376A, and T637C, that corresponded to amino acid changes Glu92Lys, Val126Ile, and Cys213Arg) and 1 synonymous mutation

(G636A). Glu92Lys was associated with E , E^R , and e^b alleles (Ling et al., 2003; Dávila et al., 2014). Although Val126Ile is found in the E allele (Kerje et al., 2003; Dávila et al., 2014), its presence does not exclude the possibility of other alleles. The presence of Cys213Arg in e^+ , E , e^b , and e^v (Ling et al., 2003; Kerje et al., 2003; Dávila et al., 2014) suggests that it has minor phenotypic effects. Sequencing data showed that the alleles of the E locus in Hamburg and Sebright chickens could be either E , E^R , or e^b and do not conflict with the report by Carefoot (1992) that the E^R allele is present in these breeds.

After comparing the known genotypes of modifier genes with the phenotypic data, it remains difficult to infer the existence of the Co allele in each individual (data not shown). Further analysis to map the Co gene cannot be applied until the Co genotypes can be inferred more accurately.

Tables and figures

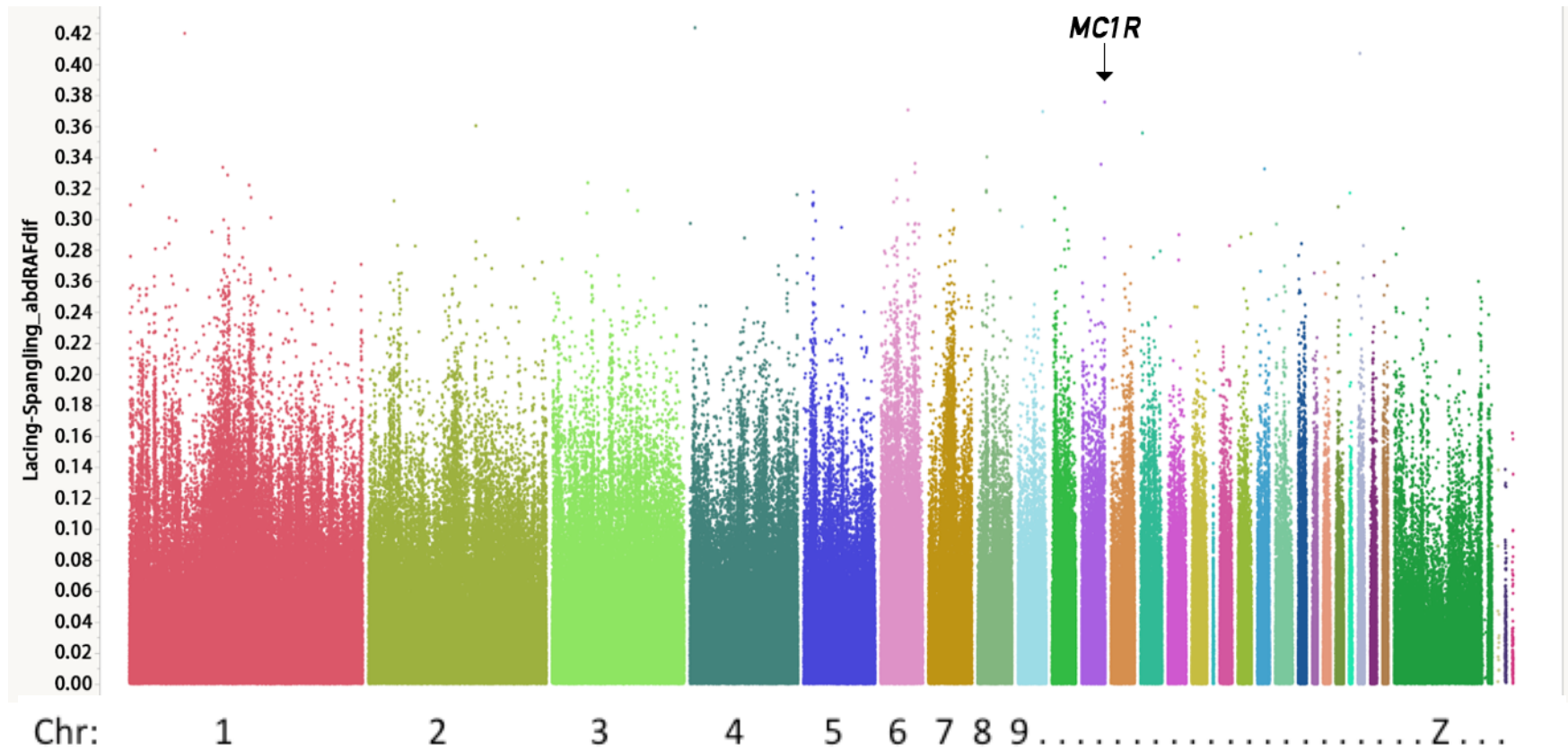


Figure 4. Genome-wide absRAFdif values, for *Co* mapping. Calculated by contrasting Pools 2_1 and 2_2 of all 600K SNPs, plotted against the genomic location.

The position of the *MC1R* gene is labeled.

References

- American Poultry Association. 1910. Pages 56 & 84 in The American Standard of Perfection. Davenport, IA, USA.
- Campo, J. L. 1997. The hypostatic genotype of the recessive White Prat breed of chickens. *Poultry Science*. 76:432-436.
- Campo, J. L., F. Orozco. 1984. A genetic study of the buff columbian color pattern in Prat chickens. *Journal of Heredity*. 75:19-22.
- Carefoot, W. C. 1987. Inheritance of the plumage pattern of the double-laced Barnevelder bantam. *British Poultry Science*. 28:173-175.
- Carefoot, W. C. 1992. Inheritance of the lace-tailed laced plumage pattern of the sebright bantam. *British Poultry Science*. 33:297-302.
- Dávila, S. G., M. G. Gil, P. Resino-Talaván, J. L. Campo, 2014. Association between polymorphism in the melanocortin 1 receptor gene and E locus plumage color phenotype. *Poultry Science*. 93:1089-1096.
- Gunnarsson, U., S. Kerje, B. Bed'hom, A. S. Sahlqvist, O. Ekwall, M. Tixier-Boichard, O. Kämpe, L. Andersson. 2011. The dark brown plumage color in chickens is caused by an 8.3-kb deletion upstream of SOX10. *Pigment Cell & Melanoma Research*. 24:268-274.
- Kerje, S., J. Lind, K. Schütz, P. Jensen, L. Andersson. 2003. Melanocortin 1 - receptor (MC1R) mutations are associated with plumage colour in chicken. *Animal Genetics*. 34:241-248.
- Ling, M. K., M. C. Lagerström, R. Fredriksson, R. Okimoto, N. I. Mundy, S. Takeuchi, H. B. Schiöth. 2003. Association of feather colour with constitutively active melanocortin 1 receptors in chicken. *European Journal of Biochemistry*. 270:1441-1449.
- Smyth, J. R. Jr., R. G. Somes Jr. 1965. A new gene determining the columbian feather pattern. *Journal of Heredity*. 56:151-156.
- Somes, R. G. Jr. 1980. The mottling gene, the basis of six plumage color patterns in the domestic fowl. *Poultry Science*. 59:1370-1374.
- Smyth, J. R. Jr. 1990. Genetics of plumage, skin and eye pigmentation in chickens. Pages 120-121 & 127 in "Poultry Breeding and Genetics". Crawford, R. D. ed. Elsevier, Amsterdam, Netherlands.
- Somes, R. G. Jr, J. R. Smyth Jr. 1965. Feather phaeomelanin intensity in buff orpington, New Hampshire and Rhode Island Red breeds of fowl 1. Age, sex and feather growth effects. *Poultry Science*. 44:40-46.

Chapter 5

Melanotic (*MI*) gene mapping

Abstract

Melanotic (*MI*) is a plumage mutation in chickens that extends black (eumelanin) in normally brown or red (pheomelanin) areas, resulting in multiple intra-feather patterns. In an attempt to identify the genomic region associated with *MI*, a mapping population was constructed by crossing Partridge Plymouth Rock males with Dark Cornish females and backcrossing the F₁ females with the F₀ male. A strong association between a 1.6 Mb region on chromosome 1 and the *MI* gene was identified by SNP analyses of pooled samples followed by linkage mapping. Further investigations are needed to identify the causal mutation.

Introduction

There are other genetic factors, in addition to the *E* and *E^R* alleles, that enhance feather eumelanization (Smyth, 1990). Among them, only melanotic (*MI*), an incompletely dominant autosomal mutation that extends eumelanin into the normally pheomelanin areas, appears to have been established (Moore and Smyth, 1971a). Since its identification, *MI* has been shown to have important roles in numerous intra-feather patterns, for example, single lacing (an outer ring of eumelanin that conforms to the edge of the feather, Moore and Smyth, 1971b) and double lacing (2 concentric eumelanic rings on a background pigmentation, that the outer ring conforms to the outer edge of the feather whilst the inner ring is separated from the outer by a ring of background pigmentation) (Carefoot, 1986a, 1986b, 2001) and spangling which is a V-shaped

eumelanic spangle located at the distal end of the feather (Carefoot, 1992) (**Figure 1.1**). Dark Cornish (Indian Game) is a standard breed with a typical double lacing pattern expressed in females. This plumage pattern is caused by e^{Wh} , MI , and Pg (Carefoot, 1986b), while other Dark Cornish populations could be e^v (Morejohn, 1955) or e^+ (Kimball, 1955). Also, e^b can cause a double lacing pattern when found with MI and Pg (Carefoot, 1986a, 1987a). As reviewed in Chapter 3, based on linkage and mapping results, an estimated physical position of MI was 46.5 Mb in Chromosome 1 (Carefoot, 1987b, 1987c. 1990; Gunnarsson et al., 2011; Wright et al., 2009).

Materials and methods

Details of matings used in this Chapter are shown in **Table 2.1** (Cross_3). Briefly 2 Partridge Plymouth Rock males were mated to 4 Dark Cornish females to produce 17 F_1 females that were then backcrossed to the F_0 males to produce 126 female progeny. Only females were considered in the analysis of the backcross population because pencilling and double lacing patterns are not observed in males. At 12 weeks of age, chickens with pencilling and double lacing patterns in the backcross population were classified by the same individual. Individual DNA samples were isolated from blood, and then combined into 3 pooled DNA samples (**Table 2.4**). Genotyping of pooled samples was via high-density 600K chicken SNP genotyping arrays. Values of absRAFdif were calculated by comparing each pair of pooled samples. Individual samples (**Table 2.3**) were genotyped via the same arrays. The associations between each SNP and the inferred genotypes were calculated by PLINK. Linkage mapping was conducted by genotyping 6 SNPs in the whole mapping population via KASP assays (**Table 2.5**). See details in Chapter 2.

Results and discussion

SNP mapping

Clear pencilling or double lacing patterns phenotypes were observed in 60 and 43 backcross females, respectively. The remaining 23 backcross females were assigned to an intermediate group.

One obvious peak in chromosome 1 (**Figure 5.1**) was observed when comparing the pencilling and double lacing groups. SNPs located within the 31.8 Mb region (blue boxed area in **Figure 5.2**) suggest the location of the *MI* mutation and linkage mapping showed that the causal mutation lies between rs314066698 (91.63 Mb) and rs314825166 (93.23 Mb) (red boxed area in **Figure 5.2**). See details of linkage mapping results in **Table 2.5**. Although no candidate gene showed a strong relationship to the plumage color within this region, *ROBO1* and *ROBO2* genes (located at 95.90 – 96.60 and 96.89 - 97.81 Mb, respectively) appear to be the only pigmentation related genes that were close to the candidate region. As reviewed in Chapter 1, Slits and its receptor Robo1, Robo2 guarantee that neural crest cells migrate dorsolaterally. More specifically, in the chicken embryo, receptor Robo1 is expressed in the closing neural tube and proximal somites while Robo2 is expressed more peripherally (Giovannone et al., 2012). Thus, Robo2 may influence melanoblasts even after the migration and settling into the feather follicles which contributes to intra-feather patterns.

Comparisons of absRAFDif between pencilling and double lacing groups (**Figure 5.1, 5.2**) revealed trends similar to those between intermediate and double lacing groups (data not shown), with the former showing a more significant candidate region. No significant candidate region, however, was found for comparisons between intermediate

and pencilling groups. The explanation could be that, as expected, a double lacing group is formed only by individuals with the Ml/ml^+ genotype; because of phenotyping errors, both pencilling and intermediate groups contain individuals with Ml/ml^+ and ml^+/ml^+ genotypes. This can also explain why the observed number of double lacing backcross individuals ($n = 43$) was less than the expected number of Ml/ml^+ individuals i.e. some Ml/ml^+ individuals may have been assigned to the pencilling and intermediate groups. This hypothesis was confirmed in part by linkage mapping where 9 backcross individuals showed double recombination of SNP markers which should not occur in a backcross mating. Therefore, these 9 individuals should be the results of phenotyping errors and thus previously assigned to the pencilling group. Namely, the previous pencilling group was formed by 51 ml^+/ml^+ and 9 Ml/ml^+ individuals while the double lacing group was formed by 43 Ml/ml^+ individuals only. The incomplete dominance of the Ml gene (Moore and Smyth, 1971a) and other gene modifiers might have had negative effects on the expression of double lacing in backcross individuals and thus contributed to phenotyping errors.

A significant associated genomic region was lacking after the analysis of individual genotypes (data not shown). The reasons could be due to different genetic backgrounds among involved individuals and/or insufficient sample size.

The next step is to apply whole genome sequencing using individual samples from the F_0 and backcross populations. The above candidate region will be the focus when reading the sequencing data. The objective is to locate candidate mutations for further investigation.

Pooled genotyping errors

In this study, the initial screening for linkage mapping involved pooled DNA samples. This provided another example of successful identification of genomic regions that are associated with phenotypes using pooled samples. However, there were considerable differences when comparing the estimated allele frequencies from array-based DNA pooling with the those calculated from individual genotyping. The former were about 0.09 higher than the latter when calculated by the average difference of the 6 SNPs used in linkage mapping (data not shown). The differences could result from pool construction error and/or array-based error (Macgregor, 2007). When genotyping individual heterozygotes, the array-based allele frequencies will not always be 0.5 because of differential intensity signals from the two dyes on the microarray (Kirov et al., 2009). Probe-specific correction (PPC) methods have been developed to adjust the array-based allele frequencies (Anantharaman and Chew, 2009). One simple and popular PPC is the k -correction method: calculating RAF as $X / (X + k_i Y)$ instead of $X / (X + Y)$, where k_i is derived from differential intensity signals for each SNP on microarrays (Butcher et al., 2005). I did not use the k -correction method because Meaburn et al. (2005) reported that although k -correction was needed to compare allelic frequency estimates from pooled DNA and individual genotyping, it was not necessary for comparisons between cases and controls. This was confirmed here where the genomic region that was associated with phenotypes was successfully identified although there was considerable error in the associated $\text{absRAF}_{\text{dif}}$ values.

Tables and figures

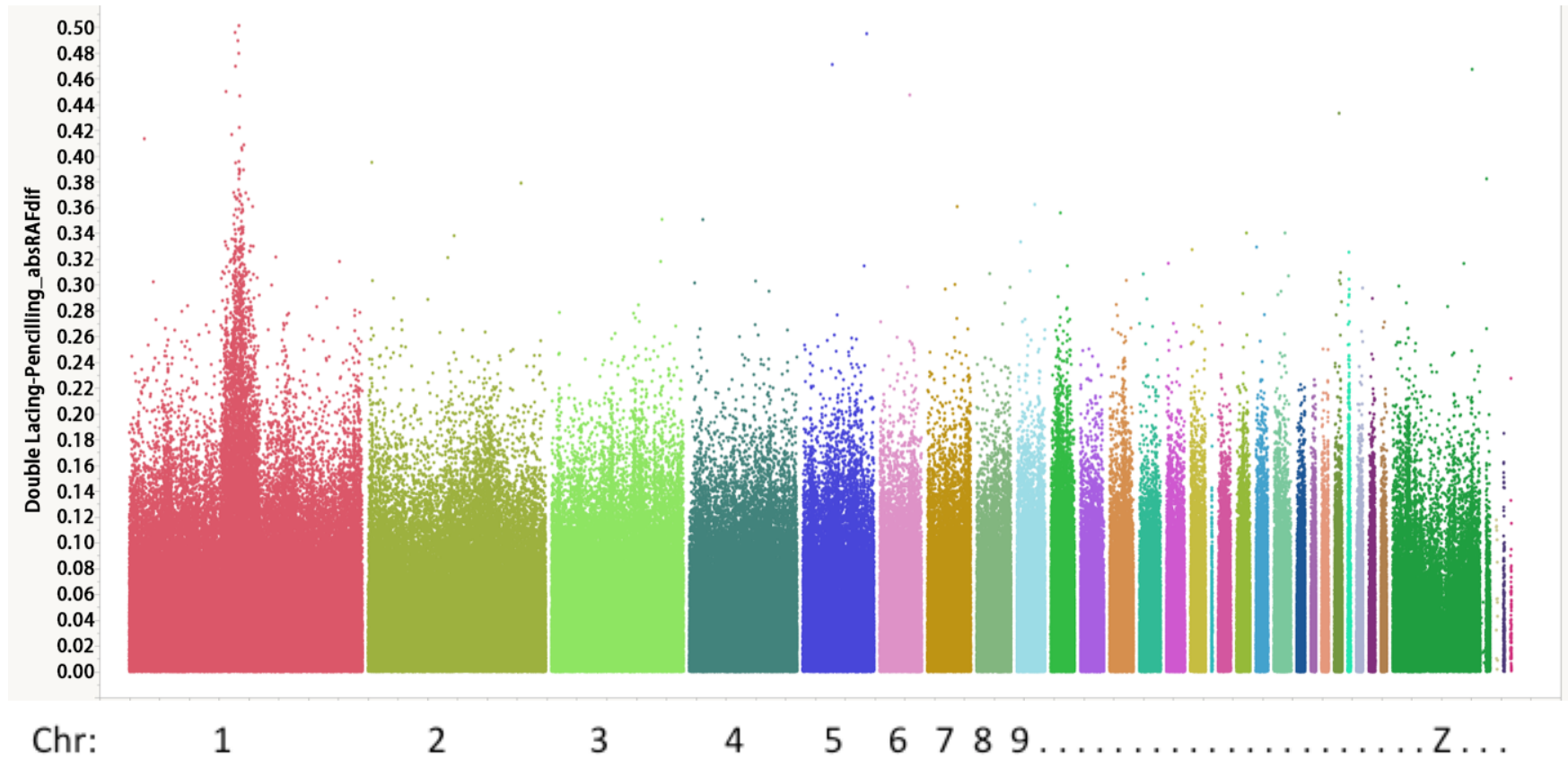


Figure 5.1. Genome-wide absRAFDif values, for *MI* mapping. Calculated by contrasting Pools 3_1 and 3_2 of all 600K SNPs, plotted against the genomic location.

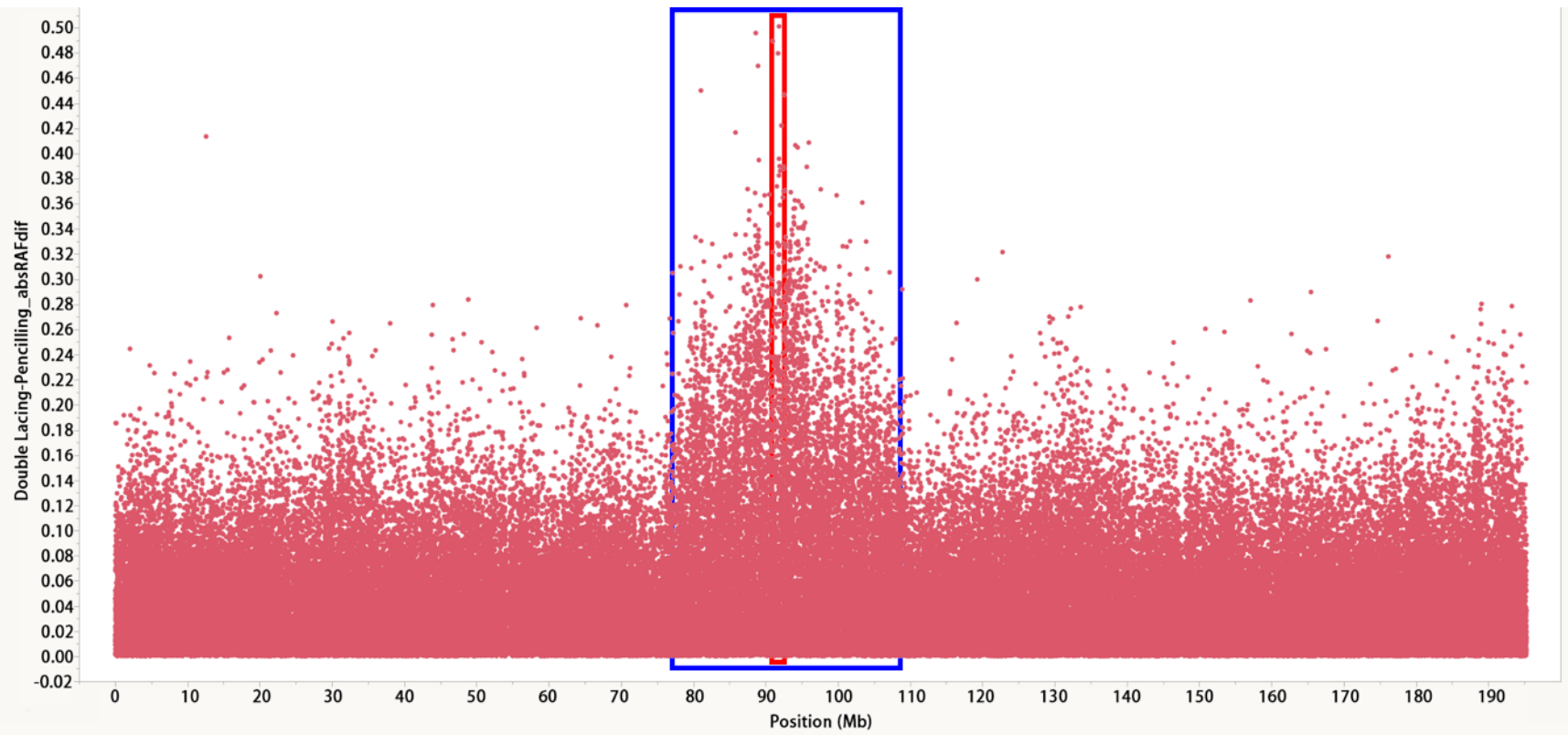


Figure 5.2. The absRAFdif values of SNPs on chromosome 1, for *MI* mapping. Calculated by contrasting Pools 3_1 and 3_2, plotted against the genomic location. SNPs located within the 31.8 Mb region (blue boxed area) gave absRAFdif values above 0.30. Red boxed area indicates the 1.6 Mb linkage mapping region, suggesting the location of the *MI* mutation.

References

- Anantharaman, R., F. T. Chew. 2009. Validation of pooled genotyping on the Affymetrix 500 k and SNP6. 0 genotyping platforms using the polynomial-based probe-specific correction. *BMC Genetics*. Doi: 10.1186/1471-2156-10-82.
- Butcher, L. M., E. Meaburn, P. S. Dale, P. Sham, L. C. Schalkwyk, I. W. Craig, R. Plomin. 2005. Association analysis of mild mental impairment using DNA pooling to screen 432 brain-expressed single-nucleotide polymorphisms. *Molecular Psychiatry*. 10:384-392.
- Carefoot, W. C. 1986a. Laced and double-laced plumage pattern phenotypes of the domestic fowl. *British Poultry Science*. 27:90-96.
- Carefoot, W. C. 1986b. Pencilled and double-laced plumage pattern phenotypes in the domestic fowl. *British Poultry Science*. 27:431-433.
- Carefoot, W. C. 1987a. Inheritance of the plumage pattern of the double-laced Barnevelder bantam. *British Poultry Science*. 28:173-175.
- Carefoot, W. C. 1987c. Relative positions of the loci of the peacomb (P), eumelanin restrictor (Db), eumelanin extension (Ml) and plumage pattern (Pg) genes of the domestic fowl. *British Poultry Science*. 28:347-350.
- Carefoot, W. C. 1990. Test for linkage between the Eumelanin dilution blue (Bl), the extended black (E) allele at the e - locus and the linked pea comb (p) and eumelanin extension (Ml) genes in the domestic fowl. *British Poultry Science*. 31:465-472.
- Carefoot, W. C. 1992. Inheritance of the lace-tailed laced plumage pattern of the Sebright bantam. *British Poultry Science*. 33:297-302.
- Carefoot, W. C. 2001. Inheritance of the black hackle of the Indian Game bantam. *British Poultry Science*. 42:274-275.
- Carefoot, W.C. 1987b. Test for linkage between the eumelanin restrictor (Db) and the eumelanin extension (Ml) genes in the domestic fowl. *British Poultry Science*. 28: pp.69-73.
- Giovannone, D., M. Reyes, R. Reyes, L. Correa, D. Martinez, H. Ra, G. Gomez, J. Kaiser, L. Ma, M. P. Stein, M. E. de Bellard. 2012. Slits affect the timely migration of neural crest cells via Robo receptor. *Developmental Dynamics*. 241:1274-1288.
- Gunnarsson, U., S. Kerje, B. Bed'hom, A. S. Sahlqvist, O. Ekwall, M. Tixier-Boichard, O. Kämpe, L. Andersson. 2011. The dark brown plumage color in chickens is caused by an 8.3-kb deletion upstream of SOX10. *Pigment Cell & Melanoma Research*. 24:268-274.
- Kimball, E. 1955. Dark cornish plumage pattern: a preliminary report. *Poultry Science*. 34:818-821.
- Kirov, G., I. Zaharieva, L. Georgieva, V. Moskvina, I. Nikolov, S. Cichon, A. Hillmer, D. Toncheva, M. J. Owen, M. C. O'Donovan. 2009. A genome-wide association study in 574 schizophrenia trios using DNA pooling. *Molecular Psychiatry*. 14:796-803.
- Macgregor, S. 2007. Most pooling variation in array-based DNA pooling is attributable to array error rather than pool construction error. *European Journal of Human Genetics*. 15:501-504.
- Meaburn, E., L. M. Butcher, L. Liu, C. Fernandes, V. Hansen, A. Al-Chalabi, R. Plomin, I. Craig, L. C. Schalkwyk. 2005. Genotyping DNA pools on microarrays: tackling the QTL problem of large samples and large numbers of SNPs. *BMC Genomics*. Doi: 10.1186/1471-2164-6-52.
- Moore, J. W., J. R. Smyth Jr. 1971a. Melanotic: key to a phenotypic enigma in the fowl. *Journal of Heredity*. 62:215-219.
- Moore, J. W., J. R. Smyth Jr. 1971b. Inheritance of the silver-laced Wyandotte plumage pattern. *The Journal of Heredity*, 63:179-184.
- Morejohn, G. V. 1955. Plumage color allelism in the red jungle fowl (*Gallus Gallus*) and related domestic forms. *Genetics*. 40:519-530.
- Smyth, J. R. Jr. 1990. Genetics of plumage, skin and eye pigmentation in chickens. Page 118 in "Poultry breeding and genetics". Crawford, R. D. ed. Elsevier, Amsterdam, Netherlands.
- Wright, D., H. Boije, J. R. Meadows, B. Bed'hom, D. Gourichon, A. Vieaud, M. Tixier-Boichard, C. J. Rubin, F. Imsland, F. Hallböök, L. Andersson. 2009. Copy number variation in intron 1 of SOX5 causes the Pea-comb phenotype in chickens. *PLoS Genetics*. 5:e1000512.

Chapter 6

Mottling (*mo*) gene mapping

Abstract

Mottling is an intra-feather pattern seen in chickens throughout the world. In a previous study, adopting a comparative-candidate-gene strategy, an amino acid substitution Arg332His in the *EDNRB2* gene was identified as responsible for the mottling phenotype seen in several Japanese breeds of chickens. Here, however, evidence is provided to show that this was not the causal mutation for mottling plumage in Mottled Houdan, a breed that originated in France. A strong association between the *EDNRB2* gene and the mottling phenotype was identified by construction of a mapping population and SNP analyses of pooled samples followed by linkage mapping. The mutation in the population studied here was the result of an amino acid change of Ala228Thr in *EDNRB2*. Together, this one with the one reported in Japanese breeds, provides an example of two different mutations resulting in a similar phenotype.

Introduction

Mottling is a common intra-feather pattern in which black feathers have white tips (Somes, 1980) (**Figure 1.1**). This single recessive gene (*mo*) described by Asmundson and Milne (1930) is also involved in the formation of tricolored patterns, such as spangling in Old English, speckling, and mille fleur, which suggests two actions of the *mo* gene on adult plumage color (Somes, 1980). First, to inhibit the pigmentation to cause the white tip, then as a eumelanin inducer to produce a V-shaped eumelanin band after the white tip. The remainder of the feather vane has the background color without the

effect of *mo*. Second, the feather pattern is tricolored when the background color is not black. When black, the V-shaped black band will not be obvious with only the white tip standing out (Somes, 1980). Because *mo* produces the V-shaped eumelanin band even when other eumelanin dilution genes are present, (e^+ , e^b , e^v , and *Co*), but not *lav* (lavender) (Somes, 1980), suggests that while it may be affected by *lav*, the molecular pathway involved in *mo* may be relatively independent from the *E* locus and *Co*.

The interactions between *mo* and *E* locus are complicated. The shape and distribution of white tips in each feather caused by *mo* is not uniform and mottling appears on approximately one of every 2 to 5 feathers (Asmundson and Milne, 1930), or one of every 2 to 3 feathers (Somes, 1980). Apparently, selection for additional mottling increases the percentage of feathers with this phenotype. A possible modifier for mottling is the *E* locus which is present in mottling, but not in tricolor chickens. The latter are more uniform than mottling and almost every feather has the V-shaped black band (Somes, 1980). The mottling gene also has an effect on chick down, which basically restricts ventral eumelanin and is probably expressed only in an *E/E* background (Schaible, 1968). Schaible (1968) also showed with grafting experiments that the mottling down pattern was caused by retarded migration of melanoblasts during early development. Early differentiation of melanoblasts may cause slow proliferation and retard migration of pigment cells in the Ancona, a mottled breed. A reduced rate of migration may also delay the arrival of melanocytes to the tip of the feather vane that are necessary to generate mottled feathers (Schaible, 1968).

Kinoshita et al. (2014) reported an allelism between mottling and tyrosinase-independent recessive white in Japanese chickens. They assigned the symbol mo^w to the

latter gene. Miwa et al. (2007) identified an Arg332His amino acid change in the endothelin receptor B2 (*EDNRB2*) gene that was causal for the panda phenotype in Japanese quail, a phenotype similar to *mo^w* in chickens. Based on the appearance of an F₁ hybrid between a panda quail and a *mo^w* chicken, Kinoshita et al. (2014) reported that a Cys244Phe amino acid substitution in the *EDNRB2* was associated with the *mo^w* mutation, while an Arg332His in the same gene was associated with the *mo* mutation in Japanese chickens. In ducks, the spot pattern was also mapped to the mutation Arg332His in *EDNRB2* (Li et al., 2015). Thus, 4 phenotypes in 3 avian species have been shown to be associated with mutations in *EDNRB2* with 3 of the 4 being the same amino acid substitution Arg332His.

It was reported by Harris et al. (2008) that the *EDNRB2* gene encodes a 7-transmembrane domain G-protein-coupled receptor EDNRB2 and participates in melanoblast differentiation and migration with its ligand, endothelin 3 (ET3). Together with Ephrin receptor B2 (EphB2), EDNRB2 mediates a repulsive response to neuronal neural crest cells and an attractive response in melanoblasts (Santiago and Erickson, 2002). Signaling from these receptors is additive because an overexpression of one receptor can rescue the loss of the other (Harris et al., 2008). As a result of whole-genome duplication events that occurred in their common ancestors, vertebrates generally possess 3 types of endothelin receptor genes, *EDBRA*, *EDNRB1*, and *EDNRB2*. In mammals, however, *EDNRB2* was lost secondarily from a chromosome that gave rise to the sex chromosomes (Braasch et al., 2009).

In this study, none of the *EDNRB2* mutations mentioned above was found in Mottled Houdan, a breed that originated in France (American Poultry Association, 1921)

with the *mo* gene. This promoted the need to study the causal mutation of *mo* in the Houdan. The procedures involved a 3-generation breeding program with SNP analyses of pooled samples followed by linkage mapping (in Chapter 2). Multiple bioinformatics methods, sequencing, and diagnostic tests (in Chapter 2) were also applied to identify the causal mutation of the mottling phenotype in Houdan.

Materials and methods

Details of matings used in this Chapter are shown in **Table 2.1** (Cross_4). Briefly, 3 Mottled Houdan males were mated to 6 Black Langshan females to produce 25 F₁ females that when backcrossed to the F₀ males produced 222 backcross progeny. Classification of mottling and black plumage patterns in the backcross population was made by the same individual at hatch and 12 weeks. DNA samples were isolated from blood of each chicken at 4 weeks, and then combined into 2 pooled DNA samples (**Table 2.4**). Genotyping of pooled samples was via high-density 60K SNP Illumina iSelect chicken arrays. Values for absRAFdif were calculated by comparing the 2 pooled samples. Individual samples were genotyped via high-density 60K chicken SNP genotyping arrays (**Table 2.3**). The association between each SNP and the inferred genotypes were calculated by PLINK. Linkage mapping was conducted by genotyping 9 SNPs for the whole mapping population via KASP assays (**Table 2.5**). See details in Chapter 2.

All exons of the *EDNRB2* gene were sequenced (**Table 2.6**) using 4 Mottled Houdans, 2 Mille Fleurs, and 3 Black Langshans; the exon 1 and the 5'-UTR sequence on exon 3 were also sequenced in 1 C (Black) female (not a standard breed), 1 American

Longtail female, and 1 A (B^{Sd}) male (not a standard breed); the 5'-UTR was also sequenced in 1 A (B^{Sd}) female, 1 Spangled Old English, 1 Speckled Sussex, 1 Blue Egg female (not a standard breed), and 1 B^{Sd} male (not a standard breed). Diagnostic tests to measure the association between the mottling phenotypes with the 3 candidate mutations were conducted using samples of 315 chickens from 85 different stocks and experimental lines (**Table 2.2**). The first candidate mutation (a non-synonymous mutation) was detected by the same KASP assay used in the linkage mapping (**Table 2.5**). The second was the causal mutation reported by Kinoshita et al. (2014). A KASP assay was designed to detect this mutation followed by the protocol of KASP-1 described in Chapter 2. The third is a 420 bp LTR/ERVK sequence located at the intron 5 of *EDNRB2* gene reported by Kinoshita et al. (2014) and also found in this study. It was detected by PCR using primers E_E6_F and E_E6_R (**Table 2.4**). Different PCR product sizes indicate the genotypes where 1107 bp represents the wild-type allele and 982 bp the mutated allele.

Results

SNP and linkage mapping

The number of mottled (*mo/mo*) and black (Mo^+/mo) individuals (113 and 108, respectively) in the backcross did not differ from a 1:1 ratio ($p = 0.74$). These results are consistent with the hypothesis that *mo* is a single recessive mutation.

There was one obvious peak in chromosome 4 (**Figure 6.1**). The region from 6.90 Mb to 17.73 Mb on the chromosome 4 contained all the SNPs with absRAFDif values greater than 0.34 (blue boxed area in **Figure 6.2**), which suggest the location of the *mo* mutation. Of the 49 SNPs found by *EDNRB2* sequencing (**Table 6.1**), only 1

(rs313943998 in dbSNP, i.e. Ala228Thr) was non-synonymous and associated with *mo*. Via the KASP assay, this candidate SNP and the other 8 flanking SNPs (**Table 2.3**) within the candidate region (blue boxed area in **Figure 6.2**) were genotyped for linkage mapping. The linkage mapping showed that the causal mutation lies between rs16360752 (10.76 Mb) and rs317734713 (11.65 Mb) (red boxed area in **Figure 6.2**). See details of linkage mapping results in **Table 2.5**. Within the region, *EDNRB2* was the only candidate gene with functions related to either melanocytes or melanosomes.

A significant associated genomic region was lacking after the analysis of individual genotypes (data not shown). The reasons could be due to different genetic backgrounds among involved individuals and/or sample size.

Identification of the causal mutation

Results of the diagnostic test showed that of the 6 populations supposed to have the *mo* gene, 5 were fixed with the Ala228Thr allele, and only the Mille Fleur D'Uccle Belgian was fixed with the wild type allele. No homozygote of Ala228Thr mutation was found in the other breeds and populations in **Table 2.5** that did not express the mottling phenotype, although some heterozygotes were present in A (B^{Sd}), American Longtail, B^{Sd}, and C (Black) (data not shown). Of the 49 mutations found by *EDNRB2* sequencing (**Table 6.1**), the only difference between Mille Fleur and Mottled Houdan was the candidate mutation Ala228Thr while the other 48 were identical. These results suggest that Mille Fleur and Mottled Houdan may have the same ancestor haplotype and share a causal mutation other than Ala228Thr.

The second candidate mutation in **Table 6.1** was a 420 bp LTR/ERVK sequence located at positions of 11,216,566 - 11,216,985 of chromosome 4, in the intron 5 of

chicken *EDNRB2* gene, which can be deleted and replaced by an unrelated 295 bp sequence. This 295 bp sequence was homologous to the genomic sequence in Japanese quail, with 91% nucleotide sequence identity (267/295 bp) (data not shown) and was also present in Japanese mottled chickens (Kinoshita et al., 2014), Mottled Houdan, and Mille Fleur. Although the diagnostic test showed that all mottled chickens were fixed with the mutate allele, the mutant alleles (homozygotes and heterozygotes) also exist in other non-mottled breeds, including Red Jungle Fowl (data not shown). These results exclude this mutation from the candidate mutations of *mo*.

The partial sequence of the *EDNRB2* gene in an American Longtail female was identical to Mottled Houdan from 5' region to exon 3, except g.11213409C>T, which was heterozygous in the American Longtail. Because the American Longtail doesn't express mottling, g.11213409C>T remains as the only possible causal mutation in this sequenced region. Another 6 individuals that were heterozygous for Ala228Thr and did not express mottling were sequenced. Two mottling individuals (1 Spangled Old English and 1 Speckled Sussex) were also sequenced. These 8 individuals showed that, g.11213409C>T was completely associated with Ala228Thr. The expression of *EDNRB2* during translation may be affected because g.11213409C>T was located on exon 3 and belonged to the 5'-UTR. Multiple regulatory cis-acting sequence elements may exist in 5'-UTR, e.g. secondary structures and upstream open reading frames (uORFs) (Wethmar et al., 2010). However, g.11213409C>T, did not disrupt or form any stable secondary structure as predicted by RNAstructure webtool (data not shown). Also, this deletion was not close to any predicted uORF (Somers et al., 2013) in chicken *EDNRB2* (data not shown).

The causal mutation for *mo* in Japanese breeds of chickens, Arg332His in *EDNRB2* (Kinoshita et al., 2014) was not detected in the Mottled Houdan. It may exist in other breeds of chicken, however, none of the 315 individuals in **Table 2.5** contained the Arg332His mutation in *EDNRB2*.

Of the 49 mutations listed in **Table 6.1**, 24 were heterozygous in Langshan. Three pure line Black Langshan chickens were involved in the *EDNRB2* sequencing and were heterozygotes for these 24 mutations suggesting duplicated genomic regions containing the *EDNRB2* gene may exist in Langshan.

Discussion

The causal mutation for the *mo* gene in Japanese chickens reported by Kinoshita et al. (2014) was not universal in other *mo* breeds of chickens, including Mottled Houdan, Mille Fleur, Spangled Old English, and Speckled Sussex. To identify the causal mutation of the *mo* gene in Mottled Houdan, construction of a backcross mating population, pooling of DNA samples, microarray analysis, linkage mapping, Sanger sequencing, and diagnostic tests were performed. The results provide strong evidence that this phenotype is caused by a mutation in *EDNRB2*. The primary candidate mutation was the Ala228Thr substitution which was completely associated with the mottling phenotype in the mapping population. Although present in all the Mottled Houdan, Spangled Old English, and Speckled Sussex samples which expressed mottling or tricolored patterns, it was not observed in Mille Fleur, a tricolored breed. Parallel evolution could be the explanation because considering that Mottled Houdan and Japanese mottled chickens have different causal mutations for *mo*, it is possible that Mille Fleur has a different causal mutation

(probably not in the coding region of *EDNRB2*) for *mo*. Among the 18 polymorphisms of *EDNRB2* that both found in this study and the one by Kinoshita et al. (2014), 15 of them are identical between *mo* in Houdan and *mo^w* in Japanese breeds; 9 of them are identical between *mo* in Houdan and *mo* in Japanese breeds (data not shown). This suggests the 2 *mo* alleles in Houdan and Japanese breeds could have evolved from *mo^w* allele independently, and thus supports the thesis of parallel evolution. Other two non-synonymous mutations found in my study (Thr8Ile and Thr15Ala), also reported by Kinoshita et al. (2014), were not associated with mottling in our samples (**Table 6.1**). In addition, heterozygotes of the Ala228Thr substitution were also observed in some non-mottled breeds. Because *mo* is recessive, it is possible that each of those heterozygotes carried only one copy of the *mo* gene and did not express the mottling phenotype. Even if a chicken carries two copies of *mo* gene, mottling may not be observed because of other pigmentation genes, e.g. dominant or recessive white. Thus, the thesis that the Ala228Thr substitution of *EDNRB2* gene in Mottled Houdan is responsible for its mottling phenotype cannot be excluded. Similarly, g.11213409C>T can also be considered as a candidate mutation because it was completely associated with Ala228Thr in the 15 samples that were sequenced with the exception of the 2 Mille Fleur. For Mille Fleur, although Ala228Thr cannot be the causal mutation for *mo*, a possibility is g.11213409C>T whose association with the mottling phenotype needs further study with larger samples.

An alternative explanation for the lack of association is that Ala228Thr is merely a physical marker linked to *mo* (Arg332His and g.11213409C>T may be the same). Thus, the causal mutation of *mo* which is shared by all breeds of mottled chickens is yet to be

identified. If such a mutation does exist, it is highly possible that it is a regulatory element of the *EDNRB2* gene. The thesis that anomalous expression of *EDNRB2* is responsible for the mottling down pattern is supported by the report of Kinoshita et al. (2014), that the expression of *EDNRB2* in skin tissues of *mo* chicks was lower than that of wild-type chicks. In other avian species, phenotypes similar the down pattern of *mo* were associated with reduced *EDNRB2* expression (Li et al., 2015; Wu et al., 2016). Wu et al. (2016) also predicted the relative expression level of *EDNRB2* was progressively reduced during melanoblast migration, suggesting the high *EDNRB2* expression is associated with melanoblast migration (Harris et al., 2008) while low expression leads to differentiation of melanocytes. In mammals, *EDNRB* is the homolog to avian *EDNRB2* and they share similar functions (Braasch et al., 2009). Mutation and reduced expression of *EDNRB* are also associated with piebald mice, a phenotype similar to the down pattern of *mo* chicks (Yamada et al., 2006). Lower *EDNRB* expression may delay melanoblast migration and stimulate maturation of melanocytes in mice (Shin et al., 1999; Lee et al., 2003).

Schaible (1968) reported that the mottling chick down pattern was caused by early differentiation and retarded migration of pigment cells, suggesting a relationship between the *mo* down pattern and the reduced *EDNRB2* expression. He also proposed an explanation that the reduced rate of migration may be responsible for the white tip on the mottled feather vane. This explanation can be strengthened when considering the proposal by Somes (1980) that the *mo* gene has two main effects on adult plumage patterns, white tips and the following V-shaped black bands. In the developing feather follicle of chickens, undifferentiated melanocytes in the lower bulge migrate upward

while differentiating into pigmented melanocytes (Lin et al., 2013). If reduced *EDNRB2* expression affects the migration of melanocytes from the lower bulge similarly to those from the neural crest, one can expect delayed migration resulting in the absence of melanocytes on the tip of the feather. Also, an early differentiation of melanocytes may be responsible to the V-shaped black bands. Based on the proposal by Somes (1980), the formation of V-shaped black bands is independent from *E* locus, i.e. Melanocortin 1-receptor (*MC1R*) (Kerje et al., 2003) and may be influenced by *lav*, i.e. melanophilin (*MLPH*) (Vaez et al., 2008). The study of chicken MC1R expression profiles suggests that MC1R should be expressed at a high level during feather replacement (Liu et al., 2010). More specifically, melanocyte stimulating hormone (MSH) is the main ligand of MC1R and can initiate the cascade of melanogenesis after binding, which is only expressed by stressed keratinocytes (Zhang et al., 2015). Therefore, the melanocytes in the lower bulge may have low expression of *MC1R* and no melanogenesis function at that time point, because they will interact with keratinocytes later as they migrate from the lower bulge. Later in the lower bulge, the expression of *MC1R* may be higher or the function of *EDNRB2* may be replaced by *EphB2* (Santiago and Erickson, 2002), which could explain the formation of tricolor patterns.

The lavender gene can dilute black pigmentation into gray in feathers (Vaez et al., 2008), skin and muscle tissues (Xu et al., 2016). It can dilute the V-shape black band in the mille fleur pattern into a slaty blue color, known as porcelain pattern (Somes 1980). The causal mutation of *lav* is a single mutation in the coding region of the *MLPH* gene (Vaez et al., 2008), which is required for melanosome transportation (Strom et al., 2002). The deficiency of this transportation pathway can affect the expression of Fibromelanosis

(*Fm*), a dermal hyperpigmentation mutation caused by the altered ET3/EDNRB2 signal (Dorshorst et al., 2011), because a different single mutation on the *MLPH* gene can dilute the ectopic black pigmentation into grey (Xu et al., 2016). Collectively, it appears that during formation of the porcelain pattern, melanocytes are fully pigmented in the lower bulge before MC1R has a role, because of low expression of *EDNRB2*. When these melanocytes migrate into the growing feather they have difficulty in transporting their pigment into keratinocytes with a mutant MLPH. In the later stage, MC1R and MLPH interact to deposit the beige color into the lower part of the porcelain feather vane.

In summary, the above thesis supports that anomalous expression of *EDNRB2* is associated with the *mo* gene. Therefore, the causal mutation is likely to be a regulatory element, which could be g.11213409C>T; further investigations are necessary to confirm the causality of g.11213409C>T and Ala228Thr.

Tables and figures

Table 6.1. Polymorphisms identified in the chicken *EDNRB2* gene

DNA position	Nucleotide polymorphism	Location	Allele in Langshan	Allele in Mottled Houdan and Mille Fleur	dbSNP
11209697 - 11209701	GAAGT>deletion	5' Region	deletion	deletion	Not in dbSNP
11209703	A>G	5' Region	G	G	rs738516435
11209770	C>T	5' Region	C	T	rs731110777
11209771	T>A	5' Region	T	A	rs318116218
11209999	C>G	5' Region	G	G	rs312750944
11210030	G>C	5' Region	G	C	rs314537375
11210053	A>G	5' Region	G	G	rs318132462
11210167	T>C	5' Region	T	C	rs315299113
11210233	A>T	5' Region	A	T	rs315709540
11210238	G>A	5' Region	A	G	rs314470926
11210290	T>C	5' Region	C	C	rs315128829
11,212,737	A>C	Intron 2	A	C	rs312457066
11,212,822	G>A	Intron 2	Heterozygote	G	Not in dbSNP
11,213,105	G>A	Intron 2	Heterozygote	G	Not in dbSNP
11,213,262	T>A	Intron 2	T	A	rs734453456

DNA position	Nucleotide polymorphism	Location	Allele in Langshan	Allele in Mottled Houdan and Mille Fleur	dbSNP
11,213,381	T>C	Intron 2	Heterozygote	T	rs313546191
11,213,409	C>T	Exon 3	C	T	Not in dbSNP
11,213,430	T>C	Exon 3	Heterozygote	C	rs314202686
11,213,498	C>T	Exon 3	Heterozygote	C	rs312956144 (Thr8Ile)
11,213,518	A>G	Exon 3	Heterozygote	A	Not in dbSNP (Thr15Ala)
11,213,706	T>C	Exon 3	T	C	rs316614064
11,213,933	T>C	Intron 3	T	C	rs313488270
11,214,052	T>C	Intron 3	T	C	rs15493999
11,215,682	T>C	Intron 4	Heterozygote	T	rs313747424
11,215,720	A>G	Intron 4	Heterozygote	G	rs731091593
11,215,722	A>C	Intron 4	Heterozygote	C	Not in dbSNP
11,215,732	A>G	Intron 4	Heterozygote	G	rs315434058
11,215,748	G>A	Intron 4	Heterozygote	A	rs318198310
11,215,756	C>T	Intron 4	Heterozygote	T	rs314103239
11,215,779	C>A	Intron 4	Heterozygote	A	rs312901123
11,215,803	C>T	Intron 4	Heterozygote	T	rs313485222
11,215,993	G>T	Intron 4	Heterozygote	T	rs317914285
11,216,005	T>G	Intron 4	Heterozygote	G	rs314022917
11,216,160	G>A	Exon 5	G	A in Houdan G in Mille Fleur	rs313943998 (Ala228Thr)
11,216,534	A>G	Intron 5	A	G	rs317721133
11,216,566 - 11,216,985	Gallus>Coturnix ¹	Intron 5	Heterozygote	Coturnix	rs736320010 ²
11,216,996	A>C	Intron 5	Heterozygote	C	rs318080604
11,217,370	A>G	Intron 6	Heterozygote	A	rs316801520
11,217,421	C>T	Intron 6	C	T	rs312594936
11,217,433	C>T	Intron 6	C	T	rs734042345
11,217,462	T>A	Intron 6	T	A	rs317818678
11,217,987	C>T	Intron 7	C	T	rs741395531
11,217,988	G>A	Intron 7	Heterozygote	G	rs315545656
11,218,085	T>A	Intron 7	T	A	rs734681357
11,218,202	T>C	Intron 7	T	C	rs16361380
11,218,235	C>T	Intron 7	Heterozygote	C	Not in dbSNP
11,218,268	A>G	Intron 7	Heterozygote	G	rs315919804
11,218,415	T>C	Intron 8	Heterozygote	C	rs315147153
11,219,434	C>A	3' - UTR	Heterozygote	A	rs315123387

¹ Gallus stands for a 420 bp LTR/ERVK sequence which located at positions of 11,216,566 - 11,216,985 of chromosome 4 on the basis of the chicken reference genomic sequence. Coturnix stands for the deletion of the that 420 bp LTR/ERVK sequence and replaced by an unrelated 295 bp sequence which is homology to quail genomic sequence.

² rs736320010 indicates the first SNP located on the 5' end of the 420 bp LTR/ERVK sequence.

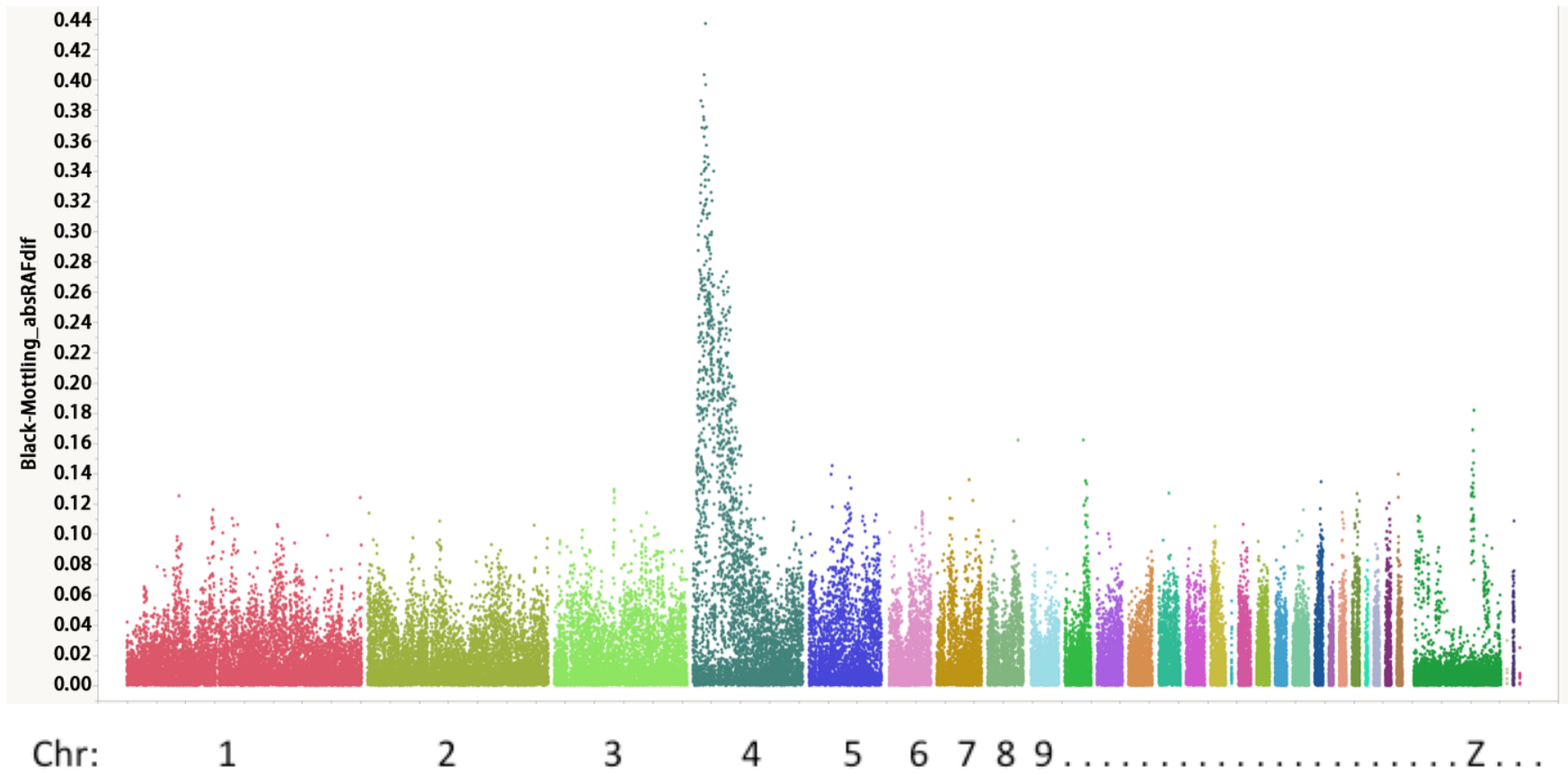


Figure 6.1. Genome-wide absRAFdif values, for *mo* mapping. Calculated by contrasting Pools 4_1 and 4_2 of all 60K SNPs, plotted against the genomic location.

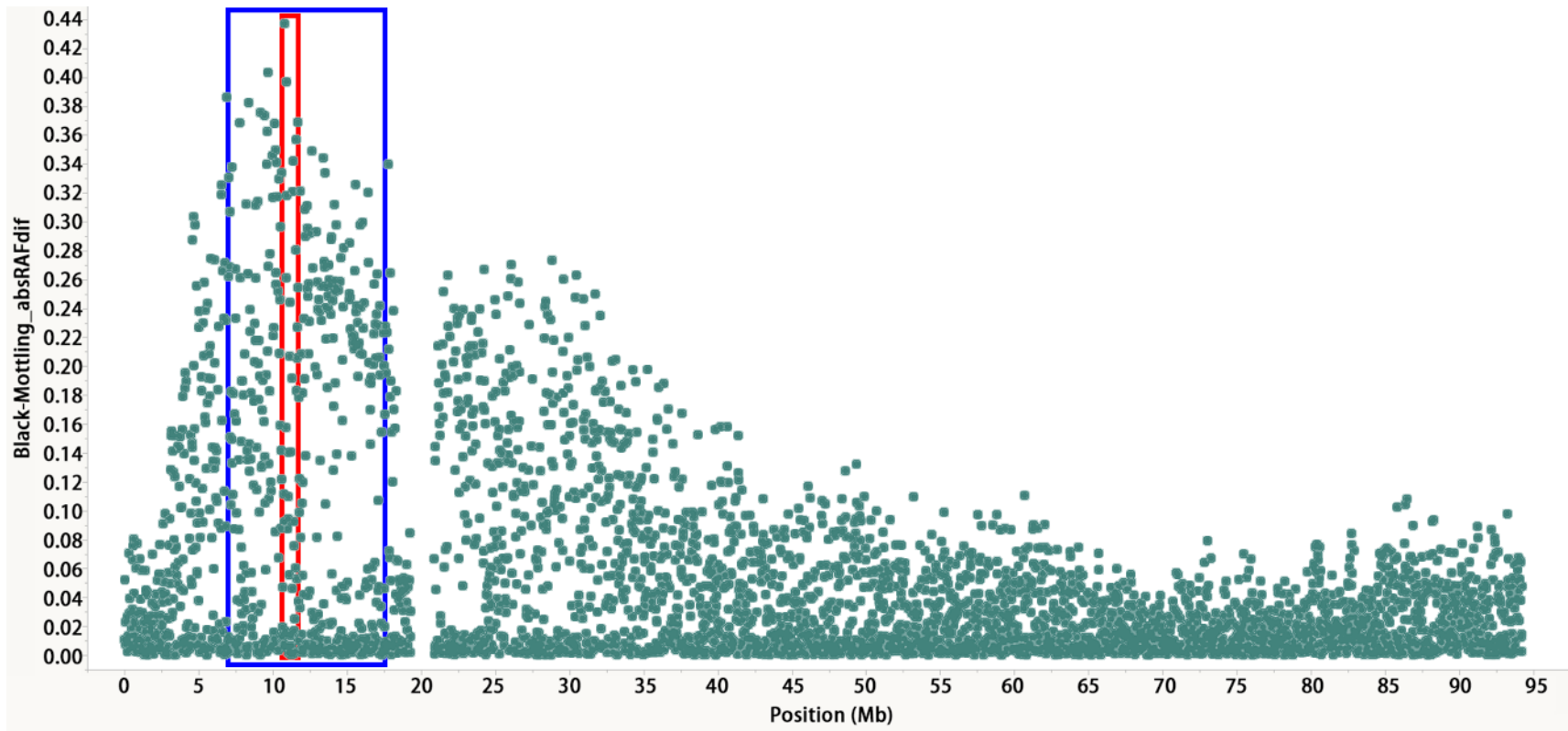


Figure 6.2. The absRAFdif values of SNPs on chromosome 4, for *mo* mapping. Calculated by contrasting Pools 4_1 and 4_2, plotted against the genomic location. SNPs located within the 10.83 Mb region (blue boxed area) gave absRAFdif values above 0.34. Red boxed area indicates the 0.90 Mb linkage mapping region, suggesting the location of the *mo* mutation.

References

- American poultry association. 1921. Pages 324 in *The American Standard of Perfection*. Davenport, IA, USA.
- Asmundson, V. S., H. I. Milne. 1930. Inheritance of plumage and skin color in the Ancona. *Scientific Agriculture*, 10:293-304.
- Braasch, I., J. N. Volff, M. Schartl. 2009. The endothelin system: evolution of vertebrate-specific ligand–receptor interactions by three rounds of genome duplication. *Molecular Biology and Evolution*. 26:783-799.
- Dorshorst, B., A. M. Molin, C. J. Rubin, A. M. Johansson, L. Strömstedt, M. H. Pham, C. F. Chen, F. Hallböök, C. Ashwell, L. Andersson. 2011. A complex genomic rearrangement involving the endothelin 3 locus causes dermal hyperpigmentation in the chicken. *PLoS Genetics*. 7:e1002412.
- Harris, M. L., R. Hall, C. A. Erickson. 2008. Directing pathfinding along the dorsolateral path—the role of EDNRB2 and EphB2 in overcoming inhibition. *Development*. 135:4113-4122.
- Kerje, S., J. Lind, K. Schütz, P. Jensen, L. Andersson. 2003. Melanocortin 1 - receptor (MC1R) mutations are associated with plumage colour in chicken. *Animal Genetics*. 34:241-248.
- Kinoshita, K., T. Akiyama, M. Mizutani, A. Shinomiya, A. Ishikawa, H. H. Younis, M. Tsudzuki, T. Namikawa, Y. Matsuda. 2014. Endothelin receptor B2 (EDNRB2) is responsible for the tyrosinase-independent recessive white (mo^w) and mottled (mo) plumage phenotypes in the chicken. *PLoS One*. 9:e86361.
- Lee, H. O., J. M. LeVorse, M. K. Shin. 2003. The endothelin receptor-B is required for the migration of neural crest-derived melanocyte and enteric neuron precursors. *Developmental Biology*. 259:162-175.
- Li, L., D. Li, L. Liu, S. Li, Y. Feng, X. Peng, Y. Gong. 2015. Endothelin receptor B2 (EDNRB2) gene is associated with spot plumage pattern in domestic ducks (*Anas platyrhynchos*). *PLoS One*. 10: e0125883.
- Lin, S. J., J. Foley, T. X. Jiang, C. Y. Yeh, P. Wu, A. Foley, C. M. Yen, Y. C. Huang, H. C. Cheng, C. F. Chen, B. Reeder. 2013. Topology of feather melanocyte progenitor niche allows complex pigment patterns to emerge. *Science*. 340:1442-1445.
- Liu, W. B., S. R. Chen, J. X. Zheng, L. J. Qu, G. Y. Xu, N. Yang. 2010. Developmental phenotypic-genotypic associations of tyrosinase and melanocortin 1 receptor genes with changing profiles in chicken plumage pigmentation. *Poultry Science*. 89:1110-1114.
- Miwa, M., M. Inoue-Murayama, H. Aoki, T. Kunisada, T. Hiragaki, M. Mizutani, S. Ito. 2007 Endothelin receptor B2 (EDNRB2) is associated with the panda plumage colour mutation in Japanese quail. *Animal Genetics*. 38:103-108.
- Santiago, A., C. A. Erickson. 2002. Ephrin-B ligands play a dual role in the control of neural crest cell migration. *Development*. 129:3621-3632.
- Schaible, R. H. 1968. Development of transitory piebald spotted and completely pigmented patterns in the chicken. *Developmental Biology*. 18:117-148.
- Shin, M. K., J. M. LeVorse, R. S. Ingram, S. M. Tilghman. 1999. The temporal requirement for endothelin receptor-B signalling during neural crest development. *Nature*. 402:496-501.
- Somers, J., T. Pöyry, A. E. Willis. 2013. A perspective on mammalian upstream open reading frame function. *International Journal of Biochemistry and Cell Biology*. 45:1690-1700.
- Somes, R. G. Jr. 1980. The mottling gene, the basis of six plumage color patterns in the domestic fowl. *Poultry Science*. 59:1370-1374.
- Strom, M., A. N. Hume, A. K. Tarafder, E. Barkagianni, M. C. Seabra. 2002. A family of Rab27-binding proteins. Melanophilin links Rab27a and myosin Va function in melanosome transport. *Journal of Biological Chemistry*. 277:25423-25430.
- Vaez, M., S. A. Follett, B. Bed'hom, D. Gourichon, M. Tixier-Boichard, T. Burke. 2008. A single point-mutation within the melanophilin gene causes the lavender plumage colour dilution phenotype in the chicken. *BMC Genetics*. 9:1-9.
- Wethmar, K., J. J. Smink, L. Achim. 2010. Upstream open reading frames: Molecular switches in (patho) physiology. *Bioessays*. 32:885-893.
- Wu, N., H. Qin, M. Wang, Y. Bian, B. Dong, G. Sun, W. Zhao, G. Chang, Q. Xu, G. Chen. 2016. Variations in endothelin receptor B subtype 2 (EDNRB2) coding sequences and mRNA expression levels in four Muscovy duck plumage colour phenotypes. *British Poultry Science*. Doi: 10.1080/00071668.2016.1259531.

- Xu, J. G., M. G. Xie, S. Y. Zou, X. F. Liu, X. H. Li, J. F. Xie, X. Q. Zhang. 2015. Interactions of allele E of the MC1R gene with FM and mutations in the MLPH gene cause the five-gray phenotype in the Anyi tile-like gray chicken. *Genetics and molecular research: GMR*. Doi: 10.4238/gmr.15027633.
- Yamada, T., S. Ohtani, T. Sakurai, T. Tsuji, T. Kunieda, M. Yanagisawa. 2006. Reduced expression of the endothelin receptor type B gene in piebald mice caused by insertion of a retroposon-like element in intron 1. *Journal of Biological Chemistry*. 281:10799-10807.
- Zhang, J., F. Liu, J. Cao, X. Liu. 2015. Skin transcriptome profiles associated with skin color in chickens. *PloS One*. 10:e0127301.

Chapter 7

Feathered-leg in chickens is associated with a SNP on chromosome 15 and a region on chromosome 12

Authors

J. Li¹, B. Dorshorst¹, S. Lamichhaney², P. B. Siegel¹ and L. Andersson^{2*}.

Affiliations

¹ Department of Animal and Poultry Sciences, Virginia Tech, Blacksburg, Virginia, United States of America

² Department of Animal Breeding and Genetics, Swedish University of Agricultural Sciences, Science for Life Laboratory, Department of Medical Biochemistry and Microbiology, Uppsala University, Uppsala Sweden

* Corresponding author

Summary:

Feathered-leg is a trait in domestic chickens and pigeons that has undergone intensive selection by fancy breeders. Populations exhibiting this phenotype provide material to study mechanisms involved with feathered-leg and to further an understanding of skin appendage differentiation and evolution of avian species. In an attempt to identify the genomic region associated with feathered-leg in chickens, a mapping population was constructed by crossing Langshan females with Houdan males and backcrossing the F₁ females to the male parental line. The backcross population was analyzed by microarrays using pooled DNA samples followed by linkage mapping and whole genome sequencing.

A single nucleotide substitution, g.12465322T>G on chromosome 15, located on the downstream of the *TBX5* gene, was strongly associated with fully feathered-leg. A second genomic region on chromosome 12, which contains two *Wnt* genes, was also associated with intermediate feathered-leg. Provided here are new insights in understanding the formations of morphological traits.

Introduction:

The ancestors of chickens had tarsometatarsus and digits that were covered with scales. A mutative transformation of part of those scales into feathers results in so-called feathered-leg, feathered feet, shank feathering, or ptilopody (Bartels 2003). It is also an important trait in avian evolution because the “4-winged” dinosaurs, which are assumed to be the ancestor of avian species, probably had feathered-legs (Sawyer & Knapp 2003). Also, as an attractive trait, “fancy chicken breeds” have been selected to have more feather coverage (heavier feathered-legs).

Although poultry geneticists have extensively studied the inheritance of feathered-leg, lacking are completely satisfactory explanations of its biology. Results from matings involving feathered-leg stocks or those between feathered and clean-leg chickens are inconsistent (Somes 1992). Two dominant genes at separate loci when presented together produce the heavy feathered-legs of the Cochin, Sultan, Belgian d’Uccle Bantam and Botted Bantam breeds (Somes 1990). Either of these genes will result in the weak feathered-leg common to Langshan, Faverolles, and Breda breeds. The slightly heavier feathered-leg observed in Brahma and Silkie breeds may be due to one of these two loci (Dunn & Jull 1927; Warren 1933), or both of them with a different allele at one locus in

other lines (Punnett & Bailey 1918; Dunn & Jull 1927). The Pavloff feathering was suggested to be due to a recessive gene. The gene symbols *Pti-1*, *Pti-2* and *pti-3* for ptilopody were assigned to these loci (Somes 1990).

Linkage mapping has shown that only one chromosome region (15.3Mb in chromosome 13) is significantly associated with feathered-leg in the Silkie (Dorshorst *et al.*, 2010). Compared with the report of Dunn and Jull (1927), this region should be either *Pti-1* or *Pti-2*. The other feathered-leg gene in the Silkie may be in a micro-chromosome, or may not exist in the Silkie line used in the study reported by Dorshorst *et al.* (2010). Sun *et al.* (2015) observed two chromosomal regions that were significantly associated with feathered-leg in Beijing-You chickens. The first region in chromosome 15 contained 5 genes including *TBX3* and *TBX5*. The second region was consistent with the one reported by Dorshorst *et al.* (2010).

The domestic pigeon is another avian species that has striking variation in feathered-leg phenotypes. By matings of different breeds of pigeons and expression studies, Domyan *et al.* (2016) reported that the decreased expression of paired-like homeodomain 1 (*PITX1*) and ectopic expression of T-box 5 (*TBX5*) were associated with feathered-leg. They also studied the expression of *TBX5* and *PITX1* in the hindlimb buds of feathered-leg Cochin and Silkie chickens. The ectopic expression of *TBX5* was observed which may be responsible to either *Pti-1* or *Pti-2*. Although there was no association between *PITX1* expression and feathered-leg in chickens (Domyan *et al.*, 2016), the position of *PITX1* (15.7Mb in chromosome 13) suggests it may be responsible for the candidate region reported by Dorshorst *et al.* (2010) and Sun *et al.* (2015). Thus, while the causal mutation

affecting TBX5 expression (in chromosome 15) in feathered-leg chickens needs to be identified, the association between *PITX1* and feathered-leg needs to be confirmed.

Here, a 3-generation mapping population was built by crossing Langshan (feathered-leg) and Houdan (clean-leg), followed by SNP analyses of pooled samples, linkage mapping, and whole genome sequencing. The aim of this study was to identify the casual mutation of feathered-leg in Langshan chicken.

Materials and methods

Animals:

Procedures for this study were approved by Institutional Animal Care and Use Committee at Virginia Tech. A linkage mapping population was initiated from 9 chickens purchased from Murray McMurray Hatchery (www.mcmurrayhatchery.com, Webster City, Iowa, USA). They consisted of 3 Mottled Houdan males and 6 Black Langshan females. Matings between 25 F₁ females and 3 F₀ Houdan males produced 222 backcross chickens.

SNP-MaP analysis:

When 12 weeks of age the feathered-leg phenotypes observed in the backcross population were classified into 3 categories. These were: 1. Feathered-leg, which resembled the phenotypes of the F₀ Langshan (n = 96); 2. Intermediate feathered-leg (n = 44); 3. Clean-leg, which resembled the phenotypes of the F₀ Houdan (n = 82). Three DNA pools were constructed based on the shared phenotypes of the backcross individuals. Each individual contributed 250ng of DNA to the pool. The feathered-leg genes or loci were initially mapped by estimating SNP allele frequencies in the 3 DNA pools. They were then

genotyped via high-density 60 K SNP Illumina iSelect chicken array and analyzed using the SNP-MaP (SNP Microarray and Pooling) approach (Docherty *et al.* 2007). The Illumina array provided an intensity reading for the two alleles (X and Y) at each of the 57,636 SNPs. Relative allelic frequencies (RAF) at each SNP for each DNA pool were calculated as $X / (X + Y)$, where X and Y represented the intensity signals of each allele. For each SNP, absolute RAF differences (absRAFdif) were calculated by contrasting every 2 of the 3 DNA pools. The absRAFdif was then plotted against the SNP genomic locations (Wells *et al.* 2012). The absRAFdif value calculated by contrasting feathered-leg and clean-leg pools of a SNP was expected to be high if it was closely linked with the feathered-leg gene.

Linkage mapping:

Because of the microarray-based error and pooled-construction error, the estimated allele frequencies from SNP-MaP are arbitrary (Macgregor 2007). Individual genotyping was therefore necessary to confirm the candidate region observed in microarray assays. We selected five SNPs which had relatively high absRAFdif values within the region for further analysis, via Kompetitive allele-specific PCR assay (KASP), developed by LGC Genomics (Beverly, MA, USA; www.lgcgenomics.com) (Semagn *et al.* 2014). These 5 SNPs were genotyped using individual samples from the entire linkage mapping population except the intermediate feathered-leg backcrosses. KASP assays were conducted with the mix of 2.5 μ l of KASP V4.0 2X Mastermix (LGC Genomics, Beverly, MA, US; www.lgcgenomics.com), 1.5 μ l PCR grade water, 1 μ l DNA (50ng/ μ l), and 0.07 μ l of primers mix (12 μ M each of allele-specific primer, carrying standard FAM or HEX compatible tails, and 32 μ M of allele-flanking primer). Amplifications using two

protocols were carried out on Bio-Rad CFX384 Touch™ Real-Time PCR Detection System. PCR amplification protocol 1 (KASP-1) began with 94°C for 15 min, 10 cycles of 94°C for 20 s and 61°C (-0.6°C/cycle) for 1 min each, followed by 26 cycles of 94°C for 20 s and 55°C for 1 min each. KASP-2 began with 94°C for 15 min, 10 cycles of 94°C for 20 s and 66°C (-0.6°C/cycle) for 1 min each, followed by 26 cycles of 94°C for 20 s and 57°C for 1 min each. KASP-3 began with 94°C for 15 min, 10 cycles of 94°C for 20 s and 58°C (-0.6°C/cycle) for 1 min each, followed by 26 cycles of 94°C for 20 s and 52°C for 1 min each. All 3 protocols ended with an endpoint fluorescence reading after 37°C for 1 min. The readings were analyzed by Bio-Rad CFX Manager™ Software. Genotyping results were validated by at least 2 amplification runs for each sample. The details of these KASP assay are shown in Table S1. Genotyping and pedigree information were inputted into CRIMAP software for analysis (Green *et al.* 1990) and the genetic distances between each SNP and feathered-leg gene were calculated.

Bioinformatics analysis:

An online GO (Gene Ontology) searching engine (Smedley et al. 2015; www.biomart.org) was used to identify genes which have a molecular function, biological process, or cellular component related to epithelial cell differentiation.

Results:

SNP and linkage mapping:

All F₁ individuals were intermediate feathered-leg. The backcross population feathered-leg phenotypes were 96 feathered-leg, 44 intermediate, and 82 clean-leg, which is

consistent with the thesis that feathered-leg is partially dominant and involved are only several genes or loci (Somes 1992).

Hypothetically, when comparing feathered-leg and clean-leg DNA pools, the highest *absRAFdif* value could be 0.5. It was observed that the region from 10.78 Mb to 12.76 Mb on chromosome 15 contained all of the SNPs with *absRAFdif* values greater than 0.35. Linkage mapping based on the 5 markers showed that at least one major gene or locus was located in a 1.04 Mb region defined by rs14096198 (11.72 Mb) and 3' end of chromosome 15 (12.76 Mb) (Table S1; Figure 1b). Among all known genes in this region (Figure 1c), those found with GO terms related to epithelial cell differentiation were *TBX5* and *TBX3*.

By contracting intermediate feathered-leg and clean-leg DNA pools, another peak of *absRAFdif* values was observed on chromosome 12. That all SNPs having *absRAFdif* values greater than 0.17 located from 2.84 Mb to 8.36 Mb (Figure 2b) suggests that at least one gene or locus on chromosome 12 affects the expression of the major feathered-leg gene or locus on chromosome 15. Within this region, *WNT7A* and *WNT5A* were functionally related to feather bud development (Li *et al.* 2013; Jin *et al.* 2006) (Figure 2c). The same peak region on chromosome 15 was also observed by contracting intermediate and clean-leg DNA pools (Figure 2a).

Whole genome sequencing:

Within the 1.04Mb candidate region on chromosome 15, only one mutation (g.12465322T>G) was associated with feathered-leg. This candidate mutation was located downstream and 44.17 Kb away from the 3' end of the *TBX5* gene's last exon

(Figure 1c). The 50 bp sequence upstream and downstream of this mutation is not homology to any other vertebrates with known genome sequences (data not shown).

Discussion:

Somes (1992) reported 93.3% penetrance of the feathered-leg gene in Langshans, while there was 100% penetrance in our F₁ population. The slight inconsistency may be due to the different clean-leg stocks involved in the matings. Therefore, inhibitor or enhancer genes for feathered-leg that exist in clean-leg stocks may not be expressed. It is not uncommon to find chickens with a slight degree of feathered-leg (stubs) in non-feathered ones (Lambert and Knox 1929). The two chromosome regions we observed were consistent with those of Somes (1992) that two loci segregate in some Langshan stocks. Prior to the mapping of feathered leg genes, results on the molecular basis of feathered-leg were contradictory. For example, by injecting a dominant negative type I bone morphogenetic protein (BMP) receptor into Leghorn embryos at day (E) 2 or 3 to block BMP signaling, Zou and Niswander (1996) observed scales transformed into feathers and resembled a feathered-leg phenotype. Harris *et al.* (2004) observed that precocious expression of BMP7 resulted in the formation of feathers from scales when they treated Leghorn embryos with recombinant BMP7 protein at day (E) 7 to 8. Such differences in embryonic ages might be explained by specific functions among BMP family proteins which have different reactions to the BMP signal. Summarized by Widelitz *et al.* (2000), the scale-feather transformation can be caused by retinoic acid and associated with changes in Hox expression. Alternations of fibroblast growth factor (FGF) or Delta pathway also can cause similar effects. Widelitz *et al.* (2000) proposed that the activity of

the β -catenin pathway, a target of the wingless-int (Wnt) pathway, contributed to the scale-feather transformation and could be regulated by the factors mentioned above. Sawyer & Knapp (2003) suggested that scale formation on the hindlimb in non-feathered-leg avian species inhibits feather formation, because scales and feathers are homologous skin appendages. This inhibition would not exist in the Silkie because there are hybrid structures in Silkie embryos. Although the scutate scale develops from its placode and interplacode regions, the feather filament is continuous with the scutate scale ridge and does not form from a feather placode (Sawyer 1972). This observation leads to the connection between feathered-leg development and pathways that regulate scale development, such as the Wnt pathway (Chang *et al.* 2015). Therefore the β -catenin and Wnt pathways, but not the BMP may have central roles in the formation of feathered-leg. These previous studies support our results and those of Domyan *et al.* (2016) that the *TBX5* gene is responsible for feathered-leg in chickens.

In chickens, *TBX5* was expressed in a restricted manner in wing buds while *TBX3* was expressed in both wing and leg buds with a much broader expression domain in wing than leg buds (Logan *et al.* 1998). Together with other *TBX* factors, *TBX5* and *TBX3* have major roles in the specification of limb-type identity, wing versus leg. Accompanied by the induction of both Wnt and FGF pathways, ectopic expression of *TBX5* in leg buds will cause wing-like feather bud patterns on the anterior surface (Takeuchi *et al.* 2003; Domyan *et al.* 2016). The hypothesis that *TBX5* regulates Wnt and other downstream pathways in feather bud development can explain the previous reports that other factors were associated with the same feathered-leg phenotype (Widelitz *et al.* 2000).

A β -catenin zone, which is induced by Wnt7a protein and localized in the posterior feather bud, is necessary and sufficient to mediate the directional elongation of feathers (Li *et al.* 2013). Overexpression of Wnt5a stimulated chondrogenic differentiation of chick wing bud mesenchymal cells *in vitro* (Jin *et al.* 2006), which may inhibit feather bud formation *in vivo*. Both of these Wnt proteins are likely to be involved in the scale-feather transformation and regulated by *TBX5*. Linkage mapping to analyze this region contains *WNT5A* and *WNT7A* genes was not feasible in our study because the absRAFdif signal was weak (the highest value was 0.24). Therefore, if the different alleles of the target gene had not been fixed in the intermediate and clean-leg backcrosses, the power of detecting target genes in linkage mapping would be decreased. Thus, further evidence is needed to confirm that mutations on these Wnt genes affect the expression of feathered-leg.

Domyan *et al.* (2016) reported, as a forelimb-specific transcription factor, ectopic expression of *TBX5* in the hindlimb changed the development of epithelial appendages and also re-patterned hindlimb into wing-like musculoskeletal system in pigeons. Similar effects can be observed in the chicken. Lambert and Knox (1929) reported that brachydactylism and syndactylism were associated with feathered-leg, which we confirmed in another 3-generation mapping population involving Silkie and Houdan that showed a significantly association between greater degree of feathered-leg and shorter 4th digit (unpublished data).

It is not feasible to use a KASP assay to genotype the candidate mutation (g.12465322T>G) because it falls in a small repeated region (Figure 1d). An alternative approach is necessary to confirm its association to feathered-leg in our mapping

populations and in other breeds expressing feathered-leg as this mutation may act as a long-range regulatory element affecting *TBX5* expression.

Acknowledgements:

We thank Giovanni Thomas, Christa Honaker, Dez-Ann Sutherland, and Michelle Jambui, for husbandry and sampling of the chickens, also for DNA isolation process. The authors declare that there are no conflicts of interest.

References:

- Bartels T. (2003) Variations in the morphology, distribution, and arrangement of feathers in domesticated birds. *Journal of Experimental Zoology Part B: Molecular and Developmental Evolution* **298**, 91-108.
- Chang K.W., Huang N.A., Liu I.H., Wang Y.H., Wu P., Tseng Y.T., Hughes M.W., Jiang T.X., Tsai M.H., Chen C.Y. & Oyang Y.J. (2015) Emergence of differentially regulated pathways associated with the development of regional specificity in chicken skin. *BMC Genomics* **16**, 1-14.
- Docherty S.J., Butcher L.M., Schalkwyk L.C. & Plomin R. (2007) Applicability of DNA pools on 500 K SNP microarrays for cost-effective initial screens in genomewide association studies. *BMC Genomics* **8**, 1-7.
- Domyan E.T., Kronenberg Z., Infante C.R., Vickrey A.I., Stringham S.A., Bruders R., Guernsey M.W., Park S., Payne J., Beckstead R.B. & Kardon, G. (2016) Molecular shifts in limb identity underlie development of feathered feet in two domestic avian species. *eLife* **5**, e12115.
- Dorshorst B., Okimoto R. & Ashwell C. (2010) Genomic regions associated with dermal hyperpigmentation, polydactyly and other morphological traits in the silkie chicken. *Journal of Heredity* **101**, 339-350.
- Dunn L.C. & Jull M.A. (1927) On the inheritance of some characters of the silky fowl. *Journal of Genetics* **19**, 27-63.
- Green P., Falls K. & Crooks S. (1990) Documentation for CRIMAP, version 2.4. Washington University School of Medicine, St Louis, MO.
- Harris M.P., Linkhart B.L. & Fallon, J.F. (2004) Bmp7 mediates early signaling events during induction of chick epidermal organs. *Developmental Dynamics* **231**, 22-32.
- Jin E.J., Park J.H., Lee S.Y., Chun J.S., Bang O.S. & Kang, S.S. (2006) Wnt-5a is involved in TGF- β 3-stimulated chondrogenic differentiation of chick wing bud mesenchymal cells. *The International Journal of Biochemistry & Cell Biology* **38**, 183-195.
- Lambert W.V. & Knox C.W. (1929) The inheritance of shank-feathering in the domestic fowl. *Poultry Science* **9**, 51-64.
- Li A., Chen M, Jiang T.X., Wu P., Nie Q., Widelitz R. & Chuong C.M. (2013) Shaping organs by a wingless-int/Notch/nonmuscle myosin module which orients feather bud elongation. *Proceedings of the National Academy of Sciences* **110**, E1452-E1461.
- Logan M., Simon H.G., Tabin C. (1998) Differential regulation of T-box and homeobox transcription factors suggests roles in controlling chick limb-type identity. *Development* **125**, 2825-2835.
- Macgregor S. (2007) Most pooling variation in array-based DNA pooling is attributable to array error rather than pool construction error. *European Journal of Human Genetics* **15**, 501-504.
- Punnett R.C. & Bailey P.G. (1918) Genetic studies in poultry. *Journal of Genetics* **7**, 203-213.
- Sawyer R.H. (1972) Avian scale development: I: Histogenesis and morphogenesis of the epidermis and dermis during formation of the scale ridge. *Journal of Experimental Zoology Part B: Molecular and Developmental Evolution*. **181**, 365-384.

- Sawyer R.H. & Knapp L.W. (2003) Avian skin development and the evolutionary origin of feathers. *Journal of Experimental Zoology Part B: Molecular and Developmental Evolution* **298**, 57-72.
- Semagn K., Babu R., Hearne S. & Olsen M. (2014) Single nucleotide polymorphism genotyping using Kompetitive Allele Specific PCR (KASP): overview of the technology and its application in crop improvement. *Molecular Breeding* **33**, 1-14.
- Smedley D., Haider S., Durinck S., Pandini L., Provero P., Allen J., Arnaiz O., Awedh M.H., Baldock R., Barbiera G. & Bardou, P. (2015) The BioMart community portal: an innovative alternative to large, centralized data repositories. *Nucleic Acids Research* **43**, W589-W598.
- Somes Jr, R.G. (1990) Mutations and major variants of plumage and skin in chickens. In: *Poultry Breeding and Genetics* (ed. By R.D. Crawford), pp. 173-4. Elsevier, Amsterdam.
- Somes Jr, R.G. (1992) Identifying the ptilopody (feathered shank) loci of the chicken. *Journal of Heredity* **83**, 230-234.
- Sun Y., Liu R., Zhao G., Zheng M., Sun Y., Yu X., L, P. & Wen J. (2015) Genome-wide linkage analysis identifies loci for physical appearance traits in chickens. *G3: Genes, Genomes, Genetics* **5**, 2037-2041.
- Warren D.C. (1933) Nine independently inherited autosomal factors in the domestic fowl. *Genetics* **18**, 68-81.
- Wells K.L., Hadad Y., Ben-Avraham D., Hillel J., Cahaner A. & Headon D.J. (2012) Genome-wide SNP scan of pooled DNA reveals nonsense mutation in FGF20 in the scaleless line of featherless chickens. *BMC Genomics* **13**, 1-10.
- Widelitz R.B., Jiang T.X., Lu J. & Chuong, C.M. (2000) β -catenin in epithelial morphogenesis: conversion of part of avian foot scales into feather buds with a mutated β -catenin. *Developmental Biology* **219**, 98-114.
- Zou H. & Niswander L. (1996) Requirement for BMP signaling in interdigital apoptosis and scale formation. *Science* **272**, 738-741.

Figures

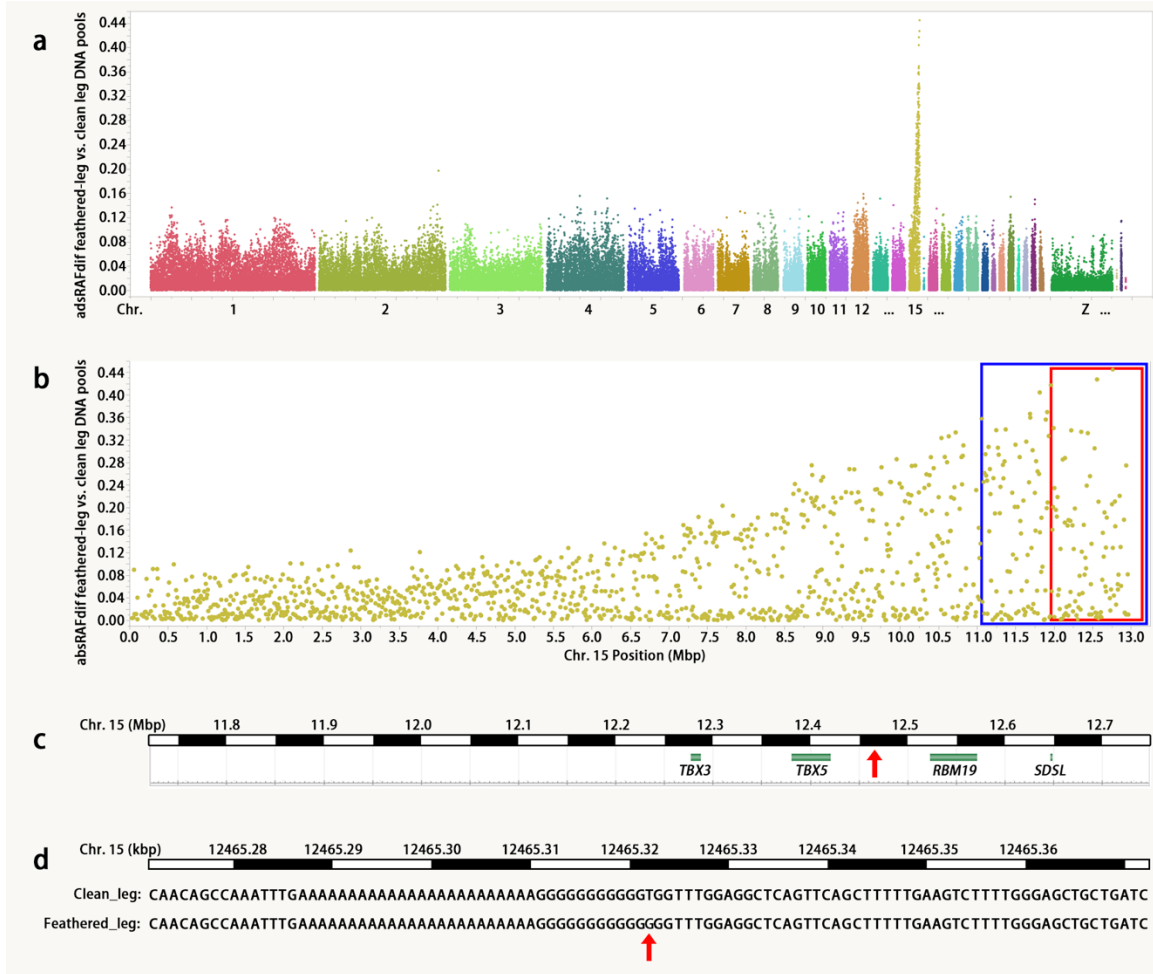


Figure 1 Linkage mapping of feathered-leg using backcross individuals. (a) Genome-wide absRAFDif values (calculated by contrasting feathered-leg and clean-leg DNA pools) of all 60K SNPs, plotted against the genomic location. (b) absRAFDif values on chromosome 15. SNPs located within the 1.98Mb region (blue boxed area) gave absRAFDif values above 0.35. Red boxed area indicates the 1.04Mb linkage mapping region, suggesting the location of the feathered-leg gene with the major effect. (c) Schematic of genes present within the 1.04 Mb region defined by linkage mapping. The candidate mutation (g.12465322T>G) is marked with a red arrow. (d) Sequence flanking the candidate mutation. The candidate mutation is marked with a red arrow.

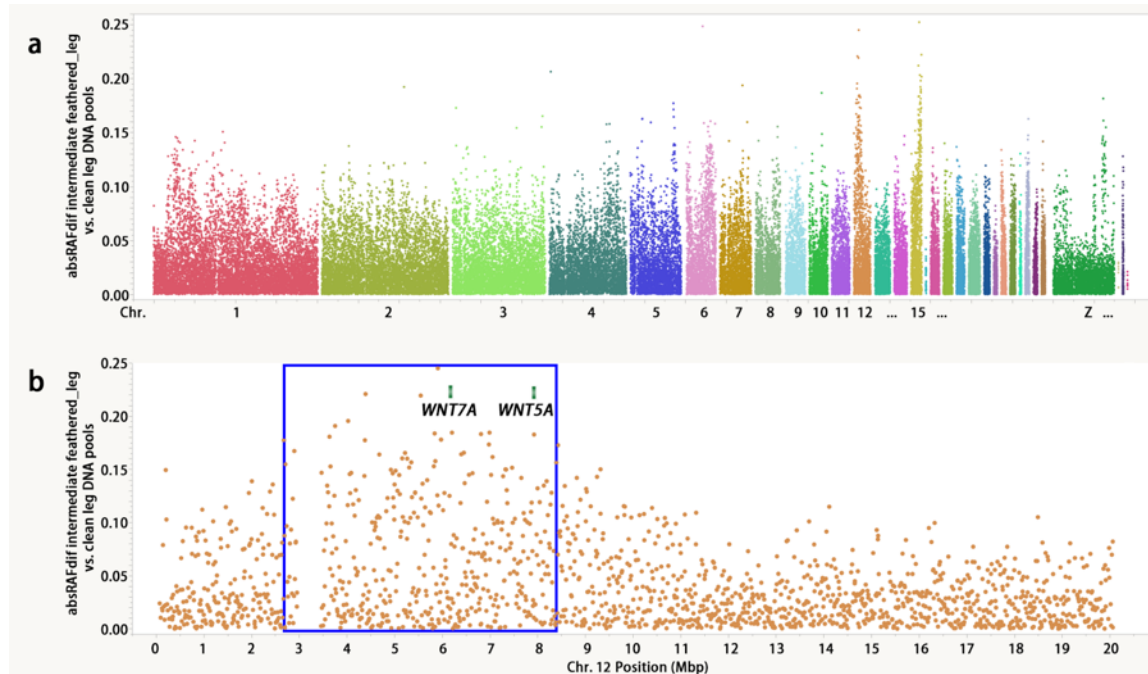


Figure 2 Genomic regions associated with intermediate feathered-leg. (a) Genome-wide absRAFDif values (calculated by contrasting intermediate feathered-leg and clean-leg DNA pools) of all 60K SNPs, plotted against the genomic location. (b) absRAFDif values on chromosome 12. SNPs located within the 5.52Mb region (blue boxed area) gave absRAFDif values above 0.17, suggesting the location of the feathered-leg gene with the major effect. Two candidate genes are labeled as green bars (*WNT7A* and *WNT5A*).

Supporting Information

Table S1. Linkage mapping of feathered-leg using individual SNP analysis.

dbSNP	absRAFDif ¹	Position on Chr. 15 (bp)	KASP protocol	Genetic distance from feathered-leg (cM) ²
rs13528978	0.358	10,784,395	KASP-3	6.783
rs14096198	0.417	11,721,706	KASP-1	1.124
rs316054667	0.427	12,316,957	KASP-2	0.000
rs14096597	0.4450	12,515,894	KASP-1	0.000
rs15787779	0.274	12,695,726	KASP-1	0.000

¹ Calculated by contrasting feathered-leg and clean-leg DNA pools RAF values

² Calculated using the CRIMAP software

Chapter 8

Polydactyly 2 (*Po-2*) gene mapping

Abstract

Polydactyly, a limb malformation occasionally observed in vertebrates, is a standard character for some of breeds of chickens. *Po-1* and *Po-2* are two different genes or alleles, and the presence of either can result in the polydactyly phenotype. In an attempt to identify the genomic region associated with *Po-2*, a mapping population was constructed by crossing Houdan males with Langshan females and mating the F₁ *inter se*. A strong association between *SHH* gene and polydactyly was identified by SNP analyses of pooled samples. Further investigations are needed to identify the candidate region and the causal mutation.

Introduction

Polydactyly (*Po*) is a limb malformation characterized by supernumerary digits that has been observed in humans, mice, chickens, and other vertebrates (Sun et al., 2014). Warren (1944) provided evidence that polydactyly in chickens was not the reappearance of the lost fifth toe from the common ancestors of birds and mammals, but had the same mechanisms as 6 toes in humans and mice.

Polydactyly is inherited as a dominant with occasional asymmetry and lack of penetrance (Hutt, 1949). A commonly observed asymmetry is heterodactyly where only one foot shows polydactyly with the frequency more on the left (sinistral heterodactyly) than the right foot (dextral heterodactyly) (Bond, 1920; Landauer, 1948). One explanation for the bilateral difference is because the left side of chicken embryo faces

toward the yolk, the formation of the extra toe on right side may be affected by environmental factors, such as lower incubation temperatures (Sturkie, 1943). Selection experiments (Landauer, 1948) support the thesis that the expression of dextral heterodactyly is affected more by environmental factors than sinistral heterodactyly because the former responded less than the latter to selection for the same condition. Penetrance is also affected at lower artificial incubation temperatures meaning that the expression of polydactyly in heterozygotes, or even in some homozygotes, is subject to environmental influences (Warren, 1944).

The usual type of polydactyly is an unaffected No. 1 digit with an extra digit added to the outside of this digit. The extra digit can be longer than digit 1, or similar in length (Somes, 1990). In other phenotypes of polydactyly such as polyphalangy, digit 1 is longer (with an extra phalanx) but without the extra digit (Warren, 1944). Another assumption is that polyphalangy is not lengthening of digit 1, but the usual extra digit with the loss of digit 1 (Dunn et al., 2011). The extra digit may appear at another position and there may be two extra digits (6-toes) (Warren, 1944). Such phenotypic variation of polydactyly is likely affected by modifier genes because with selection, there was an increase incidence of 6-toes, polyphalangy, and both sinistral and dextral heterodactyly (Landauer, 1948). An extreme example is 'duplicate', which is probably another allele on the polydactyly locus that can cause almost a complete duplication of the foot and shank, and in extreme cases a doubling of the No. 1 digits in the wings (Warren, 1941). This phenotypic variation makes classification of polydactyly difficult, and thus hinders an understanding the genetic basis.

Genes for polydactyly have been mapped in humans (Lettice et al., 2003), mice (Masuya et al., 2007), and cats (Lettice et al., 2008). All of these causal mutations are located in ~800 bp conserved noncoding element of the limb-specific cis-regulator of the Sonic Hedgehog (*SHH*) gene termed the ZPA regulatory sequence (ZRS). It is also known as a mammal-fish-conserved-sequence-1 (MFCS-1). In the developing limb, Shh is expressed in a region of the posterior mesoderm, called the zone of polarizing activity (ZPA), and is required for proper anterior/posterior limb patterning (Mariani and Martin, 2003). Shh expression is increased in the anterior of polydactyly animal limbs implying that the ZRS long-range *SHH* control element is not a posterior specific element but is general to regions of the limb that have the potential to express Shh (Dunn et al., 2011). This increased range of Shh signaling has a role in induction loss of programmed cell death in the anterior of the leg bud, which has implications in the formation of preaxial polydactyly (Bouldin and Harfe, 2009).

Although similar functions of ZRS and Shh in mammalian and avian species digit development have been observed (Butterfield et al., 2009; Bouldin and Harfe, 2009), lacking are the relationships between ZRS and Shh. Abnormal anterior Shh expression while essential is not sufficient to induce polydactyly. Thus, mutations on ZRS may have pathways other than Shh that contribute to formation of polydactyly (Dunn et al., 2011). GATA6 may have a key role in this process because it can bind to a wild-type ZRS region with at least two downstream targets, Shh and Gli1. Ectopic expression of both of them in the anterior limb bud may be necessary for expression of polydactyly (Kozhemyakina et al., 2014).

With the known importance of ZRS region in the formation of polydactyly, the causality for polydactyly of the ss161109890 SNP located within the ZRS was reported in the Silkie by Maas et al. (2011). Although this result while consistent with other studies (Huang et al., 2006; Dorshorst et al., 2010; Robb and Delany, 2012; Sun et al., 2014, Zhang et al., 2016), and the Silkie and Sultan have this SNP, it is lacking in 3 other breeds (Faverolles, Houdan, and Dorking) that exhibit polydactyly (Zhang et al., 2016). Based on the history of these breeds, there may be two alleles associated with polydactyly in chickens (Sun et al., 2014), thus a parallel evolution event (Zhang et al., 2016). Although the causality of polydactyly seen in Silkies (denoted *Po-1* in my study) is known, the mutation involved in the Houdan kind polydactyly (denoted *Po-2* in my study) remains unknown. Therefore, *SHH* is the primary candidate gene for *Po-2*.

Materials and methods

Details of matings used in this Chapter are shown in **Table 2.1**. Briefly, 3 Houdan males were mated to 6 Langshan females to produce 3 F₁ males and 24 females that were mated *inter se* to produce 175 F₂ progeny. Classification of F₂ chicks for those that were polydactyly and those with 4 toes were made at hatch by the same individual. DNA samples were isolated from blood obtained from each chicken at 4 weeks of age, and then combined into 2 pools (**Table 2.4**). Genotyping of pooled DNA samples was via high-density 600K chicken SNP genotyping array. Values of absRAFdif were calculated by comparing the 2 pooled samples. Individual samples were genotyped via the same array. The association between each SNP and the inferred genotypes were calculated by PLINK. See details in Chapter 2. Primers for ZRS sequencing followed those of Dunn et

al. (2011). Houdan, Langshan, and Silkie chickens (3 individuals from each breed) were sequenced for ZRS.

Results and discussion

Penetrance of *Po-2*

The F₁ population (expected to be all *Po-2/po-2*⁺, n = 46, included 19 individuals that were not involved in the matings to produce the F₂) showed full penetrance. Among them, only one chicken had 4 toes on both tarsometatarsi while 2 conjoined nails were found on each of its 1st digit. The extra nails are considered as an effect of *Po-2*, although less profound than typical polydactyly. There were 14 chickens with sinistral heterodactyly and none with dextral heterodactyly in F₁ population, results consistent with previous reports (Bond, 1920; Warren, 1944; Landauer, 1948). In the F₂ population, the expected ratio of polydactyly (*Po-2/Po-2* or *Po-2/po-2*⁺) and 4 toes (*po-2*⁺/*po-2*⁺) was 3:1. Observed were 108 polydactyly and 67 with 4 toes, which was less than 3:1 ratio (p < 0.01). If this deviation was because some *Po-2/po-2*⁺ chickens did not express polydactyly, the expected penetrance in F₂ population can be calculated as 73%. The difference of penetrance between the F₁ and F₂ generations could be explained by recessive modifier genes which inhibit the expression of polydactyly in *Po-2/po-2*⁺ individuals. In the F₁ the modifier loci would have been heterozygous and thus would allow the expression of polydactyly. Their segregation in F₂ would result in some of the modifiers to act as inhibitors of polydactyly. This explanation, however, does not explain the inheritance of modifier genes responsible for heterodactyly because heterodactyly

was observed in both the F₁ and F₂ populations. The reason could be because heterodactylous genes showed some degree of dominance (Landauer, 1948).

SNP mapping

The F₂ chickens with 4 toes were a mix of *Po-2/po-2⁺* and *po-2⁺/po-2⁺* individuals because penetrance was not complete, and thus would decrease the power of detecting the associated genomic region. There was one obvious peak in chromosome 2 (**Figure 8.1**) in the region from 6.02 Mb to 21.80 Mb which contained all the SNPs with absRAFDif values greater than 0.475 (blue boxed area in **Figure 8.2**). This suggests the location of the *Po-1* mutation. In an attempt to locate candidate genes within the peak region, GO terms were searched and those related to embryonic digit morphogenesis were *SHH* and limb development membrane protein 1 (*LMBR1*) genes. The mating between Silkie and Houdan suggested that the recombination rate between *Po-1* and *Po-2* was less than 0.5% (See details in Chapter 11). Because the ZRS contains the causal mutation of *Po-1*, located on an intron of *LMBR1*, regulates *SHH* (Maas et al., 2011), and is closely linked with *Po-2*, it was considered as the primary candidate region for *Po-2*. However, sequencing showed that Houdan and Langshan's ZRS regions were identical to the reference genome while the ss161109890 mutation was found in Silkies, which was consistent with the report by Zhang et al. (2016). Because there was no significant difference between the phenotypes of *Po-1* and *Po-2*, the ectopic expression of *Shh* was also likely to be involved in the expression of *Po-2*. Thus, the causal mutation could be a regulatory element of *SHH* other than ZRS.

The analysis of individual genotyping data showed peaks associated with both *Po-1* and *Po-2* in a similar genomic region as the absRAFDif peak, but less significant (data not

shown). Reasons for the weak signal could be different genetic backgrounds among involved individuals and/or sample size.

Multiple evidence supports an association of *SHH* with *Po-2*. Therefore, linkage mapping to narrow the candidate region was not considered in this project. The next step is to apply whole genome sequencing using the F₀ chicken samples from Cross_4, DNA Pools 4_5 and 4_6, and to focus on regulatory and coding regions of the *SHH* gene. The objective would be to locate candidate mutations for subsequent investigations.

Tables and figures

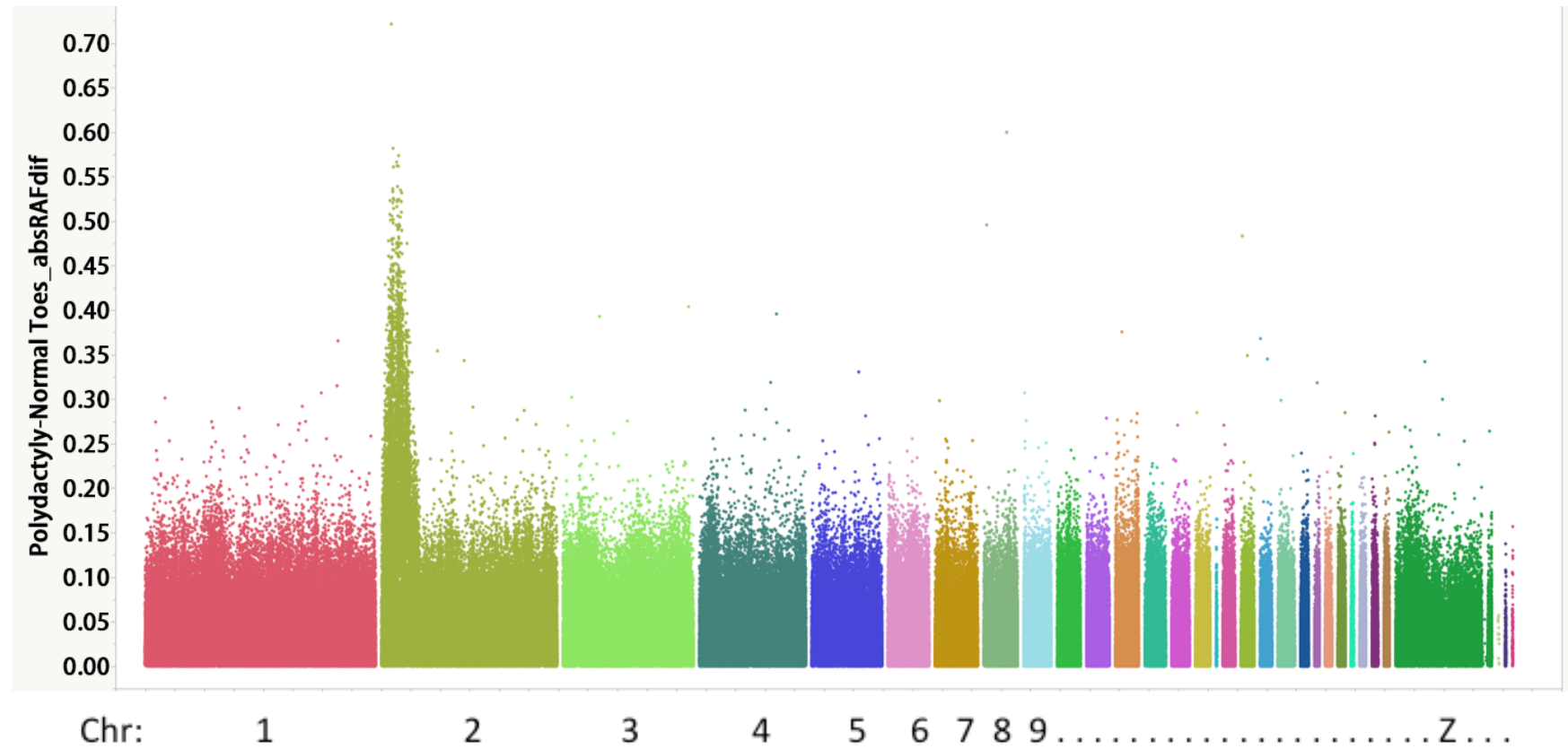


Figure 8.1. Genome-wide absRAFdif values for *Po-I* mapping. Calculated by contrasting Pools 4_5 and 4_6 of all 600K SNPs, plotted against the genomic location.

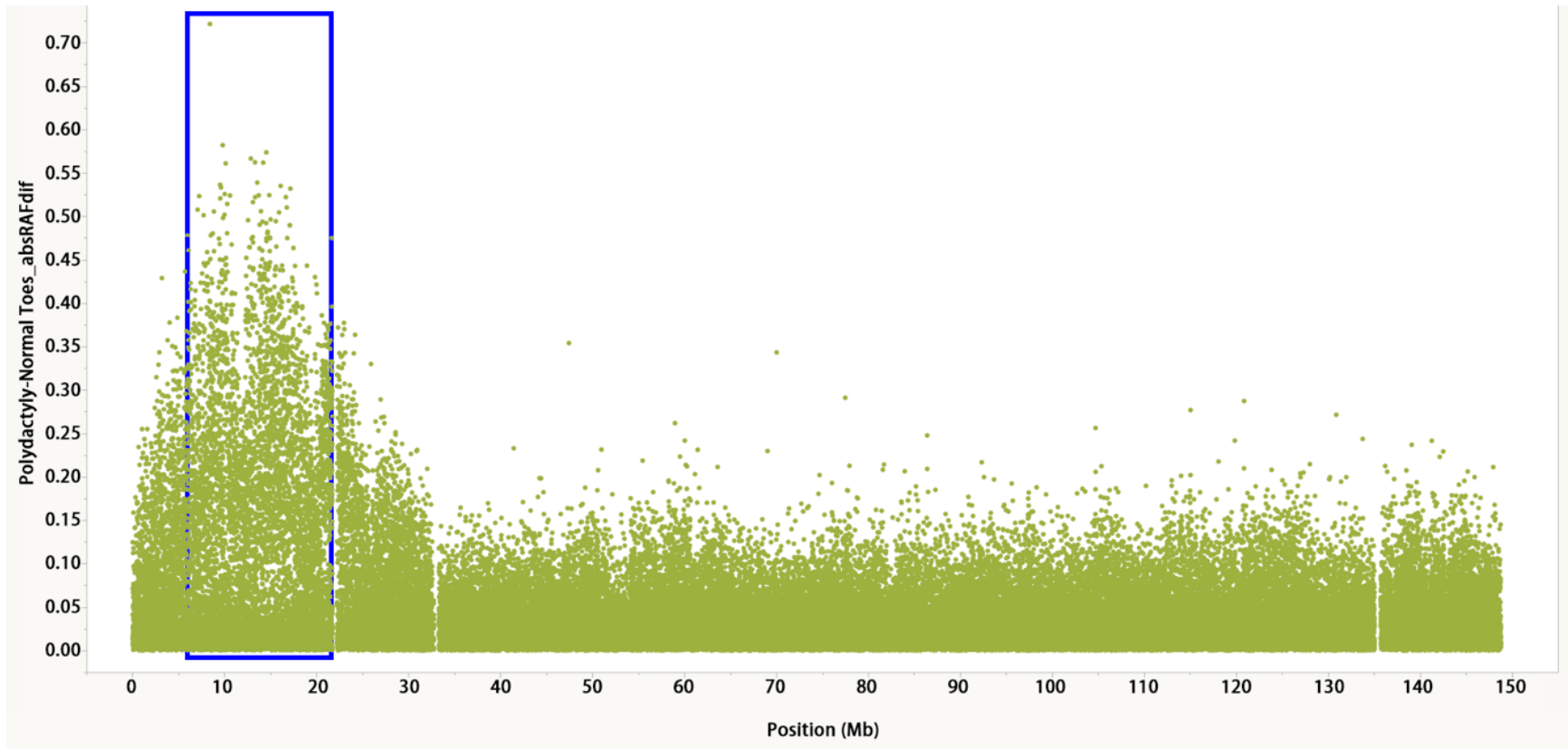


Figure 8.2. The absRAFDif values of SNPs on chromosome 2, for *Po-I* mapping. Calculated by contrasting Pools 4_5 and 4_6, plotted against the genomic location. SNPs located within the 15.8 Mb region (blue boxed area) gave absRAFDif values above 0.475, suggesting the location of the *Po-I* mutation.

References

- Bond, C. J. 1920. On the left-sided incidence of the supernumerary digit in heterodactylous fowls. *Journal of Genetics*. 10:87-91.
- Bouldin, C. M., B. D. Harfe. 2009. Aberrant FGF signaling, independent of ectopic hedgehog signaling, initiates preaxial polydactyly in Dorking chickens. *Developmental Biology*. 334:133-141.
- Butterfield, N. C., V. Metzis, E. McGlenn, S. J. Bruce, B. J. Wainwright, C. Wicking. 2009. Patched 1 is a crucial determinant of asymmetry and digit number in the vertebrate limb. *Development*. 136:3515-3524.
- Dorshorst, B., R. Okimoto, C. Ashwell. 2010. Genomic regions associated with dermal hyperpigmentation, polydactyly and other morphological traits in the Silkie chicken. *Journal of Heredity*. 101:339-350.
- Dunn, I. C., I. R. Paton, A. K. Clelland, S. Sebastian, E. J. Johnson, L. McTeir, D. Windsor, A. Sherman, H. Sang, D. W. Burt, C. Tickle, M. G. Davey. 2011. The chicken polydactyly (Po) locus causes allelic imbalance and ectopic expression of Shh during limb development. *Developmental Dynamics*. 240:1163-1172.
- Huang, Y. Q., X. M. Deng, Z. Q. Du, X. Qiu, X. Du, W. Chen, M. Morisson, S. Leroux, F. A. Ponce de Léon, Y. Da, N. Li. 2006. Single nucleotide polymorphisms in the chicken *Lmbr1* gene are associated with chicken polydactyly. *Gene*. 374:10-18.
- Hutt, F. B. 1949. *Genetics of the Fowl*. Page 47. McCraw-Hill Book Company, New York, United States.
- Kozhemyakina, E., A. Ionescu, A. B. Lassar. 2014. GATA6 is a crucial regulator of Shh in the limb bud. *PLoS Genetics*. 10:e1004072.
- Landauer, W. 1948. The phenotypic modification of hereditary polydactylism of fowl by selection and by insulin. *Genetics*. 33:133-157.
- Lettice, L. A., A. E. Hill, P. S. Devenney, R. E. Hill. 2008. Point mutations in a distant sonic hedgehog cis-regulator generate a variable regulatory output responsible for preaxial polydactyly. *Human Molecular Genetics*. 17:978-985.
- Lettice, L. A., S. J. Heaney, L. A. Purdie, L. Li, P. de Beer, B. A. Oostra, D. Goode, G. Elgar, R. E. Hill, E. de Graaff. 2003. A long-range Shh enhancer regulates expression in the developing limb and fin and is associated with preaxial polydactyly. *Human Molecular Genetics*. 12:1725-1735.
- Maas, S. A., T. Suzuki, J. F. Fallon. 2011. Identification of spontaneous mutations within the long-range limb-specific Sonic hedgehog enhancer (ZRS) that alter Sonic hedgehog expression in the chicken limb mutants oligozeugodactyly and silkie breed. *Developmental Dynamics*. 240:1212-1222.
- Mariani, F. V., G. R. Martin. 2003. Deciphering skeletal patterning: clues from the limb. *Nature*. 423:319-325.
- Masuya, H., H. Sezutsu, Y. Sakuraba, T. Sagai, M. Hosoya, H. Kaneda, I. Miura, K. Kobayashi, K. Sumiyama, A. Shimizu, J. Nagano. 2007. A series of ENU-induced single-base substitutions in a long-range cis-element altering sonic hedgehog expression in the developing mouse limb bud. *Genomics*. 89:207-214.
- Robb, E. A., M. E. Delany. 2012. The expression of preaxial polydactyly is influenced by modifying genetic elements and is not maintained by chromosomal inversion in an avian biomedical model. *Cytogenetic and Genome Research*. 136:50-68.
- Somes, R. G. Jr. 1990. Mutations and major variants of muscles and skeleton in chickens. Page 220 in "Poultry Breeding and Genetics". Crawford, R. D. ed. Elsevier, Amsterdam, Netherlands.
- Sturkie, P. D. 1943. Suppression of polydactyly in the domestic fowl by low temperature. *Journal of Experimental Zoology Part A: Ecological Genetics and Physiology*. 93:325-346.
- Sun, Y., R. Liu, G. Zhao, M. Zheng, Y. Sun, X. Yu, P. Li, J. Wen. 2014. Genome-wide linkage analysis and association study identifies loci for polydactyly in chickens. *G3: Genes, Genomes, Genetics*. 4:1167-1172.
- Warren, D. C. 1941. A new type of polydactyly in the fowl. *Journal of Heredity*. 32:3-6.
- Warren, D. C. 1944. Inheritance of polydactylism in the fowl. *Genetics*. 29:217-231.
- Zhang, Z., C. Nie, Y. Jia, R. Jiang, H. Xia, X. Lv, Y. Chen, J. Li, X. Li, Z. Ning, G. Xu. 2016. Parallel evolution of polydactyly traits in chinese and european chickens. *PloS One*. 11:e0149010.

Chapter 9

Blue (*Bl*) gene mapping

Abstract

The blue mutation (*Bl*) which generally dilutes eumelanin, is a typical example of a semi-dominant gene that in heterozygous individuals expressed an intermediate phenotype between the two homozygotes. A strong association between a 40 kb tandem duplication and *Bl* was identified by construction of a mapping population, SNP analyses of pooled DNA samples, linkage mapping, and whole genome sequencing. In addition, a putative deletion from the duplication resulted in identification of an unreported allele, which furthers our understanding of the mechanism of *Bl* mutation. The proposed gene symbol of the allele is *bl^d*.

Introduction

The blue mutation (*Bl*), first reported in Blue Andalusian chickens (Bateson and Punnett, 1906), became a classic example of semi-dominant gene (Lippincott, 1918). The blue gene dilutes eumelanin and has a dosage effect (with a black background plumage color): *Bl/bl⁺* dilutes the feather's black pigment into a grayish color (blue) across all feather tracts; *Bl/Bl* exhibits a “splash” phenotype, which is basically a white plumage with randomly scattered blue feathers (Lippincott, 1918).

The unique phenotypes of *Bl* attracted interests of early geneticists with additional details of the phenotypes described throughout the subsequent decades. These include: 1. the dilution effect of *Bl/bl⁺* is not efficient in sexual dimorphic regions (neck, back, saddle and wing bow) in male chickens which are black or very dark blue. The same

principle also applies to *Bl/Bl* males because the randomly scattered blue feathers found in sexual dimorphic regions were darker than those in other regions (Lippincott, 1918). 2. similar to “splash”, randomly scattered black feathers were observed in *Bl/bl*⁺ individuals, and described as black flecking (Lippincott, 1918). 3. the number and size of black flecking and blue flecking (blue feathers in “splash” individuals) was reduced by other genes, such as sex-linked barring and mottling that restrict eumelanin expression (Smyth, 1990). 4. small black ticks occur within a single blue feather from both *Bl/Bl* and *Bl/bl*⁺ individuals (Cock, 1953). 5. pheomelanin was not modified by *Bl* (Smyth, 1990).

The melanosomes from wild type black feathers are uniformly rod-shaped, and approximately 0.5 μm in diameter and 1.3 μm in length. In contrast, most of the melanosomes from blue feathers are spherical and approximately 0.5 μm in diameter (Bohren et al., 1943). These results are inconsistent with those from cell culture experiments, where compared to fully pigmented melanocytes, *Bl/bl*⁺ cells have larger melanosomes (Wilkins and Brumbaugh, 1979). The inconsistency might be due to different conditions between cell culture and *in vivo*, and/or that the melanosomes were modified after their translocation from melanocytes to feather vanes. Regardless, both studies showed that the poorly organized, incompletely melanized and fewer melanosomes were associated with the dilution effect of *Bl/bl*⁺.

Melanocyte heterokaryons formed between cells of the splash (*Bl/Bl*) and recessive white (*c/c*) genotypes complemented each other to produce normal pigment, previously described by Wilkins and Brumbaugh (1979). The same complementation between splash (*Bl/Bl*) and dominant white (*I/I*) was also observed later by Wilkins et al. (1982). Carefoot (1988) reported that *Bl/bl*⁺, *E/E*, *Ml/Ml*, and *Pg/Pg* genotypes resulted in a black

laced plumage pattern with a blue background. Although Bl/bl^+ and E/e^+ genotypes were effective in changing black to blue pigment, they were ineffective when the E locus was E/E (Campo and Alvarez, 1991). These reports suggest that while the blue mutation may affect aspects of pigment synthesis that are different in recessive and dominant white (*TYR* and *PMEL*, respectively), it may have a mechanism similar to that observed in lacing pattern formation interacting with MC1R.

A mutation causing a premature stop codon in microphthalmia-associated Transcription Factor (*MITF*) is responsible for “silver” plumage color in Japanese quail (Mochii et al., 1998). Subsequently, a hybrid experiment showed that “silver” in Japanese quail was homologous to “blue” in chickens (Minvielle et al., 2010). According to these reports, *MITF* was the primary candidate gene for *Bl*.

The aim of this study is to identify the causal mutation of the *Bl* gene. The procedures involved construction of a F₂ mating population, pooled DNA samples, microarray analysis, linkage mapping, whole genome sequencing, and diagnostic tests.

Materials and methods

Animals and statistical analysis

Details of matings used in this Chapter are shown in **Table 2.1**. Briefly, 2 Black Langshan males were mated to 4 D (Splash) females to produce an F₁ where 4 males and 16 females were mated *inter se* to produce 205 F₂ progeny. Classification of F₂ chickens for splash, blue, and black were made at hatch and 12 weeks by the same individual. See details in Chapter 2. The numbers of F₂ chickens with different phenotypes were analyzed by χ^2 test. Differences were considered as significant as $p < 0.05$.

Identification of the causal mutation

DNA samples were isolated from blood obtained from each chicken at 4 weeks of age, and then combined into 3 pools (**Table 2.4**). Genotyping of pooled DNA samples was via high-density 60K SNP Illumina iSelect chicken array. Values of absRAFdif were calculated by comparing each pair of the 3 pooled samples. Linkage mapping was conducted by genotyping 7 SNPs for the entire mapping population via KASP assays (**Table 2.5**). See details in Chapter 2. The candidate mutation was identified by whole genome sequencing using the pooled samples of splash and black and was confirmed by PCR and Sanger sequencing using the BP_F1, BP_F2, BP_R1, and BP_R2 primers (**Table 9.1**). The BP_F2, BP_R1, and BP_R2 primers were also used for PCR diagnostic tests of samples from 315 chickens (**Table 2.2**) and the entire mapping population. The PCRs for Sanger sequencing and diagnostic test were performed via the KAPA2G Robust HotStart PCR system and a touchdown thermal cycling protocol, which are described in Chapter 2. All exons of *MITF* were sequenced (**Table 2.6**) using 1 Blue and 1 Black Sumatra, 1 Blue and 1 Black Ameraucana, 1 Black Langshan, and 1 with splash phenotype.

Identification of the back mutation

To access genomic copy number variation (CNV), singleplex (1 probe-primers set) and duplex (2 probe-primers sets) Taqman PCRs (Ishii et al., 2006) were conducted in a total volume of 10 μ l with 2X TaqMan Genotyping Master Mix (Applied Biosystems), 0.8 mM for each of the primers, and 0.25 mM for each of the specific probes. Taqman PCRs were performed and the products detected with the ABI 7700 Fast Real-Time PCR System using the following protocol: reaction mixtures were incubated at 50 °C for 2 min

and 95 °C for 10 min followed by 40 cycles of 95 °C for 15 s, 60 °C for 1 min, and a fluorescence reading at each step. Sequences of primers and probes for the target DNA fragment (BP and LOC) were listed in **Table 9.1**, and for the house keeping gene (*SOX5*) was the same as that reported by Dorshorst et al. (2011). Quality control of all probe-primers sets was evaluated using a 7-point standard curve with a 3X dilution factor and criteria previously described by Ishii et al. (2006): slope -3.1035 to -3.7762 (PCR efficiency = 92-105%), $R > 0.995$, and y-intercept values that differ by less than 1. Taqman PCRs were performed using 7 experimental samples: 2 black and 1 white Silkie, 3 Ayam Cemani, and 1 white Frizzle. In addition, there were 6 control samples consisting of 2 D (Splash), 2 Black Langshan, and 2 F₂ individuals expressing the blue phenotype. Data were analyzed using a $\Delta\Delta C_t$ method to first normalize the target Ct value to the house keeping Ct value within the sample, and it was subsequently normalized to a known control sample (Livak and Schmittgen, 2001). Each PCR reaction has 2 technical replicates. All PCRs for standard curves were performed in one plate and all PCRs for experimental and control samples were performed in another plate.

Quantifications of copy number from genomic DNA were also conducted via a second protocol which involve the SYBR green system (Ma and Chung, 2014) instead of Taqman. PCRs were conducted in a total volume of 20 μ l with 2X Fast SYBR Green PCR Master Mix (Applied Biosystems) and 0.3 mM for each of the primers. SYBR green PCRs were performed and the products detected with the ABI 7700 Fast Real-Time PCR System using the following protocol: reaction mixtures were incubated at 95 °C for 20 s followed by 40 cycles of 95 °C for 3 s, 60 °C for 30 s, and a fluorescence reading at each cycle, ended with a standard protocol to generate melt curves. Sequences of primers for

the target DNA fragment (S1 to S5) listed in **Table 9.1**, and for the house keeping gene was the same as that used in the Taqman PCRs without the specific probe. Genomic DNA samples used in SYBR green PCRs were the same 7 experimental samples as the Taqman PCRs plus 1 D (Splash) as a control. The same $\Delta\Delta C_t$ method as in Taqman PCRs was used for data analysis. Each PCR reaction has 3 technical replicates. The PCRs for the same target DNA fragment and their controls were performed in the same plate.

Results and discussion

Plumage patterns in F₂ population

The number of splash (*Bl/Bl*), blue (*Bl/bl⁺*), and black (*bl⁺/bl⁺*) individuals (38, 104, and 63, respectively) in the F₂ population differed from a 1:2:1 ratio ($p = 0.046$). Phenotypes were consistent at both ages (hatch and 12 weeks) for each individual. That no intermediate phenotypes were observed, indicates that the expression of *Bl* was not affected by modifier or environmental factors. Therefore, the unexpected low numbers of splash and blue F₂ individuals may be associated with a side effect of *Bl* which increased mortality during early development.

Identification of candidate region

Hypothetically, when comparing between splash and black DNA pools, the highest absRAFDif value could be 1.0. It was observed that the region from 1.45 Mb to 6.73 Mb on chromosome 1 contained all of the SNPs with absRAFDif values greater than 0.65 (blue boxed area in **Figure 9.2**), which suggest the location of the *Bl* mutation. The absRAFDif calculated by comparisons involving the blue DNA pool showed a similar but less significant candidate region (data not shown). Within this region, 7 SNPs (**Table 2.3**)

were genotyped for linkage mapping via KASP assays. They showed that the causal mutation lies between rs13823450 (3.54 Mb) and rs13827135 (4.66 Mb) (red boxed area in **Figure 9.2**). See details of linkage mapping results in **Table 2.5**.

The position of candidate region (chromosome 1) showed that the causal mutation of *Bl* was not physically linked to *MITF* (chromosome 12). Meanwhile, no variation was found by the sequencing of *MITF*.

Identification of the causal mutation

Via whole genome sequencing, a tandem duplication of 40 kb (chromosome 1: 4,109,777 - 4,149,832 bp) was revealed that was associated with that splash plumage pattern. It included the entire *LOC107054603* gene and the most of the *LOC419112* gene (see **Figure 9.3**). There are multiple possibilities for this duplication to affect the functions and the expressions of genes which are responsible for *Bl*. These include, an increased expression of *LOC107054603* because of the extra copies, anomalous expressions of genes inside or flanking the duplicon because of modified regulatory elements, and an altered function of transmembrane protein 110-like (TMEM110-like, coded by *LOC419112*) because of the changes in transcripton. The break point between the two duplicons, and the junctions (5' and 3') between the duplication and the rest of genome were Sanger sequenced, which confirmed the tandem duplication and also supported the last possibility discussed above. The wild type TMEM110-like protein has 267 amino acids, while the partial sequence of *LOC419112* in the upper duplicon codes a protein with 249 amino acids. This is because the break point and a 10 bp sequence inserted 2 bp after the break point together created a premature stop codon. The protein coded by the sequence of *LOC419112* in the lower duplicon is also shorter (239 amino

acids) because a single base pair was inserted 1bp after the 3' junction, resulting in another premature stop codon (data not shown). Thus, the protein with 239 amino acids is directly related to the 1 bp insertion but not to the duplication. Diagnostic tests are needed to access the association between these 2 insertions and *Bl*. The results of such tests may provide clues about which type of protein is responsible for the phenotypes.

The duplication was also confirmed by the 6 control samples used in Taqman assays. A D (Splash) chicken has 2 copies of the break point (BP, indicates the number of the tandem duplications) and 4 copies of exon 4 of the *LOC419112* gene (LOC, indicates the number of duplicons). A blue F₂ chicken has 1 copy of BP and 3 copies of LOC. A Black Langshan has 0 copy of BP and 2 copies of LOC. Relative positions of BP and LOC amplicons were schematic summarized in **Figure 9.3**. That each *Bl* allele has 1 copy of BP and 2 copies of LOC were supported by all of these results.

In the diagnostic test, the PCR products of 339 bp fragments only suggests the absence of the break point and thus the tandem duplication; the PCR products of 339 bp and 260 bp fragments suggest the existence of the tandem duplication. However, this diagnostic test cannot differentiate between individuals with one or two copies of the break point. As the result, the break point was completely associated with blue and splash in the entire mapping population, and was found in all the other blue and splash chickens, as well as in 2 black and 1 white Silkie, 1 white Frizzle, and 5 black Ayam Cemani. If those black chickens carry the tandem duplication, then *Bl* is not completely associated with this duplication. One hypothesis is that those chickens have the break points but not the complete tandem duplication which is responsible for the *Bl*.

Identification of back mutation

In order to test the above hypothesis, assays to access genomic CNV were conducted. As the results of the assays, the control sample (*Bl/Bl*) had 2 copies of BP and 4 copies for each of the other amplicons (S3, S1, LOC, S4, S5, S2), which was consistent with the expectation for 2 complete tandem duplication. Compared with the control, each of the 2 black Silkies had 2 fewer copies of S1, LOC, and S4, suggesting a deletion containing these 3 amplicons in both *Bl* alleles. Each of the other experimental samples (white Silkie, white Frizzle, and Ayam Cemani) has 1 copy of BP, 2 copies of S1, LOC, S4, and 3 copies of the other amplicons, suggesting they were heterozygous for the wild type and the duplicated allele, while the later allele has a deletion containing S1, LOC, and S4. This duplicated-deleted allele is proposed to have gene symbol *bl^d*, which could be a back mutation from *Bl*. The CNV data suggested that these black Silkie were *bl^d/bl^d* while the other experimental samples are *bl^d/bl⁺*. It also supports the thesis that the 5' junction of the deletion lays between S3 and S1 while the 3' junction located between S4 and S5. Relative positions of all the amplicons were schematic summarized in **Figure 9.3**.

The long range PCR and sequencing experiments are currently being conducted. Complete sequences of the *Bl* and *bl^d* alleles may be obtained from them, which may provide clues of whether and how *bl^d* was back mutated from *Bl*.

Molecular mechanisms of *Bl* mutation

Because *bl^d* and *bl⁺* are phenotypically identical, they provide material to identify which parts of the tandem duplication are responsible for *Bl* and thus narrow the range of the possibilities mentioned above. Compared with *Bl*, the putative deletion in *bl^d* may contain the *LOC107054603* gene and the upper part of the *LOC419112* gene (see **Figure**

9.3). Therefore, the copy number of *LOC107054603* is decreased into the normal level and the modified TMEM110-like protein (249 or 239 AA) cannot be expressed. Thus, these two factors can possibly be the causal factors for *Bl*.

The *LOC107054603* gene is a computational predicted gene. To my knowledge, lacking are studies reporting its function. The expression of the TMEM110-like protein was observed in chicken bursal lymphocytes (Caldwell et al., 2004). Homologies of this gene are found through vertebrates, which share the 2 GO term “integral component of membrane” and “store-operated calcium entry regulator STIMATE” suggesting its function. STIMATE (stromal interaction molecule activating enhancer) is an endoplasmic reticulum (ER) transmembrane protein that serves as a positive regulator of Ca^{2+} influx in vertebrates. It activates ER-resident Ca^{2+} sensor protein STIM1 and thus induces the Ca^{2+} -NFAT signaling (Jing et al., 2015). The modified TMEM110-like protein in chickens with blue feathers may integrate into ER and affect the transformation of ER composition into premelanosome (before the stage I of melanosomes), which according to Chi et al. (2006) can explain its independence from TYR (mainly functions at stage III) and PMEL (stage I to II). In contrast, the formation of premelanosome is affected by upstream factors such as MC1R and MITF (Levy et al., 2006). The latter may explain the observed allelism between a mutation in quail *MITF* and *Bl* in chicken (Minvielle et al., 2010). The functions of the *LOC107054603* gene and the modified TMEM110-like protein need further investigation.

Phenotypes related to *bl^d*

Based on the phenotypes of blue and splash chickens, such types of back mutations may be induced instead of from a single random event. That black flecking feathers have

rod-shaped melanosomes (Lippincott, 1918) and can be affected by other eumelanin restriction factors (Smyth, 1990), indicate these feathers are independent from *Bl* in chickens carrying the *Bl* allele. Therefore, somatic mutations which eliminate the effect of *Bl* might occur in those melanoblasts before they enter the follicles of black flecking feathers. After the melanoblasts settle in the follicles, the same somatic mutations may continue to occur in their daughter cells, which is responsible for the black ticks within a single blue feather. In summary, these back mutations may constantly and randomly occur, at a higher rate than the normal mutations, which suggest they were induced, by factors such as transposons. Whether they are identical to the *bl^d* mutation identified in this study needs to be confirmed. Absence of ovarian influences may be a trigger of the back mutation, because the failure of *Bl* to express itself as fully in the sexual dimorphic regions in males is influenced by the lack of ovarian action (Lippincott, 1921). However, that it only compensates the effect of *Bl* without changing the DNA sequence is more reasonable.

In conclusion, this study showed that a tandem duplication resulting in the duplicated *LOC107054603* gene and the modified TMEM110-like protein may be responsible for the *Bl* mutation. A back mutation allele *bl^d* was identified which may associated with the induced somatic mutations.

Tables and figures

Table 9.1. PCR primers and probes used for analyzing the causal mutation of the Blue gene

Purpose	Target Element	Primer or Probe Name ¹	Primer or Probe Sequence (5'-3')	Product Size (bp)
Sequencing & diagnostic test	Break point, 5'-junction, & 3'-junction ²	BP_F1	ACACCACAGGAAACAAGCAGAA	246 ³
		BP_R1	CGTCATGGCTTTACGATTTTTG	
		BP_F2	CAGATCCTTTCATTGGTGCTTG	339 ³
		BP_R2	CTGCATTCTGCATCCTTCCTC	
Taqman	Break point ² (BP)	BP_TF	GCTGTCTGGTTGAGGACTCTG	118
		BP_TP*	CCTCTCCAGGTGCTGTTGATACTCC	
		BP_TR	GAGTTAATGCCCCAGTTCCA	
	<i>LOC419112</i> exon 4 (LOC)	LOC_TF	GCCATTTTCTTCTCCCCTTT	137
		LOC_TP*	CTTCTGACGCTGCACAGCCC	
		LOC_TR	CTGATTGGCTTGGTGTGAA	
SYBR Green	<i>LOC419112</i> intron 1 (S1)	LOC_S1F	CTGTTATTTGGGCGAGGTGT	91
		LOC_S1R	ATGGAGCATCCACAGCTTCT	
	<i>LOC419112</i> exon 6 (S2)	LOC_S2F	TGCTAGGACCCAGTCAGCTT	149
		LOC_S2R	TGACCAGGAAAAGCTCCAAC	
	5' end of the duplicon (S3)	BP5_S3F	TGGAAGTGGGGCATTAACTC	129
		BP5_S3R	AGACAAATGCTGCCCAAGAC	
	<i>LOC419112</i> intron 4 (S4 & S5)	LOC_S4F	TGGAGGCCTCTGAAGTCTGT	149
		LOC_S4R	GGAAATTTGTACGCCATCG	
		LOC_S5F	CCACAGCTTCCACTTCCTTC	140
		LOC_S5R	TATTTGCAAAGCCACTGCTG	

¹ Names with * are probes, which were 5' labeled with FAM fluorescent group and 3' labeled with MGB quencher, others are primers

² Break Point stands for the DNA sequence in the middle of the 2 duplicons; 5'-junction stands for the sequence flanking the upper boundary of the tandem duplication; 3'-junction stands for the sequence flanking the lower boundary of the tandem duplication

³ Product sizes are for amplicons containing the 5'-junction or the 3'-junction. When BP_R2 and BP_F1 work in concert to amplify the break point, the product size is 260 bp

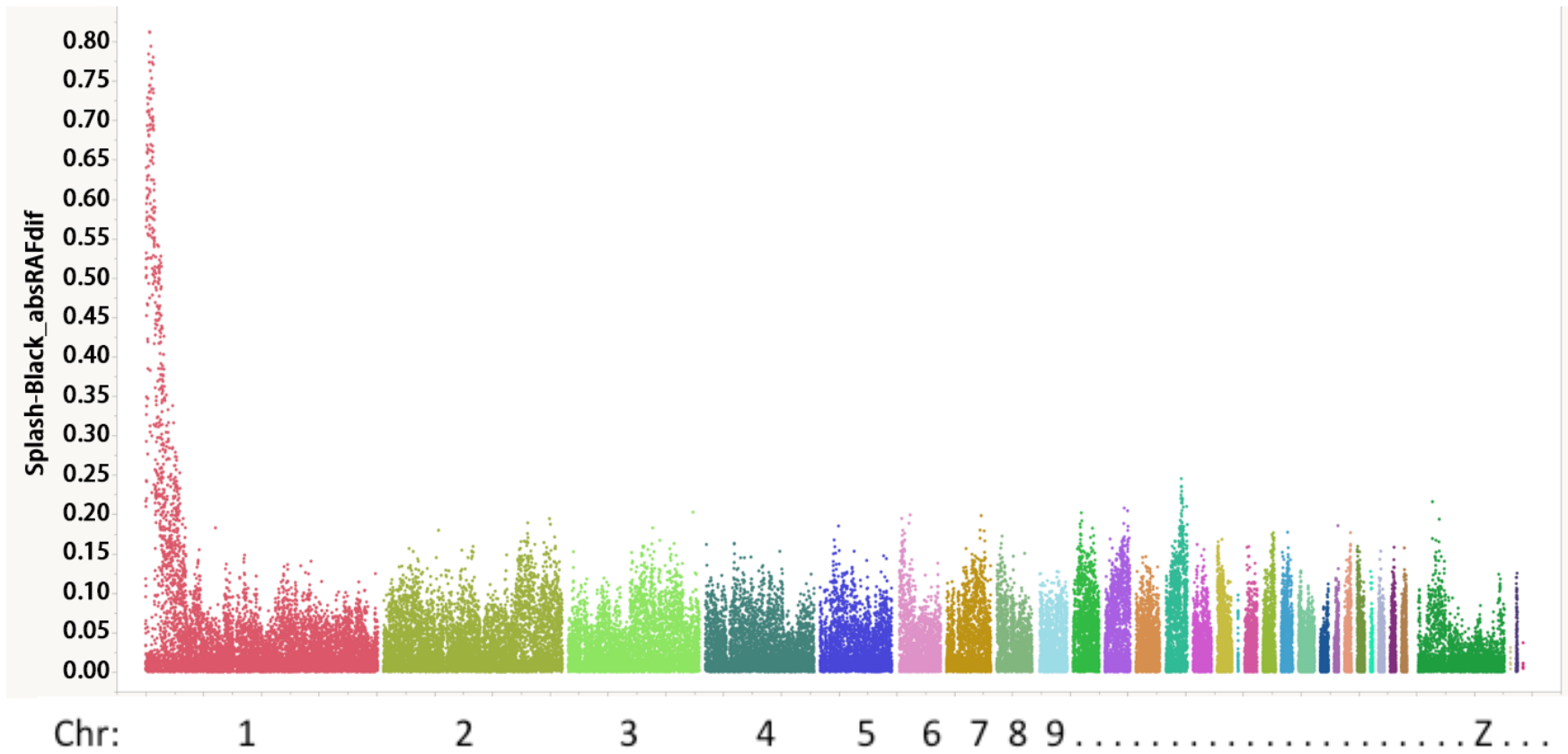


Figure 9.1. Genome-wide absRAFdif values, for *Bl* mapping. Calculated by contrasting Pools 5_2 and 5_3 of all 60K SNPs, plotted against the genomic location.

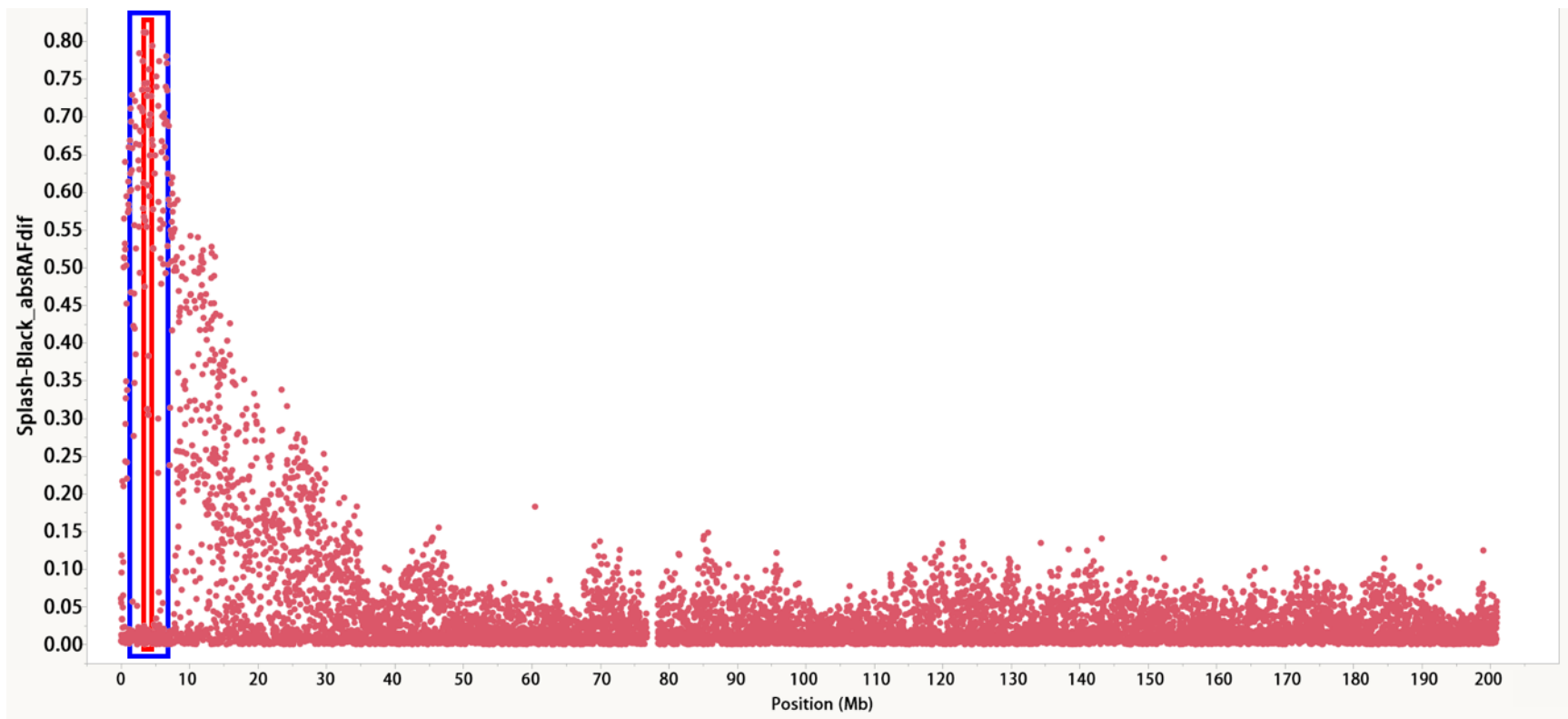


Figure 9.2. The absRAFDif values of SNPs on chromosome 1, for *BI* mapping. Calculated by contrasting Pools 5_2 and 5_3, plotted against the genomic location.

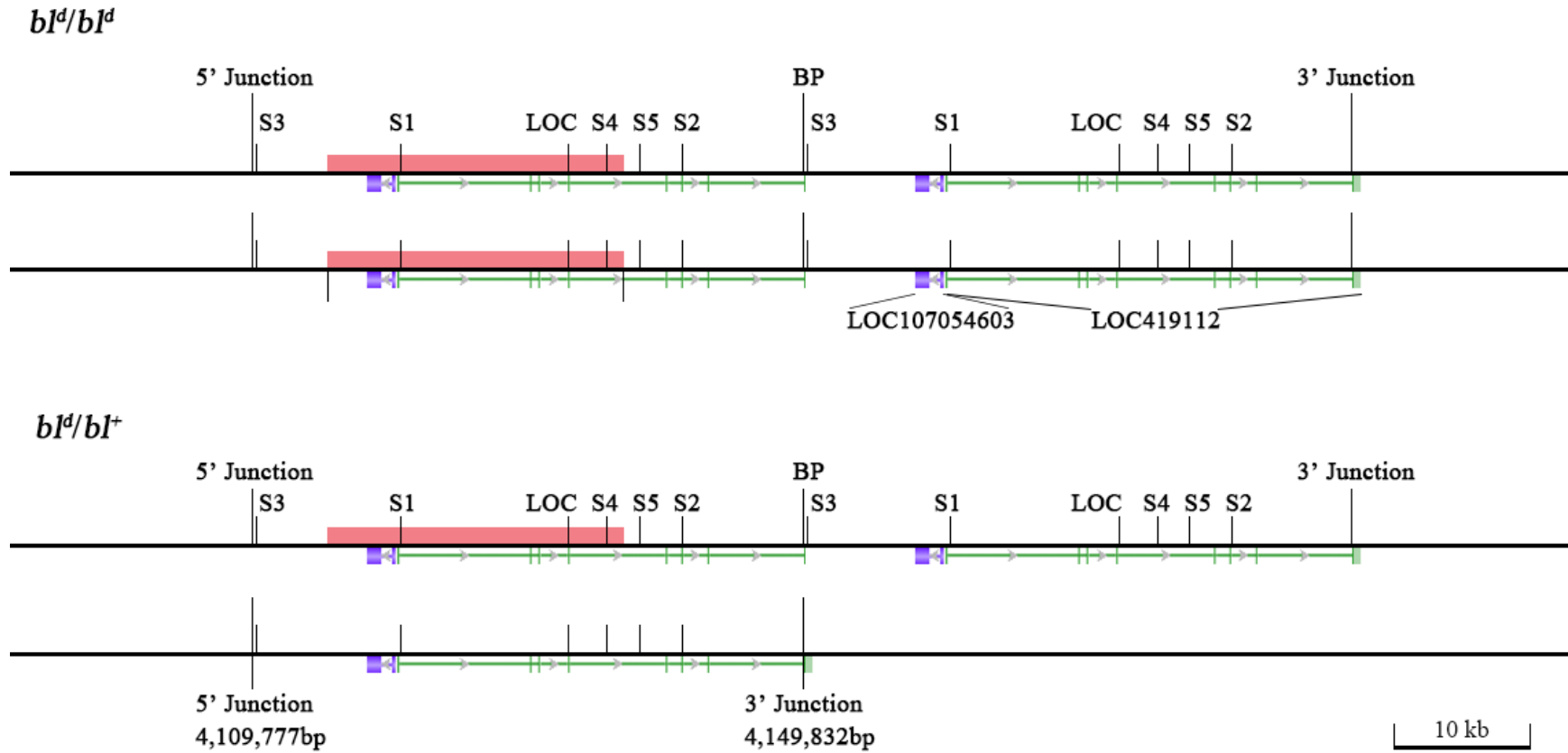


Figure 9.3. The organization of the *bl^d/bl^d* and *bl^d/bl⁺*, and the relative positions of the amplicons involved in the CNV analysis. The green bars indicate the sequence of the *LOC419112* gene, the purple bars indicate the *LOC107054603* gene. The arrows within these bars denote the direction of transcription. The red bars denote the deletion and thus the amplicons covered by the red bars cannot be detected in the CNV analysis. Without the red bars, it illustrates the organization of the *Bl* allele (a tandem duplication).

References

- Bateson, W., R. C. Punnett. 1906. Experimental studies in the physiology of heredity. Reports to the Evolution Committee of the Royal Society. 3:11-30 (Cited by Minvielle, F., B. Bed'hom, J. L. Coville, S. Ito S, M. Inoue-Murayama, G. David. 2010. The "silver" Japanese quail and the MITF gene: causal mutation, associated traits and homology with the "blue" chicken plumage. BMC Genetics. Doi: 10.1186/1471-2156-11-15).
- Bohren, B. B., R. M. Conrad, D. C. Warren. 1943. A chemical and histological study of the feather pigments of the domestic fowl. *The American Naturalist*. 77:481-518.
- Caldwell, R. B., A. M. Kierzek, H. Arakawa, Y. Bezzubov, J. Zaim, P. Fiedler, S. Kutter, A. Blagodatski, D. Kostovska, M. Koter, J. Plachy. 2004. Full-length cDNAs from chicken bursal lymphocytes to facilitate gene function analysis. *Genome Biology*. 6:R6.
- Campo, J. L., C. Alvarez. 1991. Further study on the plumage pattern of the Blue Andalusian breed. *Poultry Science*. 70:1-5.
- Carefoot, W. C. 1988. Inheritance of the laced plumage pattern of the Blue Andalusian bantam. *British Poultry Science*. 29:175-178.
- Chang, C. M., J. L. Coville, Ge. Coquerelle, D. Gourichon, A. Oulmouden, M. Tixier-Boichard. 2006. Complete association between a retroviral insertion in the tyrosinase gene and the recessive white mutation in chickens. *BMC Genomics*. Doi: 10.1186/1471-2164-7-19.
- Chi, A., J. C. Valencia, Z. Z. Hu, H. Watabe, H. Yamaguchi, N. J. Mangini, H. Huang, V. A. Canfield, K. C. Cheng, F. Yang, R. Abe, S. Yamagishi, J. Shabanowitz, V. J. Hearing, C. Wu, E. Appella, D. F. Hunt. 2006. Proteomic and bioinformatic characterization of the biogenesis and function of melanosomes. *Journal of Proteome Research*. 5:3135-3144.
- Cock, A. G. 1953. The interpretation of autosexing. *Journal of Genetics*. 51:421-433.
- Dorshorst, B., A. M. Molin, C. J. Rubin, A. M. Johansson, L. Strömstedt, M. H. Pham, C. F. Chen, F. Hallböök, C. Ashwell, L. Andersson. 2011. A complex genomic rearrangement involving the endothelin 3 locus causes dermal hyperpigmentation in the chicken. *PLoS Genetics*. 7:e1002412.
- Ishii, T., H. Sootome, L. Shan, K. Yamashita. 2007. Validation of universal conditions for duplex quantitative reverse transcription polymerase chain reaction assays. *Analytical Biochemistry*. 362:201-212.
- Jing, J., L. He, A. Sun, A. Quintana, Y. Ding, G. Ma, P. Tan, X. Liang, X. Zheng, L. Chen, X. Shi. 2015. Proteomic mapping of ER-PM junctions identifies STIMATE as a regulator of Ca²⁺ influx. *Nature Cell Biology*. 17:1339-1347.
- Kerje, S., J. Lind, K. Schütz, P. Jensen, L. Andersson. 2003. Melanocortin 1-receptor (MC1R) mutations are associated with plumage colour in chicken. *Animal Genetics*. 34:241-248.
- Kerje, S., P. Sharma, U. Gunnarsson, H. Kim, S. Bagchi, R. Fredriksson, K. Schütz, P. Jensen, G. V. Heijne, R. Okimoto, L. Andersson. 2004. The Dominant white, Dun and Smoky color variants in chicken are associated with insertion/deletion polymorphisms in the PMEL17 gene. *Genetics*. 168:1507-1518.
- Lippincott, W. A. 1918. The case of the Blue Andalusian. *The American Naturalist*. 52:95-115.
- Lippincott, W. A. 1921. Further data on the inheritance of blue in poultry. *The American Naturalist*. 55:289-327.
- Livak, K. J., T. D. Schmittgen. 2001. Analysis of relative gene expression data using real-time quantitative PCR and the 2- $\Delta\Delta$ CT method. *Methods*. 25:402-408.
- Ma, L., W. K. Chung. 2014. Quantitative analysis of copy number variants based on real-time lightCycler PCR. *Current Protocols in Human Genetics*. 80:7-21.
- Minvielle, F., B. Bed'hom, J. L. Coville, S. Ito S, M. Inoue-Murayama, G. David. 2010. The "silver" Japanese quail and the MITF gene: causal mutation, associated traits and homology with the "blue" chicken plumage. *BMC Genetics*. Doi: 10.1186/1471-2156-11-15.
- Mochii, M., T. Ono, Y. Matsubara, G. Eguchi. 1998. Spontaneous transdifferentiation of quail pigmented epithelial cell is accompanied by a mutation in the Mitf gene. *Developmental Biology*. 196:145-159.
- Smyth, J. R. Jr. 1990. Genetics of plumage, skin and eye pigmentation in chickens. Page 138 - 139 in "Poultry breeding and genetics". Crawford, R. D. ed. Elsevier, Amsterdam, Netherlands.
- Wilkins, L. M., J. A. Brumbaugh, J. W. Moore. 1982. Heterokaryon analysis of the genetic control of pigment synthesis in chick embryo melanocytes. *Genetics*. 102:557-569.
- Wilkins, L. M., J. A. Brumbaugh. 1979. Complementation and noncomplementation in heterokaryons of three unlinked pigment mutants of the fowl. *Somatic Cell Genetics*. 5:427-440.

Chapter 10

A missense mutation in *TYRPI* causes the chocolate plumage color in chicken and alters melanosome structure.

Authors

Li Jingyi¹, Bed'hom Bertrand², Marthey Sylvain², Valade Mathieu², Dureux Audrey², Moroldo Marco², Longin Christine², Coville Jean-Luc², Gourichon David³, Vieaud Agathe², Andersson Leif⁴, Dorshorst Ben¹, Tixier-Boichard Michèle².

Affiliations

¹ Department of Animal and Poultry Sciences, Virginia Tech, Blacksburg, Virginia, United States of America

² GABI, INRA, AgroParisTech, Université Paris-Saclay, 78350 Jouy-en-Josas, France

³ PEAT, INRA, 37380 Nouzilly, France

⁴ Department of Animal Breeding and Genetics, Swedish University of Agricultural Sciences, Science for Life Laboratory, Department of Medical Biochemistry and Microbiology, Uppsala University, Uppsala Sweden

Authors contribution

Li J: performed the linkage mapping experiment, KASP genotyping and candidate gene sequencing

Marthey + Valade + Bed'hom: bioinformatic analysis of the gene capture results

Moroldo + Bed'hom: designed and realized the gene capture experiment

Longin: performed the electron microscopy analysis

Dureux +Coville + Bed'hom: conceived and performed pyrosequencing tests to confirm the association between the mutation and the phenotype

Gourichon + Vieaud: set up the experimental cross and sampled the feather follicles

MTB: supervises sampling for the gene capture experiment and the backcross family, data analysis and experimental cross at INRA

Abstract

The chocolate plumage color in chickens is due to a sex-linked recessive mutation, *choc*, which dilutes eumelanin, resulting in a chocolate color. Because *TYRPI* is sex-linked in chickens, and *TYRPI* mutations are known to determine brown coat color in mammals, *TYRPI* appeared as the best candidate gene for the *choc* mutation. By combining gene mapping with gene capture, a complete association was identified between the chocolate phenotype and a missense mutation with a G to T change leading to a His214Asn change in the CuA copper-binding domain of the protein. A diagnostic test confirmed this association by screening 428 non-chocolate chickens of various origins. This is the first mutation to be described in the chicken *Tyrp1* gene. Electron microscopic analysis showed an increased number of melanosomes in feather follicles of chocolate chickens, which exhibited an abnormal structure characterized by a granular content and an irregular shape.

Significance

We describe a mutation in the chicken *Tyrp1* gene which modifies feather color by altering the number and structure of melanosomes. Our results show the importance of

the integrity of the CuA domain of the TYRP1 protein for the proper maturation of melanosomes. Although more numerous, the melanosomes of chocolate chickens have an abnormal structure which leads to a diluted color, switching from black to brown. The chocolate chicken provides a non-mammalian model for studying the role of TYRP1 and the TYRP complex in melanogenesis.

Key-words

Chicken, eumelanin, TYRP1, feather color, melanosome

Introduction

Plumage color in birds involved two types of melanin, eumelanin and pheomelanin, that constitute black/brown pigment and red/yellow pigments, respectively (Smyth, 1990). Tyrosinase (TYR), has a key role in both eumelanogenesis and pheomelanogenesis (Chang et al., 2006). Highly activated TYR recruits tyrosinase-related-protein 1 (TYRP1) and TYRP2 (also known as dopachrome tautomerase, DCT) to form the TYRP complex which is necessary for eumelanogenesis (Lamoreux et al., 1995).

In chickens, a sex-linked recessive mutation has been shown to determine the chocolate phenotype where black plumage is diluted into chocolate color (Carefoot, 1996). The mutant allele is thus named *choc* whereas the wild-type allele is named *N*. This phenotype was originally observed on one chocolate female in a small closed strain of Black Orpington bantams, suggesting the mutation occurred spontaneously. Since then, this plumage color mutation has been introduced into other breeds such as the chocolate Wyandotte. Both the chromosomal location and the phenotypic effect of the *choc*

mutation led to suggest *TYRPI* as an obvious candidate gene, since *TYRPI* mutations are generally associated with brown or chocolate coat color as in mice (Zdarsky et al., 1990), dogs (Schmutz et al., 2002), pigs (Ren et al., 2011; Wu et al., 2015), rabbits (Utzeri et al., 2014), goats (Becker et al., 2015), dun brown cattle (Berryere et al., 2003), chocolate-colored cats (Schmidt-Kuntzel et al., 2005), ‘roux’ Japanese quail (Nadeau et al., 2007), Soay sheep (Gratten et al., 2007), and blond hair in Melanesians (Kenny et al., 2012).

The aim of this study was to test the hypothesis that a *TYRPI* mutation is causing the chocolate plumage color in chickens. This was done by combining a mapping approach with a gene capture approach. Electron microscopy was undertaken to analyze the consequences of the *choc* mutation on the morphology of the melanosome.

Methods

Animals

Chocolate chickens were obtained from four origins:

- Three Chocolate Wyandotte males purchased from Greenfire Farms (USA) were crossed with five Black Langshan females purchased from McMurray Hatchery, to set up the VT linkage mapping population (8 F₀, 17 F₁ and 140 F₂),
- Two Chocolate Orpington females were sampled by Mr Bec, a French fancy breeder, one being used for the gene capture experiment,
- Two Chocolate Wyandotte animals, one male and one female, were sampled by one fancy breeder of United-Kingdom, Mr Brereton, and used to validate the diagnostic test of the mutation,

- One Chocolate Orpington male provided by Mr Bouret, a French fancy breeder, was crossed with black feathered females of the Noire du Berry breed (NDB) from the PEAT experimental facility of INRA, in order to set up a backcross (BC) family (1 F₁ male, 10 NDB females and 77 BC₁ females) used to record feather color, feathering rate (sex-linked *K* locus) and body weight at 12 weeks of age. A subset of 12 female chickens, 6 chocolate and 6 black, were slaughtered at 12 weeks of age to sample growing feather follicles. This protocol received the permit 2016021016333130-4017 delivered by the French authority for animal experiments, after a favorable advice from the Val de Loire ethical committee for animal experimentation.

In addition, 428 non-chocolate chickens from 118 different stocks or populations of experimental lines were included in this experiment (Table S1). None of these stocks or populations showed the chocolate phenotype. Virginia Tech procedures were approved by their Institutional Animal Care and Use Committee.

Linkage mapping

The segregation of chocolate and black plumage color in the F₂ of the VT linkage mapping population was observed at hatch. The sex of these F₂ was identified from blood by PCR after DNA isolation (Liu et al., 2010). Four DNA pools were prepared based on the plumage color and sex of the F₂ (Pool_1: chocolate female; Pool_2: black female; Pool_3: chocolate male; Pool_4: black male). Each individual contributed 250ng of DNA to the pool. The four pooled-DNA samples were then genotyped via high-density 60 K SNP Illumina iSelect chicken array and analyzed using the SNP-MaP approach (Docherty et al., 2007). The Illumina array provides an intensity reading for the two alleles (X and Y) at each of the 57,636 SNPs. The relative allelic frequencies (RAF) at

each SNP for each DNA pool were calculated as $X / (X + Y)$, where X and Y represent the intensity signals of the two alleles. For each SNP, the absolute RAF differences (absRAFdif) were calculated by the following contrasts: for females, Pool_1 hemizygous chocolate females (*choc/W*) versus Pool_2 black females (*N/W*); for males, Pool_3 homozygous chocolate males (*choc/choc*) versus Pool_4 heterozygous carriers (*N/choc*). absRAFdif was then plotted against the SNP genomic locations (Wells et al., 2012).

A region from 24.32 Mb to 34.26 Mb on the Z chromosome contained all SNPs with absRAFdif values greater than 0.55. Nine SNPs having relatively high absRAFdif values were chosen within or flanking this region. These nine SNPs were genotyped on all individuals of the VT mapping population via Kompetitive allele-specific PCR assay (KASP), described by Semagn et al. (2014). KASP assay was set up with 2.5 μ l of KASP V4.0 2X Mastermix (LGC Genomics, Beverly, MA, US; www.lgcgenomics.com), 1.5 μ l PCR grade water, 1 μ l DNA (50 ng/ μ l), and 0.07 μ l of primers mix (12 μ M each of allele-specific primer, carrying standard FAM or HEX compatible tails, and 32 μ M of allele-flanking primer). Two protocols were carried out on Bio-Rad CFX384 Touch™ Real-Time PCR Detection System. PCR amplification protocol 1 (KASP-1) began with 94 °C for 15 min, 10 cycles of 94 °C for 20 s and 61 °C (-0.6 °C/cycle) for 1 min each, followed by 26 cycles of 94 °C for 20 s and 55 °C for 1 min each. Protocol 2 (KASP-2) began with 94 °C for 15 min, 10 cycles of 94 °C for 20 s and 66 °C (-0.6 °C/cycle) for 1 min each, followed by 26 cycles of 94 °C for 20 s and 57 °C for 1 min each. Both KASP-1 and KASP-2 ended with endpoint fluorescence reading after 37 °C for 1 min. The readings were analyzed by Bio-Rad CFX Manager™ Software. Genotyping results were validated by at least two amplification runs for each sample. The details of these KASP assay are

shown in Table S2. The genotyping and pedigree information were analyzed with the CRIMAP software (Green et al., 1990) to calculate the genetic distances between each SNP and *choc*.

Sequencing analysis

Sequencing of *TYRPI* was performed in two steps. The first one focused on *TYRPI* exons and UTR regions in parental lines of the VT mapping cross, and the second one used target enrichment and sequence capture to analyze *TYRPI* gene and its flanking regions across 19 different populations.

Four Chocolate Wyandotte and four Black Langshan chickens were used for the first step. Seven pairs of primers were designed to amplify and sequence the exons and 5'UTR region of chicken *TYRPI* (Table S3). The KAPA2G Robust HotStart PCR system (Kapa Biosystems) was used with 1X KAPA2G GC Buffer, 0.2 mM dNTPs, 0.2 mM of each primer, 0.4 U of KAPA2G Robust HotStart DNA Polymerase, and 50 ng of DNA in a total volume of 10 μ l. A touchdown thermal cycling protocol was used for all the PCR with 95 °C for 5 min, 16 cycles of 95 °C for 30 s, 68 °C (-1.0 °C/cycle) for 30 s, and 72 °C for 30 s (60 s for primers E6&7_F and E6&7_R) each, followed by 24 cycles of 95 °C for 30 s, 52 °C for 30s, and 72 °C for 30 s (60 s for primers E6&7_F and E6&7_R) each. Amplifications were carried out on Bio-Rad CFX384 Touch™ Real-Time PCR Detection System. All sequences were visually edited, assembled and aligned with the SeqMan procedure of DNASTAR software (<http://www.dnastar.com>).

The principle of gene capture, which is to target a 'Region of Interest' (ROI) for resequencing with a very high coverage, was used for the second step. A capture array was designed for several feather color genes, including *TYRPI*, for which the captured

sequence represented 21.3 kb including the 10 kb of the gene (7 exons and 6 introns) and 10 kb flanking sequences (5 kb on 5' or 3' side). The custom Sequence Capture 385K array was designed by NimbleGen using standard parameters, except for probe uniqueness, which was set to 25 instead of the default value of 1. The capture was done for 78 samples: one chocolate female and 77 non-chocolate, males or females, from 20 different populations (Table S1).

For library preparation, 1.5 µg of genomic DNA of each sample were fragmented with a Covaris S-2 instrument (Covaris) using the following settings: number of cycles: 6, duty: 5%, intensity: 4 cycles/burst: 100, duration: 210 s. Random sheared DNAs were then assessed on a DNA 1000 Bioanalyzer chip (Agilent Technologies). For the downstream steps of end-repair, A-tailing, and adaptor ligation the TruSeq DNA Sample Preparation kit (Illumina) was used following the manufacturer's recommendations, except for the agarose gel size selection, which was skipped. Ligated samples were PCR-amplified, quantified using a Qubit (Invitrogen), and run onto a DNA 1000 Bioanalyzer chip (Agilent Technologies). Subsequently, each 385K array was used to capture samples in multiplexing. Sets of 12 uniquely indexed libraries were pooled in equimolar ratios to a final total amount of 5 µg of DNA. Then, 100 µg of *Gallus gallus* Cot-1 DNA (Applied Genetics Laboratories) and 10 µL of six different 100 µM blocking oligonucleotides (Eurofins MWG Operon) were added. The sequences of the blockers were the ones described by Meyer and Kircher (2010). The hybridization cocktail was dried in a SpeedVac at 60 °C, and for the downstream steps of hybridization, washing, and elution the protocol suggested by NimbleGen was used. Afterwards, the eluted pooled libraries were amplified through PCR. The protocol suggested by the manufacturer (Illumina) was

adopted, but the number of PCR cycles was set to 15. A final quality check was performed using a DNA 1000 Bioanalyzer chip (Agilent Technologies).

Sequencing of each multiplexed captured library was performed on a lane of HiSeq1000 (Illumina) as paired-end 101 bp reads following HiSeq1000 System User Guide. Raw image analysis and base calling were performed using the Illumina data analysis pipeline (Illumina, 2010). For removal of adaptors, custom scripts were used to trim the 3' end with base quality ≥ 10 and read lengths ≥ 40 to obtain reads for mapping. Reads were aligned initially on GalGal4 version with BWA (Li and Durbin., 2009; version 0.7.3a-r367). Following the best practices in NGS analysis (Nielsen, 2011; Van der Auwera et al., 2013), alignments files were realigned around indels and recalibrated using the GATK tool suite (McKenna et al., 2010; DePristo et al., 2011) (version 2.5-2-gf57256b), then the SNP calling was performed using the tool UnifiedGenotyper from GATK (version 3.4-46-gbc02625). Haplotypes were reconstructed using PHASE software.

In order to quickly detect SNP(s) which could be unique to the chocolate female, the mean frequency of each SNP detected in this sample was calculated for all the control samples. The position of SNPs was then updated according to the GalGal5 version of the reference genome.

Annotation of TYRP1 polymorphisms

An online GO (Gene Ontology) searching engine (Smedley et al., 2015; www.biomart.org) was used to identify genes in the candidate region of the VT design which have a molecular function, biological process, or cellular component related to pigmentation. The PROSITE webtool (Sigrist, 2013; <http://prosite.expasy.org/>) was used

to predict the motifs on TYRP1 protein sequence. The function-changing potential of the candidate mutation on *TYRP1* sequence was predicted by the PolyPhen webtool (Adzhubei et al., 2010; <http://genetics.bwh.harvard.edu/pph2/>), automatically giving a probability score for the mutation to be either possibly damaging or benign.

Diagnostic test

The candidate mutation was genotyped via the KASP assay (Table S2) using 351 non-chocolate chickens from 98 different populations (Table S1) to confirm its causality to chocolate phenotype. A pyrosequencing test was designed in order to easily distinguish the causal SNP from another neighboring missense SNP found in non-chocolate chickens (Table S4). This test can be applied to small sets of samples, from 24 to any multiple of 24. It was used to validate the association between the candidate mutation and the chocolate phenotype in the PEAT backcross family.

Melanosome morphology

Feather follicles were removed from the skin after slaughter. Feather follicle tissues were fixed with 2% glutaraldehyde in 0.1 M Na cacodylate buffer pH 7.2, for 4 hours at room temperature. Samples were then contrasted with Oolong Tea Extract (OTE) 0.5% in cacodylate buffer, postfixed with 1% osmium tetroxide containing 1.5% potassium cyanoferrate, gradually dehydrated in ethanol (30% to 100%) and substituted gradually in mix of propylene oxide-epon and embedded in Epon. (Delta microscopie – Labège France). Thin sections (70 nm) were collected onto 200 mesh cooper grids, and counterstained with lead citrate. Grids were examined with Hitachi HT7700 electron microscope operated at 80 kV (Elexience – France), and images were acquired with a

charge-coupled device camera (AMT). This work has benefited from the facilities and expertise of MIMA2 MET (GABI, INRA, Agroparistech, Paris-Saclay University).

Results

SNP and linkage mapping

In the 3-generation linkage mapping population, the 5 F₁ males that were heterozygous carriers of *choc* (*N/choc*) had black plumage, and the 12 F₁ females hemizygous carriers of *choc* (*choc/W*) had chocolate plumage. In F₂, the observed ratio of 29 chocolate males (*choc/choc*) and 45 black males (*N/choc*) did not deviate significantly from the expected 1:1 ratio ($p = 0.06$), nor for the females with 34 chocolate females (*choc/W*) and 32 black females (*N/W*) ($p = 0.81$). The result was consistent with a sex-linked recessive determinism.

The *choc* mutation was initially mapped by estimating SNP allele frequencies in DNA pools representing different phenotype classes. The *absRAFdif* value calculated by contrasting chocolate pool and black pool for a given SNP is expected to be high if it is closely linked with *choc*. In theory, the highest *absRAFdif* value could be 1.0 when comparing the pools of F₂ females (*choc/W* vs. *N/W*) and 0.5 when comparing the pools of F₂ males (*choc/choc* vs. *N/choc*). The two comparisons showed a peak of *absRAFdif* values at about the same location on Chr. Z, while the peak for the female comparison (Figure 1a) was sharper than the one for the male comparison (data not shown). Because of the microarray based error and pool construction error, the estimated allele frequencies from SNP-MaP is arbitrary (Macgregor, 2007). The individual genotyping performed with the nine chosen SNPs demonstrated that *choc* was located in a 3.57 Mb region

defined by rs16106682 (28.27 Mb) and rs14778077 (31.84 Mb) on Chr. Z (Table S2; Figure 1b). Among all known genes in this region (Figure 1c), the only one found with GO terms related to pigmentation was *TYRPI* which was a strong candidate gene for *choc*.

Sequence analysis

A total of 186 SNPs were detected by the gene capture approach in the 78 individuals for the *TYRPI* gene and its flanking regions: 25 were upstream variants, 2 were 5'-UTR variants, 102 were intronic variants, 12 were located in the coding sequence including 2 missense variants, 2 were 3'-UTR variants and 43 were downstream variants. A subset of 156 SNPs was selected according to their quality score, which covered a region of 18,659 bp between positions 30,818,152 and 30,836,811 on the Z chromosome (Figure 2). Fifteen haplotypes were identified among the 78 individuals (Table 1). These haplotypes could be organized in a network showing 4 groups of haplotypes (Figure S1). The *choc* female was the only one to carry haplotype 11 which differed by one SNP at position 30,830,367 from all other haplotypes. Sequencing the coding and UTR regions of *TYRPI* gene in the Chocolate Wyandotte and Black Langshan of the VT mapping population also showed this SNP was completely associated with *choc*. The 18,659bp region included also 42 indels, but none was specific to the *choc* female.

The SNP characteristic of chocolate animals was a missense mutation with a G to T change at position 30,830,367 leading to a His214Asn change. The ancestral haplotype where the *choc* mutation appeared, (named haplotype 10 in Table 1), was the most frequent among the 78 individuals, it occurred in White Leghorns as well as brown-egg layers. Comparing the subset of SNPs commonly detected in the gene capture with the

sequences of the VT parental lines showed that the Chocolate Wyandotte carried the same haplotype as the *choc* female used in the gene capture experiment, and that the Langshan females carried haplotypes 5 or 9 which differ at very few positions that were not studied on the VT parental lines.

Identification of the causal mutation

The sequence analysis showed that the His214Asn mutation was an obvious candidate for the '*choc*' mutation. Genotyping the SNP at position 30,830,367 in the entire VT mapping population, in the 77 BC₁ females from INRA (41 chocolate and 36 black-feathered), and in 428 non-chocolate chickens from 118 different stocks or populations of experimental lines, showed its complete association with *choc*, which strongly indicates that it is the causal mutation for the chocolate phenotype.

The TYRP1 protein in chickens has two copper-binding domains (CuA and CuB; Figure 3) and CuA contains the amino acid from 214 to 231. The His214Asn substitution changes the first amino acid of CuA from a positively-charged into a non-charged amino acid. This mutation was predicted to be POSSIBLY DAMAGING with a score of 1.000 by PolyPhen. That is because this amino acid is conserved among all sequenced vertebrates, suggesting that *TYRP1* His214Asn could determine the *choc* mutation.

The melanosomes of the chocolate females exhibited an abnormal morphology, with an irregularly shaped envelope and a granular content (Figure 4). Furthermore, the number of melanosomes tended to be 3 times higher in the chocolate females.

There was no effect of the chocolate mutation on body weight at 12 weeks of age in the BC₁ females, which reached 1285 g for the 41 chocolate females and 1280 g for the 36 black feathered females. In this family, the *choc* mutation was linked to the late-

feathering *K* mutation, since 2/3 of chocolate BC₁ females were also showing late-feathering and 1/3 exhibited a normal feather growth rate. Late-feathering tends to soften the feather structure, but there was no direct effect of the chocolate mutation on feather structure.

Discussion

In this study, linkage mapping, gene capture and SNP diagnostic tests were used to identify the causal mutation of the sex-linked chocolate plumage color in chickens. Our results provide evidence that the His214Asn mutation in *TYRP1* is causing this phenotype.

Several major plumage phenotypes of chickens, such as extended black, dominant white and recessive white, have been mapped. The causal mutations of these three phenotypes primarily influence melanogenesis within the melanocytes (Kerje et al., 2003, 2004; Chang et al., 2006). The initial step in melanogenesis is to transform tyrosine to dopaquinone, via tyrosinase (TYR), a membrane protein integrating melanosomes. Dopaquinone can become a complex quinone either when dopachrome is converted in 5, 6-dihydroxyindole (DHI) by TYRP1 enzyme, or when dopachrome is converted in DHI-2-carboxylic acid (DHICA) by TYRP2 enzyme. Then, the complex quinone is polymerized in eumelanin (Hearing, 2011).

The chicken TYRP1 protein has four distinct domains: an EGF-like domain signature 1 (98 to 109 AA), a Laminin- type EGF-like domain signature (98 to 121 AA), a Tyrosinase CuA-binding region signature (214 to 231 AA) and a Tyrosinase and hemocyanins CuB-binding region signature (396 to 407 AA) (April et al., 1998).

Furumura et al. (1998) reported that mouse TYRP1 bound neither copper, zinc nor iron, but an unknown kind of metal ion. In contrast, Olivares and Solano (2009) reported on experiments that demonstrated a CuA site of mouse TYRP1 bound copper and sustain the typical TYR activities. Thus, how metal ions cooperate with TYRP1 needs further investigation as this cooperation is likely to be functionally important because all three members of the tyrosinase protein family (TYR, TYRP1 and TYRP2) have this CuA site. Each CuA site contains three conserved histidine residues (Furumura et al., 1998). Together with the three His residues in CuB, these His directly bind to the metal ions in human and mushroom TYR (Olivares and Solano, 2009; Washington, 2015). The missense mutation (His214Asn) detected in our study disrupts one of those histidine residues and is therefore expected to have a large negative effect on TYRP1 function.

Studies using mice melanocytes showed that TYRP1 stabilizes the tyrosinase protein and that *TYRP1* mutations may result in misrouting and early degradation of tyrosinase (Manga, 2000). Indeed, tyrosinase and TYRP1 are processed together as a complex in the endoplasmic reticulum so that a mutation in one would cause the abnormal retention and degradation of the other (Kushimoto et al., 2003). Mutations of TYRP1 in mice have been associated with a reduced cell proliferation rate in melanocyte cell cultures and an impaired maturation of melanosomes with a higher proportion of immature forms, i.e. type III melanosomes (Sarangarajan et al., 2000). Generally, several dilution mutations in mice have been associated with an abnormal morphology of melanosomes: in particular, the pearl mutation was associated with an abnormal melanosomal membrane, (N'Guyen et al., 2002) which showed a granular aspect resembling the one observed on the melanosomes of the *choc* feather keratinocytes in our study. The abnormal morphology

of melanosomes in chocolate chickens brings new evidence that a proper function of TYRP1 is needed for the full maturation of the melanosome and that the three enzymes, TYR, TYRP1 and TYRP2, are not only key for pigment production but also for pigment packaging. The increased number of melanosomes in the chocolate chickens tends to suggest that the lack of fully mature melanosomes could trigger the synthesis of new melanosomes, which does not compensate for the abnormal structure, since the perceived plumage color is diluted.

Conclusion

We have shown that chickens with sex-linked chocolate plumage color carry the non-synonymous mutation His214Asn in *TYRP1*. To our knowledge, this is the first report about mutations on the chicken *TYRP1* gene. This finding strengthens the importance of the Copper-binding domain A of the TYRP1 protein, which is also mutated in dogs and rabbits exhibiting a brown coat color. The abnormal morphology of melanosomes in chocolate chickens brings new evidence that a proper function of TYRP1 is needed for the full maturation of the melanosme and that the three enzymes, TYR, TYRP1 and TYRP2, are not only key for pigment production but also for pigment packaging.

The two different approaches used, linkage mapping and sequence capture on a large range of populations, were complementary and consistent with each other. The sequence capture has proven to be very useful for the identification of the ancestral haplotype where the mutation first took place. From a breeding viewpoint, diagnostic

tests are available for breeders to distinguish heterozygous carrier males from non-mutant males which would not be distinguished at the phenotypic level.

Acknowledgements

The help of the animal caretakers of the PEAT experimental unit is gratefully acknowledged. The authors would like to thank the breeders and the colleagues who provided them with biological samples (feather pulp, blood or DNA) from chocolate and non-chocolate chickens. The gene capture experiment conducted at INRA was funded by the ANR project 'CapSeqAn'. The research contributions of Jingyi Li were conducted in the laboratory of Paul Siegel at Virginia Tech.

References:

- Adzhubei, I. A., S. Schmidt, L. Peshkin, V. E. Ramensky, A. Gerasimova, P. Bork, A. S. Kondrashov, S. R. Sunyaev. 2010. A method and server for predicting damaging missense mutations. *Nature Methods*. 7:248-249.
- April, C. S., I. J. Jackson, S. H. Kidson. 1998. The cloning and sequencing of a cDNA coding for chick tyrosinase-related protein-1. *Biochimica et Biophysica Acta (BBA)-Gene Structure and Expression*. 1395:7-12.
- Becker, D., M. Otto, P. Ammann, I. Keller, C. Drögemüller, T. Leeb. 2015. The brown coat colour of Coppernecked goats is associated with a non-synonymous variant at the TYRP1 locus on chromosome 8. *Animal Genetics*. 46:50-54.
- Berryere, T. G., S. M. Schmutz, R. J. Schimpf, C. M. Cowan, J. Potter. 2003. TYRP1 is associated with dun coat colour in Dexter cattle or how now brown cow? *Animal Genetics*. 34:169-175.
- Carefoot, W. C. 1996. Chocolate - a sex-linked recessive plumage colour mutant of the domestic fowl. *British Poultry Science*. 37:867-868.
- Chang, C. M., J. L. Coville, Ge. Coquerelle, D. Gourichon, A. Oulmouden, M. Tixier-Boichard. 2006. Complete association between a retroviral insertion in the tyrosinase gene and the recessive white mutation in chickens. *BMC Genomics*. Doi: 10.1186/1471-2164-7-19.
- DePristo, M. A., E. Banks, R. Poplin, K. V. Garimella, J. R. Maguire, C. Hartl, A. A. Philippakis, G. Del Angel, M. A. Rivas, M. Hanna, A. McKenna. 2011. A framework for variation discovery and genotyping using next-generation DNA sequencing data. *Nature Genetics*. 43:491-8. Doi: 10.1038/ng.806.
- Docherty, S. J., L. M. Butcher, L. C. Schalkwyk, R. Plomin. 2007. Applicability of DNA pools on 500 K SNP microarrays for cost-effective initial screens in genomewide association studies. *BMC Genomics*. 8:214.
- Furumura, M., F. Solano, N. Matsunaga, C. Sakai, R. A. Spritz, V. J. Hearing. 1998. Metal ligand-binding specificities of the tyrosinase-related proteins. *Biochemical and Biophysical Research Communications*. 242:579-585.

- Gratten, J., D. Beraldi, B. V. Lowder, A. F. McRae, P. M. Visscher, J. M. Pemberton, J. Slate. 2007. Compelling evidence that a single nucleotide substitution in TYRP1 is responsible for coat colour polymorphism in a free-living population of Soay sheep. *Proceedings of the Royal Society of London B: Biological Sciences*. 274:619-626.
- Green P, K. Falls, S. Crooks. 1990. Documentation for CRIMAP, version 2.4. Washington University School of Medicine, St Louis, MO.
- Hearing, V. J. 2011. Determination of melanin synthetic pathways. *Journal of Investigative Dermatology*. 131:E8-E11.
- Kenny, E. E., N. J. Timpson, M. Sikora, M. C. Yee, A. Moreno-Estrada, C. Eng, S. Huntsman, E. G. Burchard, M. Stoneking, C. D. Bustamante, S. Myles. 2012. Melanesian blond hair is caused by an amino acid change in TYRP1. *Science*. 336:554-554.
- Kerje, S., J. Lind, K. Schütz, P. Jensen, L. Andersson. 2003. Melanocortin 1-receptor (MC1R) mutations are associated with plumage colour in chicken. *Animal Genetics*. 34:241-248.
- Kerje, S., P. Sharma, U. Gunnarsson, H. Kim, S. Bagchi, R. Fredriksson, K. Schütz, P. Jensen, G. V. Heijne, R. Okimoto, L. Andersson. 2004. The Dominant white, Dun and Smoky color variants in chicken are associated with insertion/deletion polymorphisms in the PMEL17 gene. *Genetics*. 168:1507-1518.
- Kushimoto T., J. C. Valencia, G. E. Costin, K. Toyofuku, H. Watabe, K. I. Yasumoto, F. Rouzaud, W. D. Vieira, V. J. Hearing. 2003. The melanosome: an ideal model to study cellular differentiation. *Pigment Cell Research*. 16: 237–244.
- Lamoreux, M. L., B. K. Zhou, S. Rosemblat, S. J. Orlow. 1995. The pinkeyed-dilution protein and the eumelanin/pheomelanin switch: in support of a unifying hypothesis. *Pigment Cell Research*. 8:263-270.
- Li, H., R. Durbin. 2009. Fast and accurate short read alignment with Burrows-Wheeler transform. *Bioinformatics*. 25:1754-1760.
- Liu, W.Y., C. J. Zhao, J. Y. Li. 2010. A non-invasive and inexpensive PCR-based procedure for rapid sex diagnosis of Chinese gamecock chicks and embryos. *Journal of Animal and Veterinary Advances*. 9:962-970.
- Macgregor, S. 2007. Most pooling variation in array-based DNA pooling is attributable to array error rather than pool construction error. *European Journal of Human Genetics*. 15:501-504.
- Manga, P., K. Sato, L. Ye, F. Beermann, M. Lamoreux, S. J. Orlow, 2000. Mutational analysis of the modulation of tyrosinase by tyrosinase-related proteins 1 and 2 in vitro. *Pigment Cell Research*. 13:364-374.
- McKenna, A., M. Hanna, E. Banks, A. Sivachenko, K. Cibulskis, A. Kernytzky, K. Garimella, D. Altshuler, S. Gabriel, M. Daly, M. A. DePristo. 2010. The genome analysis toolkit: a MapReduce framework for analyzing next-generation DNA sequencing data. *Genome Research*. 20:1297-1303.
- Nadeau, N. J., N. I. Mundy, D. Gourichon, F. Minvielle. 2007. Association of a single-nucleotide substitution in TYRP1 with roux in Japanese quail (*Coturnix japonica*). *Animal Genetics*. 38:609-613.
- Nielsen, R., J. S. Paul, A. Albrechtsen, Y. S. Song. 2011. Genotype and SNP calling from next-generation sequencing data. *Nature Reviews Genetics*. 12:443-451.
- Olivares, C., F. Solano. 2009. New insights into the active site structure and catalytic mechanism of tyrosinase and its related proteins. *Pigment Cell & Melanoma Research*. 22:750-760.
- Ren, J, H. Mao, Z. Zhang, S. Xiao, N. Ding, L. Huang. 2011. A 6-bp deletion in the TYRP1 gene causes the brown colouration phenotype in Chinese indigenous pigs. *Heredity*. 106:862-868.
- Sarangarajan R., Y. Zhao, G. Babcock, J. Cornelius, M. L. Lamoreux, R. E. Boissy. 2000. Mutant alleles at the Brown locus encoding tyrosinase-related protein-1 (*trp-1*) affect proliferation of mouse melanocytes in culture. *Pigment Cell Research*. 13:337-344.
- Schmidt-Kuntzel, A., E. Eizirik, S. J. O'Brien, M. Menotti-Raymond. 2005. Tyrosinase and tyrosinase related protein 1 alleles specify domestic cat coat color phenotypes of the albino and brown loci. *Journal of Heredity*. 96:289-301.
- Schmutz, S. M., T. G. Berryere, A. D. Goldfinch. 2002. TYRP1 and MC1R genotypes and their effects on coat color in dogs. *Mammalian Genome*. 13:380-387.
- Semagn K., R. Babu, S. Hearne, M. Olsen. 2014. Single nucleotide polymorphism genotyping using Kompetitive Allele Specific PCR (KASP): overview of the technology and its application in crop improvement. *Molecular Breeding*. 33:1-14.
- Sigrist, C.J., E. De Castro, L. Cerutti, B. A. Cuche, N. Hulo, A. Bridge, L. Bougueleret, I. Xenarios, 2013. New and continuing developments at PROSITE. *Nucleic Acids Research*. D344-7.

- Smedley, D., S. Haider, S. Durinck, L. Pandini, P. Provero, J. Allen, O. Arnaiz, M. H. Awedh, R. Baldock, G. Barbiera, P. Bardou, T. Beck, A. Blake, M. Bonierbale, A. J. Brookes, G. Bucci, I. Buetti, S. Burge, C. Cabau, J. W. Carlson, C. Chelala, C. Chrysostomou, D. Cittaro, O. Collin, R. Cordova, R. J. Cutts, E. Dassi, A. D. Genova, A. Djari, A. Esposito, H. Estrella, E. Eyra, J. Fernandez-Banet, S. Forbes, R. C. Free, T. Fujisawa, E. Gadaleta, J. M. Garcia-Manteiga, D. Goodstein, K. Gray, J. A. Guerra-Assunção, B. Haggarty, D. J. Han, B. W. Han, T. Harris, J. Harshbarger, R. K. Hastings, R. D. Hayes, C. Hoede, S. Hu, Z. L. Hu, L. Hutchins, Z. Kan, H. Kawaji, A. Keliet, A. Kerhornou, S. Kim, R. Kinsella, C. Klopp, L. Kong, D. Lawson, D. Lazarevic, J. H. Lee, T. Letellier, C. Y. Li, P. Lio, C. J. Liu, J. Luo, A. Maass, J. Mariette, T. Maurel, S. Merella, A. M. Mohamed, F. Moreews, I. Nabihoudine, N. Ndegwa, C. Noirot, C. Perez-Llamas, M. Primig, A. Quattrone, H. Quesneville, D. Rambaldi, J. Reecy, M. Riba, S. Rosanoff, A. A. Saddiq, E. Salas, O. Sallou, R. Shepherd, R. Simon, L. Sperling, W. Spooner, D. M. Staines, D. Steinbach, K. Stone, E. Stupka, J. W. Teague, A. Z. Dayem Ullah, J. Wang, D. Ware, M. Wong-Erasmus, K. Youens-Clark, A. Zadissa, S. J. Zhang, A. Kasprzyk. 2015. The BioMart community portal: an innovative alternative to large, centralized data repositories. *Nucleic Acids Research*. 43:W589-W598.
- Smyth, J. R. Jr. 1990. Genetics of plumage, skin and eye pigmentation in chickens. Pages 109-110 in "Poultry breeding and genetics". Crawford, R. D. ed. Elsevier, Amsterdam, Netherlands.
- Utzeri, V. J., A. Ribani, L. Fontanesi. 2014. A premature stop codon in the TYRP1 gene is associated with brown coat colour in the European rabbit (*Oryctolagus cuniculus*). *Animal Genetics*. 45:600-603.
- Auwerwa, G. A., M. O. Carneiro, C. Hartl, R. Poplin, G. del Angel, A. Levy-Moonshine, T. Jordan, K. Shakir, D. Roazen, J. Thibault, E. Banks. 2013. From FastQ data to high-confidence variant calls: the genome analysis toolkit best practices pipeline. *Current Protocols in Bioinformatics*. 11-10.
- Washington, C., J. Maxwell, J. Stevenson, G. Malone, E. W. Lowe, Q. Zhang, G. Wang, N. R. McIntyre. 2015. Mechanistic studies of the tyrosinase-catalyzed oxidative cyclocondensation of 2-aminophenol to 2-aminophenoxazin-3-one. *Archives of Biochemistry and Biophysics*. 577:24-34.
- Wells, K. L., Y. Hadad, D. Ben-Avraham, J. Hillel, A. Cahaner, D. J. Headon. 2012. Genome-wide SNP scan of pooled DNA reveals nonsense mutation in FGF20 in the scaleless line of featherless chickens. *BMC Genomics*. 13:1.
- Wu, X., Y. Zhang, L. Shen, J. Du, J. Luo, C. Liu, Q. Pu, R. Yang, X. Li, L. Bai, G. Tang. 2016. A 6-bp deletion in exon 8 and two mutations in introns of TYRP1 are associated with blond coat color in Liangshan pigs. *Gene*. 578:132-136.
- Zdarsky, E., J. Favor, I. J. Jackson. 1990. The molecular basis of Brown, an old mouse mutation, and of an induced revertant to wild type. *Genetics*. 126:443-449.

Tables and figures

Table 1. Fifteen haplotypes identified in the 78 individuals. The one SNP found only in the *choc* female is boxed.

haplotype	Freq.	Haplotype sequence
11 (<i>choc</i>)	1.4%	GAAGAGTGCGAAAAACCATCCTTGATATCTCAAATCCGCATAAACCCTGCCCTGCCGCACGCTGGGAGTATGACCGGGTGAAGCTCTGTCGTTTATCCGGGAAATCCACATATATTTCCACATTTTAATCTCTACAAATGGGTAGCTTGAAAAGAGT
10 (Anc.)	29.5%	GAAGAGTGCGAAAAACCATCCTTGATATCTCAAATCCGCATAAACCCTGCCCTGCCGCACGCTGGGAGTATGACCGGGTGAAGCTCTGTCGTTTATCCGGGAAATCCACATATATGTTCCACATTTTAATCTCTACAAATGGGTAGCTTGAAAAGAGT
12	7.5%	GAAGAGTGCGAAAAACCATCCTTGATATCTCAAATCCGCATAAACCCTGCCCTGCCGCACGCTGGGAGTATGACCGGGTGAAGTCTGTCGTTTATCCGGGAAATCCACATATATGTTCCACATTTTAATCTCTACAAATGGGTAGCTTGAAAAGAGT
Reference	-	AAATCACGTAAAGCGCGTTCTTAACATCTAATAACCGAATCACTGGCCCCACCACACGCTGGGAGTATGACCGACTGAGCTCTTCCATTATGCGGGCAATCCCAAATATACGTTCCACATTTTAATCTCTACGATTAGGTAGCTTAGAAAAGAG
1	19.2%	ACGTCACGTAAGGCGCGTTCTCAGCAATCAATAACCGAATCGCTGACCCACCACACGCTGGGAATATGACCGACTGTGCTCTTCCATTATGCTGGGCAATCCAAATATGCGTTCCACATTTTAATCTCTACGATTAAAGTAGCTAGAAAAGAG
2	0.7%	ACGTCACGTAAGGCGCGTTCTCAGCAATCAATAACCGAATCGCTGACCCACCACACGCTGGGAATATGACCGACTGTGCTCTTCCATTATGCTGGGCAATCCAAATATGCGTTCCACATTTTAATCTCTACGATTAAAGTAGCTAGAAAAGAG
3	1.4%	ACGTCACGTAAGGCGCGTTCTCAGCAATCAATAACCGAATCGCTGACCCACCACACGCTGGGAATATGACCGACTGTGCTCTTCCATTATGCTGGGCAATCCAAATATGCGTTCCACATTTTAATCTCTATGATTAAAGTAGCTAGAAAAGAG
4	1.4%	ACGTCACGTAAGGCGCGTTCTCAGCAATCAATAACCGAATCGCTGACCCACCACACGATGGGAATATGACCGACTGTGCTCTTCCATTATGCTGGGCAATCCAAATATGCGTTCCACATTTTAATCTCTACGATTAAAGTAGCTAGAAAAGAG
15	0.7%	GCGTCACGTAAGGCGCGTTCTCAGCAATCAATAACCGAATCGCTGACCCACCACACGCTGGGAATATGACCGACTGTGCTCTTCCATTATGCTGGGCAATCCAAATATGCGTTCCACATTTTAATCTCTACGATTAAAGTAGCTAGAAAAGAG
5	9.6%	GAAGCGTGCAAAAACCATCCTTAATATCTAAAGAGACAATCACTGGCCGTGCCACACACTGGGAGTAAAGACATGCCAACCTTCGCAGGGTCCGTGAGTCTGCTGACGCGCACGCCACGAGACTCGGTGCCGACATTTGGACAGCTTAGAGGGGGG
6	0.7%	GAAGCGTGCAAAAACCATCCTTAATCTCTAAAGAGACAATCACTGGCCGTGCCACACGCTGGGATATGACATGCCAACCTTCGCAGGGTCCGTGAGTCTGCTGACGCGCACGTCACGAGACTCGGTGCTGGCATTGAACTTTTAGAGGAGGG
7	4.1%	GAAGCGTGCAAAAACCATCCTTAATCTCTAAAGAGACAATCACTGGCCGTGCCACACGCTGGGATATGACATGCCAACCTTCGCAGGGTCCGTGAGTCTGCTGACGCGCACGCCACGAGACTCGGTGCTGGCATTGAACTTTTAGAGGAGGG
8	1.4%	GAAGCGTGCAAAAACCATCCTTAATCTCTAAAGAGACAATCACTGGCCGTGCCACACGCTGGGATATGACATGCCAACCTTCGCAGGGTCCGTGAGTCTGCTGACGCGCACGTCACGAGACTCGGCGTGGCATTGAACTTTTAGAGGAGGG
9	3.4%	GAAGCGTGCAAAAACAATCCTTAATATCTAAAGAGACAACAATCACTGGCCGTGCCACACACTGGGAGTATGACATGCCAACCTTCGCAGGGTCCGTGAGTCTGCTGACGCGCACGCCAAGAGACTCGGTGCCGACATTTGGACAGCTTAGAGGGGGG
13	1.4%	GAATCACATAGAGCGCGTTTCTAACATCTCGAATCCGCATAAAATGAACCGTGATCTGCCACAAGCTACGATGCCAACCTTCGCAGGGTCCGTGAGTCTGCTGACGCGCACGTCACGAGACCCGGTCCGGCATTGAACTTTTAGAGGAGGG
14	17.8%	GAATCACATAGAGCGCGTTTCTAACATCTCGAATCCGCATAAAATGAACCGTGATCTGCCACAAGCTACGATGCCAACCTTCGCAGGGTCCGTGAGTCTGCTGACGCGCACGTCACGAGACCCGGTCCGGCATTGAACTTTTAGAGGAGGG

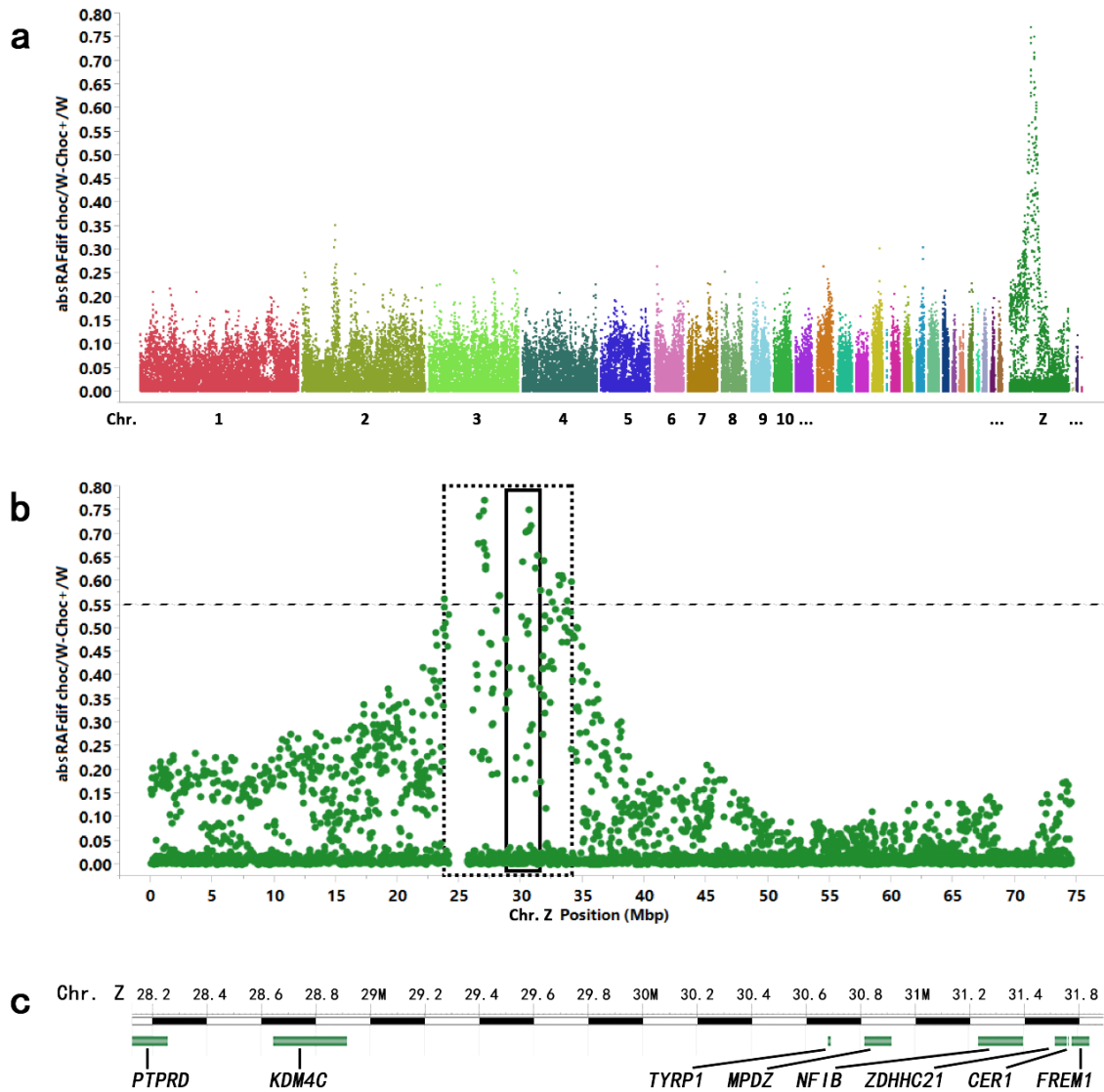


Figure 1 Linkage mapping of the *chocolate* mutation using F₂ females. (a) Genome-wide absRAFDif values (calculated by contrasting *choc/W* and *N/W* RAF values) of all 60K SNPs, plotted against genomic location. (b) absRAFDif values for chromosome Z. SNPs located within the 9.94 Mb region (dote lined area) gave absRAFDif values above 0.55. Solid lined area indicates the 3.57 Mb linkage mapping region, suggesting the location of the *choc* mutation. (c) Scheme of genes present within the 3.57 Mb region defined by linkage mapping.

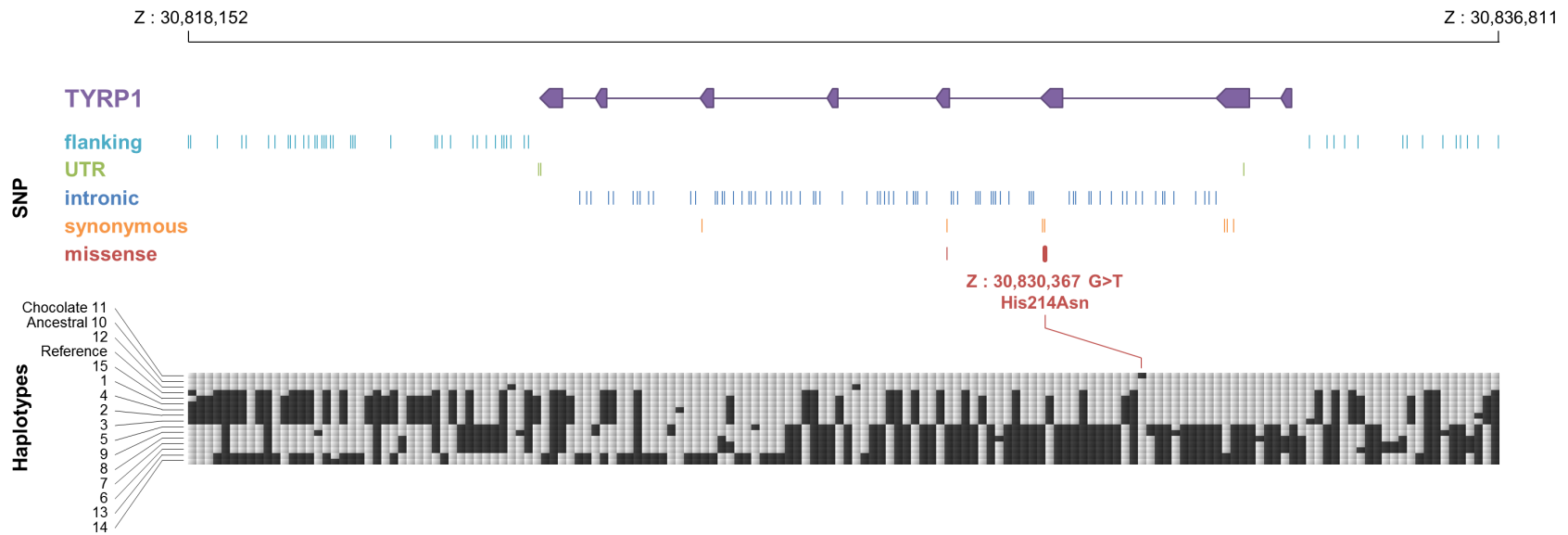


Figure 2. Position of the SNP identified in the gene capture experiment according to the structure of the *TYRP1* gene. Sequence coverage is shown along the whole region. The 15 haplotypes identified in the 78 individuals are summarized according to a color code where all SNPs found in the *choc* female and in any of the control non-chocolate individuals are in gray whereas all positions differing between the *choc* female and the controls are in black. There is only one position where a SNP is found only in the *choc* female.

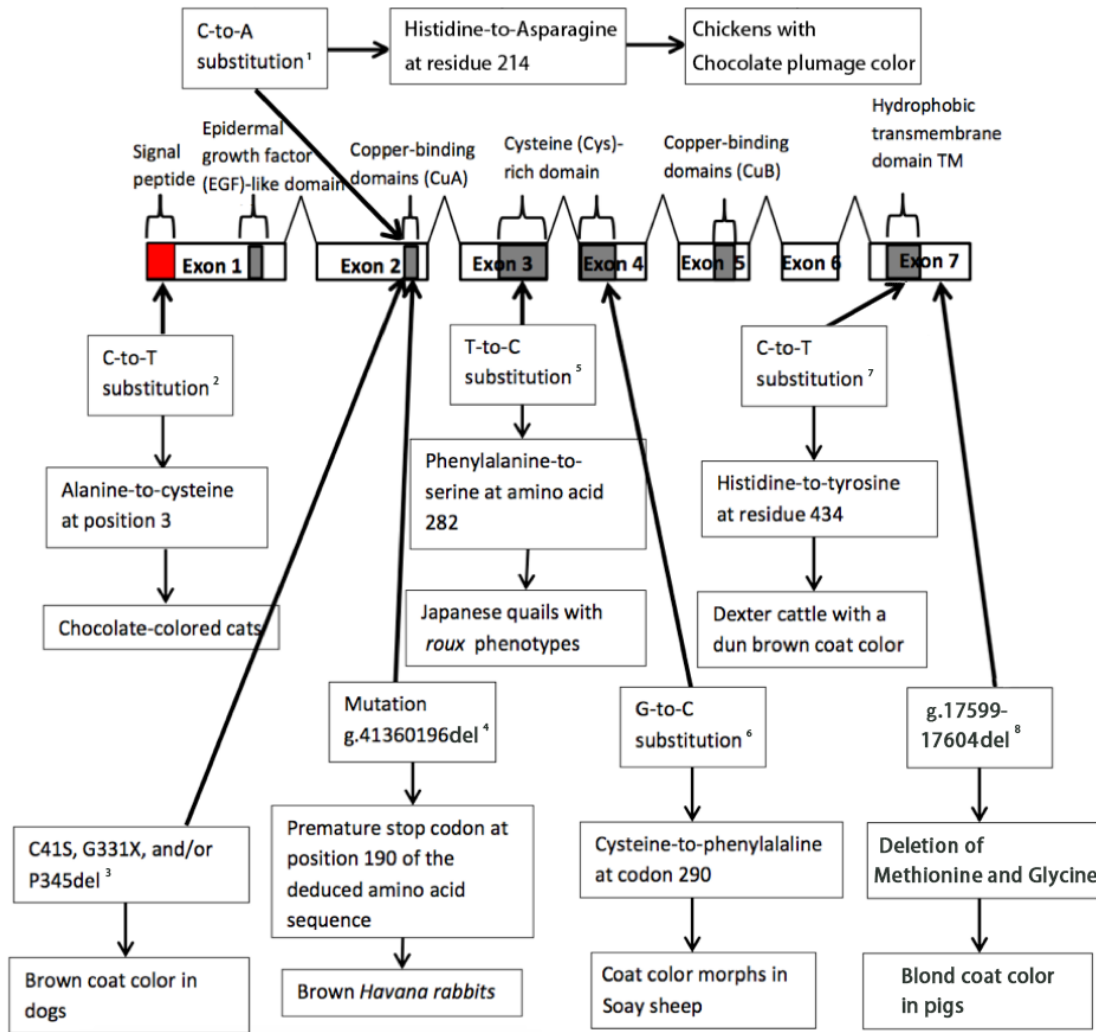


Figure 3 Scheme of the *TYRP1* gene summarizing the various polymorphisms associated with coat color or feather color variation in domestic animals. The arrows show their positions on the gene and shaded areas represent patterns of the *TYRP1* gene. Viewing the position of these polymorphisms on the gene *TYRP1* allows comparing between different species.

¹ Mutation found in our study.

² Schmidt-Kuntzel et al., 2005.

³ Schmutz et al., 2002.

⁴ Utzeri et al., 2014.

⁵ Nadeau et al., 2007.

⁶ Gratten et al., 2007.

⁷ Berryere et al., 2003.

⁸ Ren et al., 2011; Wu et al., 2015.

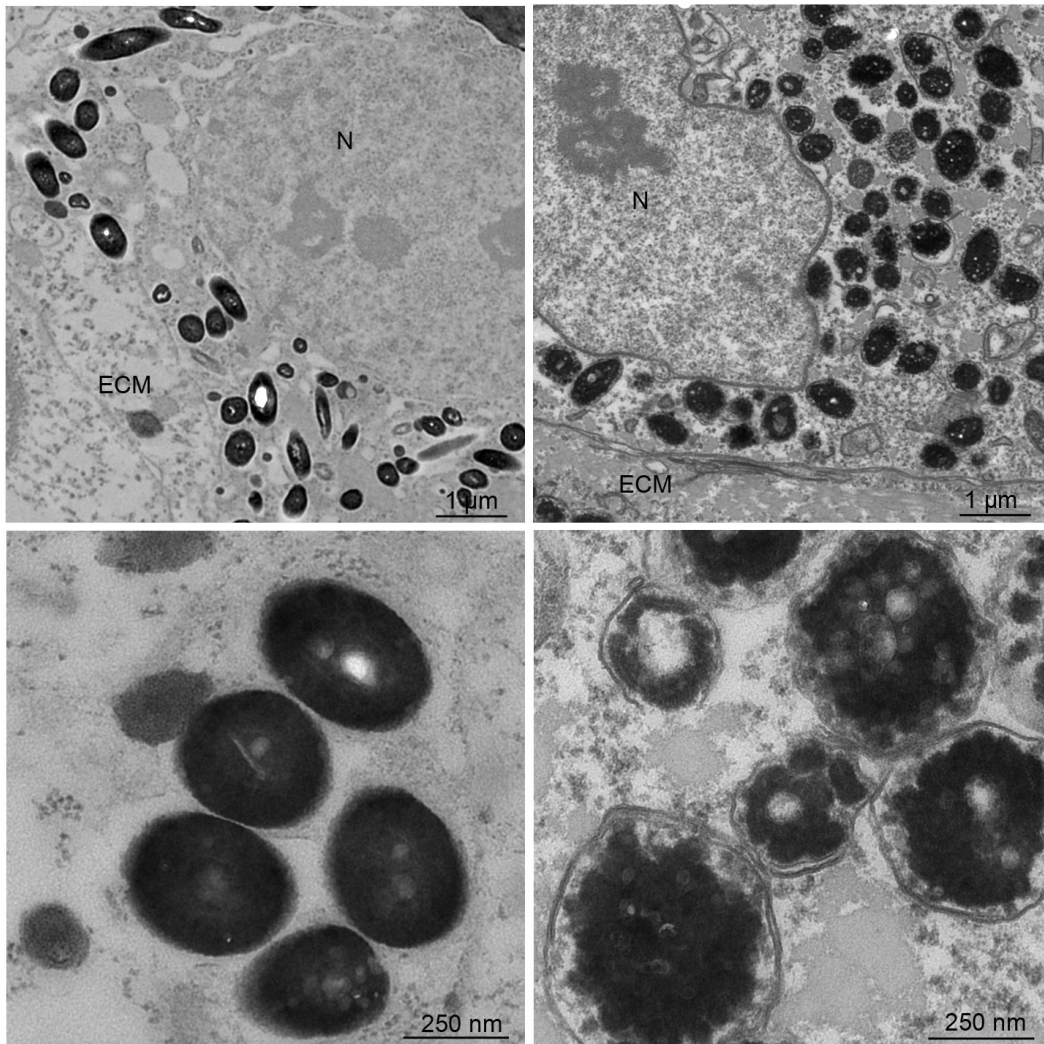


Figure 4. Electron microscope pictures of melanosomes from feather follicles: (A) from a black feathered hen with a 3000 magnifying power (B) from a black feathered hen with a 20000 magnifying power (C) from a Chocolate feathered hen with a 3000 magnifying power (D) from a Chocolate feathered hen with a 20000 magnifying power.

Supporting information

Table S1. List of non-chocolate breeds or lines used to provide control samples for the *TYRPI* His214Asn genotyping. The samples used for the gene capture experiment are marked with a *.

Breed	Plumage color	Source	Number of animals
A (B ^{Sd}) ¹	B ^{Sd}	Arizona, U.S.	10
Ameraucana	uncharacterized	Cary, NC, U.S.	1
Ameraucana	Black	APA Show Lucasville, OH, U.S.	2
Ameraucana	Blue	APA Show Lucasville, OH, U.S.	2
American Longtail	Wild-type	H & H Longtails	10
Andalusian	Blue	Marshfield, WI, U.S.	1
Araucana	uncharacterized	Cape Fear Poultry Assoc.	4
Araucana*	uncharacterized	Jaime Gongora	4
Australorp	Black	Marshfield, WI, U.S.	1
Ayam Cemani	Black	Minnesota, U.S.	7
B (Wild-type)	Wild-type	Arizona, U.S.	7
Black castellana*	black	AvianDiv DNA bank§	1
Blue Egg	uncharacterized	Arizona, U.S.	10
Brahma	Buff	Cape Fear Poultry Assoc.	2
Brahma	Dark	APA Show Lucasville, OH, U.S.	1
Brahma	Light	NC State University	2
BSd	BSd	Arizona, U.S.	10
Buckeye	uncharacterized	APA Show Lucasville, OH, U.S.	1
Buttercup	Buttercup	Murray McMurray	9
Buttercup	Buttercup	APA Show Lucasville, OH, U.S.	10
C (Black)	Black	Arizona, U.S.	8
Campine	Golden	NC State Fair	2
Chantecler	Partridge	APA Show Lucasville, OH, U.S.	1
Cochin	Buff	Cape Fear Poultry Assoc.	1
Cochin	Golden Laced	APA Show Lucasville, OH, U.S.	1
Cochin	Partridge	Murray McMurray	2
Cornish	Dark	Murray McMurray	10
Czech golden penciled*	gold	AvianDiv DNA bank	1
D (Splash)	Splash	Arizona, U.S.	10
Delaware	uncharacterized	APA Show Lucasville, OH, U.S.	1
Dorking	Silver Gray	Murray McMurray	6
D'Uccle Belgian	Mille Fleur	APA Show Lucasville, OH, U.S.	2
Faverolles	uncharacterized	NC State Fair	4
Faverolles	Salmon	Murray McMurray	6
Faverolles	White	APA Show Lucasville, OH, U.S.	2
Fayoumi*	silver autosomal barring	INRA	3
Flyfishing			
Limousin*	dirty white silver autosomal	Lycée Agricole Neuvic, France	2
Friesian Fowl*	barring	AvianDiv DNA bank	1
Frizzle	Red	NC State Fair	1
Frizzle	White	NC State Fair	2
Godollo New			
Hampshire *	gold	AvianDiv DNA bank	2

Green-legged partridge*	gold	AvianDiv DNA bank	1
Hamburg	Golden Penciled	Murray McMurray	2
Hamburg	Silver Spangled	Murray McMurray	10
Hamburg	Silver Spangled	Cape Fear Poultry Assoc.	2
Hedemora	uncharacterized	Uppsala, Sweden	2
Houdan	Mottled	Murray McMurray	1
Houdan	Mottled	APA Show Lucasville, OH, U.S.	10
Houdan	Mottled	Murray McMurray	6
Houdan*	black mottled	AvianDiv DNA bank	1
Icelandic *	mottled	AvianDiv DNA bank	3
	color		
Icelandic*	uncharacterized	AvianDiv DNA bank	1
Junglefowl	Wild-type	NC State University	2
Junglefowl	Wild-type	Richardson line	6
Langshan	Black	Murray McMurray	2
Langshan	Black	APA Show Lucasville, OH, U.S.	10
Leghorn	Black tail, Red	APA Show Lucasville, OH, U.S.	2
Leghorn	Single Comb Dark Brown	NC State University	1
Leghorn	Single Comb Light Brown	NC State University	1
Leghorn	Single Comb Light Brown	APA Show Lucasville, OH, U.S.	1
Leghorn	White		10
Mantes*	black mottled	check name	1
Marans	Birchen	Greenfire	3
Marans	Birchen		5
Marans	Copper	APA Show Lucasville, OH, U.S.	2
Marans	Wheaten	APA Show Lucasville, OH, U.S.	2
New Hampshire	uncharacterized	APA Show Lucasville, OH, U.S.	1
New Hampshire x Silkie	uncharacterized	NC State University	2
Old English	Spangled	APA Show Lucasville, OH, U.S.	2
Orlov*	mottled	AvianDiv DNA bank	1
Orpington	Black	Marshfield, WI, U.S.	1
Orpington	Buff	Cape Fear Poultry Assoc.	2
Orpington	Buff	APA Show Lucasville, OH, U.S.	1
Phoenix	Silver	Marshfield, WI, U.S.	1
Plymouth Rock	Barred	NC State University	2
Plymouth Rock	Barred	Virginia Tech	1
Plymouth Rock	Barred	NC State University	6
Plymouth Rock	Partridge	Murray McMurray	10
Plymouth Rock	Silver Penciled	Murray McMurray	2
Polish	Buff Laced	Cape Fear Poultry Assoc.	2
Polish	White Crested Black	NC State University	1
Polish	White Crested Black	Marshfield, WI, U.S.	2
Polish	White Crested Black, non-bearded	APA Show Lucasville, OH, U.S.	1
Polish	White Crested Blue, non-bearded	APA Show Lucasville, OH, U.S.	1
Polish	White, non-bearded	APA Show Lucasville, OH, U.S.	1
Polish x Silkie	uncharacterized	NC State University	1
Poltava Clay*	gold	AvianDiv DNA bank	1

Rhode Island	Red	Cape Fear Poultry Assoc.	1
Rhode Island	Red	APA Show Lucasville, OH, U.S.	2
Rhode Island Red*	gold	AvianDiv DNA bank	2
Sebright	Golden	Cape Fear Poultry Assoc.	1
Sebright	Golden	APA Show Lucasville, OH, U.S.	2
Sebright	Silver	Murray McMurray	10
Sebright	Silver	Cape Fear Poultry Assoc.	2
Silkie	uncharacterized	China	10
Silkie	Black	NC State Fair	5
Silkie	White	NC State Fair	3
Silkie	White	NC State University	10
Silkie	White	University of Wisconsin-Madison	3
Spitzhauben	German	NC State University	2
Sultan	White	Cape Fear Poultry Assoc.	2
Sultan	White	NC State University	2
Sumatra	uncharacterized	APA Show Lucasville, OH, U.S.	1
Sumatra	Black	APA Show Lucasville, OH, U.S.	2
Sumatra	Black	NC State University	10
Sumatra	Blue	APA Show Lucasville, OH, U.S.	2
Sumatra	Blue	Marshfield, WI, U.S.	1
Sussex	Speckled	Cape Fear Poultry Assoc.	2
Svarthöna	Black	Uppsala, Sweden	4
brown-egg layer line*	gold	INRA	3
Transsylvanian			
Naked neck*	black	AvianDiv DNA bank	1
Welsummer	uncharacterized	APA Show Lucasville, OH	1
Westfälische			
Totleger*	autosomal barring	AvianDiv DNA bank	1
White Leghorn*	white	Janet Fulton	45
	white with black		
White Leghorn*	spots	Janet Fulton	2
Wyandotte	Partridge	Murray McMurray	2
Wyandotte	Silver Penciled	Murray McMurray	1
Yokohama	Red Shoulder	APA Show Lucasville, OH, U.S.	1
		Total	428

¹ B^{SD}: Barred Sex-linked Dilution

Table S2. List of the 9 SNPs found to be associated with the *choc* mutation and subsequently used for linkage mapping with either KASP1 or KASP2 protocol. The candidate SNP in the *TYRP1* coding sequence is also indicated.

dbSNP	absRAFdif ¹	Position on Chr. Z (bp GalGal5)	KASP protocol	Genetic distance from <i>choc</i> (cM) ²
rs316461371	0.563	24,320,139	KASP-2	10.2
rs16106682	0.476	28,269,887	KASP-1	1.0
rs16080645	0.641	30,154,038	KASP-1	0
rs14687394	0.704	30,485,550	KASP-2	0
TYRP1 ³	-	30,830,367	KASP-1	0
rs14778077	0.580	31,836,731	KASP-2	5.7
rs14762884	0.642	32,081,991	KASP-1	5.7
rs312841286	0.592	33,347,891	KASP-1	7.2
rs14764310	0.408	35,683,084	KASP-2	15.8
rs14765167	0.261	37,190,373	KASP-2	18.685

¹ calculated by contrasting *choc/W* and *N/W* RAF values

² Calculated using the CRIMAP software

³ SNP for His214Asn substitution, not reported by dbSNP

Table S3. PCR primers and conditions for *TYRP1* sequencing.

Target element	Primer name	Primer sequence (5'-3')§	Product size(bp)	Tm(°C)
5'-UTR	5'_F	ACGTCGGAGTGTTC AATTTCT	916	60.0
	5'_R	TACAAACCTCCAGTCCAGTCCT		60.0
Exon 1	E1_F	TCTGGGA ACTGCTTAGATGTCA	746	59.9
	E1_R	AAATCAACATGCCAACAGACAG		60.0
Exon 2	E2_F	CATTCAAAAAGGGCTGAATAAGG	717	60.0
	E2_R	TGAAATTGAAGCAA AATTTCAATG		60.3
Exon 3	E3_F	ACCGCTGTTGTGAGGCTTTT	934	62.1
	E3_R	CTCCGCTCCTGGAGACATTC		62.3
Exon 4	E4_F	TGTGCAAAGGACTAGCACACA	909	60.5
	E4_R	ATCCTTCAGCACATCCAGCA		61.8
Exon 5	E5_F	AAACGTAACGGCTGGCAAAT	996	61.7
	E5_R	AGGATGTGCAAGGCAACTGA		61.8
Exon 6 & 7	E6&7_F	GACCTTTGACGCTGTTGCAG	1597	62.0
	E6&7_R	CCAGCACAAATGGAAGCACAT		62.1

§ Primer sequences were designed according to the *TYRP1* DNA sequence of chicken (GenBank

accession numbers NC_006127.3) using Primer3Plus software ([http://www.bioinformatics.nl/cgi-](http://www.bioinformatics.nl/cgi-bin/primer3plus/primer3plus.cgi)

[bin/primer3plus/primer3plus.cgi](http://www.bioinformatics.nl/cgi-bin/primer3plus/primer3plus.cgi)).

Table S4: design of the pyrosequencing test for the Chocolate mutation

Target: SNP G/T (forward strand of the genome, at position chrZ: 30,830,367 (galGal5) -> p.H214N (TYRP1))

Other nearby SNP: C/T (forward strand of the genome, at position chrZ: 30;830,362 (rs315736514, galGal5))

Targeted region: >chrZ:30689087-30689387 (galGal4 +)

CTATTACGAGATAATATGAGAATACAAAATTCATCCATACAAACCACAATAGGAGCACATGACTCAACATTAATGCTAACCTTACCTGCATGTCT
 CTTTCAAGTTGCAGTAGATGATACCTATGCCATGTGACAAAAGCTGGTCCYTCATKAGAGAAATCAACTCTTTCAAAGCTCTGCTGCCCTGCACC
 AAGGAAAGTCTTCCTGACGGAATAATAATGAGACCACACAAAGTAGTTATAAATGGAGATATTCTCAAAGTGTGGTGTGTTGCCATCTGGCCCA
 AATATTTCTTCACGTC

Design:

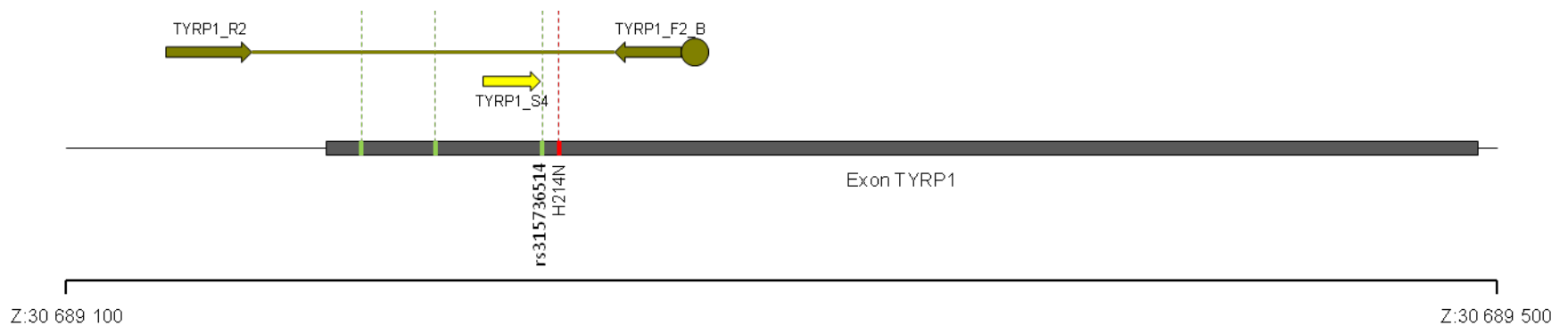
Primer Set Score: 96

Primer	Id	Sequence	Nt	Tm °C	%GC
Forward PCR primer	F2-biot	AGGGCAGCAGAGCTTTGAA	19	70.2	52.6
Reverse PCR primer	R2	AAACCACAATAGGAGCACATGACT	24	70.0	41.7
Sequencing primer	S4	TGACAAAAGCTGGTCC	16	52.6	50.0

Amplicon length: 145

Amplicon %GC: 41.4

Sequence to Analyze: YTCATKAGAGAAATCAACTCTTTCAA



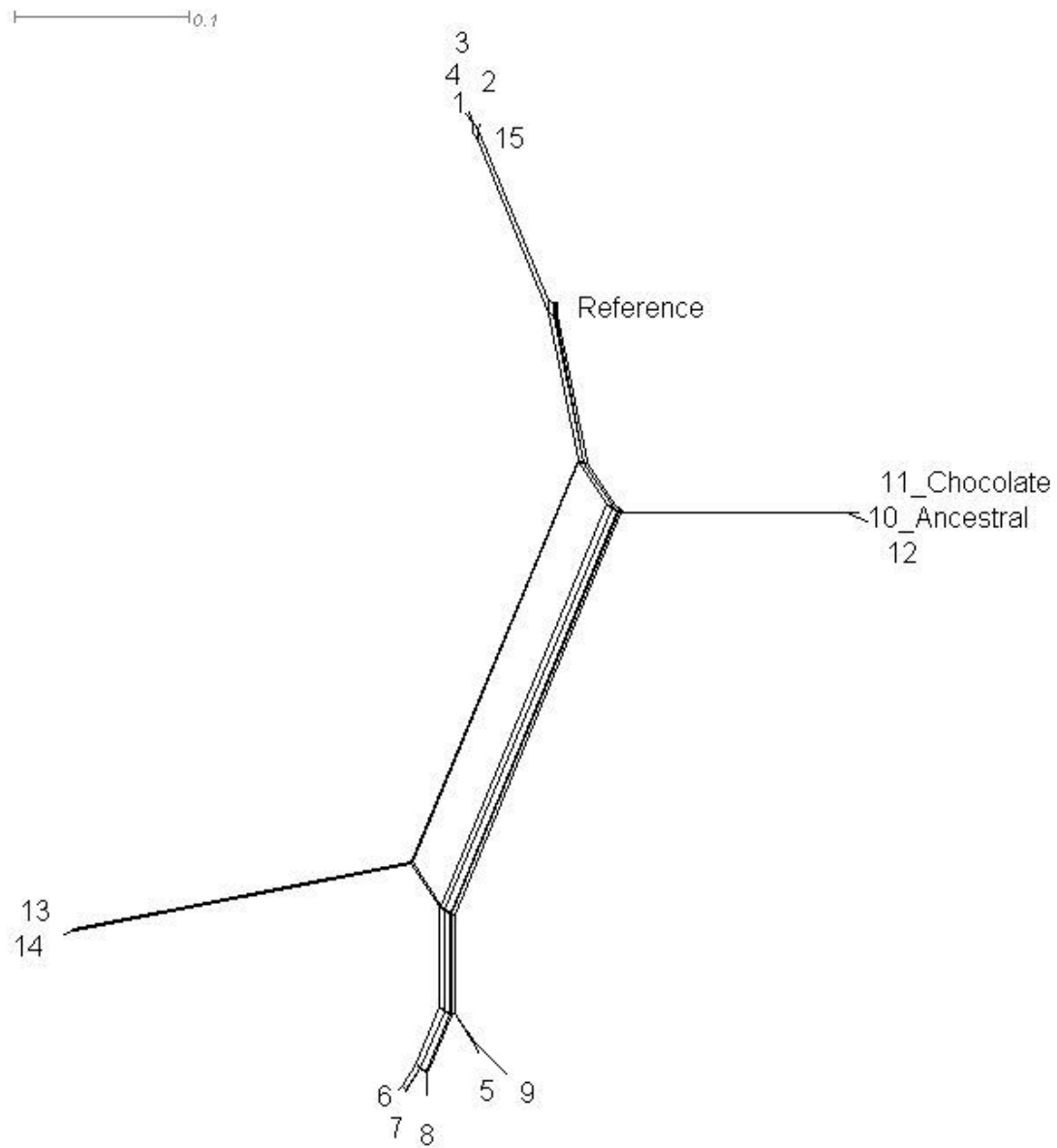


Figure S1. The network of TYRP1 haplotypes extracted from the gene capture experiment.

Chapter 11

Peripheral Experiments

Abstract

The research for my dissertation also included the mapping of 4 genes or loci other than the 8 genes or loci covered in Chapters 3 to 10. These 4 genes or loci were: dark brown egg shell color in Marans, vulture hock (*v*), feathered-leg 2 (*Pti-2*), and Creeper (*Cp*). Although these projects have not been completed, there is still a considerable amount of data which are summarized in this Chapter. In addition, a 3-generation population was built, which can be used to study interactions between blue and chocolate plumage colors.

Literature review

Dark brown egg shell color in Marans

The origin of Marans can be traced to 12th century when English ships would dock at La Rochelle (near Marans in France) and unload gamecocks. The progeny from a cross between those gamecocks and local hens were larger and laid darker brown eggs that were preferred by the local people and hence were the foundation for the early form of Marans, a breed selected for meat and egg production. During the second half of the 19th century two Chinese breeds, Brahma and Langshan, were imported to La Rochelle. They were introgressed into the early form of Marans to improve the meat quality while retaining the dark brown eggshell color. Since 1921, those Marans have been strictly selected for the large body size and the dark brown color of the eggshells. (Marans of America Club, <http://www.maransofamericaclub.com/marans-history.html>). Today, the

eggshell color trait is selected mainly for show purposes. It provides excellent material to study the inheritance of eggshell color because the major genes affecting this trait should be at or almost at fixation.

Although the genetics of eggshell color of chickens is of considerable interest, little progress has been made especially in understanding its molecular basis (Samiullah et al., 2015). Heritabilities of eggshell color are generally moderated to high (Blow et al., 1950; Farnsworth and Nordskog, 1955; Hunton, 1962) and different methods have been used to measure the color of eggshells, e.g. reflectivity meter, spectrophotometer, image analysis software, and High Performance Liquid Chromatography (HPLC) (Samiullah et al., 2015). Among them, perhaps the most widely used is a spectrophotometer which employs on the $L^* a^* b^*$ color space system that generates 3 values from one read of one spot on the eggshell. L^* has a maximum of 100 (white) and a minimum of 0 (black) and is the important component for simply measuring shell chromaticity. For a^* , green is towards the negative end of the scale and red towards the positive end. For b^* , blue is towards the negative end and yellow towards the positive end of the scale (Roberts and Chousalkar, 2013). When measuring eggshell color, these 3 measurements are probably measuring amounts of the same material because protoporphyrin is a major component of the brown eggshell color (Sasaki et al., 2004). In the use of Chroma Meter, a popular kind of spectrophotometer, quantitative trait loci (QTL) of eggshell color were reported to be located on chromosomes 2, 4, 6, 11, and 12 (Sasaki et al., 2004; Schreiweis et al., 2005; Wolc et al., 2014). Zheng et al. (2014) studied the expression of candidate genes and reported that 7 genes were associated with eggshell color. Among them, the gene that encodes ATP-binding cassette, subfamily G, member 2 (ABCG2) may be responsible for

the previous QTL signal on chromosome 6. In addition, by using a candidate gene strategy, Fulton et al. (2012) reported that ovocalyxin-32 (OCX32), a matrix protein in the outer layers of the eggshell and the cuticle, was associated with eggshell color and other egg quality traits. These QTL and genes may be involved in the dark brown color of eggs laid by Marans. The intense selection for eggshell color in Marans may have also altered correlated traits such as shell strength (Yang et al., 2009; Şekeroğlu and Duman, 2011). The implications of these factors to a multitude of fitness traits remain to be addressed.

Gene mapping of morphological traits in the Silkie chicken

There are morphological traits observed in Silkie chickens that are not commonly seen in other domestic breeds of chickens. Dorshorst et al. (2010) provided examples of these traits and the genes involved. They include: inhibitor of dermal melanin (*Id*), fibromelanosis (*Fm*), polydactyly 1 (*Po-1*), silkie feathering or hookless (*h*), feathered-legs (*Pti-1* or *Pti-2*), vulture hock (*v*), rose comb (*R*), and duplex comb (*D*), and crest (*Cr*). Among them, the causal mutations of *Fm*, *Po-1*, *h*, *R*, *D*, and *Cr* have been identified (Dorshorst et al., 2011; Maas et al., 2011; Imsland et al., 2012; Wang et al., 2012; Feng et al., 2014; Dorshorst et al., 2015). The hyperpigmentation phenotype of the Silkie chicken is associated with 2 genes: *Fm* an autosomal dominant and *Id* which is sex-linked and incompletely dominant (Bateson and Punnett, 1911). That *Id* is incompletely epistatic to *Fm* further complicates studies involving these two genes (Dunn and Jull, 1927). Although intensively studied, the *Id* gene hasn't been mapped. Li et al. (2014) reported 3 SNP located at a 0.7 Mb region on the Z chromosome that were significantly associated with *Id*. However, because the genomic context of this region is complex, no causal

mutations have been identified. Therefore, to avoid duplicated studies, the mapping *Id* gene is not included in the research for my dissertation.

Feathered-legs and vulture hock are two other traits that were included in my dissertation proposal. By crossing the Silkie and Houdan (no feathered-leg or vulture hock) chickens, the interaction between *Po-1* in Silkie and *Po-2* in Houdan, as well as the known causal mutation of hookless (*h*) could be studied.

As reviewed in Chapter 7, the existence of two feathered-leg genes in the Silkie is questionable. The validity of one or two genes models can be tested by crossing Silkie and Houdan, and then mapping the feathered-leg gene(s) in the Silkie. Also, the effect of brachydactylism and syndactylism on expression of the feathered-leg gene (Lambert and Knox, 1929) can be tested by measuring the total length of toes of chickens with or without feathered-leg. In addition, recording of feathered-leg in this mapping population is necessary for mapping of vulture hock (*v*), in which feathers in the crural feather tract of the tibia are increased in length and rigidity, thus giving the appearance of a flight feather (Dorshorst et al., 2010). This is because the expression of this incompletely dominant trait is dependent on the presence of feathered-leg, i.e., a “clean-leg chicken” will not express vulture hock regardless of how many copies it has of the *v* gene (Jull, and Quinn 1931). Vulture hock and feathered-leg are phenotypically and genetically related. Dorshorst et al. (2010) showed that in Silkies, two SNP (rs14999343 and rs13505642, 2.6 Mb away from each other) on chromosome 13 were associated with both *v* and *Pti*. A satisfactory explanation, however, is lacking because segregations of *v* and *Pti* occur in cross breeding experiments even though clean-leg and vulture hock were not observed together in the same individual (Danforth 1929; Jull and Quinn 1931). These results

suggest that these two genes are not closely linked. Similar to feathered-leg with its possible evolutionary importance, flight-feather-like vulture hock may be expressed in “4-winged” dinosaurs (Sawyer and Knapp, 2003). The possibility of same origin of these two traits may explain their phenotypic and genetic relationships.

Ectopic expression of *SHH* is responsible for *Po-1* in Silkie (Dunn et al., 2011). The *SHH* gene is also associated with *Po-2* based on the result of Chapter 8 in my dissertation. The presence of these 2 genes in the same individual have not been reported yet. Their interaction may provide new insights in understanding the formations of polydactyly.

Creeper

The Creeper trait in chickens is caused by a single autosomal gene (*Cp*), initially described in 1925 by Cutler. Homozygous *Cp/Cp* is lethal and heterozygotes are generally characterized by a pronounced shortness of the extremities (reviewed by Jin et al., 2016). The linkage of genes for Creeper and rose-comb (Serebrovsky and Petrov, 1928) was the first reported autosomal linkage case in farm animals. Creeper has been widely used as an illustration of an autosomal dominant semi-lethal gene and an example of linkage. Somes (1990), in his review, pointed out that phenotypes of Creeper chickens were intensively studied during the 1930s by Landauer (1932; 1933) and others including Cairns and Gayer (1943). Landauer reported that in heterozygotes, embryonic mortality was reduced by 5%. The heterozygous effects on adult chickens, other than shortened extremities, include susceptibility to vitamin D deficiencies and to the toxic effects of selenium. Homozygous embryos die around the fourth day of incubation, with only 2% surviving and developing to later stages (referred to as phocomelic embryos). No homozygotes hatch. He also reported that the percentage of phocomelic embryos was

increased by changing incubation temperatures. These observations suggested that the causal mutation of *Cp* should affect a gene or genes involved in multiple important pathways during early embryonic development as well as during later stages. However, the hypothesis of a general retardation of growth in *Cp* homozygotes seemed implausible (Elmer, 1968a).

Transplantation experiments suggested that the effect of *Cp* acted directly and locally in the cartilaginous cells from the donor limb primordia (Hamburger, 1941). In contrast, transplantation of eye primordia showed no local gene action and the effect of *Cp* occurred indirectly from the host embryo (Gayer and Hamburger, 1943). Based on co-culture experiments using heterozygous Creeper embryo extracts, Elmer (1968a) presented evidence that the reduced growth rate of extremities was due to an inhibitory substance by Creeper chondrocytes. This inhibitory effect might be related to aberrant leucine metabolism (Elmer, 1968b). Although these studies expanded our understanding of *Cp* gene action, the molecular basis of this phenotype was unknown until Jin et al. (2016) reported a 11.9 kb deletion on chicken chromosome 7 which contained the whole sequence of Indian hedgehog (*IHH*) gene. Large scale segregation and expression analyses suggested that the deletion of *IHH* was the causative mutation for the Creeper trait in chickens. They also proposed that the phenotypes of *IHH* deletion in other animals including humans resemble Creeper in chickens. Their findings explain most of the results from previous studies except that the deletion of *IHH* has an inhibitory effect on wild-type tissue. The contradiction is that it does not explain the recombination between Creeper and rose-comb genes.

There are 3 alleles at rose-comb locus, *r*, *R1* and *R2*. Either *R1* or *R2* can cause the rose-comb phenotype while *r* is the wild-type allele. The genetic basis of the *R1* allele is a 7.4 Mb inversion on chromosome 7, and it is assumed that the *R2* allele arose by a non-homologous recombination between *r* and *R1*, which resulted in a 91 kb duplicated sequence reversely inserted into chromosome 7 and 7.4 Mb away from its original copy (Imstrand et al., 2012). They also detected rose-comb alleles in 8 Western European chicken breeds. Of these only *R1* alleles were found in 5 of these breeds with both *R1* and *R2* alleles present in other 3 breeds. They also observed that in 3 Russian breeds with rose-comb, *R2* alleles were exclusive in 2 and both alleles were in the third. Thus, the *R1* allele is most frequent in Western European chickens and *R2* allele is most frequent in Eastern European chickens. Serebrovsky and Petrov (1928) reported a recombination rate between rose-comb and Creeper of 8.3%, while it was only 0.4 to 0.5% in subsequent studies (Landauer, 1932, 1933; Taylor, 1934). These may be explained as different rose-comb alleles have different genetic distances from Creeper gene because the former study used a Russian stock with rose-comb trait and the latter studies used Western European stocks. There are difficulties in explaining the recombination between *Cp* and either *R1* or *R2* because the deletion of the *IHH* gene is the causal mutation of *Cp*. The reason is that *IHH* is located within the 7.4 Mb inversion in *R1* allele, and also within the 91 kb duplication in *R2* allele. A single homologous recombination that occurred within a chromosome inversion in heterozygote individuals should lead to the formation of dicentric or duplication-deficiency chromosomes (Lefort et al., 2002). Such chromosomes are usually unstable and consequently lethal to the embryo (Novitski and Braver, 1954). Thus, the recombination rate between *R1* and *Cp* should be suppressed to

0% because of the 7.4 Mb inversion. A recombination between *R2* and *Cp* is possible because the original copy of *IHH* in *R2* is not inverted, and after such recombination the reversed copy of *IHH* may still be functional and would compensate for the loss of *IHH* from the *Cp* gene.

In summary, although it is unlikely from recombination experiments that Creeper and rose-comb can be expressed in the same individual, such individuals have been reported (Serebrovsky and Petrov, 1928; Landauer, 1932, 1933; Taylor, 1934). One possibility is that an unknown mechanism allows nonhomogeneous recombination to occur in that chromosomal region without obvious deleterious effects. This reasoning is supported by the hypothesis that *R2* evolved from *R1* by a nonhomogeneous recombination. If the causal mutation of *Cp* is located ~0.5 Mb downstream of the *R1* inversion's distal breakpoint (so it can't be the deletion of *IHH*), there is no difficulty in explaining the reported recombination rates.

Materials and methods

Animals

To study the dark brown egg trait in Marans, two mapping population were constructed. Another two mapping populations were also constructed to study the morphological traits in Silkie and the interaction between blue and chocolate plumage colors. Each mapping population (Cross_7, Cross_8, ... Cross_10) consisted of 2 parental populations (F_0), 1 crossbred population (F_1), and 1 F_2 population (**Table 11.1**). Blood samples were collected for each individual in Cross_9 and Cross_10.

Phenotyping analyses

For each of the 12 F₁ females in Cross_8, ten eggs were collected. A Chroma Meter (Minolta, Osaka, Japan) from Department of Food Science and Technology at Virginia Tech was used to quantify the color of the eggshells. The blunt end, apex end, and side of each egg were measured. During measurement, the reflected light is divided three ways, passed through filters, and strikes silicon photocells. Upon striking the silicon photocells, light energy is converted into an electrical signal and sent to a microprocessor where it is converted into coordinates for the chosen color space (Muizzuddin et al., 1990). Data output is in the form of L*, a*, and b* values.

For each F₂ in Cross_9, a total of 30 phenotypes were collected with 27 of them listed in **Table 11.2**. The other 3 phenotypes (down, plumage, and shank color) recorded were not objectives involved in this research. In addition, LT7, 1D7, and 4D7 (in **Table 11.2**) for left and right tarsometatarsus, were also measured on 20 Red Jungle Fowl (wild-type for all the genotypes) that were raised in the similar environment, and served as controls. All calculations were conducted using means, standard deviations, correlations, oneway ANOVA, Student's t test, 2-sided F test, or Shapiro-Wilk W test procedures in JMP software (JMP 11, 2015). Effects model for the ANOVA:

$$Y_{ij} = \mu. + \tau_i + \varepsilon_{ij}$$

where $\mu.$ is the grand mean, τ_i is the effect of the i th factor level, ε_{ij} are the error terms (Kutner et al., 2004). An absolute value of asymmetry was calculated as left minus right (L – R) for each bilateral trait at 7 weeks. Relative asymmetry (RA) was defined as the ratio of the absolute value of asymmetry divided by the value for the size of the bilateral trait:

$$RA = (|L - R| / [(L + R) / 2]) \times 100$$

Prior to analysis, each RA was transformed to an arcsine square root (Yang et al., 1998).

Except RA, the ratio data (original length data divided by the total length of the tarsometatarsus) which contains less than 90% values within the range of 0.3-0.7 was also transformed to an arcsine square root (Jaeger, 2008). The means, standard deviations and variances for each original length data were calculated and correlations between those means and their standard deviations or variances were calculated. If they were significantly correlated, log10 or square root transformation should apply to those original length data (Bland and Altman, 1996).

Genotyping analyses

Whole genome DNA was isolated from blood samples of Cross_9 chickens. KASP primers were designed to genotype two causal mutations for *Po-1* and *h* (Maas et al., 2011; Feng et al., 2014), and KASP-1, KASP-2 protocols (described in Chapter 2) were used to genotype these two mutations, respectively. Sex of these Cross_9 chickens was identified by PCR (Liu et al., 2010).

A total of 24 DNA samples from 2 families of Japanese Bantams were received from North Carolina State University (NCSU). There were 6 and 18 samples for families 1 and 2, respectively. Each family consisted of half Creeper (Cp/cp^+) and half normal (cp^+/cp^+) individuals. Individual genotyping data obtained by high-density 60K SNP Illumina iSelect chicken arrays was also provided by NCSU. Results from each SNP for each individual was one of AA, AB, BB (3 genotypes), or No Call. For each SNP, the absolute value of the differences of heterozygosity (ABSdif_H) was calculated as:

$$ABSdif_H = \left| \frac{\text{number of heterozygotes in Creeper individuals}}{\text{number of total Creeper individuals except No Calls}} - \frac{\text{number of heterozygotes in normal individuals}}{\text{number of total normal individuals except No Calls}} \right|$$

In addition, two ABSdif_H values were calculated for each SNP using family 2 or pooling of two families. Using family 1 only to calculate ABSdif_H was not considered because of the small sample size. The ABSdif_H values were plotted against the SNP genomic locations. PLINK software was used to calculate the association between genotypes and phenotypes for each SNP, following the methods described in Chapter 2, however no data filter methods were applied. The same bioinformatics analyses described in Chapter 2 were also used to search for candidate genes.

Results and discussion

Fertility of Maran-Houdan crossbred

Crossbred progeny from Marans and Houdan matings was built in Cross_7 to study the inheritance of dark brown eggshells. The offspring of two nonrelated parental lines may be expected to exhibit relatively higher viability and fertility because of hybrid vigor. However, most of the F₁ females in Cross_7 laid their first egg at older ages or in some cases never commenced egg production. Over a period of 3 weeks, 33 eggs were collected from 28 females, and 20 F₂ chicks were hatched from these eggs. Such a small number of F₂ chickens was not adequate for a QTL analysis, and thus Cross_8 was built as a replacement for Cross_7. This cross of Marans and Leghorn (Cross_8) reproduced well. The reason of low reproduction among the F₁ in Cross_7 may be the combination of

Marans' and Houdan's genes. One or several major genes may have had epistatic effects or overdominance to mask the expected hybrid vigor.

Statistical analyses of eggshell color

Correlations between measurements for two different locations of eggs (blunt end, side, or apex end) are shown in **Table 11.3**. All the correlations were highly significant ($p < 0.0001$). The correlations between apex and blunt ends of the egg were lower than others, indicating the different conditions of where the pigmentation was deposited to the apex and blunt ends of the eggshell (greater surface area on blunt than apex end).

All the correlations between two different color measurements (L^* , a^* , or b^*) were also highly significant (**Table 11.4**). The measurement involving b^* was less associated with other two, suggesting pigmentations other than protoporphyrin that affect blue and yellow colors may be involved in the dark brown eggshell.

Effects of F_1 females, F_0 males, and F_0 females were estimated by ANOVA, using color data based on different combinations between color measurements (L^* , a^* , or b^*) and locations (blunt end, side, or apex end) (data not shown). In general, significant effects were observed among F_1 and F_0 females but not F_0 males, indicating Leghorn females may contribute more to the phenotypic variation in the F_1 than Marans males. The reasons could be: 1. Marans are more inbred than Leghorns, so that the Marans have less genetic variation. 2. Marans have been intensely selected for dark brown eggshell color which decreased the standing genetic variation. Although Leghorns have also been selected for white egg color, the genes or loci for white egg may have epistatic effects on other eggshell related genes and inhibit the effect of other genes (Punnett and Bailey, 1920). Thus, other genes might be under low selection pressure and genetic variation was

preserved in Leghorns. 3. Maternal effects may contribute to egg related traits from Leghorn females to F₁ females. All 3 factors (F₁ female, F₀ male, and F₀ female) have effects ($p < 0.01$) on all measurements of b*, but not on L* and a* (data not shown). As discussed above, pigmentations other than protoporphyrin that mainly affects blue and yellow colors may be involved in dark brown eggshell, which might be influenced by genes or loci in Marans males, in Leghorn females, and maternal effects. Finally, all 3 of the factors have significant effects ($p < 0.05$) on measurements from the blunt end of eggs (data not shown). Thus, the b* values from the blunt end of eggs were more affected by individual and family effects. However, it's relatively smaller repeatability (calculated by using 10 eggs from each of the 12 F₁ females, shows in **Table 11.5**) suggested that slightly greater environmental variation was involved. Unlike other two values, L* didn't follow the trend of apex end > side > blunt end, after multiple comparisons (**Table 11.5**). The lower L* value (i.e. whiter) at blunt end is consistent with Nys et al. (1991) that the upward orientation of the blunt end of the egg determines its accumulation of whitening. When averaging the measurements from different locations of eggs, (**Table 11.6**), F₁ female effects were still significant. Few conclusions can be made based on the F₁ results, however they provided the possibility of providing insights if F₂ genotypic and phenotypic data were collected and analyzed.

Phenotypic data of feathered-leg and vulture hock

Feathered-leg was recorded for Cross_9 F₂ chicks at hatch, 7 weeks, and 27 weeks (FL0, FL7, and FL27). FL0 was classified into 5 categories: very heavy feathered, heavy feathered, light feathered, very light feathered, and clean. When all the very heavy feathered and heavy feathered chicks were combined into a single feathered-leg group

and the rest combined into a clean-leg group, the numbers did not differ from a 3:1 ratio ($p = 0.62$). Classifying of FL7 was more difficult than FL0 because more intermediate phenotypes were observed and the feathered-leg to clean-leg ratio was different from the 3:1 ratio ($p = 0.01$). At week 27, the classification of the phenotypes into 5 categories was impossible and a 10-category (0 to 9) system was designed. This way, although the FL27 data were more precise and contained more information, it was difficult to study the ratios between feathered-leg and clear leg groups. One hypothesis to explain these observations could be: one dominant major gene (assumed to be *Pti-2*) in Silkie influences feathered-leg at hatch, so that when it segregated in the F_2 , a 3:1 ratio was observed. The categories of “light feathered” or “very light feathered” at hatch were considered as no *Pti-2* gene. Their light feathering might be influenced by other modifier genes. During development at later stages, these modifier genes and environmental factors continued to influence the feathered-leg phenotype, and segregation of *Pti-2* was no longer obvious based on phenotype. Therefore, the same mapping population could be used in two ways: mapping *Pti-2* using FL0 and mapping QTLs associated with adult feathered-leg by treating FL27 data as a numeric trait.

Vulture hock was not observed at hatch. VH7 was recorded as only two categories: vulture hock and non-VH. The ratio between these two categories was significantly different from 1:3 ($p < 0.01$). However, when clean-leg and intermediate FL individuals were excluded based on FL7, the ratio between vulture hock and non-VH was almost an exact 1:3 ($p = 0.96$). VH27 was recorded with one additional category: intermediate VH, which was considered to be caused by heterozygotes. The data had a similar trend so that when all F_2 were included, the ratio between vulture hock, intermediate VH, and non-VH

was different from 1:2:1 ($p < 0.01$). When individuals with the FL27 record of 0 to 3 (clean-leg to light feathered leg) were excluded, the ratio matched 1:2:1 ($p = 0.74$). There may be advantages and disadvantages to using either VH7 or VH27 data to map the v gene. The phenotype is not fully expressed at week 7, thus the non-VH category in VH7 should be a mix of V^+/V^+ and V^+/v , resulting in difficulty in the detection of the causal mutation. However, the expression of vulture hock might be affected by feathered-leg more at 27 weeks of age, with the result of the exclusion of more individuals for v mapping because of FL27. The non-VH, intermediate VH, and vulture hock individuals at 27 weeks which have feathered-leg (4 to 9 based on FL27) are supposed to have the genotypes of V^+/V^+ , V^+/v , and v/v , respectively. This may be a more powerful method for mapping of the v gene but with a smaller sample size. Genotyping results from pooling of DNA samples both ways should show which is the more useful procedure to map the v gene.

Phenotypic and genotypic data of hookless and polydactyly

Hookless (Silkie feather) was recorded as hookless or Non-HL at 7 and 27 weeks of age. For each chicken, the classifications for HL7 and HL27 were consistent with each other. The ratio (132:44) between Non-HL and hookless perfectly matched a 3:1 ratio ($p = 1.00$). These results agreed with those of Feng et al. (2014) that hookless is affected by a single recessive gene. The causal mutation of hookless on *PDSS2* gene was genotyped by a KASP assay and the results matched all the phenotypic data.

Each individual of F_2 ($n = 199$) should have at least one copy of either *Po-1* or *Po-2*, because polydactyly was observed in every chick at hatch, suggesting the recombination rate between *Po-1* and *Po-2* was less than 0.5% (1/199). The close linkage of these two

genes was consistent with results reported by Maas et al. (2011) and those in Chapter 8. They also suggest that recombination events between these two genes might not occur in Cross_9, meaning that they can be treated as two alleles at one locus. Therefore, the genotype of each F₂ could only be one of *Po-1/Po-1*, *Po-1/Po-2*, or *Po-2/Po-2*. Under this assumption, the genotypes of F₂ progeny were inferred by detecting the copy numbers of *Po-1* from a KASP assay.

Statistical analyses in regard to polydactyly

Total length of the extra digit was recorded on 199 chicks at hatch (ED0) as long, middle, or short on both left and right tarsometatarsus. Only 5 middle and short extra digits on the left tarsometatarsus and 7 on the right were observed. Although each of them had the genotype of either *Po-1/Po-2* or *Po-2/Po-2* (namely, all *Po-1/Po-1* individuals were recorded as long in ED0), no differences ($p > 0.05$) were detected among genotypes. The reason for these results might be that *Po-1* and *Po-2* genes influence the development of the extra digit to the same degree at hatch, or because of the 3-category system used for recording lacked sufficient information. Thus, quantification was needed at later ages via a vernier caliper. The angle between the extra digit and the 3rd digit on both left and right tarsometatarsus (AG) for each individual was recorded as one of acute, right, or obtuse, at hatch (AG0) and 7 weeks (AG7). No significant genotypic effect was detected on both AG. Due to its less likelihood of being influenced by *Po* genes and the difficulty in quantifying the phenotype, angles were not recorded at older ages.

Because ED7 was quantified, a control measurement was needed to adjust the measurements from other growth factors that generally affect the length of all the

phalanges. 1D7, 4D7, and LT7 were selected as candidates for the control. The reasons of choosing these three phenotypes were: 1. The 1st digit is the closest to the extra digit and they may share the similar conditions during development except for the effect of *Po* genes. 2. The expression of *Po* genes may also act as a morphogen to affect a larger range. Therefore, the 4th digit, which is the furthest from the extra digit, may be more independent from the effect of *Po* genes, than the 1st digit. 3. Length of tarsometatarsus may be a better phenotype to represent the general growth of limb bones other than digits, because the development of digits may be further affected by the cage or pen where the chickens had been raised (except the extra digit, which does not touch the ground when the chicken is standing or walking). In order to examine the effectiveness of each candidate for control, they were analyzed by ANOVA to detect genotypic effects. No significant effect of the *Po* gene was found on 1D7, 4D7, or LT7, meaning they were independent from the influence of *Po* genes. There were significant differences, however, in variances of 1D7 and 4D7 between the Cross_9 F₂ and the Red Jungle Fowl for both left and right tarsometatarsus, while such a difference was not found on LT7 (**Table 11.7**). Thus, it may be assumed that genetic factors other than the *Po* genes (such as feathered-leg or other unknown genes) which segregated in the Cross_9 F₂ population affected 1D7 and 4D7, but not the LT7. In summary, LT7 and also LT27 were better measurements as a control.

Correlations between the means and their standard deviations ($r = 0.86$, $p < 0.0001$) and variances ($r = 0.84$, $p = 0.0002$) were positive for the 14 original length traits. After log₁₀ transformation, such correlations still existed but were negative ($r = -0.81$, $p = 0.0005$; $r = -0.76$, $p = 0.0016$, respectively), while after square root transformation, they

were not significantly correlated ($r = 0.04$, $p = 0.89$; $r = 0.08$, $p = 0.77$, respectively). Therefore, the 14 original lengths data were square root transformed prior to ANOVA. The data of adjusted total length of the 1st and 4th digit (1D/LT and 4D/LT, for both ages and sides) had less than 90% values within the range of 0.3-0.7. Thus, together with all the RA data, 1D/LT and 4D/LT were arcsine square root transferred prior to analysis. The different genotypes (*Po-1/Po-1*, *Po-1/Po-2* and *Po-2/Po-2*) had significant effects on the ED/LT and HE/LT (**Table 11.8**), but not on the 1D/LT, 4D/LT, and LT. The *Po-1* gene was associated with a longer extra digit and a higher extra digit, indicating that polydactyly had a greater effect on phenotypes in the Silkie than in the Houdan. This difference was consistent with the observations that a few double extra digits (6 toes) were observed in Silkie, but not in Houdan pure lines. To my knowledge, no phenotypic differences between Silkie's and Houdan's polydactyly have been reported. In addition, the dominance of *Po-1*'s effects on the length and the height of the extra digit are different (**Table 11.8**), suggesting different pathways are involved that affect these two phenotypes. Furthermore, the causal mutations of *Po-1* and *Po-2* may affect polydactyly in different pathways.

Statistical analyses with regard to other factors in Cross_9

Eggs were incubated at two-week intervals resulting in three hatches of the Cross_9 F₂ over a period of 4 weeks. Hatch effects were significant between the 1st hatch and other two hatches for 1D, 1D/LT, 4D, 4D/LT, and LT (for both sides at 7 weeks). Two possible reasons for the hatch effects are: 1. The measurements of the 1st hatch at 7 weeks was the first time the vernier caliper was used and there might be systematic errors because of inexperience. 2. Environment factors might have affected only hatch 1

chickens during their incubation or the early development after hatch. Either of these reasons could have reduced hatch effects at older ages because they were not significant for any measurements at 27 weeks (data not shown). Therefore, the data at 27 weeks should be more reliable than those obtained at the 7 weeks.

There was sexual dimorphism at 1D, 4D, LT, and HE for both left and right tarsometatarsus at both ages (males had larger values than females, data not shown), but not when adjusted for LT. Sex effects were also significant on ED7_Left, ED/LT7_Right, ED27_Left and ED/LT27_Left, but not on ED7_Right and ED/LT7_Left (data not shown). The different pattern of sex affecting ED from other length data suggested that the development of the extra digit might involve different mechanisms than those for other toes and shank.

4D/LT27 was negatively correlated ($r = -0.60$, $p < 0.0001$) with FL27 (0~9, treated as a numeric trait). Significant differences were also found in 4D/LT7 among FL7 phenotypes (**Table 11.9**). These results were consistent with previous reports that the feathered-leg gene had a side effect of brachydactylism (Lambert and Knox, 1929) and may be explained by the ectopic expression of TBX5 in the hindlimb which is responsible for feathered-leg (See Chapter 7). As a forelimb-specific transcription factor in avians, TBX5 changed the development of epithelial appendages and also re-patterned the hindlimb into wing-like musculoskeletal system (Domyan et al. 2016). Leg feathers grow mainly on the outside of the shank and the dorsal side of the 4th digit which could explain why feathered-leg did not affect phenotypes other than the total length of the 4th digit. As with feathered-leg, different vulture hock phenotypes at both ages were not associated with other phenotypes except the length of the 4th digit (**Table 11.9**). Similar

effects of vulture hock effects were noted when viewed either for all individuals or those without leg feathers (including feathered-leg and intermediate FL phenotypes). Again, phenotypic and genetic similarities were observed between feather-leg and vulture hock. Although, the feathered-leg and vulture hock phenotypes decreased the total length of 4th digit as a recessive at both ages, the exception was VH27 when clean-leg and light feathered-leg individuals (with a 0-3 FL27 record) were excluded, which had an overdominant influence on 4D/LT (**Table 11.9**). There may be compensating mechanisms that allow the *Pti* gene to decrease the total length of 4th digits to a greater degree in the absence of the *v* gene.

Effects of HL7 were observed on LT7_Right (**Table 11.10**), while there was no HL27 effect on any phenotype at 27 weeks. HL7 also negatively influenced ED7 and HE7, but not ED/LT7 or HE/LT7 (data not shown). Namely, such effects were cancelled by dividing the LT. The *h* gene may have a pleiotropic effect which negatively affects the general growth of juvenile chickens, however such effects may be compensated with age.

Asymmetry and developmental stability in Cross_9

Asymmetry was assessed using all the measurements at 7 weeks (**Table 11.11**). For ED7 and ED/LT7, the extra digits were longer on the left than the right tarsometatarsus. This result was consistent with previous reports that more chicks had left polydactyly and right normal than right polydactyly and left normal tarsometatarsus (Warren, 1944). Thus, the *Po* genes have stronger effect on ED_Left than ED_Right, while with similar effects on HE_Left and HE_Right. Directional asymmetry was found in LT7, with the right longer than the left tarsometatarsus, a result consistent with that of Yang et al (1998), although the difference they observed was not significant ($p > 0.05$). 4D/LT7 showed the

4th digits were longer on the left tarsometatarsus, which was likely caused by the shorter tarsometatarsus on the left but not the absolute total length of the 4th digit.

Reviewed by Møller and Swaddle (1997), there are 3 types of asymmetry:

Directional asymmetry (DA) occurs when there is a propensity of one side of a trait to develop more than the other. Antisymmetry (AS) occurs when one side is larger than the other, but there is no handed-bias as to which side will be larger. Fluctuating asymmetry (FA) occurs when an individual is unable to undergo identical development on both sides of a bilaterally symmetrical trait. FA is a direct result of the inability of individuals to undergo identical development on both sides. FA is thought to be the only type of asymmetry that relates to accidents during morphogenesis and hence developmental instability, which is due to intra- (genetic) and extra- (environmental) stressors. However, asymmetry other than FA is suggested to be affected by 'development noise' or random accidents during morphogenesis and thus could also be used as indicators of developmental stability and genetic stress. Sex effects on RA of 4D/LT and LT were found but not on 4D. Therefore, different RA of 4D/LT between sexes may be caused by different RA of LT. Females had higher RA of LT than males (**Table 11.11**), which is consistent with T RINTAMÄKI's study (1997) that suggested male birds with more symmetric LT were advantageous in mating because of female preference. Thus, sexual selection might decrease the RA of LT in males over time. Vulture hock was associated with RA of 4D and HE, using both original length data and adjusted ratio data. The higher RA of 4D in vulture hock individuals (**Table 11.11**) could be explained by resource allocations because the shorter 4D associated with vulture hock might suffer from a lack of resources which means higher developmental stability. The vulture hock

might provide an extra protection to part of the shank so that the position of the extra toe is more stable in development, i.e. vulture hock was associated with lower RA of HE (**Table 11.11**). Besides, considering the possible similarity of genetic makeup between vulture hock and feathered-leg, and no effects of feathered-leg were found on any RA, the developmental stability associated with vulture hock might be influenced more by environmental than genetic stresses. No other significant differences were found for any RA using other factors recorded at 7 weeks of age (data not shown).

Identification of genes associated with Creeper

The mapping results for *Cp* were similar when using data only for family 2 and the pooling of two families. Thus, figures for the pool of the two families are presented (**Figures 11.1 to 11.4**). Both had the same peak region on Chromosome 7 which was associated with *Cp* using both ABSdif_H and -logp values, and 4 SNP (rs14611160, rs13780563, rs431898418, and rs314469969, positions on Chr_7: 16.6 Mb, 18.4 Mb, 22.4 Mb, and 22.4 Mb respectively) had the highest association (**Figures 11.2 and 11.4**). GO terms were searched in an attempt to locate candidate genes within the peak region. The candidate genes (**Table 11.12**) were compared with the 4 SNP and 2 (rs431898418 and rs314469969) were only 14 and 28 kb away from a strong candidate gene: *IHH*. The other two highest SNP had relatively longer distances from any candidate genes. In addition, the two SNP close to *IHH* were detected by two methods of calculation (ABSdif_H and -logp), strengthening the likelihood that they were associated with *Cp*. These results support that *IHH* could be the priority candidate gene for *Cp* and are consistent with previous gene mapping results (Jin et al., 2016). However, because of the limitations of sample size, these results should not be considered as a strong evidence.

Also, still remaining is the paradox of recombination between Creeper and rose comb genes.

Interactions between blue and chocolate plumage color

Theoretically, there should be 6 different phenotypic combinations found in Cross_10 F₂. However, the splash (*Bl/Bl*) phenotype strongly inhibited black pigmentation, which masked the effect of chocolate. Lacking may be epistatic effects between blue and chocolate plumage colors because the 5 F₂ individuals with the combination of these two dilution factors had a more diluted plumage color. Therefore, these two genes dilute pigmentation via different mechanisms, which is consistent with findings reported in Chapters 9 and 10. Because one of the candidate gene for *Bl*, TMEM110-like protein, may affect the development of melanosomes before its stage I, while the causal mutation of chocolate alters the function of TYRP1 which affect the melanosomes mainly at stage III (Chi et al., 2006). In addition, as showed in Chapter 10, increased number of melanosomes is associated with chocolate mutation. When it is decreased by blue mutation, a further diluted color should be expected. Even though the small population size of Cross_10 limited the study of the gene separations, the difference between the actual and expected ratios of different phenotypes ($p = 0.001$) might have resulted from the higher mortality noted in Chapter 9 for splash (*Bl/Bl*) chickens.

Tables and figures

Table 11.1. Details of 4 chicken populations discussed in Chapter 11

Population	Target Gene/Trait	Number, Breed and Genotype/Phenotype of F ₀ Males	Number, Breed and Genotype/Phenotype of F ₀ Females	Number and Genotype/Phenotype of F ₁		Number of F ₂
				Males	Females	
Cross_7	dark brown egg	1 Marans ² dark brown egg	6 ¹ Houdan ³ white egg	brown egg		20
				6 ¹	28 ¹	
Cross_8	dark brown egg	2 Marans ² dark brown egg	7 Leghorn ⁴ white egg	brown egg		229
				3	12	
Cross_9	<i>Pti</i> (<i>Pti</i> -1 and/or <i>Pti</i> -2), <i>v</i> , <i>Po</i> -1, <i>Po</i> -2, <i>h</i>	2 ⁵ Silkie ⁶ <i>Pti/Pti v/v Po-1/Po-1 h/h</i>	5 Houdan ³ <i>pti⁺/pti⁺ V⁺/V⁺ Po-2/Po-2 H⁺/H⁺</i>	<i>Pti/pti⁺ V⁺/v Po-1/Po-2 H⁺/h</i>		199
				5	9	
Cross_10	<i>Bl</i> , <i>choc</i>	1 Wyandotte ² <i>Choc/Choc bl⁺/bl⁺</i>	1 D (Splash) ⁷ <i>choc⁺/W Bl/Bl</i>	<i>Choc/ choc⁺ Bl/bl⁺</i>	<i>Choc/W Bl/bl⁺</i>	26
				1	2	

¹ Only some of them contributed to their F₂.

² Purchased from Greenfire Farms.

³ Purchased from Murray McMurray Hatchery.

⁴ Low antibody selection line from Virginia Tech.

⁵ Semen from these 2 males are pooled for the mating to produce F₁.

⁶ Pure line from North Carolina State University.

⁷ Not a standard breed, provided by David D. Caveny.

Table 11.2. Phenotypes recorded in the Cross_9 F₂ population

Age (weeks)	Phenotype	Left or Right	Abbreviation	Data Type
0	Degree of feathered-leg	Recorded together	FL0	Categories ¹
7	Degree of Feathered-leg	Recorded together	FL7	Categories ²
27	Degree of Feathered-leg	Recorded together	FL27	Categories ³
7	Vulture hock	Recorded together	VH7	Categories ⁴
27	Vulture hock	Recorded together	VH27	Categories ⁵
7	Hookless	Recorded together	HL7	Categories ⁶
27	Hookless	Recorded together	HL27	Categories ⁷
0	Angle between the extra digit & the 3 rd digit	Left and Right	AG0	Categories ⁷
7	Angle between the extra digit & the 3 rd digit	Left and Right	AG7	Categories ⁷
0	Total length of the extra digit	Left and Right	ED0	Categories ⁸
7	Total length of the extra digit	Left and Right	ED7	Numeric
27	Total length of the extra digit	Left only	ED27	Numeric
7	Total length of the 1 st digit	Left and Right	1D7	Numeric
7	Total length of the 4 th digit	Left and Right	4D7	Numeric
27	Total length of the 4 th digit	Left only	4D27	Numeric
7	Total length of the tarsometatarsus	Left and Right	LT7	Numeric
27	Total length of the tarsometatarsus	Left only	LT27	Numeric
7	Distance between the extra toe and the bottom of the tarsometatarsus	Left and Right	HE7	Numeric
27	Distance between the extra toe and the bottom of the tarsometatarsus	Left only	HE27	Numeric

¹ Very heavy feathered, heavy feathered, light feathered, very light feathered, and clean

² Feathered, intermediate FL, or clean.

³ Recorded as 10 categories (0 to 9), larger number means heavier feathered-leg.

⁴ Vulture hock or non-VH.

⁵ Vulture hock, intermediate VH, or non-VH.

⁶ Hookless or Non-HL.

⁷ Acute, right, or obtuse.

⁸ Long, intermediate, or short.

Table 11.3. Correlations (r) between different locations on the eggshell for color measurements

r	L* (n = 120)	a* (n = 120)	b* (n = 120)
Blunt end vs. side	0.91	0.86	0.84
Side vs. apex end	0.90	0.91	0.86
Apex end vs. blunt end	0.72	0.68	0.60

L* is a measurement of shell chromaticity; a* is a measurement of greenness (negative) and redness (positive); b* is a measurement of blueness (negative) and yellowness (positive). All the correlations are significant (p -value < 0.0001).

Table 11.4. Correlations (r) between different color measurements at 3 locations of the eggshell

r	Blunt End (n = 120)	Side (n = 120)	Apex End (n = 120)
L* vs. a*	-0.87	-0.90	-0.91
a* vs. b*	0.64	0.65	0.70
b* vs. L*	-0.63	-0.64	-0.70

L* is a measurement of shell chromaticity; a* is a measurement of greenness (negative) and redness (positive); b* is a measurement of blueness (negative) and yellowness (positive). All the correlations are significant (p -value < 0.0001).

Table 11.5. Means, their standard errors, and estimated repeatability of Cross_8 F₁ eggshell color for different locations of egg and color measurements

Color Measurement ¹	Location of Egg ²	Mean ³ (in mm, n = 120)	F ₁ Female (n = 12) Repeatability
L*	Blunt end	67.99 ± 0.27 ^{AB}	0.74
	Side	68.48 ± 0.26 ^A	0.78
	Apex end	67.31 ± 0.29 ^B	0.74
a*	Blunt end	12.63 ± 0.18 ^A	0.69
	Side	13.16 ± 0.16 ^B	0.79
	Apex end	13.45 ± 0.18 ^B	0.78
b*	Blunt end	23.96 ± 0.24 ^A	0.67
	Side	25.14 ± 0.18 ^B	0.74
	Apex end	25.98 ± 0.16 ^C	0.68

¹ L* is a measurement of shell chromaticity; a* is a measurement of greenness (negative) and redness (positive); b* is a measurement of blueness (negative) and yellowness (positive).

² Significant differences were detected between F₁ females on all the 9 measurements, data not shown.

³ Within each color measurements, means sharing the same superscript are not different from each other (Each pair, student t, *p*-value < 0.05).

Table 11.6. Means, their standard errors, and estimated Cross_8 F₁ individual effects on F₁ eggshell color using the average color measurements of each egg

F₁ Female ID	L* Mean^{1, 2, 3} (n = 10)	a* Mean^{1, 2, 3} (n = 10)	b* Mean^{1, 2, 3} (n = 10)
917	66.72 ± 0.43 ^F	13.32 ± 0.27 ^{EF}	27.19 ± 0.26 ^{AB}
918	67.35 ± 0.35 ^{EF}	13.47 ± 0.06 ^{DEF}	25.73 ± 0.26 ^{CD}
920	65.08 ± 0.54 ^G	14.79 ± 0.40 ^{AB}	26.62 ± 0.24 ^B
921	67.22 ± 0.44 ^{EF}	14.07 ± 0.16 ^{CD}	23.25 ± 0.35 ^F
922	72.97 ± 0.30 ^A	9.61 ± 0.11 ^I	21.56 ± 0.27 ^G
923	71.71 ± 0.55 ^B	10.81 ± 0.13 ^H	24.46 ± 0.12 ^E
925	63.63 ± 0.36 ^H	15.19 ± 0.32 ^A	27.53 ± 0.23 ^A
928	68.90 ± 0.42 ^{CD}	12.87 ± 0.22 ^F	25.17 ± 0.28 ^{DE}
929	69.95 ± 0.28 ^C	11.68 ± 0.29 ^G	24.40 ± 0.35 ^E
930	66.91 ± 0.27 ^F	13.69 ± 0.21 ^{CDE}	26.36 ± 0.27 ^{BC}
931	66.56 ± 0.40 ^F	14.26 ± 0.28 ^{BC}	24.54 ± 0.46 ^E
932	68.10 ± 0.49 ^{DE}	13.18 ± 0.29 ^{EF}	23.52 ± 0.40 ^F

¹ L* is a measurement of shell chromaticity; a* is a measurement of greenness (negative) and redness (positive); b* is a measurement of blueness (negative) and yellowness (positive).

² Each value is the mean of three measurements from the apex end, side, and blunt end of each egg.

³ Within each color measurements, means sharing the same superscript are not different from each other (Each pair, student t, *p*-value < 0.05).

Table 11.7. Means, their standard errors, and homogeneity test of variances of LT7, 1D7, and 4D7¹
between the Cross_9 F₂ and the red jungle fowl

Phenotype	Cross_9 F₂ Mean (in mm, n = 184)	Red Jungle Fowl Mean (in mm, n = 20)
LT7_Left	62.46 ± 0.34	56.44 ± 0.85
LT7_Right	63.10 ± 0.34	57.44 ± 0.98
1D7_Left ¹	13.50 ± 0.19	10.94 ± 0.20
1D7_Right ¹	13.59 ± 0.18	11.16 ± 0.15
4D7_Left ¹	19.98 ± 0.27	25.63 ± 0.44
4D7_Right ¹	19.82 ± 0.27	25.84 ± 0.37

¹ LT7 is the total length of the tarsometatarsus at week 7; 1D7 is the total length of the 1st digit at week 7;
4D7 is the total length of the 4th digit at week 7.

² Standard deviations of Cross_9 F₂ and red jungle fowl are significantly different (data not shown, *p*-value < 0.01).

Table 11.8. Means, their standard errors, and estimated *Po* genotypic effect on ED, 1D, 4D, HE, and LT¹ in

Cross_9 F₂

Phenotype	<i>Po-1/Po-1</i> Mean (n = 45) ³	<i>Po-1/Po-2</i> Mean (n = 87) ³	<i>Po-2/Po-2</i> Mean (n = 52) ³	Dominance of <i>Po-1</i>
ED/LT7_Left ²	0.428 ± 0.007 ^A	0.412 ± 0.005 ^{AB}	0.403 ± 0.006 ^B	Non-dominant
ED/LT7_Right ²	0.418 ± 0.007 ^A	0.390 ± 0.005 ^B	0.391 ± 0.007 ^B	Recessive
1D/LT7_Left ²	0.216 ± 0.005 ^A	0.213 ± 0.004 ^A	0.220 ± 0.005 ^A	
1D/LT7_Right ²	0.213 ± 0.005 ^A	0.217 ± 0.004 ^A	0.213 ± 0.003 ^A	
4D/LT7_Left ²	0.332 ± 0.007 ^A	0.315 ± 0.007 ^A	0.319 ± 0.007 ^A	-
4D/LT7_Right ²	0.324 ± 0.007 ^A	0.309 ± 0.006 ^A	0.315 ± 0.008 ^A	-
HE/LT7_Left ²	0.389 ± 0.009 ^A	0.377 ± 0.006 ^A	0.350 ± 0.005 ^B	Dominant
HE/LT7_Right ²	0.388 ± 0.007 ^A	0.375 ± 0.006 ^A	0.344 ± 0.006 ^B	Dominant
LT7_Left	62.88 ± 0.73 ^A mm	61.86 ± 0.49 ^A mm	63.11 ± 0.57 ^A mm	-
LT7_Right	63.49 ± 0.77 ^A mm	62.69 ± 0.49 ^A mm	63.45 ± 0.59 ^A mm	-
	<i>Po-1/Po-1</i> Mean (n = 44) ³	<i>Po-1/Po-2</i> Mean (n = 85) ³	<i>Po-2/Po-2</i> Mean (n = 46) ³	
ED/LT27_Left ²	0.367 ± 0.006 ^A	0.350 ± 0.004 ^B	0.336 ± 0.006 ^B	Recessive
4D/LT27_Left ²	0.286 ± 0.006 ^A	0.271 ± 0.006 ^{AB}	0.263 ± 0.007 ^B	Non-dominant ⁴
HE/LT27_Left ²	0.340 ± 0.007 ^A	0.330 ± 0.005 ^A	0.306 ± 0.006 ^B	Dominant
LT27_Left	92.96 ± 1.38 ^A mm	90.44 ± 1.02 ^A mm	92.36 ± 1.23 ^A mm	-

¹ ED is the total length of the extra digit; 1D is the total length of the 1st digit; 4D is the total length of the 4th digit; HE is the distance between the extra toe and the bottom of the tarsometatarsus; LT is the total length of the tarsometatarsus.

² Data was adjusted for LT. e. g. ED/LT7 represents the total length of the extra digit at week 7 divided by the total length of the tarsometatarsus at week 7.

³ Within each phenotype, means sharing the same superscript are not different from each other (Each pair, student t, P<0.05).

⁴ No genotypic effect was found by ANOVA.

Table 11.9. Means, their standard errors, and estimated feathered-leg and vulture hock effects on the total length of the 4th digit (4D) in Cross_9 F₂

Trait ¹	Feathered-leg (week 7) Mean (n = 124) ^{2,3}	Intermediate FL (week 7) Mean (n = 41) ^{2,3}	Clean-leg (week 7) Mean (n = 19) ^{2,3}	Dominance of Feathered-leg
4D/LT7_Left	0.296 ± 0.004 ^A	0.367 ± 0.005 ^B	0.375 ± 0.006 ^B	Recessive
4D/LT7_Right	0.293 ± 0.005 ^A	0.353 ± 0.005 ^B	0.368 ± 0.007 ^B	Recessive
	Vulture Hock (week 7, All⁴) Mean (n = 31)²		Non-VH (week 7, All⁴) Mean (n = 153)²	
4D/LT7_Left	0.273 ± 0.008 ^A		0.330 ± 0.004 ^B	
4D/LT7_Right	0.268 ± 0.011 ^A		0.324 ± 0.004 ^B	
	Vulture Hock (week 7, within FL⁵) Mean (n = 31)²		Non-VH (week 7, within FL⁵) Mean (n = 93)²	
4D/LT7_Left	0.273 ± 0.008 ^A		0.304 ± 0.005 ^B	
4D/LT7_Right	0.268 ± 0.011 ^A		0.302 ± 0.005 ^B	
	Vulture Hock (week 27, All⁶) Mean (n = 19)²	Intermediate VH (week 27, All⁶) Mean (n = 49)²	Non-VH (week 27, All⁶) Mean (n = 107)²	
4D/LT27_Left	0.229 ± 0.010 ^A	0.268 ± 0.005 ^B	0.283 ± 0.005 ^B	Recessive
	Vulture Hock (week 27, within FL 4-9⁷) Mean (n = 19)²	Intermediate VH (week 27, within FL 4-9⁷) Mean (n = 42)²	Non-VH (week 27, within FL 4-9⁷) Mean (n = 24)²	
4D/LT27_Left	0.229 ± 0.010 ^A	0.263 ± 0.006 ^B	0.233 ± 0.010 ^A	Over dominance

¹ The total length of the 4th digit was adjusted for LT. e. g. 4D/LT7 represents the total length of the 4th digit at week 7 divided by the total length of the tarsometatarsus at week 7.

² Within each row, means sharing the same superscript are not different from each other (Each pair, student t, P<0.05).

³ Based on all the FL7 records. The effect of FL27 (treated as a numeric trait) on 4D/LT27 was also estimated but not shown in the table which was significant negatively correlated ($r = -0.60$, $p < 0.0001$).

⁴ Based on all the VH7 records.

⁵ Based on the VH7 records while individuals with an intermediate FL or clean-leg record in FL7 were excluded.

⁶ Based on all the VH27 records.

⁷ Based on the VH27 records while individuals with a 0-3 FL27 record were excluded.

Table 11.10. Means, their standard errors, and estimated hookless and its genotypic effects on the total length of the tarsometatarsus in Cross_9 F₂

Trait ¹	Hookless (week 7) Mean (n = 47) ^{2,3}		Non-HL (week 7) Mean (n = 137) ^{2,3}	Dominance of <i>h</i>
LT7_Left	61.36 ± 0.68 ^A mm		62.84 ± 0.38 ^A mm	
LT7_Right	61.60 ± 0.68 ^A mm		63.62 ± 0.38 ^B mm	
	<i>h/h</i> (week 7) Mean (n = 47)^{2,4}	<i>H/h</i> (week 7) Mean (n = 86)²	<i>H/H</i> (week 7) Mean (n = 51)^{2,4}	
LT7_Left	61.36 ± 0.68 ^A mm	62.53 ± 0.47 ^{AB} mm	63.37 ± 0.66 ^B mm	Non-dominance
LT7_Right	61.60 ± 0.68 ^A mm	63.46 ± 0.47 ^B mm	63.87 ± 0.67 ^B mm	Recessive
	Hookless (week 27) Mean (n = 45)^{2,3}		Non-HL (week 27) Mean (n = 130)^{2,3}	
LT27_Left	91.23 ± 1.33 ^A mm		91.69 ± 0.81 ^A mm	
	<i>h/h</i> (week 27) Mean (n = 45)^{2,4}	<i>H/h</i> (week 27) Mean (n = 83)^{2,4}	<i>H/H</i> (week 27) Mean (n = 47)^{2,4}	
LT27_Left	91.23 ± 1.33 ^A mm	91.31 ± 0.96 ^A mm	92.37 ± 1.45 ^A mm	-

¹ Numbers in this column represent the ages. e. g. LT7 represents the total length of the tarsometatarsus at week 7.

² Within each row, means sharing the same superscript are not different from each other (Each pair, student t, P<0.05).

³ Hookless stands for the Silkie-like feather; Non-HL stands for wild-type feather with hock.

⁴ *h* stands for the recessive mutant allele of the hookless gene; *H* stands for the dominant wild-type allele of the hookless gene.

Table 11.11. Means, their standard errors, and estimated sex and vulture hock effect on percentage relative asymmetry (RA) in Cross_9 F₂ at week 7

Trait ¹	Type ³	Larger Side	Percentage RA ^{4, 5}		Percentage RA ^{4, 5}	
			Male (n = 100)	Female (n = 84)	VH ⁶ (n = 31)	Non-VH ⁶ (n = 153)
1D	AS	-	12.43 ± 1.02 ^A	11.57 ± 1.16 ^A	10.52 ± 1.37 ^A	12.33 ± 0.87 ^A
1D/LT ²	AS	-	12.12 ± 1.03 ^A	11.57 ± 1.15 ^A	10.84 ± 1.39 ^A	12.07 ± 0.87 ^A
4D	AS	-	6.36 ± 0.57 ^A	9.35 ± 1.46 ^A	14.22 ± 3.44 ^A	6.41 ± 0.50 ^B
4D/LT ²	DA	Left	6.61 ± 0.59 ^A	10.18 ± 1.46 ^B	15.21 ± 3.43 ^A	6.82 ± 0.52 ^B
ED	DA	Left	7.63 ± 0.72 ^A	7.76 ± 0.94 ^A	7.47 ± 1.26 ^A	7.73 ± 0.65 ^A
ED/LT ²	DA	Left	8.20 ± 0.74 ^A	8.29 ± 0.94 ^A	7.73 ± 1.30 ^A	8.34 ± 0.65 ^A
HE	FA	-	8.37 ± 0.75 ^A	9.14 ± 0.84 ^A	5.12 ± 0.62 ^A	9.45 ± 0.64 ^B
HE/LT ²	FA	-	8.39 ± 0.70 ^A	8.72 ± 0.83 ^A	5.12 ± 0.70 ^A	9.23 ± 0.61 ^B
LT	DA	Right	1.66 ± 0.13 ^A	2.49 ± 0.23 ^B	1.57 ± 0.21 ^A	2.14 ± 0.15 ^A

¹ 1D is the total length of the 1st digit; 4D is the total length of the 4th digit; ED is the total length of the extra digit; HE is the distance between the extra toe and the bottom of the tarsometatarsus; LT is the total length of the tarsometatarsus.

² Data was adjusted for LT. e. g. 1D/LT represents the total length of the 1st digit divided by the total length of the tarsometatarsus.

³ AS = antisymmetry (mean zero, not normal distribution); FA = fluctuating asymmetry (mean zero, normal distribution); DA = directional asymmetry (mean not zero).

⁴ Within each trait and each factor (sex or VH), means sharing the same superscript are not different from each other (Each pair, student t, P<0.05).

⁵ $RA = (|L - R| / [(L + R) / 2]) \times 100$. Only in multiple comparison analyses, each RA was transformed to an arc sine square root.

⁶ Vulture hock (VH) and Non-VH (wild-type) data were based on all the available individuals without considering the feathered-leg phenotype at week 7 (FL7). When chickens with a clean-leg or intermediate feathered-leg record of FL7 were excluded, similar significant differences were found (data not shown).

Table 11.12. Candidate genes of *Cp*

Gene Name	Ensembl Gene ID	Position (Mb, Galgal4)	Gene Ontology Terms
<i>BMPR-2</i>	ENSGALG00000008459	11874050~11976212	limb development, osteoblast differentiation
<i>HOXD3</i>	ENSGALG00000023420	16325200..16354477	skeletal system morphogenesis
<i>HOXD4</i>	ENSGALG00000023419	16340652..16342299	skeletal system morphogenesis
<i>HOXD8</i>	ENSGALG00000028128	16355644..16357729	skeletal system morphogenesis
<i>HOXD9</i>	ENSGALG00000027513	16361241..16364705	skeletal system morphogenesis
<i>HOXD10</i>	ENSGALG00000009270	16364830..16369516	skeletal system development
<i>HOXD11</i>	ENSGALG00000009273	16374464..16378904	skeletal system development
<i>HOXD12</i>	ENSGALG00000009274	16383785..16385462	skeletal system development
<i>HOXD13</i>	ENSGALG00000009277	16389450..16391995	skeletal system development
<i>SP3</i>	ENSGALG00000009327	17146668..17177953	ossification
<i>IHH</i>	ENSGALG00000011347	22427441..22435414	skeletal system development, ossification

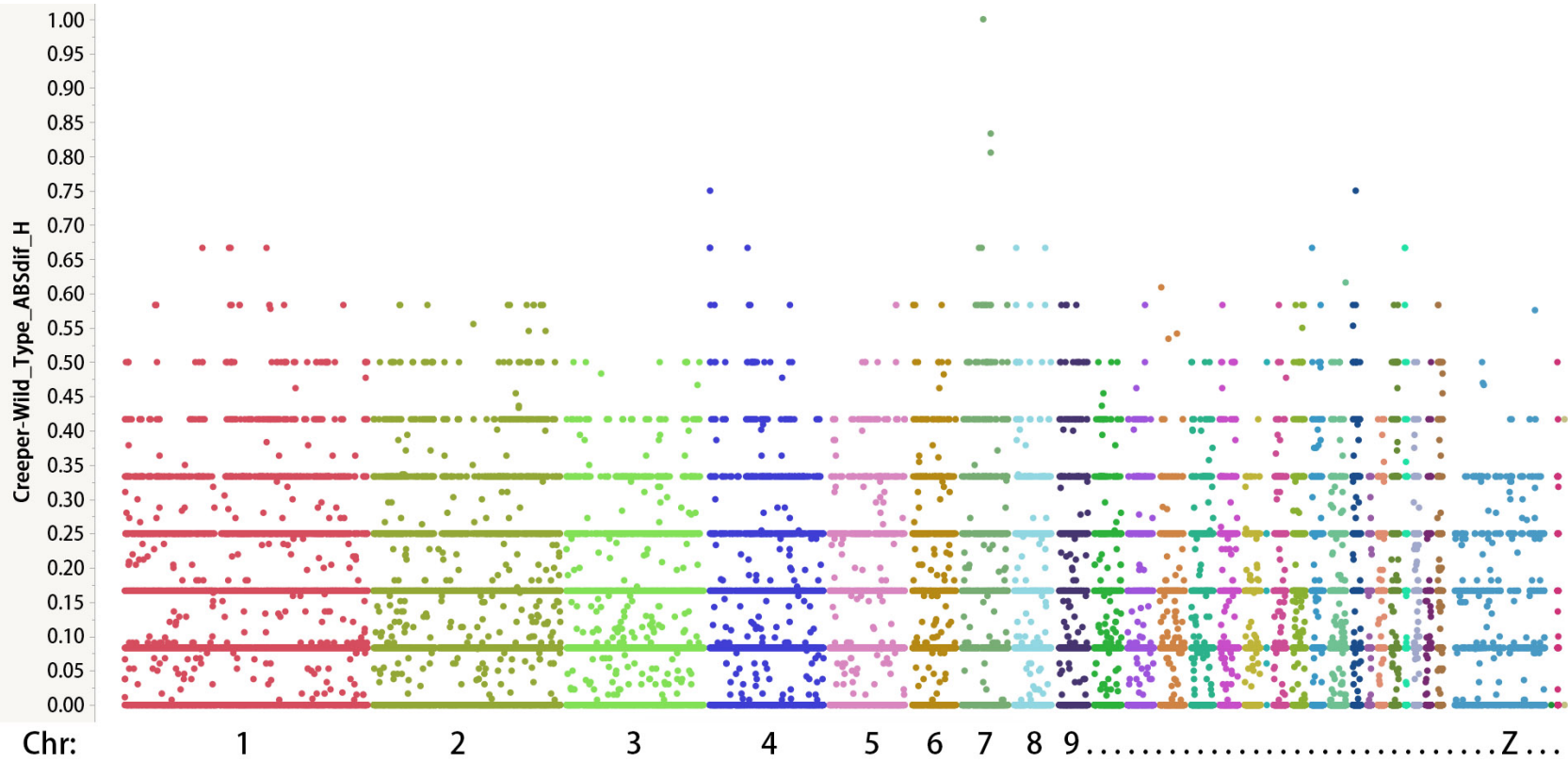


Figure 11.1. Genome-wide ABSdif_H values for *Cp* mapping. All 60K SNPs were plotted against the genomic location.

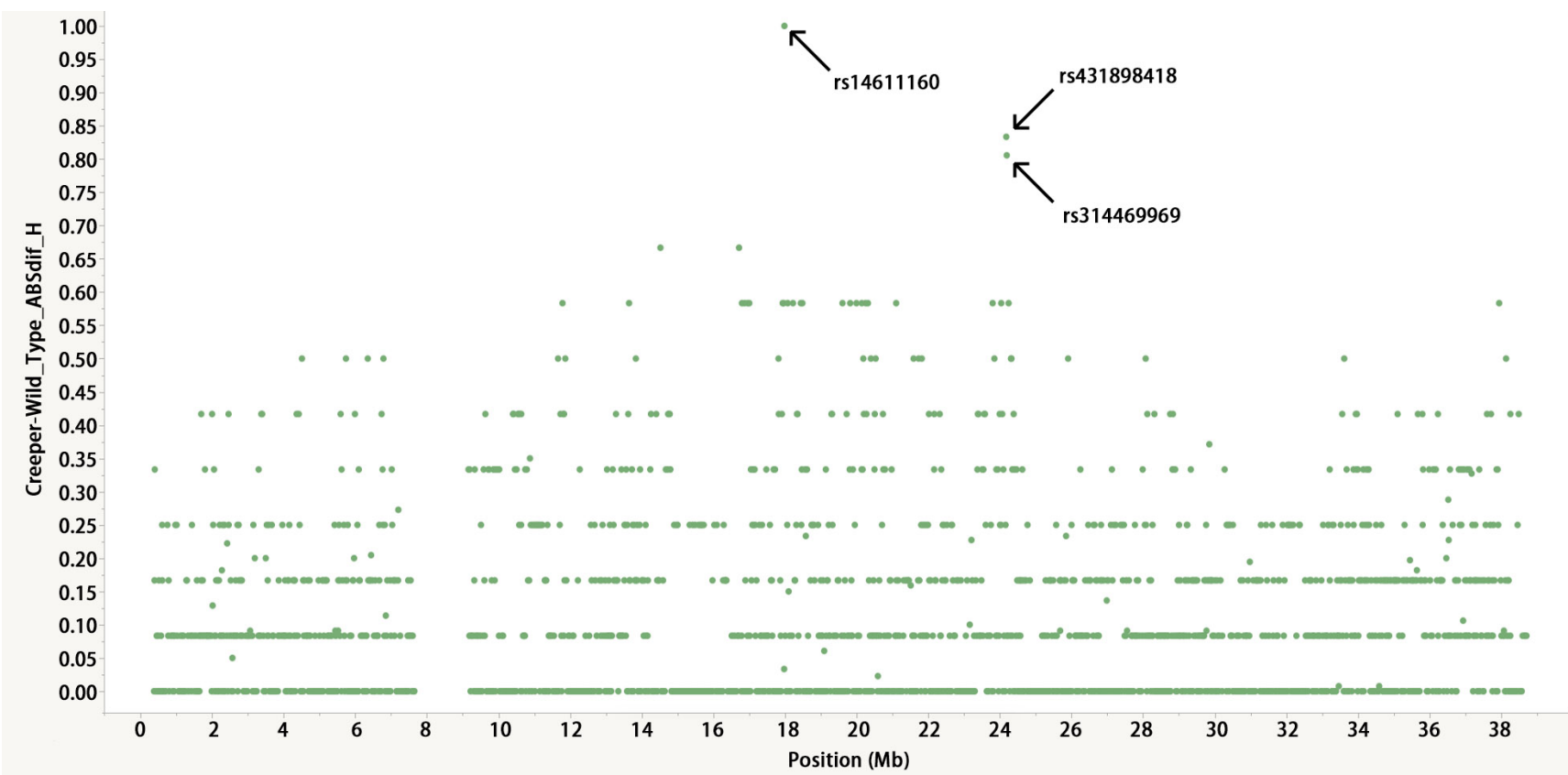


Figure 11.2. The ABSdif_H values of SNPs on chromosome 7 for *Cp* mapping. Plotted against the genomic location. SNP with highest ABSdif_H values were labeled.

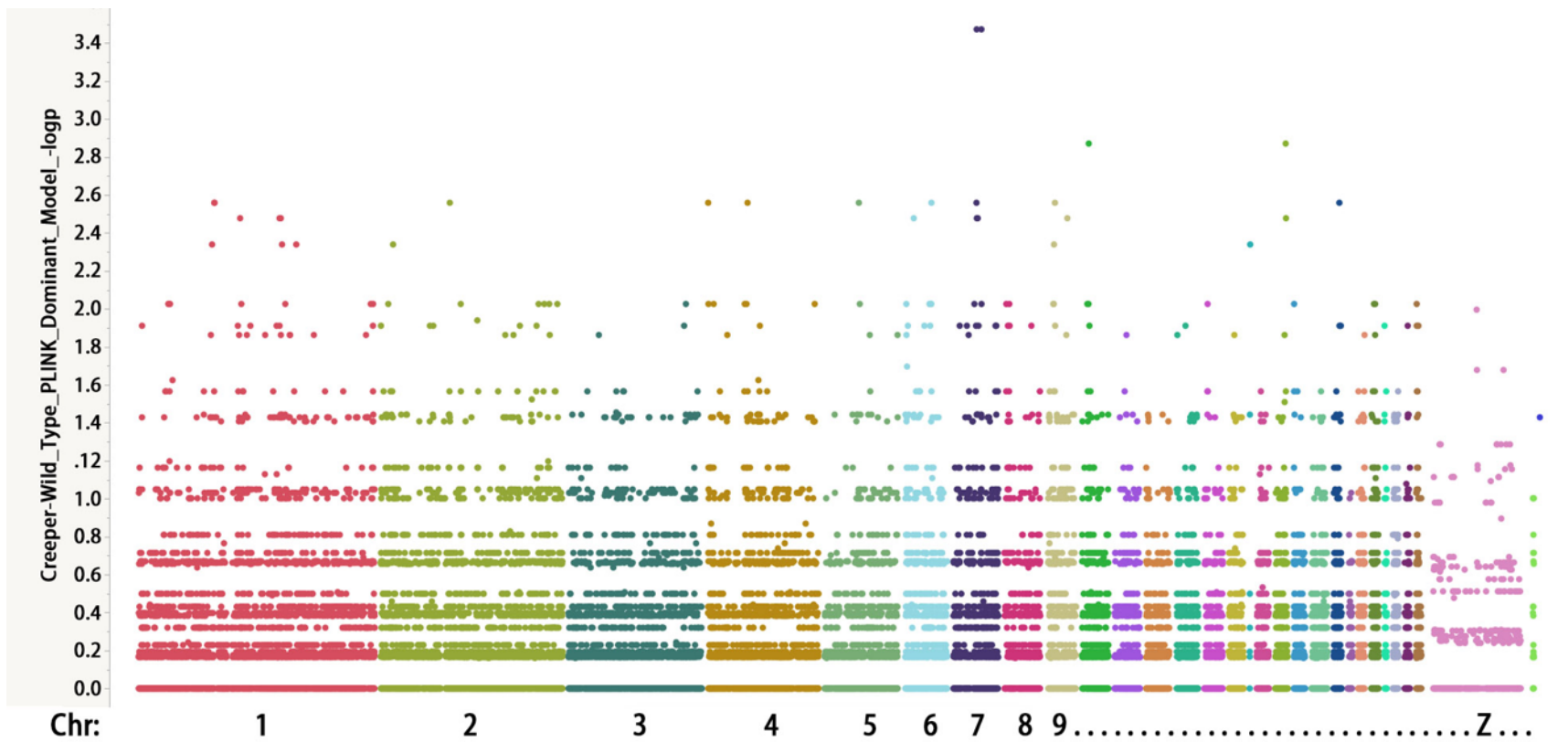


Figure 11.3. Genome-wide $-\log p$ values calculated by dominant model in PLINK, for C_p mapping. All 60K SNPs were plotted against the genomic location.

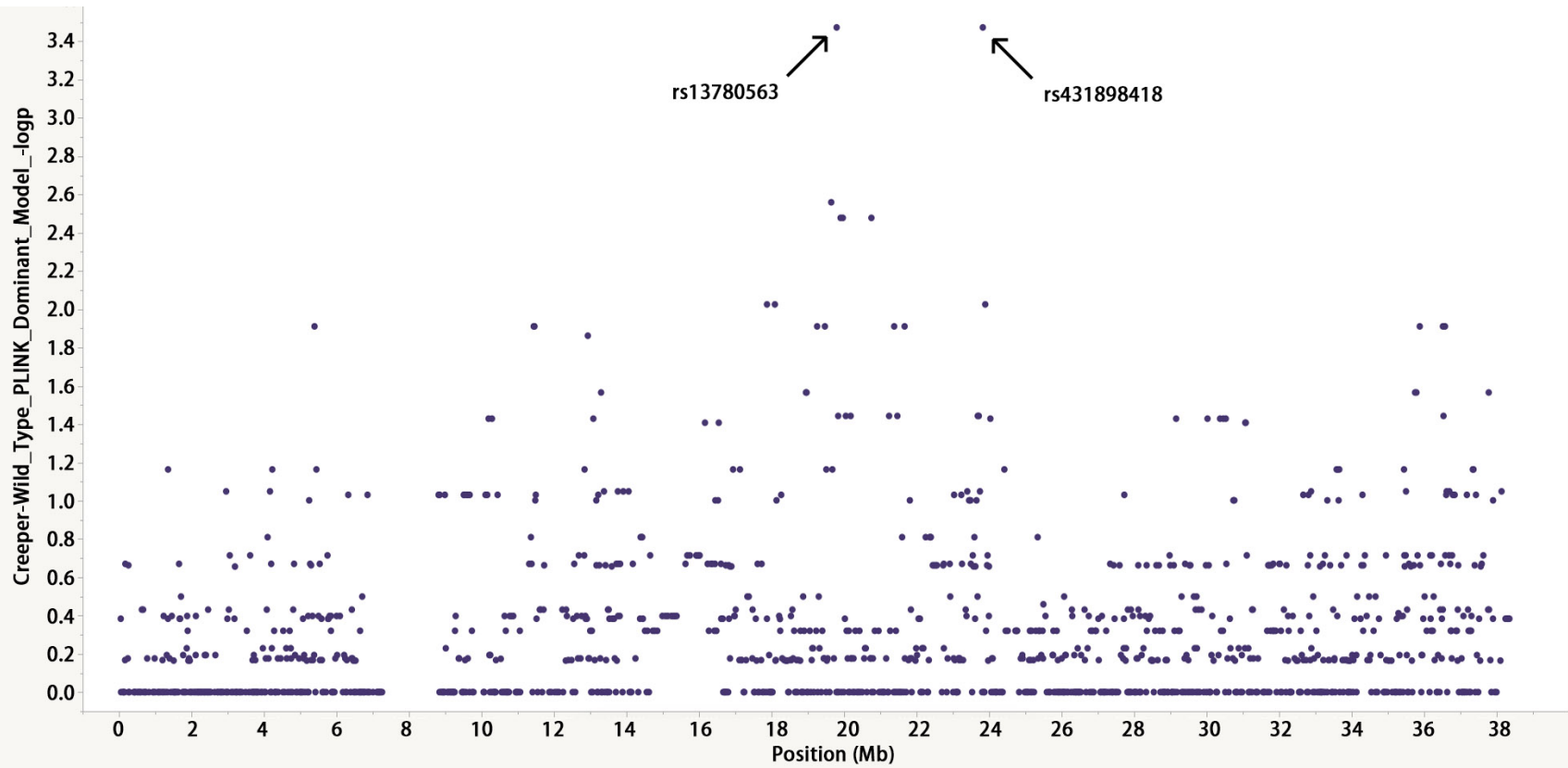


Figure 11.4. The $-\log p$ values calculated by dominant model in PLINK of SNPs on chromosome 7, for C_p mapping. Plotted against the genomic location. SNP with highest $-\log p$ values were labeled.

Reference

- Bateson, W., R. C. Punnett. 1911. The inheritance of the peculiar pigmentation of the silky fowl. 1911. *Journal of Genetics*. 1:185-203.
- Bland, J. M., D. G. Altman. 1996. Transforming data. *British Medical Journal*. 312:770.
- Blow, W. L., C. H. Bostian, E. W. Glazener. 1950. The inheritance of egg shell color. *Poultry Science*. 29:381-385.
- Cairns, J. M., K. Gayer. 1943. Identification of chick embryos homozygous for the Creeper factor. *Journal of Experimental Zoology*. 92:229-245.
- Chi, A., J. C. Valencia, Z. Z. Hu, H. Watabe, H. Yamaguchi, N. J. Mangini, H. Huang, V. A. Canfield, K. C. Cheng, F. Yang, R. Abe, S. Yamagishi, J. Shabanowitz, V. J. Hearing, C. Wu, E. Appella, D. F. Hunt. 2006. Proteomic and bioinformatic characterization of the biogenesis and function of melanosomes. *Journal of Proteome Research*. 5:3135-3144.
- Danforth, C. H. 1929. Bantam genetics: distribution of traits in a Sebright-Mille Fleur cross. *Journal of Heredity*. 20:573-582 (Cited by Somes, R. G. Jr. 1990. Mutations and major variants of plumage and skin in chickens. Page 176 in "Poultry Breeding and Genetics". Crawford, R. D. ed. Elsevier, Amsterdam, Netherlands).
- Domyan, E. T., Z. Kronenberg, C. R. Infante, A. I. Vickrey, S. A. Stringham, R. Bruders, M. W. Guernsey, S. Park, J. Payne, R. B. Beckstead, G. Kardon. 2016 Molecular shifts in limb identity underlie development of feathered feet in two domestic avian species. *ELife*. 5:e12115.
- Dorshorst, B., A. M. Molin, C. J. Rubin, A. M. Johansson, L. Strömstedt, M. H. Pham, C. F. Chen, F. Hallböök, C. Ashwell, L. Andersson. 2011. A complex genomic rearrangement involving the endothelin 3 locus causes dermal hyperpigmentation in the chicken. *PLoS Genetics*. 7:e1002412.
- Dorshorst, B., M. Harun-Or-Rashid, A. J. Bagherpoor, C. J. Rubin, C. Ashwell, D. Gourichon, M. Tixier-Boichard, F. Hallböök, L. Andersson. 2015. A genomic duplication is associated with ectopic eomesodermin expression in the embryonic chicken comb and two duplex-comb phenotypes. *PLoS Genetics*. 11:e1004947.
- Dorshorst, B., R. Okimoto, C. Ashwell. 2010. Genomic regions associated with dermal hyperpigmentation, polydactyly and other morphological traits in the Silkie chicken. *Journal of Heredity*. 101:339-350.
- Dunn, L. C., M. A. Jull. 1927. On the inheritance of some characters of the silky fowl. *Journal of Genetics*. 19: 27-63.
- Elmer, W. A. 1968a. In vitro and in situ analyses of the inhibitory effect of Creeper tissues. *Journal of Experimental Zoology*. 169:381-389.
- Elmer, W. A. 1968b. Experimental analysis of the Creeper condition in chickens: effect of embryo extract on elongation, protein content, and incorporation of amino acids by cartilaginous tibiotarsi. *Developmental Biology*. 18:76-92.
- Farnsworth, G. M., A. W. Nordskog. 1955. Breeding for egg quality 3. Genetic differences in shell characteristics and other egg quality factors. *Poultry Science*. 34:16-26.
- Feng, C., Y. Gao, B. Dorshorst, C. Song, X. Gu, Q. Li, J. Li, T. Liu, C. J. Rubin, Y. Zhao, Y. Wang. 2014. A cis-regulatory mutation of PDSS2 causes silky-feather in chickens. *PLoS Genetics*. 10:e1004576.
- Fulton, J. E., M. Soller, A. R. Lund, J. Arango, E. Lipkin. 2012. Variation in the ovocalyxin-32 gene in commercial egg-laying chickens and its relationship with egg production and egg quality traits. *Animal Genetics*. 43:102-113.
- Gayer, K., V. Hamburger. 1943. The developmental potencies of eye primordia of homozygous Creeper chick embryos tested by orthotopic transplantation. *Journal of Experimental Zoology*. 93:147-183.
- Hamburger, V. 1941. Transplantation of limb primordia of homozygous and heterozygous chondrodystrophic ("Creeper") chick embryos. *Physiological Zoology*. 14:355-365.
- Hunton, P. 1962. Genetics of egg shell colour in a light sussex flock. *British Poultry Science*. 3:189-193.
- Imsland, F., C. Feng, H. Boije, B. Bed'hom, V. Fillon, B. Dorshorst, C. J. Rubin, R. Liu, Y. Gao, X. Gu, Y. Wang, D. Gourichon, M. C. Zody, W. Zecchin, A. Vieaud, M. Tixier-Boichard, X. Hu, F. Hallböök, N. Li, L. Andersson. 2012. The Rose-comb mutation in chickens constitutes a structural rearrangement causing both altered comb morphology and defective sperm motility. *PLoS Genetics*. 8:e1002775.
- Jaeger, T. F. 2008. Categorical data analysis: Away from ANOVAs (transformation or not) and towards logit mixed models. *Journal of Memory and Language*. 59:434-446.
- Jin, S., F. Zhu, Y. Wang, G. Yi, J. Li, L. Lian, J. Zheng, G. Xu, R. Jiao, T. Gong, Z. Hou, N. Yang. 2016. Deletion of Indian hedgehog gene causes dominant semi-lethal Creeper trait in chicken. *Scientific Reports*. 6:30172.
- JMP version 11. 2015. SAS Institute Inc., Cary, NC.
- Jull, M. A., J. P. Quinn. 1931. Inheritance in poultry: data on the genetics of vulture hock, hen feathering and "crooked neck" in the domestic fowl. *Journal of Heredity*. 22:147-154.
- Kutner, M. H., C. J. Nachtsheim, J. Neter, W. Li. 2004. *Applied Linear Statistical Models*. 5th ed. Page 701. McGraw-Hill/Irwin, New York, United States.
- Lambert, W. V., C. W. Knox. 1929. The inheritance of shank-feathering in the domestic fowl. *Poultry Science*. 9:51-64.

- Landauer, W. 1932. Studies on the Creeper fowl. V. the linkage of the genes for Creeper and single-comb. *Journal of Genetics*. 26:285-290.
- Landauer, W. 1933. Creeper and single-comb linkage in fowl. *Nature*. 132:606.
- Lefort, G., P. Blanchet, N. Belgrade, F. Rivier, A. M. Chaze, P. Sarda, J. Demaille, F. Pellestor. 2002. Stable dicentric duplication-deficiency chromosome 14 resulting from crossing-over within a maternal paracentric inversion. *American Journal of Medical Genetics*. 113:333-338.
- Li, G., D. Li, Ni. Yang, L. Qu, Z. Hou, J. Zheng, G. Xu, S. Chen. 2014. A genome-wide association study identifies novel single nucleotide polymorphisms associated with dermal shank pigmentation in chickens. *Poultry Science*. 93:2983-2987.
- Liu, W. Y., C. J. Zhao, J. Y. Li. 2010. A non-invasive and inexpensive PCR-based procedure for rapid sex diagnosis of Chinese gamecock chicks and embryos. *Journal of Animal and Veterinary Advances*. 9:962-970.
- Maas, S. A., T. Suzuki, J. F. Fallon. 2011. Identification of spontaneous mutations within the long-range limb-specific Sonic hedgehog enhancer (ZRS) that alter Sonic hedgehog expression in the chicken limb mutants oligozeugodactyly and silkie breed. *Developmental Dynamics*. 240:1212-1222.
- Møller, A. P., J. P. Swaddle. 1997. *Asymmetry, Developmental Stability and Evolution*. Pages 9-20. Oxford University Press, New York, United States.
- Muizzuddin, N., K. Marenus, D. Maes, W. P. Smith. 1990. Use of a chromameter in assessing the efficacy of anti-irritants and tanning accelerators. *Journal of the Society of Cosmetic Chemists*. 41:369-378.
- Novitski, E., G. Braver. 1954. An analysis of crossing over within a heterozygous inversion in *Drosophila melanogaster*. *Genetics*. 39:197.
- Punnett, R. C., P. G. Bailey. 1920. Genetic studies in poultry II. Inheritance of egg-colour and broodiness. *Journal of Genetics*. 10:277-292.
- Roberts, J. R., K. Chousalkar. 2013. Egg quality and age of laying hens: implications for product safety. *Animal Production Science*. 53:1291-1297.
- Samiullah, S., J. R. Roberts, K. Chousalkar. 2015. Eggshell color in brown-egg laying hens - a review. *Poultry Science*. 94:2566-2575.
- Sasaki, O., S. Odawara, H. Takahashi, K. Nirasawa, Y. Oyamada, R. Yamamoto, K. Ishii, Y. Nagamine, H. Takeda, E. Kobayashi, T. Furukawa. 2004. Genetic mapping of quantitative trait loci affecting body weight, egg character and egg production in F2 intercross chickens. *Animal Genetics*. 35:188-194.
- Sawyer, R. H., L. W. Knapp. 2003. Avian skin development and the evolutionary origin of feathers. *Journal of Experimental Zoology Part B: Molecular and Developmental Evolution*. 298:57-72.
- Schreiweis, M. A., P. Y. Hester, D. E. Moody. 2005. Identification of quantitative trait loci associated with bone traits and body weight in an F2 resource population of chickens. *Genetics Selection Evolution* 37:106-112.
- Şekeroğlu, A., M. Duman. 2011. Effect of egg shell colour of broiler parent stocks on hatching results, chickens performance, carcass characteristics, internal organ weights and some stress indicators. *Kafkas Üniversitesi Veteriner Fakültesi Dergisi*. 17:837-842.
- Serebrovsky, A. S., S. G. Petrov. 1928. A case of close autosomal linkage in the fowl. *Journal of Heredity*. 19:305-306.
- Somes, R. G. Jr. 1990. Mutations and major variants of plumage and skin in chickens. Pages 223-224 in "Poultry Breeding and Genetics". Crawford, R. D. ed. Elsevier, Amsterdam, Netherlands.
- T RINTAMÄKI, P. E. K. K. A., R. V. Alatalo, J. Höglund, A. Lundberg. 1997. Fluctuating asymmetry and copulation success in lekking black grouse. *Animal Behaviour*. 54:265-269.
- Taylor, L. W. 1934. Creeper and single-comb linkage in the fowl. *Journal of Heredity*. 25:205-206.
- Wang, Y., Y. Gao, F. Imsland, X. Gu, C. Feng, R. Liu, C. Song, M. Tixier-Boichard, D. Gourichon, Q. Li, K. Chen. 2012. The crest phenotype in chicken is associated with ectopic expression of HOXC8 in cranial skin. *PLoS One* 7:e34012.
- Warren, D. C. 1944. Inheritance of polydactylism in the fowl. *Genetics*. 29:217-231.
- Wolc, A., J. Arango, T. Jankowski, I. Dunn, P. Settari, J. E. Fulton, N. P. O'Sullivan, R. Preisinger, R. L. Fernando, D. J. Garrick, J. C. M. Dekkers. 2014. Genome-wide association study for egg production and quality in layer chickens. *Journal of Animal Breeding and Genetics*. 131:173-182.
- Yang, A., E. A. Dunnington, P. B. Siegel. 1998. Developmental stability in different genetic stocks of white rock chickens. *The Journal of Heredity*. 89:260-264.
- Yang, H. M., Z. Y. Wang, J. Lu. 2009. Study on the relationship between eggshell colors and egg quality as well as shell ultrastructure in Yangzhou chicken. *African Journal of Biotechnology*. 8:2898-2902.
- Zheng, C., Z. Li, N. Yang, Z. Ning. 2014. Quantitative expression of candidate genes affecting eggshell color. *Animal Science Journal*. 85:506-510.

Chapter 12

Summary

This dissertation consists of gene mapping of 12 morphological traits in chickens. Results from these studies showed that morphological traits can be influenced by single mutations on DNA sequences. These mutations can be a SNP in the coding region (*choc*, Chapter 10), in the UTR (*mo*, Chapter 6), or in the regulatory region (*Pti-1*, Chapter 7). It also can be a genomic duplication, deletion, or an insertion of a single base pair (*Bl*, Chapter 9). Candidate genes associated with morphological traits identified in this dissertation include *ROBO2* (*MI*, Chapter 5), *EDNRB2* (*mo*, Chapter 6), *TBX5* (*Pti-1*, Chapter 7), *SHH* (*Po-2*, Chapter 8), *LOC419112* (*Bl*, Chapter 9), and *TYRPI* (*choc*, Chapter 10). Their identifications provides insights of cellular and molecular mechanisms involved in morphogenesis.

It was hypothesized that the ancestors of avian species had a feathered-leg phenotype. Therefore, the feathered-leg mutation identified in this dissertation could be identical to that of the ancestors of avian species and thus provide material to study the evolution of birds. Experiments involving *Po-1*, *Po-2*, two different *mo* alleles, and feathered-leg traits in chickens and pigeons provide three examples of parallel evolution. The mapping of *choc* will further our understanding of the domestication process, because this mutation which occurred spontaneously in a female of a backyard flock has spread from England throughout the world within two decades. Genomic duplications, insertions, and deletions can trigger significant phenotypic changes and thus have important roles during evolution. All were observed in the *Bl* allele which thus can facilitate the study of the interactions among them.

It was proposed in this dissertation that the *mo* mutation has a similar effect on melanocytes during embryonic development and follicle development. The same was proposed regarding the *Bl* mutation. They illustrate an advantage for using the chicken as a model organism because it allows similar mechanisms to be studied at two different stages within the same individual.

Research conducted in this dissertation revealed factors including genomic context, modifiers, and environmental factors that influenced the phenotypic expression of single genes. There are candidate regions still waiting to be discovered. They can further our understanding of gene \times genetic background and gene \times environment interactions. This dissertation also provides examples demonstrating that the SNP-MaP strategy is a reliable and cost-efficient way to identify the causal mutations for phenotypes.

Abbreviations

1D	Total length of the 1 st digit
1D7	Total length of the 1 st digit at 7 weeks of age
4D	Total length of the 4 th digit
4D27	Total length of the 4 th digit at 27 weeks of age
4D7	Total length of the 4 th digit at 7 weeks of age
A	Adenine
AA	Amino acid
<i>Ab</i>	Autosomal barring
ABCG2	Adenosine triphosphate-binding cassette, subfamily G, member 2
ABSdif_H	Differences of heterozygosity
absRAFdif	Absolute RAF difference
AG	Angle between the extra digit & the 3 rd digit
AG0	Angle between the extra digit & the 3 rd digit at hatch
AG7	Angle between the extra digit & the 3 rd digit at 7 weeks of age
Ala	Alanin
Anc.	Ancestor
ANOVA	Analysis of variance
Arg	Arginine
AS	Antisymmetry
ASIP	Agouti signaling protein
Asn	Asparagine
ATP	Adenosine triphosphate

<i>B</i>	Sex-linked barring
BC	Backcross
BC ₁	First backcross generation
<i>Bg</i>	Autosomal barring
<i>Bl</i>	Blue
BMP	Bone morphogenetic proteins
BMPR-2	Bone morphogenetic protein receptor type 2
bp	Base pair
B ^{SD} :	Barred Sex-linked Dilution
C	Cytosine
<i>c</i>	Recessive white
Ca	Caesium
CDKN2A/B	Cyclin-dependent kinase inhibitor 2A/B
<i>choc</i>	Chocolate
Chr.	Chromosome
cM	Centimorgan
CNV	Copy number variation
<i>Co</i>	Columbian
<i>Cp</i>	Creeper
<i>Cr</i>	Crest
Ct	Cycle threshold
CuA	Copper-binding domains A
CuB	Copper-binding domains B

Cys	Cysteine
Cys	Cysteine
<i>D</i>	Duplex comb
DA	Directional asymmetry
<i>Db</i>	Dark brown
DCT	Dopachrome tautomerase
del	Deletion
DHI	Dihydroxyindole
DHICA	Dihydroxyindole-2-carboxylic acid
DNA	Deoxyribonucleic acid
dNTP	Deoxyribose nucleoside triphosphate
<i>E</i>	Extended black
ED	Total length of the extra digit
ED0	Total length of the extra digit at hatch
ED27	Total length of the extra digit at 27 weeks of age
ED7	Total length of the extra digit at 7 weeks of age
EDBRA	Endothelin receptor A
EDNRB	Endothelin receptor B
EDNRB1	Endothelin receptor B subtype 1
EDNRB2	Endothelin receptor B subtype 2
EGF	Epidermal growth factor
EPHB2	Ephrin receptor B2
ER	Endoplasmic reticulum

ET3	Endothelin3
F ₀	Parental population
F ₁	First filial generation
F ₂	Second filial generation
FA	Fluctuating asymmetry
FAM	6-Carboxyfluorescein
FGF	Fibroblast growth factor
FL	Degree of feathered-leg
FL0	Degree of feathered-leg at hatch
FL27	Degree of feathered-leg at 27 weeks of age
FL7	Degree of feathered-leg at 7 weeks of age
<i>Fm</i>	Fibromelanosis
Freq.	Frequency
G	Guanine
GATA6	GATA binding protein 6
Gli1	GLI family zinc finger 1
Glu	Glutamine
GO	Gene ontology
<i>h</i>	Hookless
HE	Distance between the extra toe and the bottom of the tarsometatarsus
HE27	Distance between the extra toe and the bottom of the tarsometatarsus at 27 weeks of age

HE7	Distance between the extra toe and the bottom of the tarsometatarsus at 7 weeks of age
HEX	6-Hexachlorofluorescein
His	Histidine
HL	Hookless
HL27	Hookless at 27 weeks of age
HL7	Hookless at 7 weeks of age
HOXD	Homeobox D
HPLC	High Performance Liquid Chromatography
<i>I</i>	Dominant white
<i>Id</i>	Inhibitor of dermal melanin
IHH	Indian hedgehog
Ile	Isoleucine
indel	Insertion and deletion
KASP	Kompetitive allele-specific polymerase chain reactions assay
kb	Kilobase pairs
KGF	Keratinocyte growth factor
KGFR	Keratinocyte growth factor receptor
kV	Kilovolt
<i>lav</i>	Lavender
Leu	Leucine
<i>Lg</i>	Lacing
<i>LMBR1</i>	Limb development membrane protein 1

LT	Total length of the tarsometatarsus
LT27	Total length of the tarsometatarsus at 27 weeks of age
LT7	Total length of the tarsometatarsus at 7 weeks of age
LTR/ERVK	Long terminal repeats/ endogenous retroviruses group K
Lys	Lysine
MaP	Microarray and pooling
MATP	Membrane-associated transporter protein
Mb	Megabase pairs
MC1R	Melanocortin 1 receptor
Met	Methionine
MFCS-1	Mammal-fish-conserved-sequence-1
MGB	Minor groove binder
min	Minute
MITF	Microphthalmia-associated transcription factor
<i>Ml</i>	Melanotic
MLPH	Melanophilin
mM	Millimolar
mm	Milimeter
<i>mo</i>	Mottling
mRNA	Messenger RNA
MYOVA	Myosin VA
Na	Sodium
NDB	Noire du Berry breed

NFAT	Nuclear factor of activated T cells
ng	Nanogram
NGS	Next-generation sequencing
nm	Nanometer
OCX32	Ovocalyxin-32
<i>P</i>	Pea comb
PAR-2	Protease-activated receptor-2
PAX3	Paired box gene 3
PCR	Polymerase chain reactions
<i>Pg</i>	Pattern
pH	Potential of hydrogen
Phe	Phenylalanine
PITX1	Paired-like homeodomain 1
PMEL	Premelanosome protein
PNA	Peanut agglutinin
<i>Po-1</i>	Polydactyly-1
<i>Po-2</i>	Polydactyly-2
PPC	Prob-specific correction
<i>Pti-1</i>	Ptilopody 1
<i>Pti-2</i>	Ptilopody 2
<i>pti-3</i>	Ptilopody 3
QTL	Quantitative trait locus
<i>R</i>	Rose comb

RA	Relative asymmetry
Rab27a	RAS oncogene family
RAF	Relative allelic frequency
Robo1	Roundabout1
Robo2	Roundabout2
ROI	Region of interest
s	Second
S	Silver
SHH	Sonic Hedgehog
SLC45A2	Solute carrier family 45, member 2, protein
Slits	Slit-family proteins
SNP	Single nucleotide polymorphism
SOX10	SRY-box containing gene 10
SOX5	SRY-box containing gene 5
Sp3	Specificity protein 3 transcription factor
STIM1	Stromal interaction molecule 1
STIMATE	Stromal interaction molecule activating enhancer
T	Thymine
TBX3	T-box 3
TBX5	T-box 5
Thr	Threonine
Tm	Melting temperature
TMEM110	Transmembrane protein 110

TYR	Tyrosinase
Tyr	Tyrosine
TYRP1	Tyrosinase-related-protein 1
TYRP2	Tyrosinase-related-protein 2
U	Unit
uORFs	Upstream open reading frames
UTR	Untranslated region
v	Vulture hock
Val	Valine
VH	Vulture hock
VH27	Vulture hock at 27 weeks of age
VH7	Vulture hock at 7 weeks of age
W	W chromosome
Wnt	Wingless-int
WNT5A	Wingless-int family protein 5A
WNT7A	Wingless-int family protein 7A
ZPA	Zone of polarizing activity
ZRS	Zone of polarizing activity regulatory sequence
α -MSH	α -melanocyte stimulating hormone
μ g	Microgram
μ l	Microliter
μ M	Micromolar